

Max-Planck-Institut für Eisenforschung GmbH

Max-Planck-Straße 1
D-40237 Düsseldorf

Phone: +49-211-6792-0
Fax: +49-211-6792-268
E-mail: mpi@mpie.de
Homepage: <http://www.mpie.de>

Access

from Central Railway Station:
by Bus 834 (direction Belsenplatz)
Stop Sohnstraße

by Taxi to Sohnstraße/Max-Planck-
Straße, 10 minutes

from Airport:
by Taxi to Sohnstraße/Max-Planck-
Straße, 15 minutes



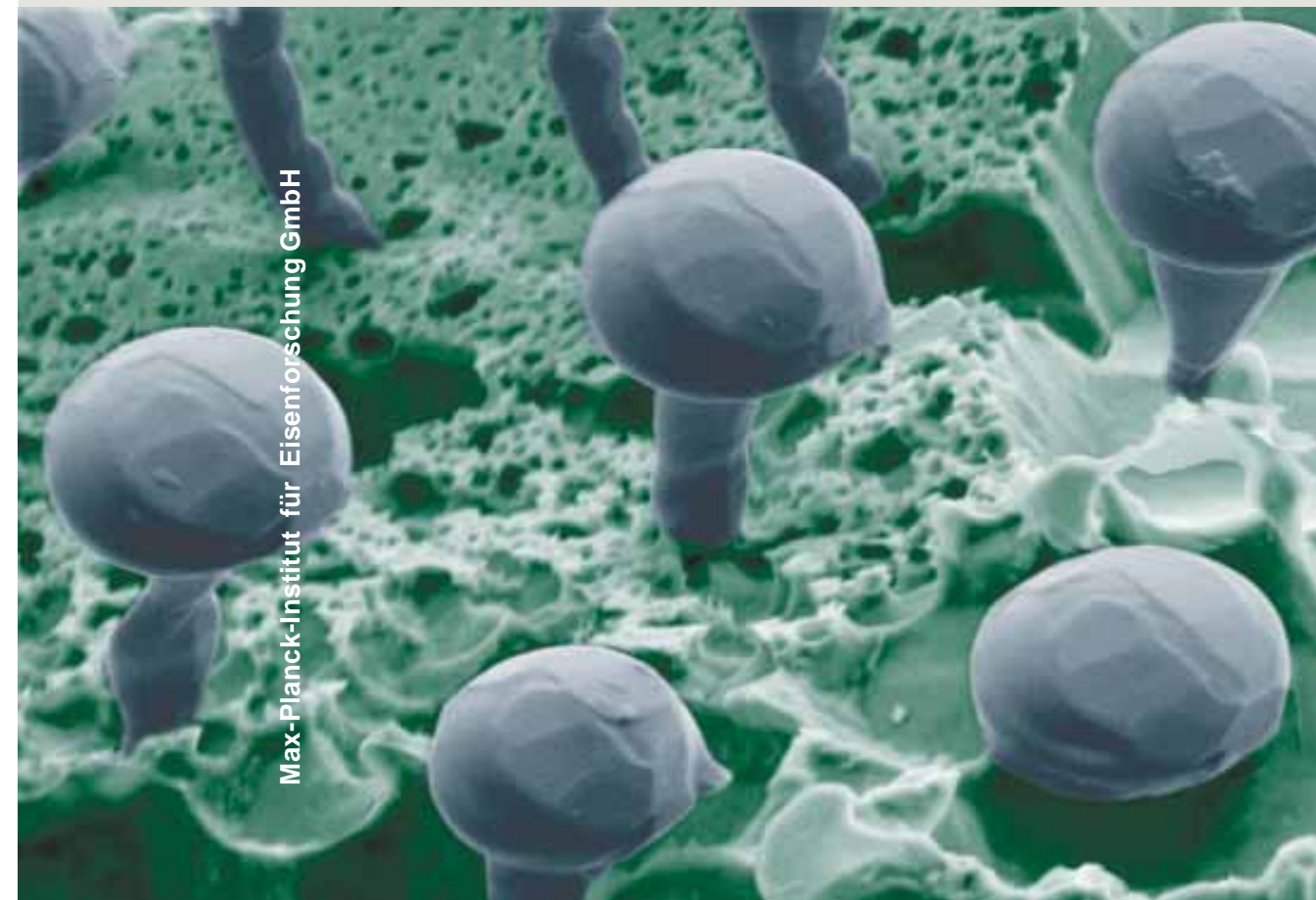
Scientific Report 2003 / 2004

Scientific Report 2003 / 2004

Max-Planck-Institut
für Eisenforschung GmbH



MAX-PLANCK-GESELLSCHAFT



Max-Planck-Institut für Eisenforschung GmbH

Scientific Report 2003/2004

December 2004

Max-Planck-Institut für Eisenforschung GmbH
Max-Planck-Str. 1 · 40237 Düsseldorf
Germany

Front cover

Image of a nanostructured array of rhenium „nanollipops“ recorded with a field emission scanning electron microscope. A pseudo binary NiAl – 1.5 at.% Re eutectic was directionally solidified in a Bridgman furnace using a temperature gradient of $\sim 40 \text{ K cm}^{-1}$ and a growth rate of 30 mm h^{-1} . The structure shown was obtained in an etch pit that formed during anisotropic selective dissolution of the NiAl matrix. Every single rhenium nanowire (diameter $\sim 450 \text{ nm}$) bears a prominent rhenium head (diameter $\sim 4 \mu\text{m}$). The chemical composition was confirmed by energy dispersive X-ray analysis to be pure rhenium. It is clearly visible that each of these „nanollipops“ has identical morphological features – indicating that each is a clone of the others on the same plain. All single crystalline „nanollipops“ have the same azimuthal orientation since the crystal morphology and direction are identical. For details, see also the Selected Scientific Topic on pages 119-122.

Imprint

Published by

Max-Planck-Institut für Eisenforschung GmbH
Max-Planck-Str. 1, 40237 Düsseldorf, Germany
Phone: +49-211-6792-0
Fax: +49-211-6792-440
E-mail: mpi@mpie.de
Homepage: <http://www.mpie.de>

Editors

Frank Stein
Ulrich Gahn

Graphics

Petra Siegmund

Layout and Typesetting

Frank Stein

Printed by

Lausitzer Druck- und Verlagshaus GmbH,
Bautzen, Germany

© December 2004 by Max-Planck-Institut für
Eisenforschung GmbH, Düsseldorf
All rights reserved.

PREFACE

During the last two years a lot of new research activities have been started in our institute as is demonstrated in the following report. Besides, the institute has continued its efforts to reorganize its departmental structure and to renovate its laboratories and buildings.

After the retirement of Prof. Peter Neumann, head of the Department of Physical Metallurgy, in 2004 the institute has experienced a major shift in its departmental structure. The former more experimentally oriented Department of Physical Metallurgy will now focus on theoretical calculations concerning phase equilibria, phase transformations and the prediction of materials properties using among others ab-initio computer calculations. Prof. Jörg Neugebauer has been appointed as head of this new Department of Computational Materials Design and as a Director at the Institute. The remaining departments deal with issues of forming and the mathematical modelling of microstructures (Prof. Dierk Raabe), the stability of surfaces and interfaces and the development of functional coatings for structural materials (Prof. Martin Stratmann) and with lightweight materials and novel steels (Prof. Georg Frommeyer). As head of the fifth department, the former Department of Metallurgy, a new director still has to be appointed.

Besides the new departmental structure, a number of new research groups have been established which will be presented in detail in Part I of this report. Among them is a Leibniz group which was set up by Prof. Raabe after he had obtained the Gottfried Wilhelm Leibniz award for the year 2004, a Christian Doppler Laboratory funded by the Christian Doppler Society in Austria, and the International Max Planck Research School on Surface and Interface Engineering of Advanced Materials. This confirms the increasing attractiveness of the institute for young scientists who join the institute from all over the world. The newly established research school – a collaborative effort of this institute, the MPI für Kohlenforschung and the Ruhr Universität Bochum – is financed by the Max Planck Society, the State of North Rhine-Westphalia and industrial grants and started its programme in 2004. Already now this school is quite essential for attracting young PhD students to work at the institute.

The major renovation work of the institute has been continued over the last two years. During this period of time cutting edge laboratories have been established in a second large renovation step which includes the departments of Prof. Raabe and Prof. Frommeyer described in more detail in Part I of this report. The renovation activities are scheduled to be finished in 2006.

This report consists of three parts: Part I deals with the organization of the institute including the new research groups, the progress in the institute renovation and the new scientific laboratories. Part II covers the research activities of the institute and Part III summarizes the statistically relevant information of the institute.



Martin Stratmann

CONTENT

| | | |
|------------------|--|------------|
| PART I. | THE INSTITUTE | 7 |
| | Management of the Institute | 9 |
| | Scientific Organization | 10 |
| | New Research Groups | 12 |
| | International Max Planck Research School <i>surmat</i> | 19 |
| | Central Facilities | 21 |
| | Institute Renovation in Progress and Newly Established Scientific Laboratories | 33 |
| | | |
| PART II. | RESEARCH ACTIVITIES | 45 |
| | Inter-Departmental Research Activities | 47 |
| | Research Activities within the Departments | 57 |
| | Selected Scientific Topics | 99 |
| | | |
| PART III. | GENERAL INFORMATION AND STATISTICS | 173 |
| | Boards, Scientific Members, Heads of Departments, and Scientists at the Institute | 175 |
| | Scientific Honours | 179 |
| | Participation in Research Programmes | 180 |
| | Collaborations with Research Institutes and Industrial Partners | 183 |
| | Patents and Licenses | 188 |
| | Conferences, Symposia, and Meetings Organized by the Institute | 189 |
| | Institute Colloquia and Invited Seminar Lectures | 191 |
| | Lectures and Teaching at University | 195 |
| | Oral and Poster Presentations | 196 |
| | Publications | 208 |
| | Doctoral and Diploma Theses | 219 |
| | Budget of the Institute | 221 |
| | Personnel Structure | 222 |
| | The Institute in Public | 224 |

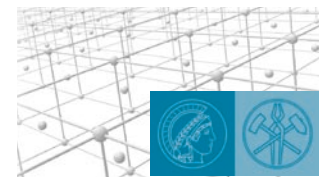


PART I.

THE INSTITUTE

| | |
|---|-----------|
| Management of the Institute | 9 |
| Scientific Organization | 10 |
| New Research Groups | 12 |
| Leibniz Group on Biological Chitin-Based Nano-Composites | 12 |
| Christian Doppler Laboratory for Polymer / Metal Interfaces | 15 |
| Atomistic Modelling in Interface Science | 17 |
| International Max Planck Research School for Surface and Interface Engineering in Advanced Materials | 19 |
| Central Facilities | 21 |
| Materials Preparation | 21 |
| Electron Microscopy | 23 |
| Electron Probe Microanalysis | 24 |
| Metallography | 25 |
| Chemical Analysis | 26 |
| Computer Centre | 27 |
| Electronics Workshop | 29 |
| Technical Services | 30 |
| Library | 31 |
| Administration | 32 |
| Institute Renovation in Progress and Newly Established Scientific Laboratories | 33 |
| Institute Renovation in Progress | 33 |
| New Scientific Laboratories | 34 |

Vakaat



Management of the Institute

The Max-Planck-Institut für Eisenforschung (MPIE) is a joint venture between the Max Planck Society and the Steel Institute (VDEh). Since half of the institute's budget is supplied indirectly through industry, this institute is unique within the Max Planck Society.

The institute was founded in 1917 by the Verein Deutscher Eisenhüttenleute (VDEh) and incorporated into the Kaiser Wilhelm Gesellschaft, the predecessor of the Max Planck Society. The institute was first located in Aachen and was associated with the Technical University of Aachen. The institute later moved in 1934/35 to its present location on a site donated by the city of Düsseldorf.

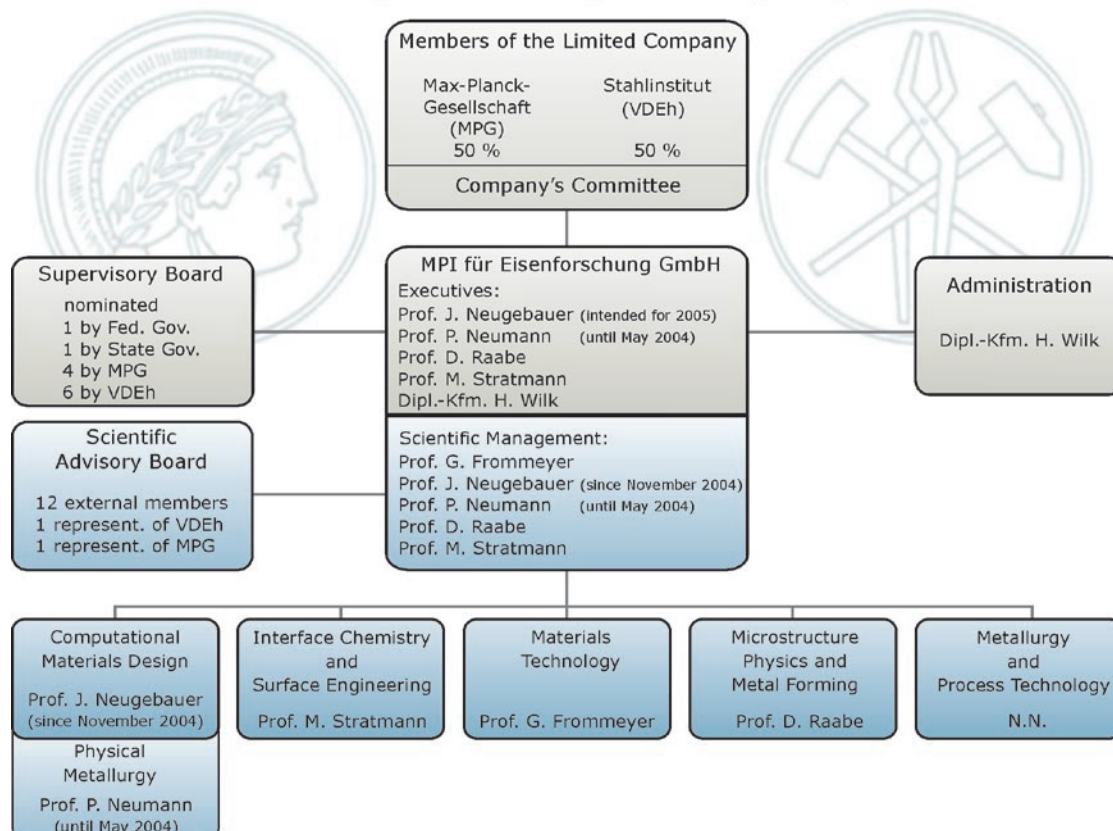
In 1946, the institute's heavily damaged buildings were reconstructed, work resumed and the institute was incorporated into the Max Planck Society. The institute rapidly expanded and new laboratory buildings were erected in the early 1960s. Following the appointment of H.J. Engell as director in 1971, a complete reorganization of the institute was carried out. Up to 2002, the institute was headed by a chief executive director (1971-1990: Prof. Engell, 1990-2002: Prof. Neumann) and an associated administrative director.

Since 2002, all scientific members of the institute form an executive board of directors. The position of a managing director will be filled, in rotation, by one of the board members. A board, which supervises the institution's activities, consists of representatives from the federal government, the state of North Rhine-Westphalia, the Max Planck Society and the Steel Institute (VDEh). A Scientific Advisory Board comprised of prominent scientists assists the institute in finding the right balance between fundamental research and technological relevance.

From 1971 until the present, the institute has operated on the legal basis of a limited liability company (GmbH) and its budget is equally covered by the Steel Institute (VDEh) and the Max Planck Society. Nearly 100 employees on permanent positions including scientists, technicians and administrative staff are working at the institute, and an additional 80 scientists are financially supported through third party funds and scholarships.

Since 2000, the institute is again under reconstruction which will result in nearly 7500 m² of new laboratories and offices. The second phase of the building project now is finished and new laboratories were opened in 2004. The renovations are expected to be completed in 2006.

Max-Planck-Institut für Eisenforschung GmbH
Management and Organization (2004)





Scientific Organization

The institute devotes its research to iron, steel and related materials. In addition to the development of new materials, the institute focuses on the physical and chemical processes and reactions which are of importance for material production, processing, materials characterisation and properties.

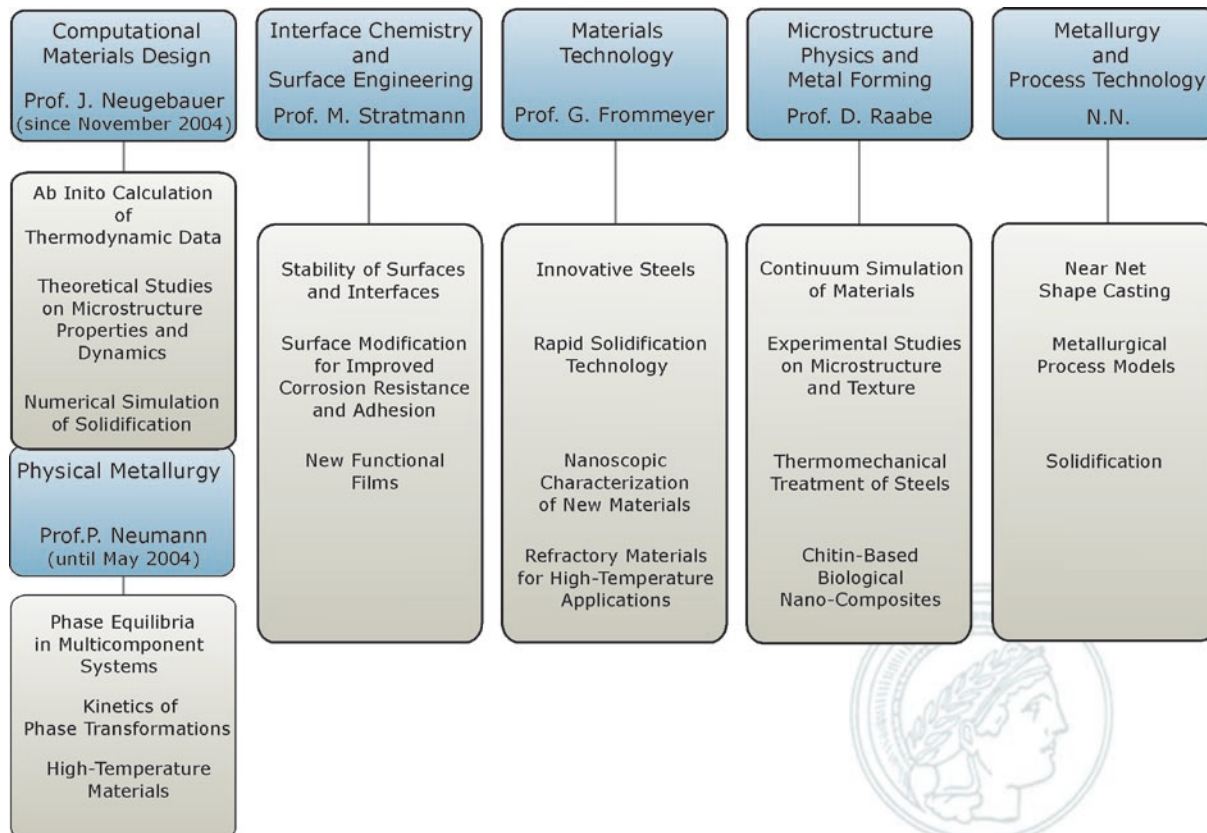
The institute is organized into five departments. In November 2004, one of these departments was closed due to the retirement of its director, and a new department has been established:

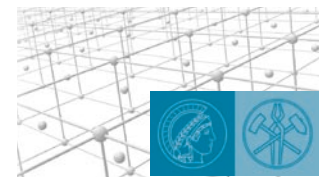
- *Physical Metallurgy* (Prof. P. Neumann, until May 2004; Dr. G. Sauthoff, provisionally until Nov. 2004): phase equilibria, phase transformations in multi-component systems and high-temperature materials
- *Computational Materials Design* (Prof. J. Neugebauer, since Nov. 2004): development and application of multiscale simulation techniques to describe materials properties and design

Within three of the five departments the work has been continued under the direction of their heads throughout the last two years:

- *Interface Chemistry and Surface Engineering* (Prof. M. Stratmann): aspects of environmentally accelerated degradation of surfaces and interfaces like corrosion and deadhesion and the engineering of new and stable surfaces and interfaces
- *Materials Technology* (Prof. G. Frommeyer): novel lightweight steels, new intermetallic materials and rapid solidification processes
- *Microstructure Physics and Metal Forming* (Prof. D. Raabe): mathematical modelling of microstructures and properties during processing and their experimental investigation using microscopy and diffraction methods

Scientific Scopes of the Departments





For the fifth department, which only has a provisional head at the moment, a new director still has to be appointed:

- *Metallurgy and Process Technology* (N.N., Dr. Büchner provisionally): modelling of metallurgical processes and near net shape casting

- New steels
- Iron aluminium based materials
- Carburisation and metal dusting
- Surface mechanics and adhesion
- Microstructure and reactivity
- Numerical modelling

The main scopes of the departments are summarized in the figure on the left side.

Each department is broken down into research groups which are typically managed by group heads. The figure below shows the organization of the groups within the departments. Included are the newly established Leibniz group and the Christian Doppler laboratory which are described in detail on the following pages.

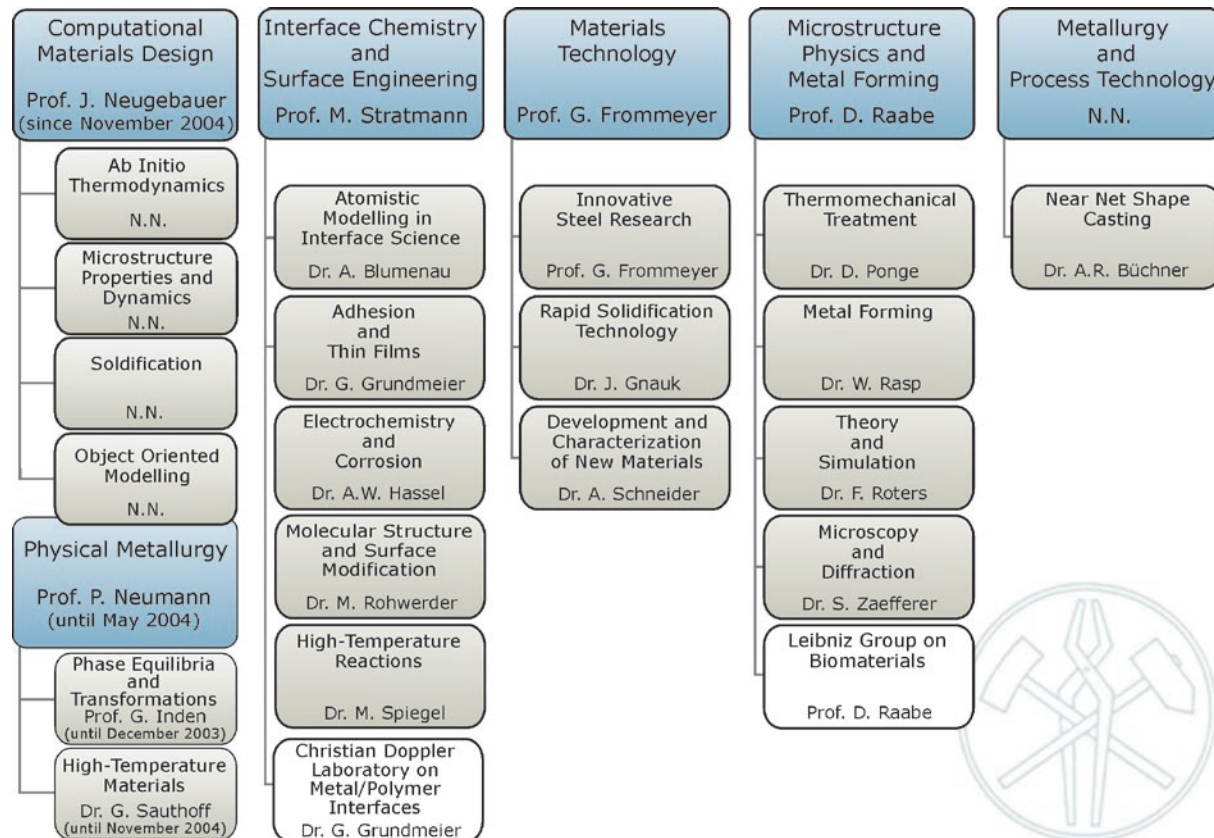
Each research group has its own specific focus and research activities. Part II of this status report summarizes the scientific concepts of the departments and provides several short papers on selected scientific topics giving an overview of the results obtained during the last two years.

In addition to departmental research, certain research activities are of common interest within the institute. These research areas are highly interdisciplinary and combine the experimental and theoretical expertise available from within the different departments in order to achieve a scientific and technological breakthrough in highly competitive areas of research. Such inter-departmental research activities are also described in Part II and include:

The research within the institute is therefore organized vertically in highly specialized departments and research groups and horizontally in inter-departmental research activities. We believe that this form of organization encourages a high level of individual scientific work within the departmental framework of research groups as well as the development of new materials with complex properties combining e.g. high mechanical strength with high surface functionality. In a typical university setting, research activities such as metallurgy or surface science are carried out in different university departments. In contrast, these research activities are linked through the institute's research structure leading to a more efficient use of the scientific equipment and a homogeneous research profile.

Service groups provide the scientific departments with valuable experimental expertise. These services include the production of materials, chemical analysis of metallic substrates, electron microscopy, metallography, a workshop equipped for the handling of unusually hard and brittle materials, facilities to build scientific equipment, a library and a computer centre.

Organization of the Scientific Groups within the Departments





New Research Groups

Leibniz Group on Biological Chitin-Based Nano-Composites

D. Raabe, P. Romano, C. Sachs, A. Al-Sawalmih

The materials encountered in the exoskeleton of most arthropods are biological chitin-protein-based mineralized nano-composites which are characterized by highly directional mechanical and functional properties and an intricate microstructure. These materials, which have evolved in part over a period as long as 600 million years, are typically

very lightweight with a specific weight similar to that of water and at the same time very strong exceeding in part the compression strength of some aluminium alloys (Fig. 1). They mostly consist of highly textured biological polymer tissues (Fig. 2) in which various amounts of nanosized ceramic particles are embedded (Fig. 3).

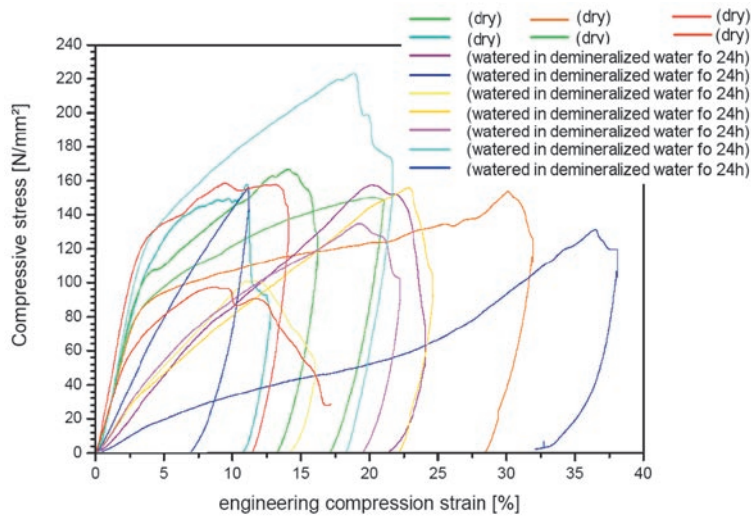


Fig. 1: Stress-strain curves for cylindrical lobster compression samples in different states.

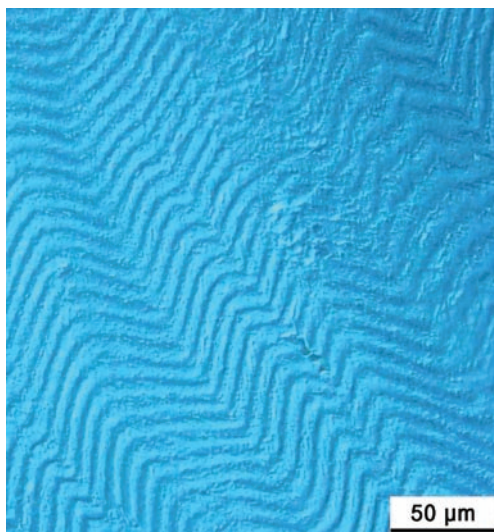


Fig. 2: Polarized optical microscopy showing the woven chitin-protein matrix which is characteristic of the arthropod cuticula. Local changes in the mechanics of the exoskeleton of the lobster are realized by embedding different numbers of ceramic nano-particles into the chitin-protein matrix and by changing the wavelength and stiffness of the woven matrix.

The fact that the various ingredients are arranged with pronounced structural, topological, and crystallographic directionality (Fig. 4) relative to the mechanical loads they encounter suggests the notion of *smart anisotropy* as a main feature of these materials. This term is introduced in order to describe the intimate connection between matter and construction which is a typical principle of natural creations but a rare feature of man-made engineering structures.

This report gives a concise introduction to the newly established Leibniz group on biological chitin-based nano-composites which is kindly funded by the DFG under the framework of the Gottfried

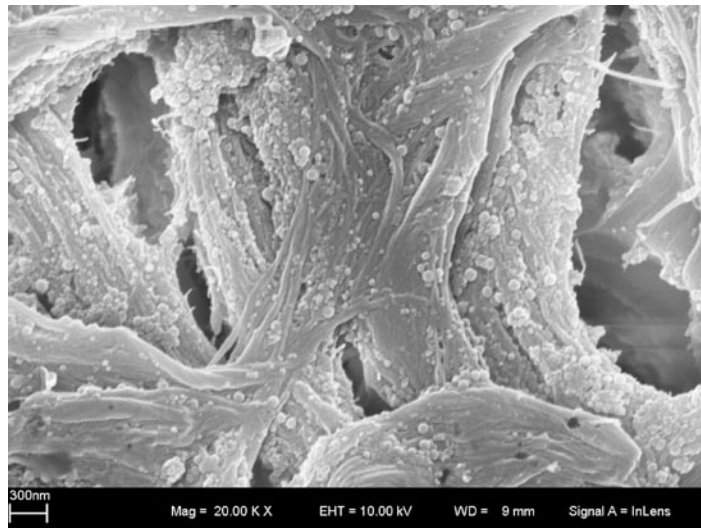


Fig. 3: The lobster cuticle consists of highly textured biological polymer tissues in which various amounts of nanosized ceramic particles are embedded. The microstructure is very porous.

Wilhelm Leibniz award. The aim of the work in this group is to understand and – if possible – to mimic the relationship between the microstructure and

the properties of these exciting composites from a materials science point of view. For this purpose we organise the work in the form of five initiatives:

| Initiative | Main research task within the Leibniz group |
|---|--|
| Structure analysis | Structure, phase, and texture analysis by lab-scale X-ray and wide angle X-ray synchrotron experiments |
| Microstructure analysis | Optical and electron microscopy of the microstructure of deformed and undeformed specimens |
| Electrical properties | Measurement of the directional electrical properties |
| Mechanical properties | Measurement of the mechanical properties by compression, tensile, and hardness testing |
| Modelling of the mechanical behaviour (starts Febr. 2005) | Constitutive modelling and finite element analysis of the stress-strain response of honeycomb-type chitin-based composites |

We currently conduct experiments on one particular material, namely, on the graded and directional properties of the crustacean shell of lobster (*homarus americanus*). It is an excellent example of a bio-nano-composite with variable properties

and substantial structural and mechanical anisotropy which manifests itself both, at the microscopic and at the macroscopic scale. The cuticle of the *homarus americanus* is a multilayer chitin-protein-based biological composite containing variable

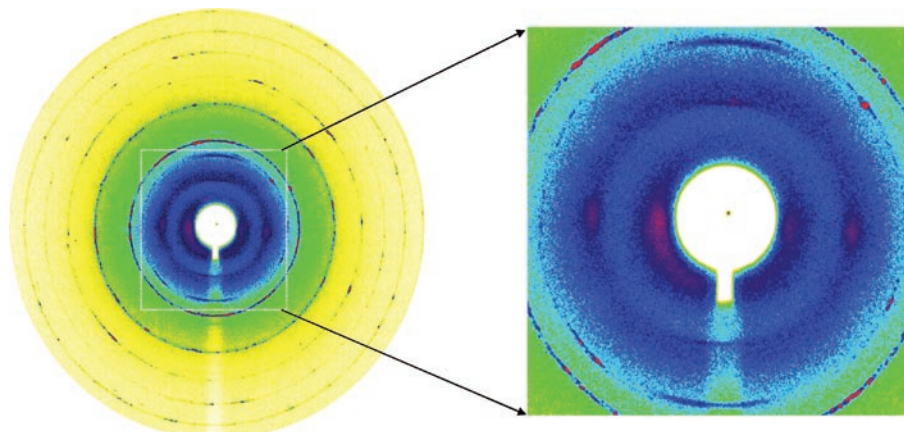


Fig. 4: Wide angle X-ray synchrotron experiments on the lobster cuticle conducted by the group of Brokmeier at DESY show pronounced crystallographic textures both of the chitin matrix as well as of the mineral phase.

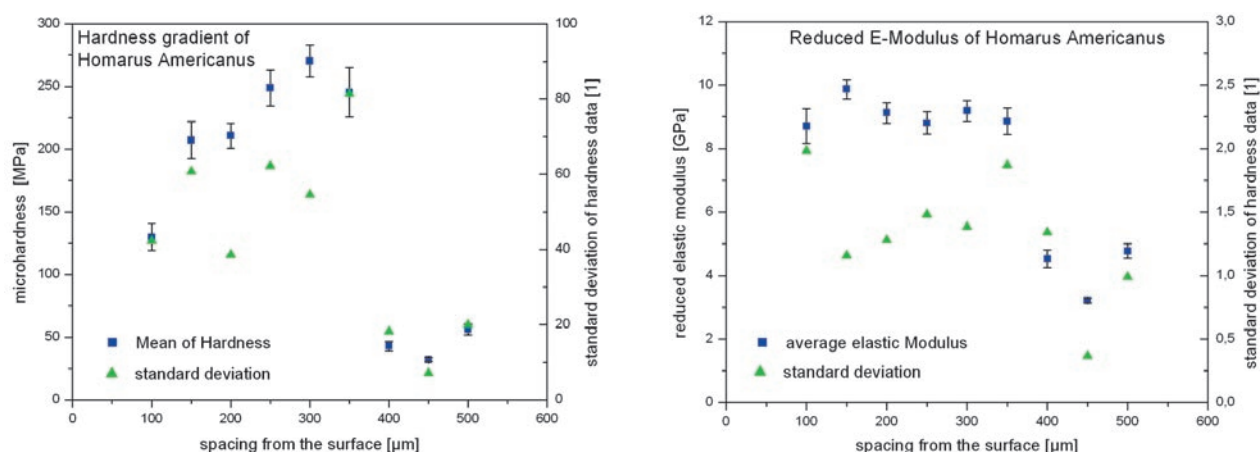


Fig. 5: Pronounced mechanical gradients exist through the thickness of the exoskeleton of lobster. It is, therefore, an excellent model of a naturally graded material which might serve as an example to related engineering applications.

amounts of nanoscopic biominerals (mainly calcite). Basically, the cuticle consists of three layers, namely, the epicuticle, the exocuticle, and the endocuticle. The epicuticle is an outer thin waxy layer providing a permeability barrier to water and gas. The exocuticle and endocuticle layers below are made up of chitin fibers arranged in lamellas of different thickness (Figs. 2,3). Local variations in composition and structure of the material provide a wide range of the local mechanical properties within the flat skeleton plane as well as through the thickness of the cuticle (cross-section, Fig. 5). For instance, small changes in the local biomineralisation content, can lead either to a rigid material serving as a highly protective exoskeleton or it can render the material highly flexible serving as a constructional element as in articular membranes at joints.

The aim of the group now consists in the correlation between the microscopic structure and composition

of the lobster cuticle on the one hand (Figs. 2-4) and the resulting local mechanical properties on the other (Figs. 1,5). The mechanical experiments are conducted using micro-tensile tests (Fig. 6), micro-compression tests, micro-indentation, and nano-indentation. For the structure and microstructure characterization experiments we use light optical transmission microscopy, laboratory-scale x-ray diffraction in conjunction with an area detector, synchrotron radiation (DESY), high resolution scanning electron microscopy, and transmission electron microscopy. In order to identify all the different components in the material, some of them were gradually removed by tailored chemical etching. Particular attention is placed on the effect of the local grade of biomineralisation via embedded calcium salts and the resulting mechanical properties of the cuticle.

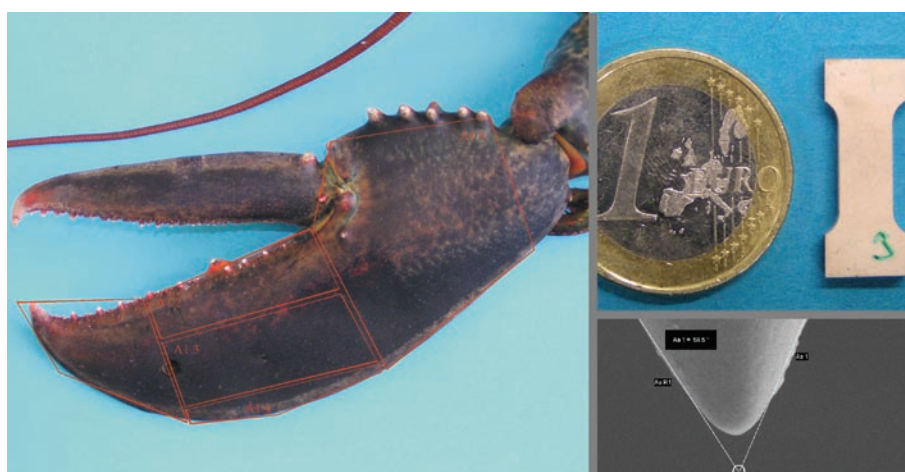


Fig. 6: Mechanical testing on the lobster cuticula requires the design of small scale specimens.



Christian Doppler Laboratory for Polymer / Metal Interfaces

G. Grundmeier, N. Fink, V. Popova, B. Wilson, R. Vlasak

The Christian Doppler Laboratory for Polymer/Metal Interfaces funded by the Christian Doppler Society in Austria was established at the MPI for Iron Research in April 2003. Dr. Guido Grundmeier is leading this laboratory, which cooperates with voestalpine Stahl Linz and Henkel Austria as industrial partners. Currently, four scientific co-workers are working in the frame of two research modules.

It is the primary goal of the research work in the Christian Doppler Laboratory for Polymer/Metal Interfaces to understand fundamental mechanisms of adhesion and de-adhesion at modified polymer/metal interfaces. This fundamental understanding is used to design new advanced polymer/metal interfaces with increased long-term stability in corrosive environments. Within the CD laboratory, work is currently being undertaken to advance the knowledge of adhesion and delamination processes occurring at polymer/metal interfaces. In addition, a fundamental understanding of the function of new environmental friendly thin conversion layers and their influence on the stability of interfaces is underway as in the near future these new layers will widely replace the established methods of metal pre-treatment.

Methods of electrochemical, spectroscopic and microscopic analysis are further developed to enable the characterisation of processes like film formation

on heterogeneous metal surfaces or degradation of interfaces. Scanning Kelvin Probe (SKP - detection of potential changes due to corrosion processes), Infrared Reflection Absorption Spectroscopy (IRRAS - detection of changes in surface chemistry) and Surface-Enhanced Infrared Absorption (SEIRA - analysis of water at the polymer/metal interface) are adapted to the tailored materials. These techniques allow the analysis of ultra thin layers and buried interfaces even under corrosive conditions. Complementary investigations of micro mechanics and adhesion of thin films are based on the application of scanning force microscopy (AFM).

Research module 1: Analysis of ultra-thin layer formation on metals in aqueous solution

The need for environmental friendly alternatives to chromate containing conversion layers has been subject to intense research over the last 15 years. The chemistry of these alternative systems is far from being completely understood, so it is the focus of this module to utilise a combinatorial approach to promote a better understanding of the chemical processes and kinetics that occur during the formation of advanced thin amorphous conversion layers on galvanized steel surfaces. The use of SEIRA-Attenuated Total Reflection (SEIRA-ATR) allows the uptake of water at the interface of thin films and the underlying substrate to be determined, thus enabling a swift

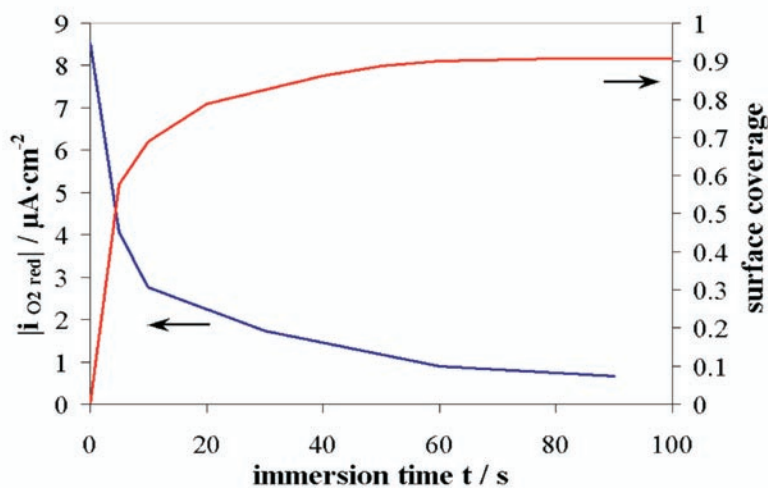


Fig. 1: Comparison of surface coverage of the conversion layer as determined by cyclic voltammetry and the corresponding decrease in the oxygen reduction current density as measured in the transfer controlled potential region on a modified hot dip galvanized surface.

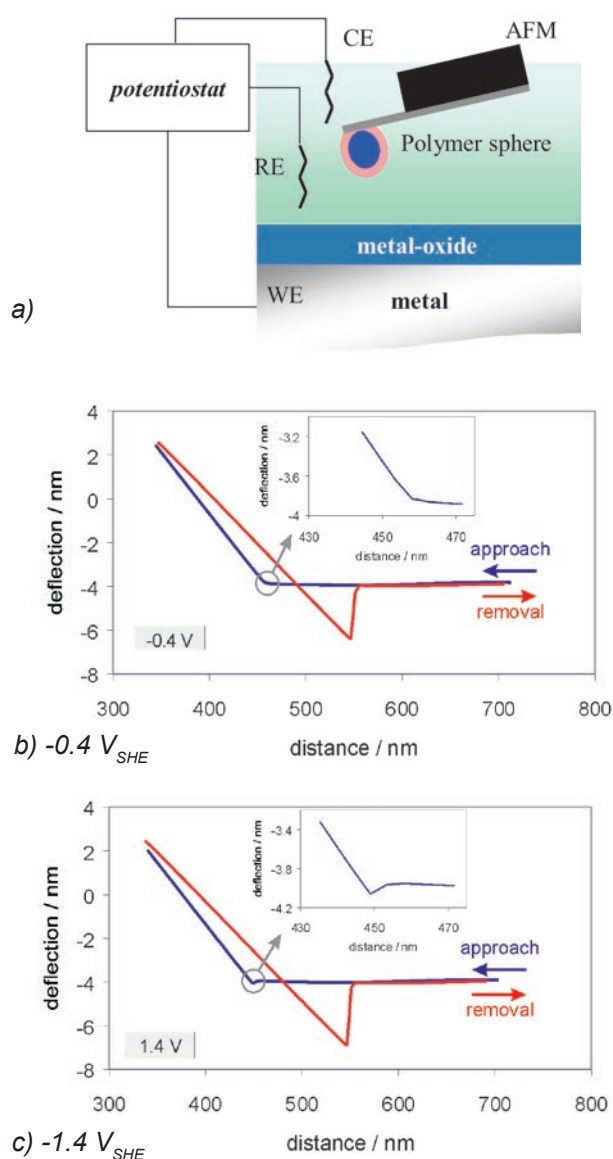


Fig. 2: Schematic of the experimental set-up for Force-Distance analysis under potential control (a). Force-Distance curves on HOPG in 1mM KCl and KOH (pH 10.9) at two different potentials (b,c).

analysis of the corrosion kinetics. In addition, the utilisation of Infrared Reflection Absorption Spectroscopy in conjunction with localised electrochemical analyses and Electron Backscattered Diffraction (EBSD) measurements provide pertinent information about the film formation kinetics depending on the grain orientation of the metal on a fundamental level.

Research module 2: Nanoscopic measurements of polymer/metal adhesion under control of the electrode potential

A high resolution AFM has been optimised to investigate the initial states of the conversion film formation on a nanoscopic scale depending on the grain orientation of the polycrystalline Zn-coating (see EBSD measurements in module I). By means of the AFM, force distance curve measurements are performed under control of the electrode potential to study the mechanisms of polymer/metal de-adhesion in corrosive environments (see Fig. 2 for details of the experimental set-up and force distance curves under potential control). A defined potential was applied to the sample (working electrode). Ag/AgCl microelectrode was used as reference electrode. At $-0.4 V_{SHE}$ and pH 10.9 the tip (Si) encountered a repulsive force that decayed exponentially with a decay length similar to the Debye-length. In contrast, at $+1.4 V_{SHE}$ an attractive force was observed in agreement with Döppenschmidt and Butt (A. Döppenschmidt, H.-J. Butt, *Colloids and Surfaces* 149 (1999) 145).

The formation of microscopic defects of thin films on metals is studied by forming experiments. Scanning Electron Microscopy microscopic analysis of the films is combined with EBSD to observe changes in the surface structure and de-adhesion phenomena as a function of the grain orientation of the metal.



Atomistic Modelling in Interface Science

A.T. Blumenau

This new research group, established in September 2004, is integrated into the Department of Interface Chemistry and Surface Engineering. It will mainly focus on ab initio and density functional theory (DFT) based atomistic modelling of interface structures and phenomena. In contrast to mesoscopic parameter models, which are based on empirical parameters and often are only able to reproduce existing knowledge, first principle-based atomistic methods allow a predictive modelling, which can help to interpret and understand experiments on an atomistic or molecular level and additionally guide and inspire new experiments.

Initially research will focus on the semiconducting properties of thin oxide films, their interaction with organic molecules, and on the chemical and electronic structure of metal/oxide/polymer interfaces. After testing the limitations of various ab initio and DFT based approaches for the problems mentioned above, the modelling of adhesion and de-adhesion processes is planned. As for the latter often electrochemical corrosion plays a crucial role, it is envisaged to couple the field of electrochemistry with atomistic modelling to address the respective corrosion phenomena.

To achieve a better understanding of these interface related phenomena on the molecular and atomistic scale in more detail than possible by sophisticated experiments only, experiment and theory have to be combined in a process of mutual validation and guidance. Therefore a close interaction with the department's experimental groups will be established, in order to design new experiments on well defined model systems and structures, which are feasible for the computational modelling. This will in particular be supported by the preparation of well defined substrate surfaces in the UHV system of the department.

Methodology

For most investigations the primary methods will be based on density functional theory, where the highly complex many-electron-wave function is replaced by an overall spatial electron density, which is much easier to handle computationally. DFT based methods have proven to be very successful in a variety of fields, such as semiconductor defect science, the modelling of surfaces and reconstruc-

tions, nanostructures, bio-chemistry – to name just a few. In terms of phenomena, DFT based methods can predict and describe low energy structures, binding energies, elastic properties, vibrational and electronic spectra, diffusion paths and many more.

With the practical implementations of DFT including many approximations, they will probably fail for some specific bonding configurations and reaction paths. Whenever this is the case, the application of less approximate but computationally more demanding methods becomes inevitable. Furthermore, to span over larger length and time scales at acceptable computational costs, the multiscale combination of methods becomes crucial, where only the reactive core of a system is modelled using the computationally most demanding method, whereas the surrounding spatial regions are treated less accurately. Here the group will test different parameter transfer and embedded multiscaling approaches with respect to their applicability in interface modelling.

Collaborations

Besides intra-departmental efforts to combine experiment and predictive simulation, the group will also strongly interact with other departments of the institute. E.g. the group will collaborate closely with the department of Prof. J. Neugebauer, sharing computational infrastructure, code modules and participate in joint projects on selected topics. Furthermore, together with the Department of Microstructure Physics and Metal Forming it is planned to test possibilities of parameter transfer from ab initio methods to finite element modelling.

Internationally the group closely collaborates with several theoretical groups dedicated to ab initio and DFT-based modelling of complex materials.

In particular close links exist with groups involved in the development of DFT-based computer codes: These are the developers and users consortium of the AIMPRO density functional code [1] (R. Jones, University of Exeter, P.R. Briddon, University of Newcastle, and M.I. Heggie, University of Sussex, all in the UK), and the group of T. Frauenheim, University of Paderborn, Germany, which develops and maintains the density functional-based tight-binding code DFTB [2], a useful tool whenever model



- NEW RESEARCH GROUPS -

systems are too large or time scales in dynamic simulations become too long to be simulated with pure ab initio or DFT methods. The DFTB method can also include dispersive interaction (weak bonding) through an empirical approach.

Further collaboration exists with S. Öberg, Department of Mathematics, Luleå University of Technology, Sweden, where research focuses on the ab initio description of the interaction of water with mineral surfaces and collector molecules as used in ore flotation processes in the mining industry.

References

1. Jones, R.; Briddon, P.R.: in: Semiconductors and Semimetals, Vol. 51A: Identification of Defects in Semiconductors, ed. M. Stavola, Academic Press, Bristol, Boston, MA (1998), Chap. 6.
2. Frauenheim, T.; Seifert, G.; Elstner, M.; Hajnal, Z.; Jungnickel, G.; Porezag, D.; Suhai, S.; Scholz, R.: Phys. Status Solidi (b) 217 (2000) 41.



International Max Planck Research School for Surface and Interface Engineering in Advanced Materials (imprs surmat)



Introduction. In 1999, the Max Planck Society together with the Association of Universities and Other Education Institutions in Germany launched an initiative to promote junior scientists called the International Max Planck Research Schools. In the winter semester 2000/2001, the first Research Schools were started as cooperative efforts involving Max Planck Institutes together with German and foreign universities and research facilities. These Schools offer outstanding students from Germany and abroad the possibility to prepare for their PhD exam in a structured program providing excellent research conditions.

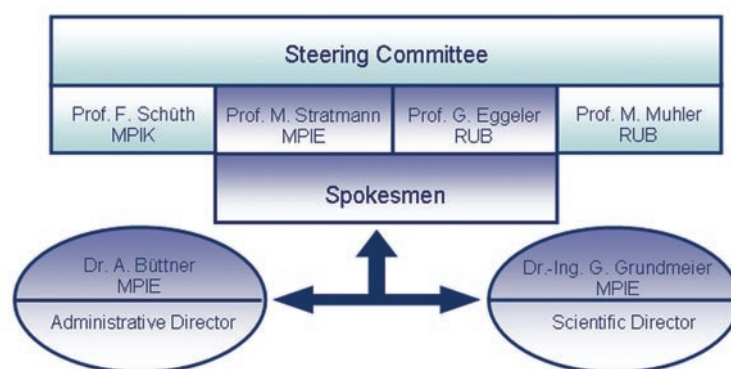
imprs-surmat. One of the youngest Research Schools is the International Max Planck Research School for Surface and Interface Engineering in Advanced Materials. The application for this Research School was considered and allowed by a scientific commission of the Max Planck Society in January 2003. It is a collaborative project involving the Max Planck Institute for Iron Research in Düsseldorf, the Max Planck Institute for Coal Research in Mülheim an der Ruhr, and four engineering and sciences departments of the Ruhr-University in Bochum. The Max Planck Institute for Iron Research takes over the lead management. In addition to the aforementioned German partners Prof. Tian Zhongqun and Prof. Lin Changjian from the State Key Laboratory for Physical Chemistry

of Solid Surfaces, Xiamen University, Prof. Mao Weimin from the Department of Materials, University of Science and Technology, Beijing, and Prof. Zhao Dongyuan from the Department of Chemistry, Fudan University are involved in this Research School.

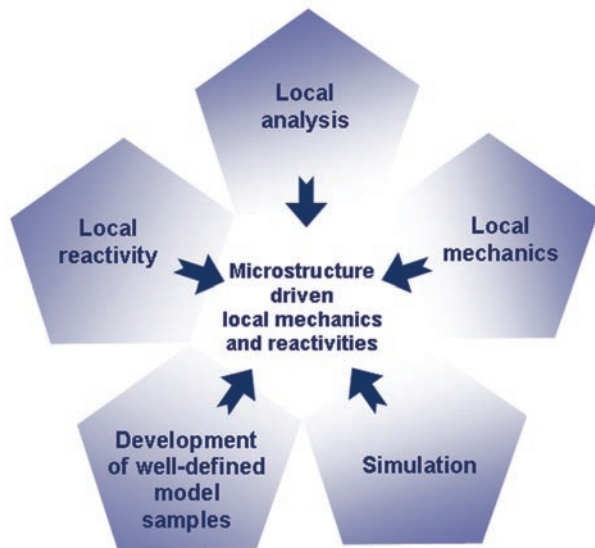
China. The cooperation with the associated partner universities in China includes exchange of students and staff in both directions, a formal agreement that any thesis examination may take place in the home university but part of the research is performed also in the partners university and active participation of the Chinese colleagues in the summer and winter classes.

Scientific focus. The main research objective is to correlate the chemical structure, morphology and mechanical properties of heterogeneous surfaces and buried interfaces with functional properties of the materials and to optimize them by means of advanced surface modification technique. All research projects are assigned to the five subtopics of imprs-surmat.

Status quo. Until now fifteen high-qualified doctoral students have been selected out of a multiplicity of applicants for the participation in imprs-surmat. Most of them already began with their scientific work. The coordination office received hundreds of applications from more than 30 nations, which is a clear indicator for the world wide interest young



Lead management and organisational structure of imprs-surmat.



The imprs-surmat covers topics ranging from fundamental scientific issues to engineering applications.

scientists take in the participating institutions of imprs-surmat respective in the graduate program offered.

Opening ceremony. To emphasize the importance of imprs-surmat a great opening ceremony took place on December, 17th, 2004.

At this opportunity the concept of imprs-surmat has been presented as an instrument for the promotion of young scientists and furthermore as a place of scientific and cultural exchange to the public respective to our invited guests. The doctoral students which have been accepted to imprs-surmat in its first year of existence were officially awarded their scholarships by high-ranking representatives of our financial partners from industry, from the government of North Rhine-Westphalia, the Max Planck Society and the Ruhr University in Bochum.

External sources of scholarships. As a supplement of the scholarships regularly financed by the basic budget of our Research School, two German steel companies financially support the imprs-surmat. The ThyssenKrupp Stahl AG covers the costs of two scholarships, the Salzgitter AG contributes one scholarship, each for the duration of three years.

These activities underline the convincing concept of imprs-surmat. The possibility to get in contact with representatives of the German industry especially attracts high qualified foreign graduates.

Outlook. In addition to research, the interdisciplinary education of students is of particular importance for imprs-surmat. The aim is that each student will gain an insight in the concepts and methods of interface analysis and engineering that can be applied in various fields of advanced materials development such as metals, coatings, electronics and medicine.

Therefore imprs-surmat includes intensive teaching in four summer and winter schools and research symposia. The schools focuses on the physical chemistry of surfaces and interfaces, phase transformations induced by the presence of interfaces and the mechanical properties of interface dominated materials, thin films, and nano-scale patterning and processing of thin film covered materials. Topics include corrosion, adhesion, tribology, catalysis, and the physical properties of thin functional layers.

The first summer school will take place in March 2005. It focuses on the basic concepts in materials science and will be coordinated by Prof. G. Eggeler (RUB) and Prof. D. Raabe (MPIE).



Central Facilities

Materials Preparation

A.R. Büchner, J. Gnauk

Research and development of new materials and processes require the capability to produce materials according to particular specifications. The institute has specific facilities for the production and refinement of materials according to the scientific and technological needs of the research groups within the institute.

In the course of the evolution and restructuring of the institute, it seemed to be necessary to reorganise all facilities of melting and specimen preparation. In order to concentrate activities and to assure that facilities and know-how will remain available in the future, a new service group for materials preparation was established. After a certain time of disturbances due to building renovation this group starts now working within the Department of Metallurgy. In the following the most important fields of application and the available facilities are outlined.

Alloy preparation: The three materials related departments of the institute: Metallurgy and Process Technology, Physical Metallurgy and Materials Technology have a variety of sophisticated technical equipments to prepare special alloys as single and polycrystalline samples.

Several induction furnaces are available to produce different quantities of materials. Small amounts (about 350 to 850 g) of special alloys with melting temperatures up to about 1850 °C are routinely prepared by induction melting in ceramic crucibles in vacuum ($2 \cdot 10^{-5}$ mbar) or inert gas to obtain cylindrical ingots with 20 to 40 mm in diameter and up to 200 mm in length. For the production of medium amounts of pure metals and alloys (ingots up to 7 kg), two vacuum induction furnaces with a basic pressure of 10^{-7} mbar are available. Melting of larger amounts of material melts in vacuum or desired atmosphere can be performed in two bigger furnaces, coupled with a facility for pilot test sampling with a maximum capacity of 80 kg and equipped with a 100 kW medium frequency generator. A typical application is the production of iron-based alloys possessing melting temperatures up to 1800 °C.

Some electrical resistance carbon furnaces (Tammann furnaces) with maximum operation temperature of 3000 °C enable to process non-metallic, non-inductive coupling materials under inert gas atmosphere. A high pressure induction furnace with maximum pressures of 100 bar with a capacity

of 10 kg material, operating with a maximum power supply of 50 kW allows to keep melts of earth alkaline, manganese or rare earth metals with higher partial vapour pressure at high temperature in order to prevent volatile vaporisation.

For melting highly reactive materials, two different facilities are available. One is an electric arc furnace with 300 g capacity, equipped with a tilting mould. In addition to this, an induction levitation melting unit is used for the preparation of small amounts (350 g maximum) of polycrystalline high-purity alloys exhibiting high oxygen, nitrogen or hydrogen affinity. Melting temperatures up to about 1900 °C are achieved, and for subsequent solidification cold copper moulds are installed in a vacuum or inert gas chamber.

Specific solidification performances: Single crystals with up to 40 mm in diameter and 130 mm in length of diverse alloys with melting temperatures up to 1700 °C can be prepared in ceramic crucibles in vacuum or inert gas atmosphere using a modified Bridgman technique. The crystal orientation will be determined by laser light reflection at the etched crystal surface. Another Bridgman furnace with similar geometry, operating with temperatures up to 2000 °C, serves for directional solidification purposes. Single crystal growth and high purification of metals using the method of zone refining can be performed by a 75 kW electron beam melting furnace. The molten zone is produced by a circular cathode of tungsten, which is moved vertically along the sample.

In addition to the type of „Bridgman furnaces“, which are specifically designed for controlled slow cooling processes, two units for rapidly solidified materials are also available. These are a melt drop furnace and a splat cooling facility, operating with a modified levitation melting unit.

Near net shape casting: Worldwide and uniquely two thin strip casters for direct strip casting related to Bessemer's process are operating in the Department of Metallurgy. The as-cast materials may be peritectic or other low carbon steels as well as stainless steels and non-ferrous metals. One caster is equipped with a 150 kW induction furnace with a maximum crucible capacity of 200 kg. The produced steel strips possess a thickness of 1 to 4 mm and a strip width of 120 mm. The second caster is a slightly



smaller facility (30 kW furnace, maximum capacity 10 kg, strip width of 65 mm). It has the unique feature of a full housing of the caster and of the strip casting process and therefore it can be carried out in an inert gas atmosphere.

The institute is also equipped with a shape flow casting (SFC) and a planar flow casting (PFC) facility for the fabrication of metallic fibres, wires and ribbons or foils. The PFC meltspinning equipment enables to produce rapidly solidified ribbons with maximum cooling rates of 10^6 K/s and with a variable thickness of about 50 μm to 250 μm and 30 mm in width by ejecting the melt stream onto an actively cooled rotating wheel surface. The SFC facility produces wires of diameters ranging from 1 to 3 mm directly by casting the melt into a guiding groove of a horizontally rotating wheel. The shape flow caster can also be used as in-rotating-liquid-spinning (INROLISP) method, where the melt is injected into a liquid cooling medium (water or other coolants), which produces metal fibres of 80 to 400 μm in diameter. All these products possess the microstructural features and related properties of

rapid solidification, e.g. fine grained microstructure and less (or no) segregation in combination with final or near net shape geometries.

Thermal treatment: In addition to the casting facilities mentioned above, several annealing furnaces to manipulate the microstructure and phase distribution after the casting process are available. For the heat treatment several annealing furnaces in various geometries and dimensions with temperatures up to 1700 °C are present, partially with protective atmosphere or under vacuum.

Mechanical alloying: Powder metallurgical processing like mechanical alloying can be carried out using a planetary ball mill, partially filled with hard and heat resistance steel or cemented carbide balls (5 to 11 mm in diameter) and a capacity of 500 ml in an inert gas atmosphere. Another high energy ball mill (attritor) with a total capacity of 8 litres serves for the production of larger amounts of material. To form billets of metal powder, isostatic pressing with pressures up to 3500 bar can be performed with a cold isostatic press possessing a cylindrical chamber of 400 mm in length and 200 mm in diameter.



Electron Microscopy

S. Zaefferer, A. Schneider

Electron microscopy is one of the most important and universal techniques in the study of microstructures of crystalline materials. In particular, the combination of imaging, diffraction techniques and chemical microanalysis allows a precise and complete characterization of the material on scales ranging from several mm to nm using scanning electron microscopy (SEM) and down to the sub-nm scale using transmission electron microscopy (TEM). The institute provides a number of instruments most of which are particularly well equipped for diffraction techniques and chemical analysis. A particular focus of the EM laboratory lies on orientation microscopy, a technique which, by automatic mapping of crystal orientations and phases, allows to study crystalline microstructures and textures in a detail that cannot be reached by any other technique.

The flagship of the instruments with regard to orientation microscopy is the high-resolution SEM JEOL JSM 6500 F. With this instrument extremely high beam currents at high resolution can be reached due to a special construction of the field emission gun (FEG). This system is therefore dedicated to the high-speed and high-precision measurement of electron backscatter diffraction (EBSD) patterns and EDX spectra. The instrument is equipped with a highly sensitive, high-speed digital CCD camera for EBSD measurements and software programmes for automatic crystal orientation mapping (ACOM - OIM 3 software by TSL) and phase analysis (Delphi software by TSL). The system allows to obtain a lateral resolution of orientation determination of about 30 to 100 nm (depending on the material). A standard of up to 60 orientation measurements per second is obtained during ACOM analysis. Alternatively, high quality images with 1200×1200 pixels can be acquired for crystallographic analysis. The combination of EBSD and EDX allows the investigation of complex materials containing a variety of different phases and microstructures. Since recently the instrument is equipped with a combined compression-tensile and heating stage which allows to perform in-situ observations of deformation and annealing processes with high lateral resolution.

A second high-resolution SEM with FEG (LEO Gemini 1540 VP) is available which permits measurements to be made under variable pressures. This instrument is currently used for ultrahigh resolution imaging, for investigations of non-conductive polymer coatings and for the in-situ observation of oxidation experiments. It is therefore

equipped with a heating stage with a gas-inlet. Also this microscope is equipped with an ACOM system (TSL).

An SEM with a standard tungsten filament gun (JEOL JSM 840A), which is also equipped with ACOM facilities (software Crystal of HKL Technology), is used particularly for large orientation mappings, in the order of several 10 mm^2 , where the sample stage rather than the electron beam is scanned during the measurement. In addition, the instrument can be equipped with a micro-tensile testing machine for in-situ deformation experiments.

The most recent and most advanced achievement in the park of SEM with ACOM facilities is the Zeiss Crossbeam XB1560 FIB which is the combination of a high-resolution SEM and a focussed ion beam (FIB) microscope. While the SEM part is used to observe and analyse the sample, the FIB part serves to cut and structure the sample surface. One particular application will be three-dimensional orientation microscopy by a cut-and-analyse serial section technique. To this end a surface is prepared by FIB and analysed by EBSD. Subsequently the next section is cut and observed again and so on. In this way, resolutions of about 50 nm in depth will be achievable and material volumes of about $50 \times 30 \times 30 \text{ }\mu\text{m}^3$ will be investigable in the future. Besides standard electron detectors, the instrument is furthermore equipped with a transmitted electron detector for the acquisition of scanning transmission electron images from thin foils. These foils are made by cutting with FIB at well defined positions. In this way the Crossbeam instrument is an ideal tool for the preparation of TEM samples from difficult, for example multiphase materials.

For transmission electron microscopy, a Philips CM20 with 200 kV TEM is available. This TEM is a standard analytical instrument for diffraction, tilt experiments and energy dispersive X-ray (EDX) investigations. A unique aspect of this instrument is a software system for on-line, semiautomatic crystallographic analysis. The system is connected to the TEM via a high-resolution, high-dynamics, wide-angle CCD camera and makes it possible to index all kinds of diffraction patterns quickly and directly for the purpose of orientation and phase determination. Furthermore, tilt experiments can be calculated in advance on the computer and then performed with greater ease on the microscope. This allows, for example, a simple quantitative characterisation of dislocations and grain boundaries.

Electron Probe Microanalysis

M. Palm

A CAMECA Camebax SX50 electron microprobe equipped with four wavelength dispersive spectrometers is available at the institute. It is mainly employed for qualitative and quantitative analysis of phases, mapping of element distributions and measurements of concentration gradients.

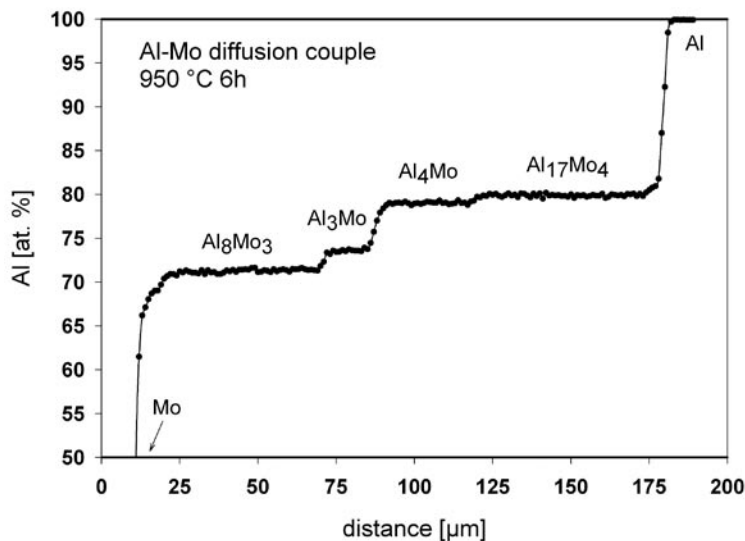
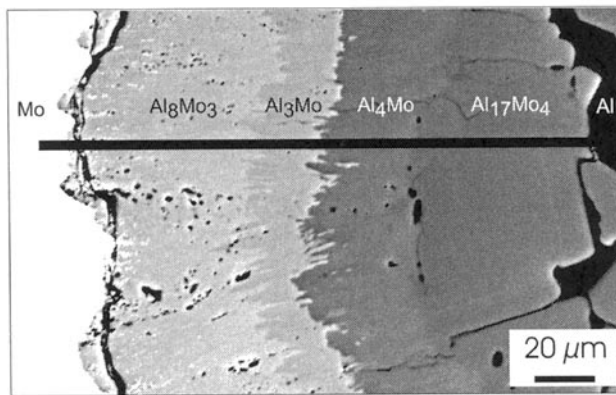
An important example for the latter kind of measurement is the evaluation of diffusion profiles within diffusion couples. The diffusion couple technique is a valuable experimental method in studying phase relations in multicomponent systems. A diffusion couple is a combination of two or more starting materials of differing chemical compositions, which are welded together and then heat treated for a certain time. During annealing a concentration profile develops due to interdiffusion. After quenching the sample down to room temperature the diffusion couple is sectioned along the diffusion path, i.e. perpendicular to the original weld between the different starting materials. The diffusion profile is evaluated by electron probe microanalysis (EPMA)

by scanning the stage in discrete steps along the diffusion path and performing a quantitative chemical analysis at each scanning step. The step size can be varied down to 1 μm .

Among other applications the diffusion couple technique is employed for the determination of phase diagrams. The figure shows an example from the experimental determination of the Al-Mo system [M. Eumann, Phasengleichgewichte und mechanisches Verhalten im ternären Legierungssystem Fe-Al-Mo; Shaker Verlag Aachen (2002) p. 120]. In this case the diffusion couple has been assembled by squeezing an aluminium rod into a cylinder machined out of molybdenum. During annealing at 950 °C the aluminium is molten and reacted with the molybdenum. The back scattered electron image reveals that a sequence of different phases has formed in the diffusion couple. The compositions of the phases are shown in the diffusion profile obtained by EPMA. Steps in the concentration profile indicate the presence of two-phase fields and by extrapolating

the concentration profiles of individual phases onto the phase boundary the compositions of the phases in equilibrium with each other, i.e. the tie-lines between the phases, can be determined. Another example of evaluating a diffusion profile by EPMA is given in the scientific research topic „Theoretical and Experimental Investigations of Structure Type Variations of Laves Phases“ in Part II of this report.

The growing importance of the diffusion couple technique including evaluation of the diffusion profiles by EPMA has been demonstrated in the workshop „The Diffusion Couple Technique“ held on December 6 & 7th, 2004 at the Max Planck Institute for Iron Research.



Back scattered electron image of a sequence of phases formed in a Mo / Al diffusion couple after annealing at 950 °C (top) and respective diffusion profile obtained by EPMA (bottom).



Metallography

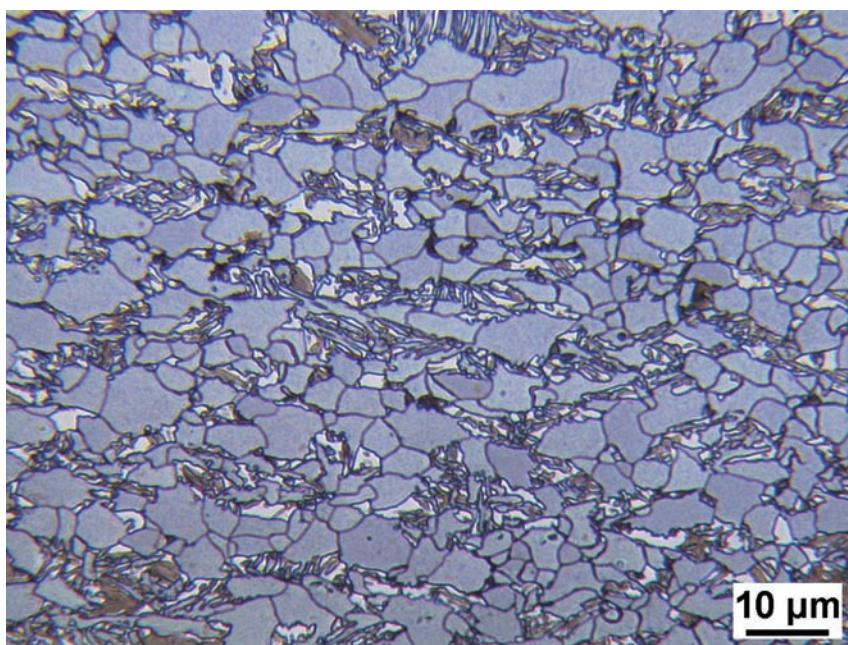
S. Zaefferer

Task of the service group metallography is to perform metallographic work for the different groups of the institute or to instruct and support the members of the groups (for example PhD students and postdocs) with these tasks. Currently the group consists of five experienced metallographic assistants. The services offered by the group include the metallographic preparation of metallic, intermetallic and non-metallic samples for different observation techniques or for further processing and the observation and documentation of samples by optical and scanning electron microscopy.

For preparation, a large variety of different techniques are available. These include cutting with various techniques, sample mounting (hot and cold, conductive or non-conductive resin, resin-free sample mounting), grinding and various polishing techniques with a wide range of different polishing solutions. Also available is electrolytic polishing. After polishing samples may be chemically or electrochemically etched to develop the microstructure for further observation. For these tasks, a variety of different recipes with focus on the preparation of microstructures of steels and intermetallics are available. Finally, specimens can be coated by sputtering of gold, iron, copper or carbon.

For the observation of microstructures by optical microscopy various instruments by Leica (Aristomet), Zeiss (Axiomat) and others are available. A wide variety of observation techniques including bright field, dark field, differential interference contrast, polarized light microscopy and macro photography with perpendicular illumination can be applied. Furthermore, a hot stage microscope for observation at high temperatures and a micro-hardness tester are provided. Photos are either acquired conventionally on photographic film or by high-resolution CCD cameras. Digital images are automatically sorted into an electronic data base and can be analyzed by software for digital quantitative metallography. An example of a photograph is given in Fig. 1 showing the microstructure of martensite developed in an Ni_3Al alloy as observed by polarized light microscopy.

For observations at higher resolutions, a scanning electron microscope Camscan CS4 equipped with an EDX system with a detector with ultra thin window for light element analysis is used. The instrument is run and maintained full time by one of the group members.



Light optical micrograph of a TRIP steel. The colours signify the following structures: blue: ferrite with low carbon content, brown: ferrite with high carbon content and high lattice distortion (often a part of the bainite structure), white: residual austenite or martensite; needle-like structure indicates bainite.

Chemical Analysis

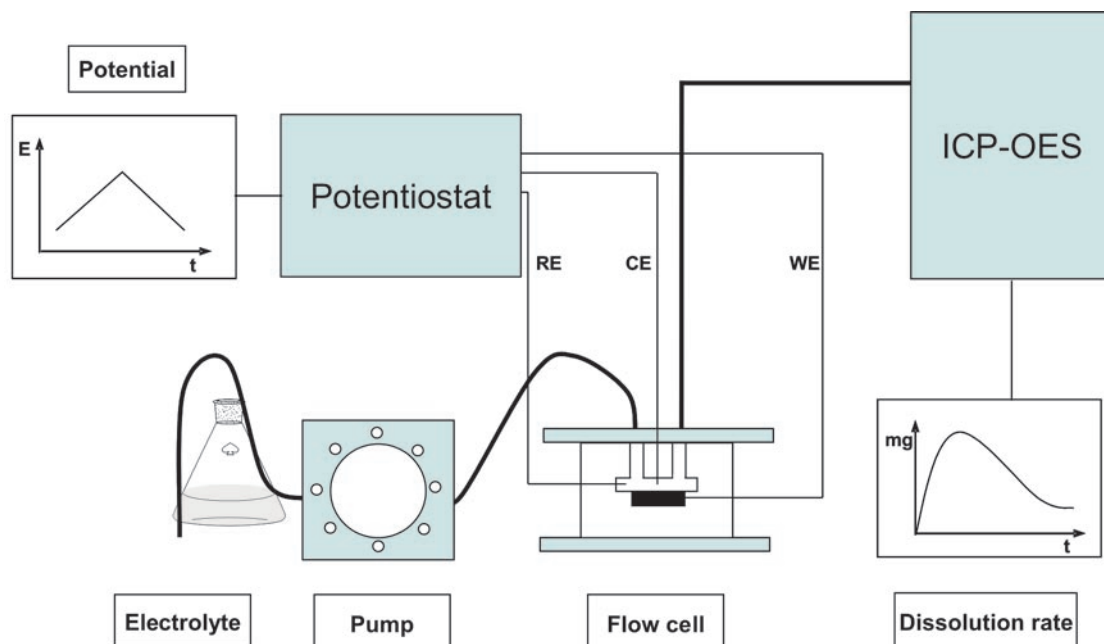
D. Kurz

The knowledge of the chemical composition is an important requirement for the use of materials in chemical experiments. Simultaneous atomic emission spectrometry with inductively coupled plasma and dual view optics (ICP-OES), atomic absorption spectrometry with a flame and hydride technique (FAAS, CVAAS), ion chromatography (IC), thermal conductivity and infrared absorption are the standard methods used by the group for the analysis of nearly 60 elements in different materials and matrices.

Approximately 70 percent of the analyses are measured with the ICP-OES, which has high performance Echelle optics with a wavelength range from 165 nm to 1000 nm and a spectral resolution of 0,005 nm. The dual view optics and the detector, which is a charge injection device (CID), allow the simultaneous measurement of element concentrations in a dynamic range covering 4-5 orders of magnitude and make it possible to simultaneously

analyse low and high contents of elements without having to prepare a new sample. This technique consists of an inductively coupled plasma source which is used to dissociate the sample into its constituent atoms or ions and excite them to a level where they emit light of a characteristic wavelength. A detector measures the intensity of the emitted light and the data processing calculates the concentration of the particular element in the sample.

A thin electrochemical flow cell was designed, which can be directly connected to the ICP-OES in order to measure the composition of the electrolyte downstream from the corroding metallic sample. The experimental setup is shown in the figure below. This permits a qualitative identification of the soluble products and a quantitative measurement of the simultaneous dissolution rates of the sample components over a time interval of less than 1 second.



Schematic of the experimental setup for measuring the composition of an electrolyte downstream from a corroding metallic sample with a special electrochemical cell.



Computer Centre

H. Kemnitz

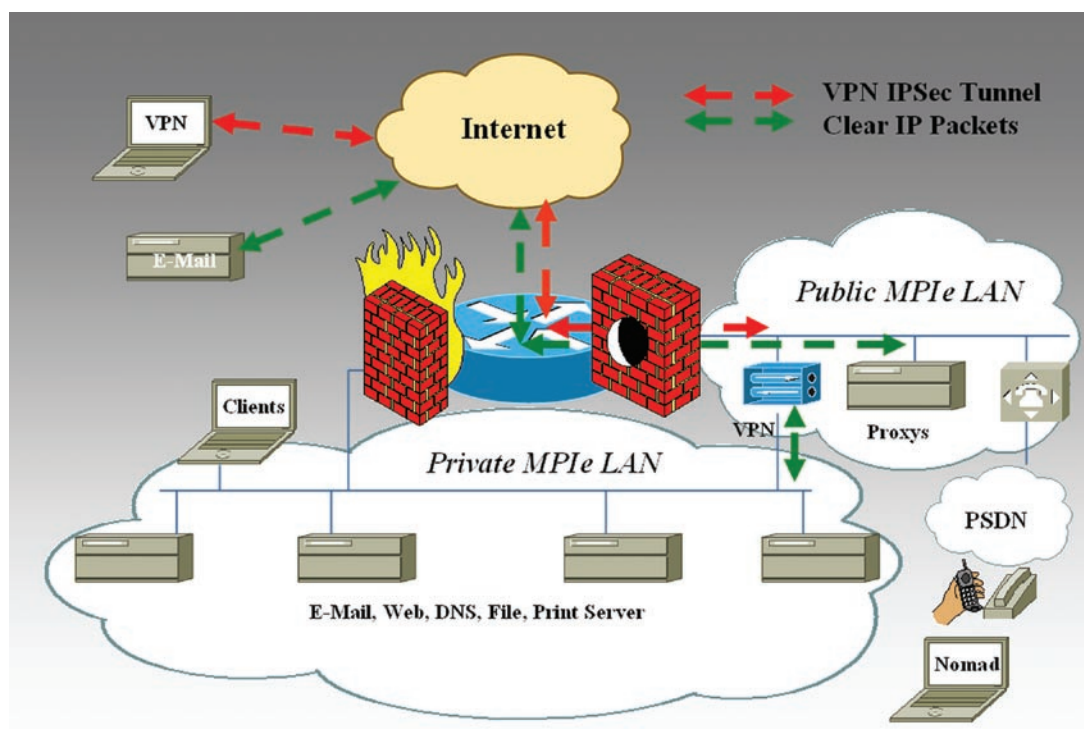
Bridging the gap between scientific research and information interchange, a high performance data network offers the essential telecommunication capabilities. In the year 2000, the computer centre has planned a new generation network for the institute, state of the art and realized to coincide with the structural renovation of the institute, which is still taking place.

The new network infrastructure of the institute consists of a local area network (LAN) with access to wide area networks (WAN) such as the Internet or public switched data or telephone net (PSDN) as shown in the figure below. Sites connected to a WAN are usually targets of electronic sabotage from the outside. To secure the institute's campus network, a design concept was chosen which redirects the flow of data from the WAN through an additional security layer, the so called „Public MPIe LAN“. The advantage of this complex technique is that several application proxies for Name Services, E-Mail, Web, FTP etc. inspect the traffic from the outside to the „Private MPIe LAN“ for malicious contents. Additional

protection is provided by Packet Filters (Firewall), which restrict access to the different LAN's. Hardly screened is the „Private MPIe LAN“, to which all institute computers and services are connected.

The physical network looks like a spider's net, as shown schematically in the figure on the next page. Radial Gbps trunk lines link the edge switches to the core in the centre. The red dotted lines are redundant links, which are enabled in case of trunk loss by a spanning tree mechanism. Twenty edge switches build the „Private MPIe LAN“ with more than 40 Gigabit- and 550 Fast Ethernet-data ports all together in its current state. The inner structure of the network was set up for highest throughput rate with non-blocking and wire speed property. The core switch has a bandwidth of 128 Gbps, the edge switches 17,5 Gbps; some trunk lines are link-aggregated.

Besides setting up and running the data network, the computer centre provides all necessary communication services for end user connectivity. This support was focused on platform-independent



Logical layout of the MPIe network.



- CENTRAL FACILITIES -

accessibility. Among routing, DNS and NAT, the important services are:

INTERNET: high-speed access (34 Mbps) secured by Firewall and Application Proxies

VPN: encrypted access from the Internet to institute network resources

RAS: ISDN and analogue telephone data dial in data service

E-MAIL: gateways check E-Mail from the outside for malicious content;
inhouse user access their mailboxes via POP3 or IMAP4 protocols,
travelling user via SSL encrypted Webmail

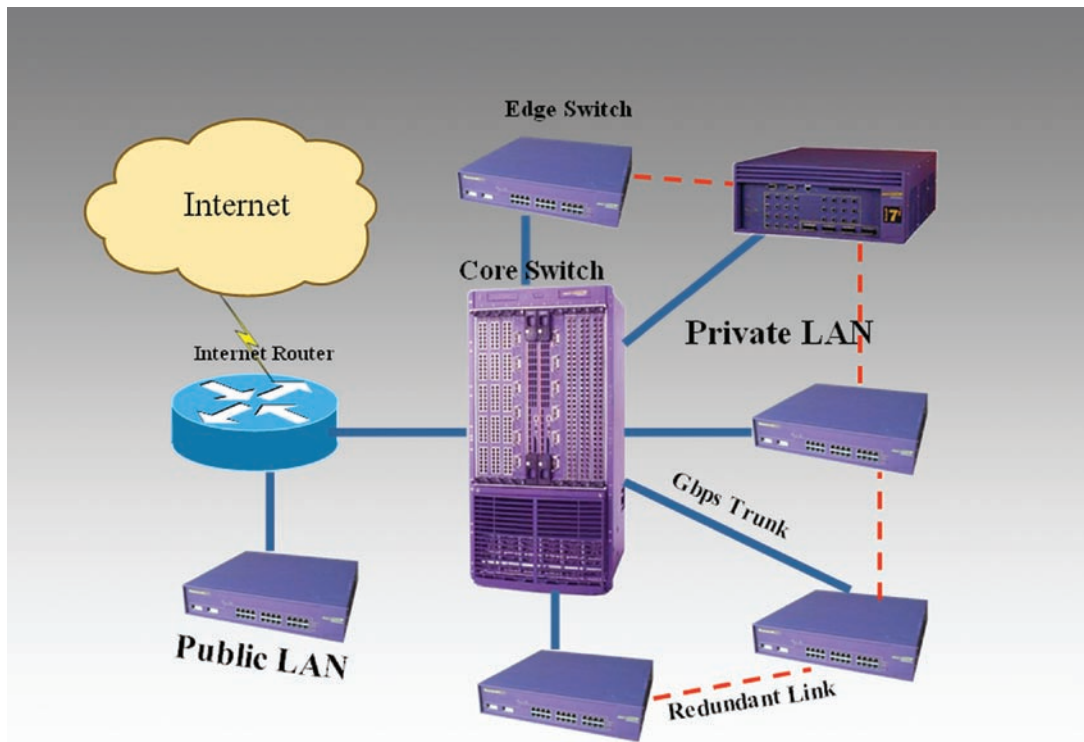
WWW: institute's home page and intranet design and maintenance;

imprs surmat research-school page operating

INFO: CD-ROM service for the distribution of information, databases and software

CALENDAR: network-wide work flow for the institute's executive staff

Planned and outstanding is to offer directory (LDAP), mass storage (SMB) and backup service (TSM). most



Physical layout of the MPIE network.

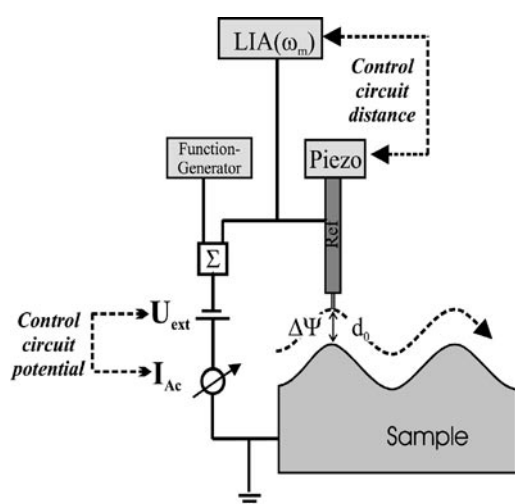


Electronics Workshop

H. Kemnitz

The experimental research character of the institute requires a wide range of laboratory equipment, which has to be designed, built and tested by the electronics workgroup in close cooperation with the scientific staff. By combining commercially available devices for process control, data acquisition and data analysis, most research demands can be satisfied. However, it is of particular importance to respond for special research requirements with unique prototype design for low-level measurements, special sensory and high-quality process instrumentation. In recent years, the electronics workgroup has developed exceptional experimental instrumentation, which is considered unique.

An example for this task is the „Height Regulation for a Scanning Kelvin Probe“ that allows simultaneously the measurement of volta potentials and the profiling of the sample topography on macroscopically rough and curved surfaces inside a climate chamber. As can be seen in the figure below, the scanning sensor tip of the probe has to be kept in constant distance to the surface profile within a z-resolution of below 200 nm, related to a lateral spatial resolution of about 10 μm . The mechanical part of the height regulation is performed by a piezoelectric translator stack and a stepping motor in combination. Two independent control circuits are provided for distance and potential measurement. The high accuracy is gained by processing the demodulated signals of a double modulation of an external voltage at different frequencies. Two process computer control the experiment.

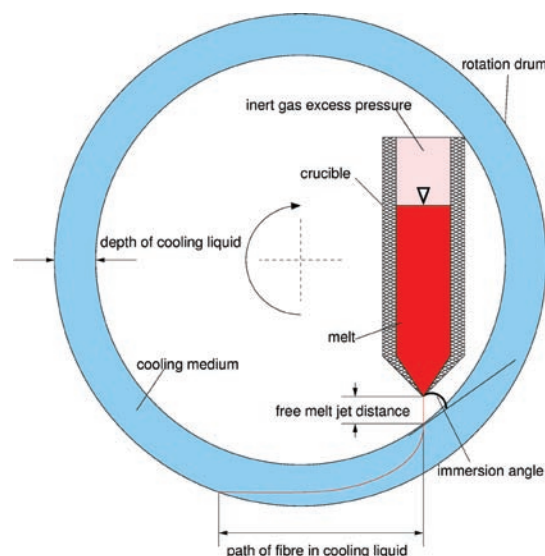


Distance control of the sensor tip of a Scanning Kelvin Probe. The resolution in z-direction is in the range of 200 nm related to a tip-sample distance of about 10 μm .

Another highlight is a new process instrumentation for the „In-Rotating Liquid-Spinning“ (INROLISP) experiment. This near-netshape-casting facility casts metallic fibres with diameters in the micrometer range into a rotating cooling liquid as is schematically shown in the figure below. For that purpose, the melt-ejecting nozzle has to be positioned as close as possible to the surface of the cooling medium. In detail, the optimal distance of about 1 to 5 mm is dependent upon the fibre diameter, the unrelaxed velocity profile and the collapsing free melt jet and has to be positioned within an accuracy of less than 100 μm . Additionally the immersion angle has to be adjusted very accurately in the range of 40° to 50° and the speed of the cooling liquid should be approximately 8 to 10 km/h.

Besides compiling prototypes, the electronic workgroup improves the behaviour of the present high end laboratory equipment. The resolution of a newly acquired field emission electron microscope with heating stage was increased by a factor of 10. This was achieved by smoothing the heating current to prevent a force interaction between a rough ripple of the heating current and the scanning electron beam.

Current projects are: „Process instrumentation of a thin strip casting equipment“; „Precise control of a roll slit and rotary motion of a rolling mill“; „Thermomechanical heat treatment in a rolling mill“ and a „Melt spinning facility to study the kinetic processes during solidification“.



„In-Rotating-Liquid-Spinning“ experiment.



Technical Services

H. Voges

Mechanical Workshop

R. Selbach

Apart from the production of round (type A/B) and flat (type E) tensile test and Charpy test specimens from a wide range of materials, a variety of interesting projects and devices were carried out.

The highlights of our work include, e.g., the construction of an in-situ plasma reaction chamber, an infrared liquid cell made of Plexiglas (PMMA) and an electrochemistry/plasma cell made of Delrin (POM), to name just a few. The construction of the in-situ plasma reaction chamber was one of our most challenging and time-consuming tasks. The chamber is completely made of stainless steel and was fitted with an adjustable, prism-controlled sample table which is controlled electrically from the outside.

Because of the many years of experience of the staff of the workshop in the machining of exotic materials and our modern machining equipment with a state-of-the-art selection of tools, we are able to occupy a top position in the field of machining of metals. With respect to our tooling equipment, we are very well prepared to cope with new materials produced at our institute in the future.

Operational Engineering

M. Winkler

The technical service has several working areas, which ensure the trouble-free operation of the technical installations within the institute.

Electric workshop. The *electricity service* is currently, and will continue to be, updated to the state-of-the-art standard in the present and upcoming stages of construction. The in-house power line is supplied by two 1000 kVA transformers. In case of a loss of power, the most relevant (e.g. security) facilities are powered by an emergency generator.

A safety lighting along evacuation routes, such as stairways and corridors is guaranteed by a separate battery facility. All emergency routes are monitored

by an automatic fire alarm system. In case of an emergency, the entire staff located in the buildings is warned by an acoustic alarm. The electricity service division assists all departments of the institute with the set-up and operation of their testing facilities. In the course of the institute's renovations, a new telephone system was installed and the data network was extended.

Central building control system. A newly installed *central building control system* regulates all new facilities of the buildings management *centrally*. The implementation of the new facilities was indispensable in order to fulfil the operational requirements of laboratories and offices.

Air conditioning systems such as extractor hood ventilation systems, deaeration facilities and constant air-conditioned rooms are controlled by the central building control system. The majority of laboratories are partially air-conditioned and are equipped with a circulating air cooling unit. A partially installed heat recuperation unit is applied for the purpose of energy saving. Two refrigerating machines with a total power of 1000 kW guarantee the supply of cooling. A low temperature vessel is used for heat supply.

The institute's dual plumbing system ensures that incoming laboratory and potable water is strictly separated. Consequently, waste water also leaves the building separated. In addition, there is a neutralisation facility for chemically polluted wastewater.

The *gas and water services* are subdivided while being controlled centrally by the building control system and by a local supply. The centrally controlled media supply facilities provide compressed air, deionised/demineralised water and special gases such as nitrogen, argon, etc. For critical gases, gas warning devices are installed.

In order to handle the requirements mentioned above, the buildings management uses the digital data control (DDC) technique, where the relevant data from all areas merge prior to recording and processing. The single stations of this service are located in technical centres, distributed throughout the building and are digitally linked to each other and controlled by the central building service.



Library

W. Rasp

The institute's library is organized – in contrast to most other public libraries – as a reference library, so that the service function of a lending library is not provided. Unfortunately, there is some restriction to have a direct access to the library because at present it is lodging in a neighbouring building which is part of the Steel Institute (VDEh). All together the collection contains nearly 5000 catalogued scientific books. They are grouped into 19 topics, which cover most of the broad range of the institute's scientific interest. Institute employees are allowed to borrow a book temporarily or, with special permission, for a longer term. A searchable database is provided via intranet for all institute co-workers.

Among the basic collection of books, there are a lot of valuable, old volumes as e.g.: Georgius Agricola 'De Re Metallica', Basel 1556; J.K. Kunst und Werckschul/Anderer Theil 'Chymiae ac aliarum Artium Cultore', Nürnberg 1707; Monsieur de Reaumur, de Academie Royale des Sciences, 'L'Art de Convertir le Fer', Paris 1722; Jars Gabriel 'Metallurgische Reisen, I-IV', Berlin 1777-1785.

Many scientific journals (about 10,000 volumes) are also collected in the library. The oldest of them are 'Zeitschrift für Angewandte Physik' beginning in 1848, 'Stahl und Eisen' starting in 1881, 'Zeitschrift für Metallkunde' since 1919 and 'Archiv für das Eisenhüttenwesen' first issued 1927/28 and renamed into 'steel research' in 1985.

These days the number of paper journals in the institute's library is decreasing because of the increasing importance of publications via electronic media. So the institute takes advantage of the Virtual Library (VLib) offered by the Max Planck Society. VLib allows free access to all sort of basic information resources on different electronic platforms by means of the internet. Thus the staff members and guests have a run of about 4300 journals, 1450 of them being licensed for permanent storage by the Max Planck Society. The VLib portal also makes available the library catalogues from 70 different Max Planck Institute libraries as well as those from external libraries. In view of this immense supply of information the institute was able to reduce its own budget for scientific journals considerably.



G. Agricola
De Re Metallica
Basel 1556

Georgius Agricola's 'De Re Metallica' printed in Basel in the year 1556.



Administration

H. Wilk

In the end of 2003, preparations to introduce the SAP R3-Software-module „Human Resources“ were concluded. Since January 2004, salaries and wages of the employees are again calculated in the institute and the outsourced computation was discontinued. The new module extends the possibilities to integrate personal data from the personnel division into the accounting system of the institute. External consultants assisted in introducing and customizing this module. The entire information-system SAP R3 will be maintained by the Max Planck Society.

The introduction of another SAP module is scheduled for the near future. This module will integrate cost accounting into the information system and will further refine the already existing possibilities to create statements for revenues and expenditures. A detailed time schedule for the implementation has not yet been fixed.

Research contracts funded by third parties are concluded increasingly with industrial partners, besides contracts with public financing. Particularly, agreements on intellectual property rights and their exploitation are object of difficult negotiations. A support agreement with the consulting society

Garching Innovation GmbH, Munich, which also carries out the marketing of the know-how of the Max Planck Society, has been signed.

In October 2004, 26 foreign nations were represented at the institute. The large number of foreign employees leads to growing language problems. The fact that research contracts are formulated in increasing number in English is also a special challenge for the administration. Therefore, it is necessary to offer the employees English language courses.

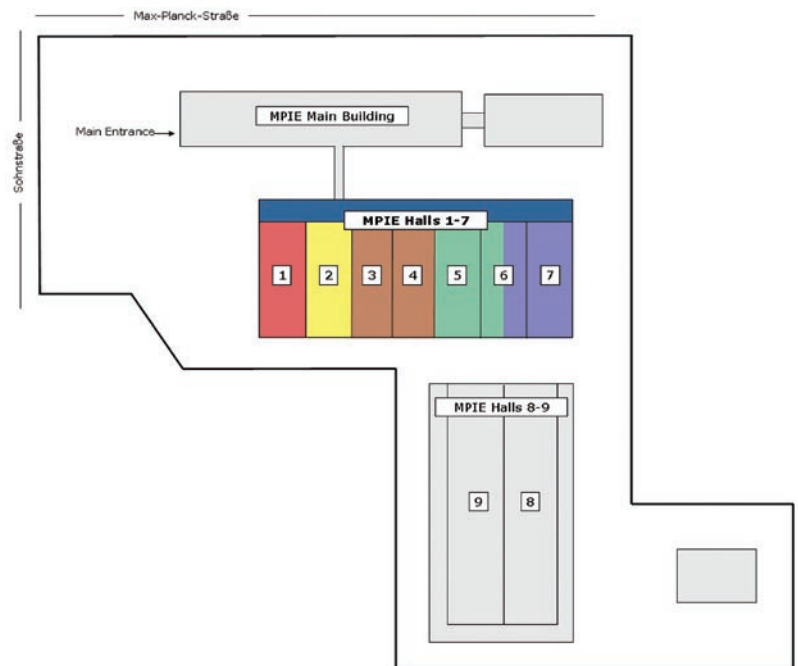
A new structure for budgetary planning will be prepared. It is intended to define a core budget for the institute which takes the necessary financial means needed by the institute into account. Structure and financial requirements of this core budget shall not be negotiated on a yearly basis with the Max Planck Society and the Steel Institute VDEh. Changes in the structure lead to adjustments of the financial means. Special influences (expensive investments, appointments etc.) will not be part of the core budget and these financial requirements have to be negotiated separately.



Institute Renovation in Progress and Newly Established Scientific Laboratories

Institute Renovation in Progress

The renovation of the institute has been continued during the last two years. After the renovation of the main building was finished in spring 2002, work on the halls 1 to 7 on the institute's back-yard started. The figure on the right side shows the institute's grounds with the arrangement of the buildings. The total area of the halls 1 to 7 is about 3100 m² with nearly 2500 m² for laboratories and workshops and about 600 m² for office rooms on the 1st floor (marked dark blue in the figure). The architecture of the halls is illustrated by the photograph below showing hall 3 with the mechanical workshop inside.



Map of the area of the MPIE buildings with the newly renovated halls 1 to 7.

As indicated by the colours, the halls are assigned to various departments and workshops. Hall 1 was completely transformed to office rooms and laboratories on two floors housing the Department of Microstructure Physics and Metal Forming as well as rooms for the Department of Metallurgy and Process Technology and the electron microscope of the Department of Materials Technology. Hall 2 is used as goods depot for technical services and office supplies. The above mentioned mechanical workshop is in hall 3. The central electric power supply, the building control system and the highspeed data network resources are in hall 4 (two stories and a cellar). Hall 5 and part of hall 6 are occupied by the experimental equipment of the Department of Metallurgy and Process Technology. The other part

of hall 6 and the complete hall 7 belong to the Department of Materials Technology.

The newly established scientific laboratories of the departments in halls 1 to 7 are described in the following section.



View into the renovated hall 3 containing the mechanical workshop (Photo: O. Schoplick).

Newly Established Scientific Laboratories

High resolution scanning orientation electron microscopy

S. Zaeferrer

The new scanning electron microscopy laboratory is equipped with a standard tungsten filament scanning electron microscope (JEOL JSM 800A) and a high resolution scanning electron microscope with a thermal field emission gun (JEOL JSM 6500 F). Both instruments are optimized for the investigation of microstructures and textures of crystalline materials by means of electron backscatter diffraction (EBSD). In this technique a stationary electron beam illuminates a steeply inclined sample (60° - 70°). The inclination is necessary in order to allow a significant fraction of backscattered electrons to leave the sample. Some of these backscattered electrons are diffracted in the sample and form Bragg cones. The cones form corresponding diffraction patterns on a

fluorescent screen which is positioned close to the sample. The patterns resemble in their geometry the well known Kikuchi patterns observed in transmission electron microscopy. The position and width of the Kikuchi bands in the patterns allows one to determine the positions and interplanar distances of the crystal lattice planes (hkl) in the illuminated crystal. The positions and width of the Kikuchi bands are used to determine the orientation and phase of the illuminated area. This technique is the basis of an automated crystal orientation mapping (ACOM) system where the primary beam is scanned on a regular grid. At each grid point a diffraction pattern is acquired and both, the phase and the crystallographic orientation are determined. From these measurements crystal orientation and phase maps are constructed. In these mappings each point can be colored according to a reference coordinate system. The crystal orientation maps provide a set of detailed informations (Fig. 1).

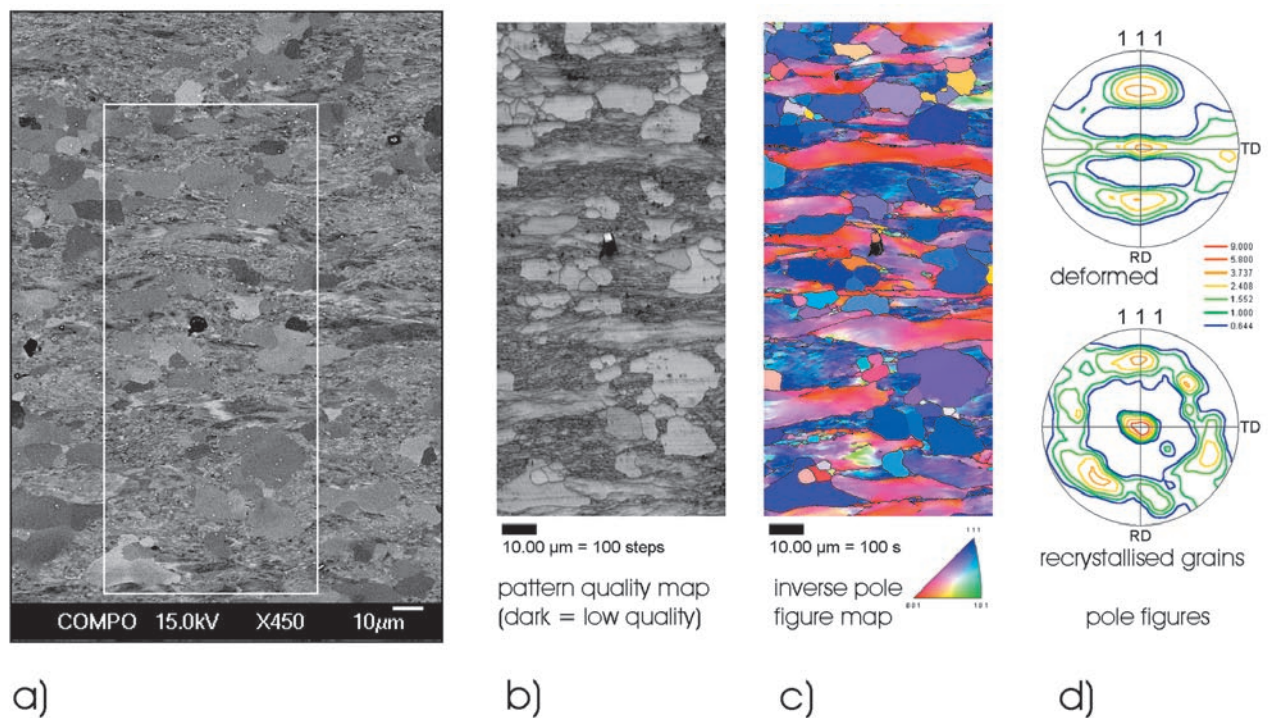


Fig. 1: Orientation Mapping: ACOM from a microstructure of a partially recrystallised IF steel:
a) Electron channelling contrast image obtained with the backscattered electron (BSE) detector
b) Diffraction pattern quality map of the observed area
c) Crystal direction map indicating the crystal directions pointing parallel to the sample normal direction (ND)
d) (111) pole figures of the deformed and recrystallised partition of the sample, showing that recrystallisation strongly supports crystal orientations with (111) || ND (centre of pole figure) (I. Thomas and S. Zaeferrer).



First, a high resolution image of the microstructure is given where grain sizes, grain shapes, and their topological arrangement can be determined. The crystal orientation distribution function of any freely selectable area can be calculated. Furthermore the misorientations across grain and phase boundaries or between any two reference points in the mapping can be calculated. In-grain or kernel average misorientation measures or corresponding numbers quantifying diffraction pattern quality can be calculated and used, for example, to differentiate between deformed and recrystallized areas. The tungsten filament microscope is mainly used to map large areas by stage movement of the sample. This allows one to scan sample areas in the square-centimeter range with medium spatial resolution (at best 500 nm step size). The FEG microscope, in contrast, reaches the ultimate theoretical resolution of the EBSD technique which is of the order of some

10 nm. Due to the particularly high beam current delivered by this instrument, either a very high measurement speed, currently reaching up to 60 measurements per second, or a very high pattern quality with a high signal to noise ratio can be obtained. The high measurement rate is important when large mappings are to be measured with high resolution. A field which is explored in detail only since recently is the determination of known and unknown phases from material volumes significantly smaller than $1 \mu\text{m}^3$ by the combination of crystallographic analysis via EBSD and chemical analysis by EDX in the SEM (see Fig. 2). In this way the SEM simplifies tasks which were traditionally carried out by TEM. The efforts for sample preparation are significantly reduced, the observable areas are much larger and new software packages simplify the determination process.

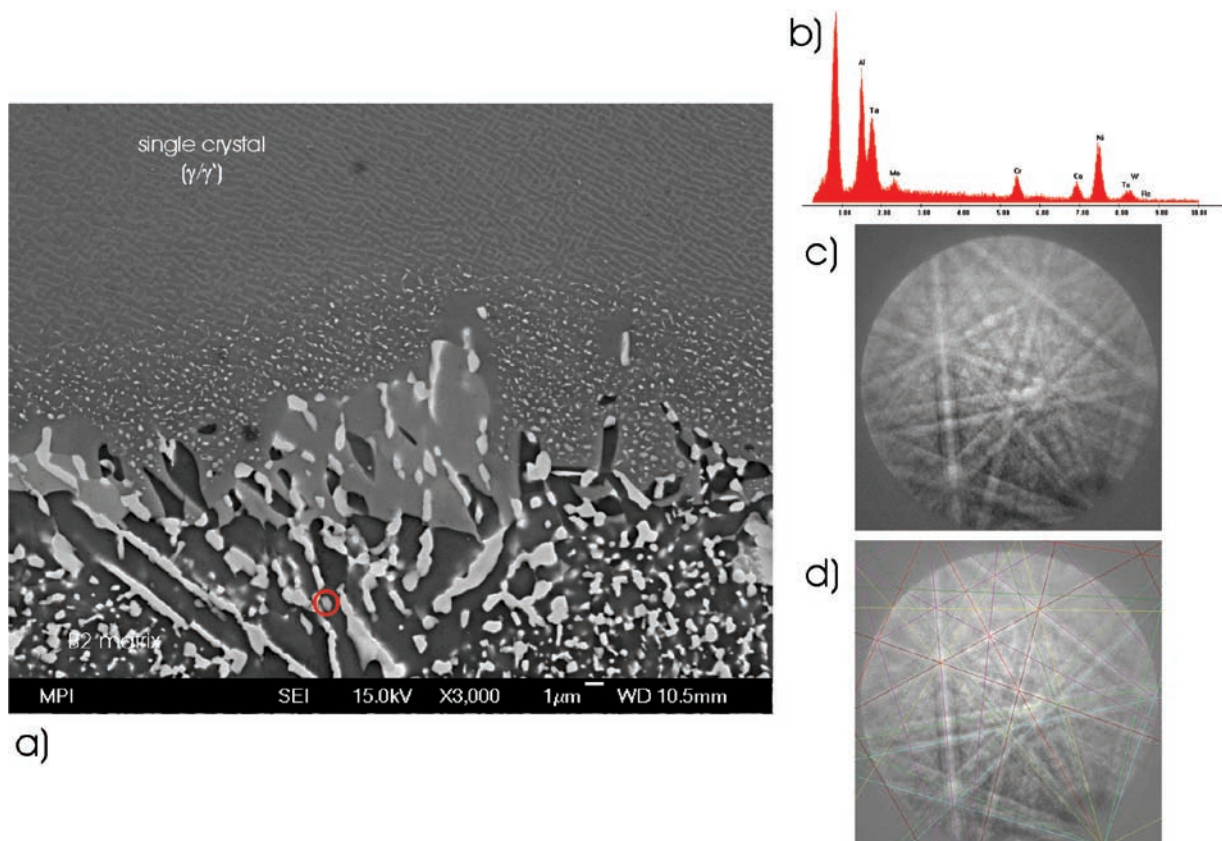


Fig. 2: Phase Identification: Phase identification by EDX and EBSD for a precipitate in the diffusion zone of an Al-coated Ni-based superalloy:

- a) BSE image of the interface (the cross marks the investigated particle).
- b) EDX spectrum obtained by spectral mapping
- c) EBSD pattern
- d) EBSD pattern overlaid with the indexing for hexagonal NiAlTa (S. Zaeferrer).

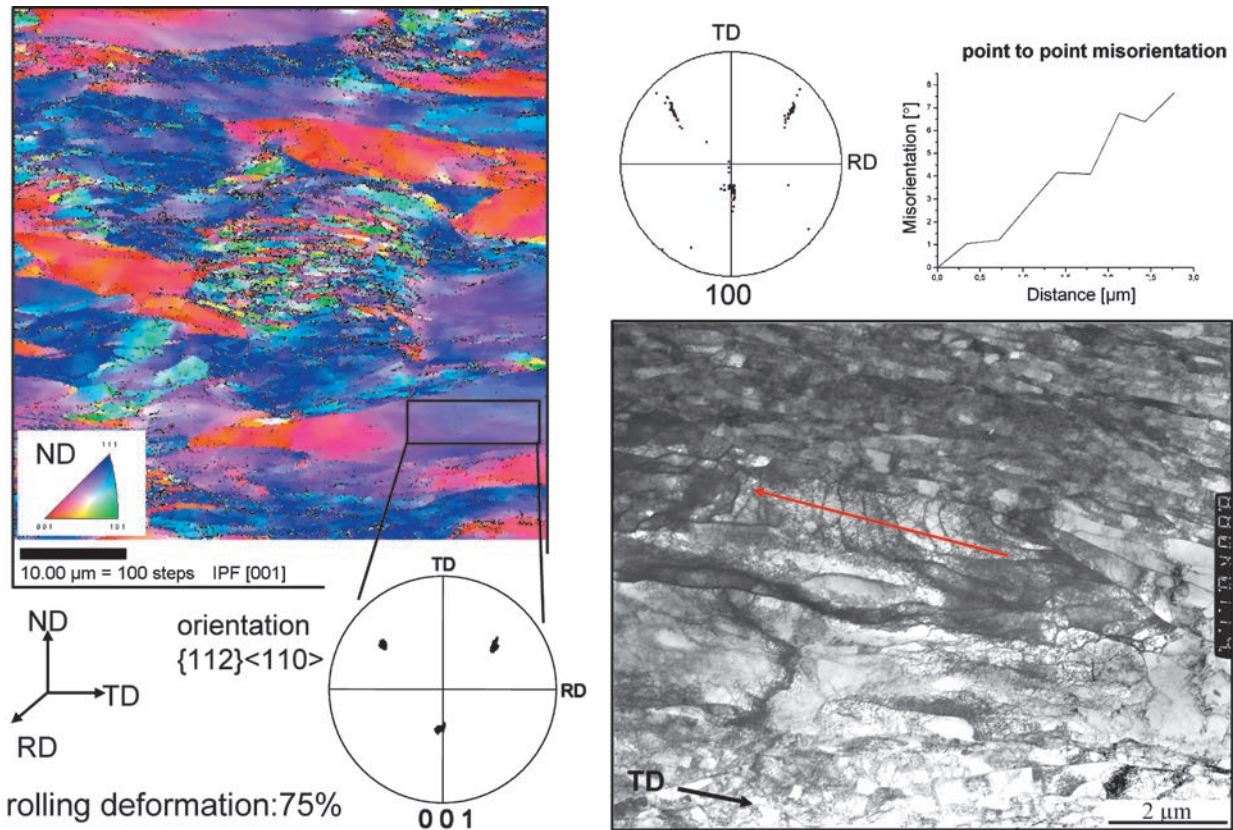


Fig. 3: Comparison between high-resolution EBSD measurements and TEM data taken in an interstitial free steel. TEM texture maps are of importance in cases where the high resolution EBSD-SEM is not sufficient or where microstructural details are to be observed that do not appear in SEM data such as the subgrain structure of a heavily deformed IF steel (I. Thomas and S. Zaefferer).

Transmission electron microscopy laboratory
A. Schneider, S. Zaefferer

The new TEM facilities consist of a Philips CM20 TEM and a fully equipped sample preparation laboratory (focused on the preparation of metallic samples). The TEM is equipped with a standard pole piece for large angle sample tilt, a STEM (scanning TEM) system, an EDX detector, a TV rate CCD camera mounted below the viewing chamber and a high angle high resolution CCD camera mounted on top of the viewing chamber. This digital camera (AMT) is characterized by very high contrast dynamics and a resolution of 1300 x 1000 pixels what makes it particularly well suited for the observation of diffraction patterns or high contrast images (such as dark field images). What makes the TEM laboratory special and particularly dedicated to the quantitative investigation of crystallographic texture and microstructure is a software system that allows the on-line and semi-automatic analysis of diffraction patterns (spot and Kikuchi patterns) for the determination of crystal structure, crystal orientation, and lattice defects. Orientation maps with a resolution of 10 nm can be obtained. These maps are of great importance in cases where the high resolution EBSD-SEM is not sufficient or where microstructural details are to be

observed that are hidden in SEM data. While the EBSD-SEM maps more or less continuous orientation gradients in crystals the TEM reveals the existence of sharp cells with discontinuous orientation changes in grains of similar orientations (see Fig. 3).

Combined focused ion beam and electron scanning microscopy and 3D nanotexture laboratory (FIB-SEM-EBSD-EDX)

S. Zaefferer, M. Nellesen, D. Raabe

This new research laboratory is dedicated to the joint measurements of crystallographic texture, microstructure, structure, phase, and chemical composition with very high lateral resolution and in 3 dimensions by using a ZEISS 1540 XB CrossBeam Workstation equipped with electron back scatter diffraction (EBSD) and EDX. This ultimate microstructure research and mapping tool combines a high resolution scanning electron microscope equipped with a ultra high resolution GEMINI field emission column with the high performance Canion FIB column into one single integrated system for a full three dimensional analysis of grain and subgrain



structures (Figs. 4,5). The Canion FIB ion source can be focused into a beam of a diameter in the order of few nanometers to image (similar to the scanning electron microscope) and to cut (similar to a sputter gun) specimen surfaces. With this configuration simultaneous observation and structuring of the specimen surface is possible. The Ga⁺-ion beam of the FIB gun is capable of subsequently cutting slices from a sample. Imaging of each surface slice can be carried out by using either the FIB mode exploiting the excellent contrast of the Ga⁺-ions or the high resolution scanning electron microscope in SEM or EBSD mode. From such series of slices the complete 3D microstructure can be reconstructed. The focused Ga⁺-beam can be positioned at the surface with very high accuracy and produces a fine, defined cut. Thus, also the manufacturing of mechanical specimens in the micrometer area or tailored thin foils for TEM taken from well defined areas is possible. The live SEM imaging capability of the 1540XB CrossBeam during FIB operation mode gives full control when analyzing complicated microstructures. The super eucentric stage makes the 1540XB CrossBeam an excellent research tool for 3D nano- and microtexture projects. Besides EBSD and EDX the machine is equipped with a spectrum of additional tools: a multi-channel gas injection system allows the targeted deposition of a variety of materials; a transmitted electron detector permits to observe thin foils in transmission mode (STEM). The backscattered electron detector allows to take images with high density and orientation contrast. A micromanipulator, finally, is a dedicated robot to handle micrometer-scale samples for the preparation of TEM thin foils, for example. This novel microscope can be used for ultra high resolution FEG-SEM analysis, high performance FIB imaging, high resolution live imaging during milling and polishing, endpoint detection for automated milling, cross section investigation, three dimensional microstructural examination, failure and MEMS analysis, automated TEM sample preparation, and 3D nanotexture analysis to name but a few essential fields of application.



Fig. 4: FIB-SEM column with the various detectors marked.



Fig. 5: The complete instrument in working condition.

X-ray diffraction laboratory

S. Zaeferrer

The projects pursued in the X-ray diffraction laboratory are essentially concerned with quantitative texture investigation by means of wide angle X-ray Bragg measurements. Experiments can be carried out in back reflection and in transmission mode. Additionally, phases and lattice parameters, residual stresses, and internal strain tensors can be determined. The laboratory is equipped with two

X-ray goniometers. The Bruker D500 is used mainly for the determination of crystallographic textures. It is equipped with a 4 circle Eulerian cradle, a semiconductor point detector and a multi-purpose software package for texture and stress analysis. The Bruker D8 GADDS system has a more versatile setup (Fig. 6). On the side of the X-ray source a polycapillary beam guide is used to collect a large amount of the (monochromatic) radiation into a fine collimated beam. By this method a bright almost parallel X-ray beam of about 1 mm diameter is obtained on the

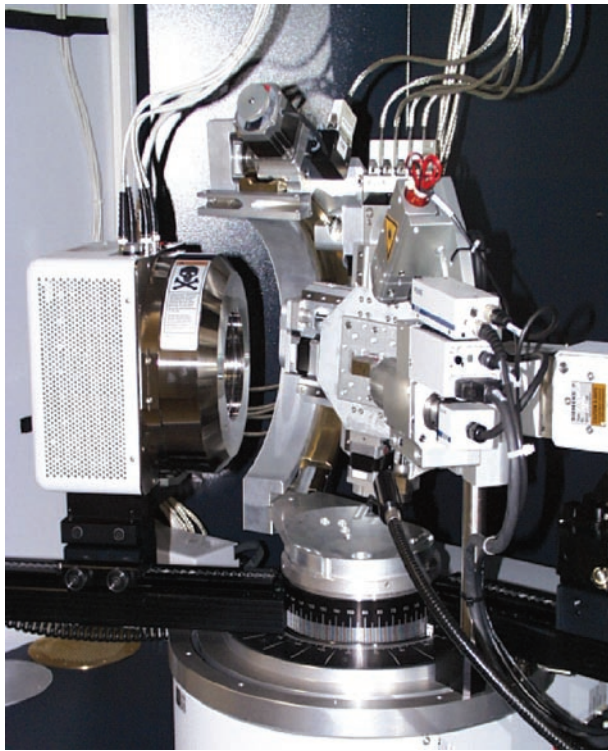


Fig. 6: X-ray texture goniometer equipped with an area detector for texture, stress, and phase analysis.

sample. By means of various apertures the beam size can be reduced to below 100 μm . The sample is positioned on a sophisticated sample stage. First, an open Eulerian cradle allows arbitrary 3D rotations of the mounted sample as required for pole figure determination in reflection and transmission mode or for internal stress determination. Onto this cradle a 3-D sample stage is fixed that permits the movement of the sample in all three lateral directions and, therefore, enables the user to precisely position the sample in the beam or perform various types of

scans. Sample positioning is performed by aid of a laser positioning system. On the detection side an area detector is used. This proportional gas counter detector has an X-ray sensitive area of 100 mm in diameter and consists of 1024 x 1024 pixels. Each pixel can register up to 200 counts per second and has a depth of 16 bit (i.e. 64.000 counts). The Debye-Scherrer rings of different lattice planes are immediately visible (Fig. 7). The detector allows one to index the rings for texture-corrected phase identification. The intensity distribution along each of the Debye-Scherrer rings is used to obtain pole figure data. Three different methods can be used for the reproduction of the orientation distribution functions from pole figures. These are the various variants of the harmonic series expansion methods which consider the non-negativity condition, direct inversion methods, and the texture component method. Finally, the detector precisely monitors the peak position and the peak profile for the different reflections. These data allow one to determine residual stresses by means of peak profile analysis as a function of texture.

Strain mapping photogrammetry laboratory
M. Adamek

In this new laboratory the determination of the plastic displacement field and the subsequent calculation of some tensor components of the plastic strain field at the surface of mechanically strained specimens is for sets of subsequent deformation steps conducted by using photogrammetry (Fig. 8). This is a digital image analysis method which is based on the recognition of geometrical changes in the gray scale distribution of surface patterns before and after straining. Both, the natural characteristics of an unprepared sample surface or an artificial quasi-

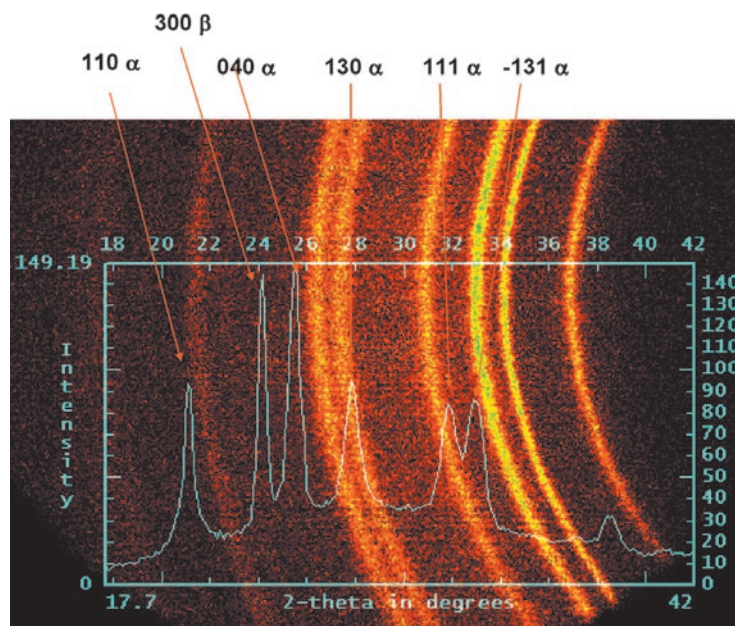


Fig. 7: Debye-Scherrer diagram of a multiphase polymeric material (N. Chen).

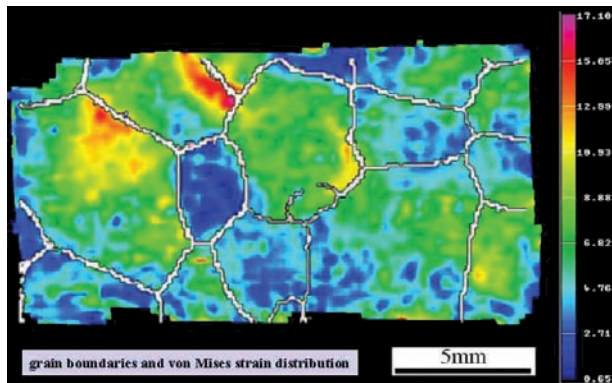
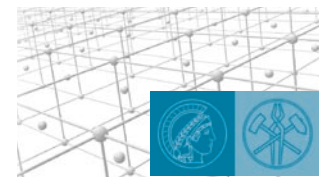


Fig. 8: Plastic von Mises equivalent strain distribution in a deformed polycrystal. The black lines show the large angle grain boundaries as determined by use of an EBSD measurement.

stochastic color spray applied to a polished surface may serve as input pattern. In order to measure the three dimensional surface coordinates digital stereo pair images of the sample are acquired using two high resolution CCD cameras. Pattern recognition is carried out by a digital image processing procedure which maps a rectangular grid onto the image. The grid points are characterized by three dimensional coordinates and by the gray scale distribution in their proximity. After straining, the pattern is again recognized based on the assumption that the gray scale distribution around a certain coordinate remains constant during straining. From the change in border coordinates containing the correct initial gray scale distribution around the grid point the three dimensional displacement gradient tensor field is determined at each grid point. These data serve as input for deriving the surface components of the local strain tensor. The strain tensor is used in the definition as the symmetric portion of the first order approximation of the standard polar decomposition of the displacement gradient tensor. The photogrammetric method works without a

regular grid on the sample surface. The displacement gradient field is derived exclusively from changes in the border coordinates for a gray scale distribution at each coordinate. The spatial resolution of the method is, therefore, independent of some external grid size but it is of the order of the respective light optical or electron-optical setup (ranging from cm to nm). The strain resolution is below 1% since the method uses the match of the complete gray scale distribution before and after loading as a measure to determine the exact shift in border coordinates. This procedure provides a larger precision than the determination of the new border coordinates in the form of discrete pixel steps.

Surface topography laboratory

M. Adamek

In the new surface laboratory the 3D surface topography of a specimen can be measured by using a white-light confocal microscope (Fig. 9). Confocal microscopy works by a point distance measurement using a depth discrimination method in reflection mode. In a first focusing step, light which is emitted from a point source is imaged into the object focal plane of a microscope objective. An in-focus specimen location results in a maximum flux of the reflected light through a detector pinhole (second focusing), whereas light from defocused object regions is partly suppressed. Therefore, the detector signal, as limited by the pinhole size, is reduced drastically when defocusing the specimen. For the current laboratory equipment this principal design was improved for fast 3D measurements by use of a spinning multiple pinhole mast (Nipkow disk) in an intermediate image plane of a microscope. The Nipkow disk consists of an array of pinholes arranged

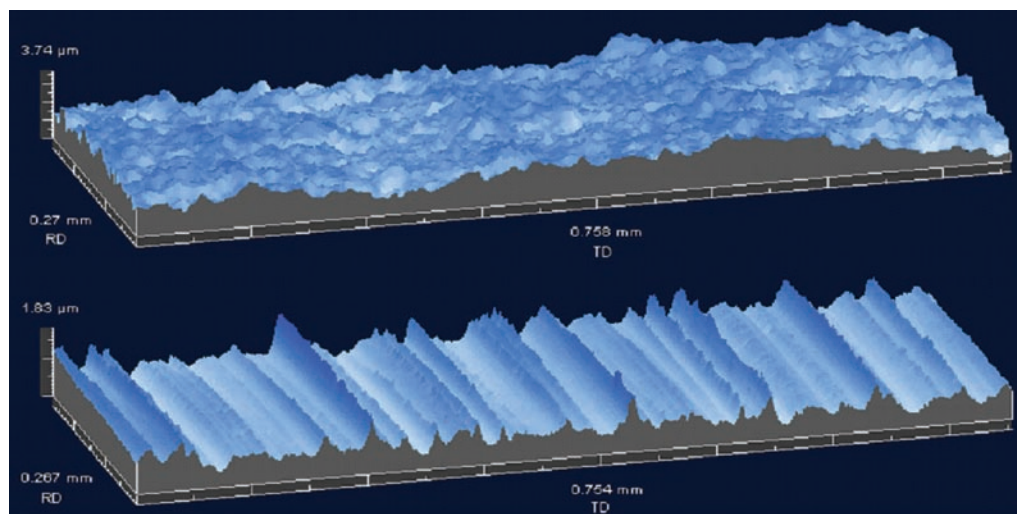


Fig. 9: Examples of different surface roughness patterns obtained on the same material.

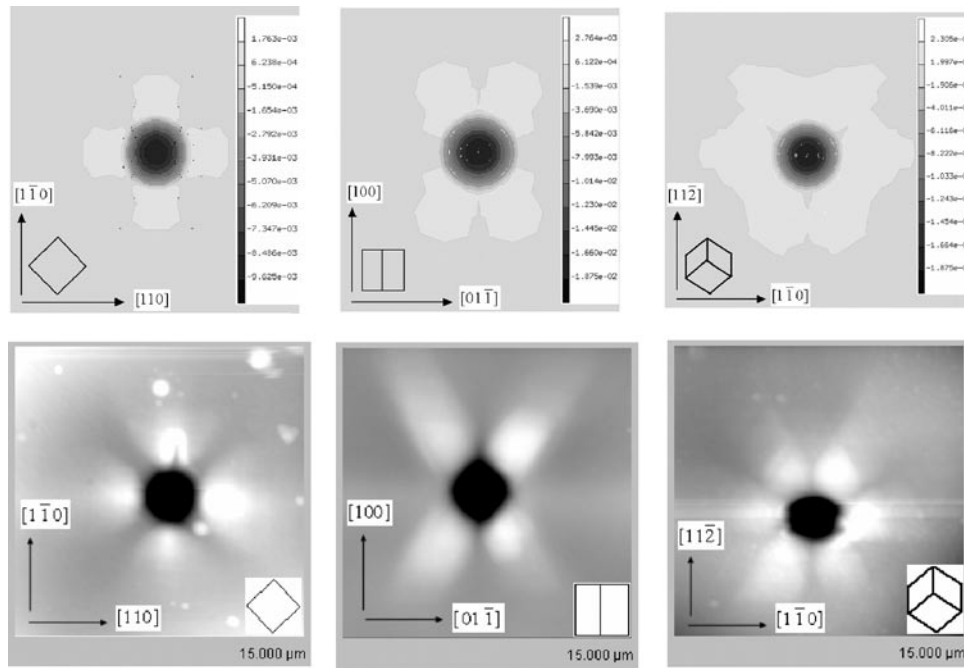


Fig. 10: Examples of different nanoindentation surface patterns taken from single crystals. Upper row: Crystal plasticity finite element simulations; lower row: experimental surface maps.

in a spiral shape. The disk which is operated in a spinning mode is illuminated by a plane wave and acts as a scanning multiple point light source which is imaged into the object focal plane of the microscope objective. After the reflection of light,

each illuminating Nipkow pinhole acts as its own detector pinhole. Combined with fast CCD image processing the rotating Nipkow disk affects the in-plane-scan of the object field in video-real-time. Therefore, only the additional out-of-plane scan is required for 3D acquisition. The Nipkow-disk expands the effect of depth discrimination to the area of the microscope object field, which allows optical sectioning like in computer tomography.

Nanomechanical testing and atomic force microscopy laboratory

N. Zaafarani, H. Bögershausen, H. Faul

The laboratory for nanomechanical testing is equipped with a joint Hysitron nanoindenter and atomic force microscopy system (*TribolIndenter*). The instrument includes an XYZ-sample-stage and a set-up which combines a piezo-scanner as known from conventional atomic force microscopy with a transducer and a diamond indenter-tip (Figs. 10,11). The XYZ-stage is used to position the sample under the piezo scanner, which then conducts the fine positioning as well as the approach of the indenter in normal direction. A three-plate capacitor (transducer) with the indenter fixed to the middle plate is being used to move the indenter tip in normal direction by applying a bias DC voltage on the bottom plate of the capacitor. The electric field potential between the plates varies linearly with the displacement of the indenter and the middle plate it is attached to in normal direction. In this way the displacement of the indenter can be measured accurately. Once the indenter tip is positioned on

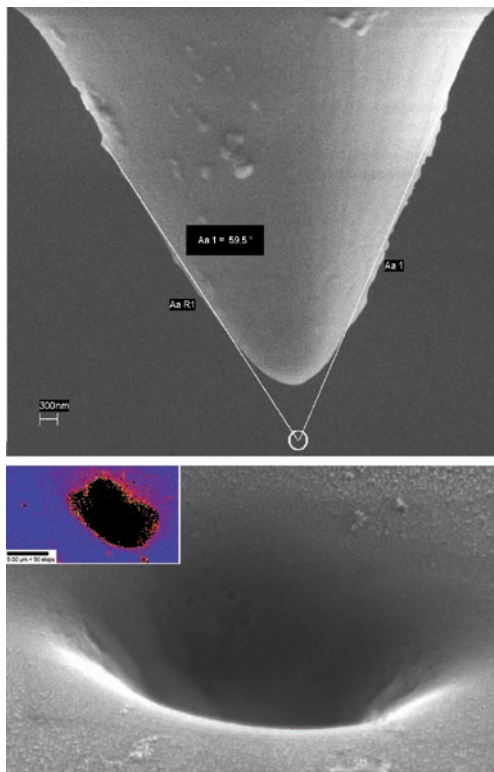


Fig. 11: For most experiments a conical nanoindenter geometry instead of the conventional Berkovitch set-up is used in order to avoid artificial symmetries other than those of the crystals indented.



top of the sample, it can either be forced into the sample by applying a bias voltage on to the bottom capacitor of the transducer (hardness test) or it can be moved in lateral direction (x-y-plane) with help of the piezo controller to image the sample surface comparable to an conventional atomic force microscope. A further set-up allows one to conduct scratching experiments which are increasingly important to analyze the mechanics of metal-polymer interfaces.

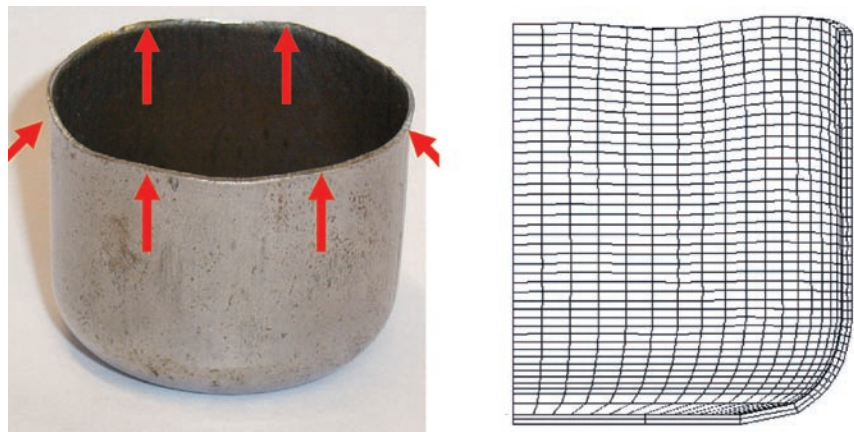


Fig. 12: Plastic anisotropy resulting in earing in experiment and simulation.

Computational materials science laboratory

F. Roters, A. Kuhl, B. Beckschäfer

The new laboratory for computational materials science is equipped with a set of 10 fast Unix workstations, some of them with a dual-processor set-up, and a pool of about 40 and high end Windows-based workstations. The network is based on an optical fiber backbone. The laboratory uses MARC, ABAQUS, and DEFORM as standard commercial finite element solvers as well as a set of cellular automaton and Potts-Monte Carlo simulation programs which have been designed by the group for theory and simulation in the Department for Microstructure Physics and Metal Forming. The commercial finite element software packages are used by incorporating novel physically based constitutive models in the form of user-defined subroutines into these codes. Important projects are in the fields of the large scale and small scale prediction of crystalline anisotropy during elastic-plastic mechanical loading of polycrystalline matter

(Fig. 12). The novelty of the current approaches developed in the department consists in merging formerly separated concepts from metal physics, crystallography and variational mathematics into a new method which is referred to as texture component crystal plasticity finite element method (TCCP-FEM). This approach is based on the direct integration of a small set of spherical crystallographic orientation components into a non-linear finite element model. It allows for the first time to integrate fundamental theory from the fields of crystallography and crystal plasticity into the theoretical treatment of the microscopic and macroscopic behavior of polycrystals at reasonable computation times. The method is hence particularly suited also in industrial context for instance for predicting the mechanical properties of novel light-weight constructional materials (Fig. 13). The various cellular automaton and Potts-type simulation models are particularly used for the prediction of non-equilibrium transformation and coarsening phenomena such as recrystallization, grain growth, and spherulite expansion.

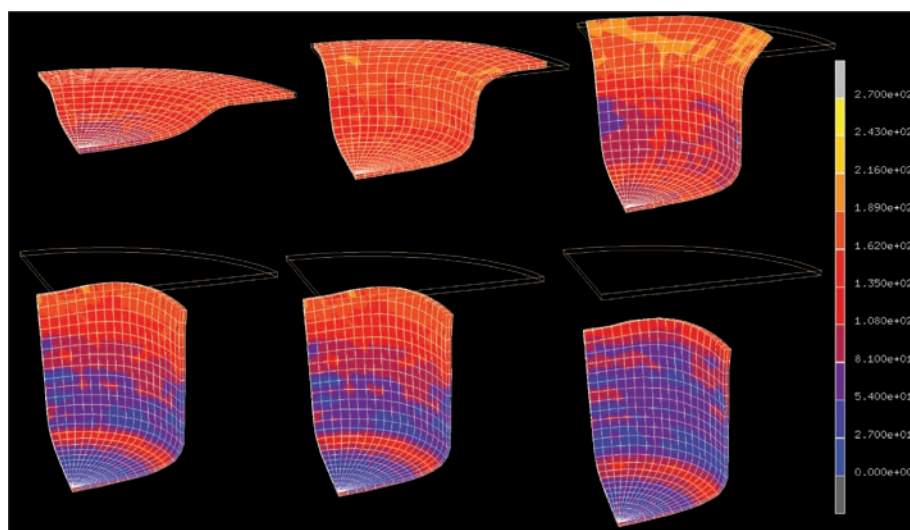


Fig. 13: Simulation deep drawing operation for the automotive industry including texture update.

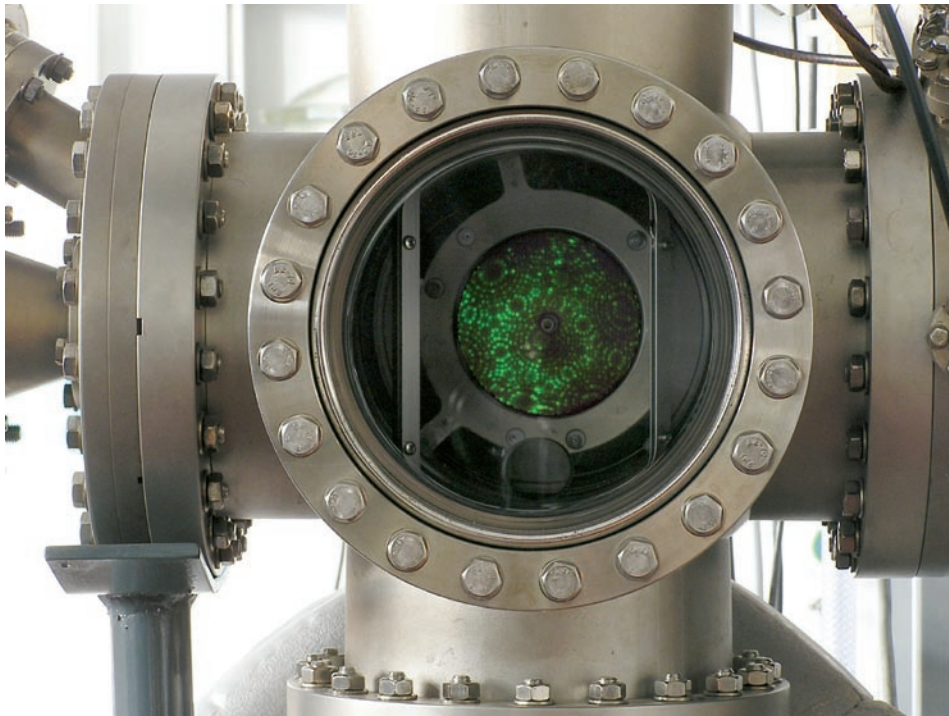


Fig. 14: Phosphor screen of the field ion microscope (FIM) with the image of a [110] oriented tungsten sample tip revealing atomic resolution. The concentric rings represent edges of atomic planes. In the centre of the screen the probe hole can be recognized which is used for the time-of-flight-measurements of field desorbed atoms (atom probe). The screen is viewed through a mirror whose aperture can be moved to the bottom of the image to improve the image quality.

Atom probe field ion microscopy laboratory

A. Schneider

An atom probe field ion microscope (APFIM) is employed for imaging and time-of-flight spectroscopy of metallic materials on the atomic scale (Fig. 14). FIM sample tips in the shape of sharp needles are imaged by the ionisation of noble gas atoms on top of surface in an strong inhomogeneous electrical field of extremely high field strength of the order of several 10^7 V/cm. Special features of interest can be selected on the FIM image and analysed in the atom probe. Surface atoms are field desorbed by applying short voltage pulses and identified by time-of-flight measurements. In this way the compositions and compositional fluctuations can be determined with the highest possible spatial resolution.

The main topics of the APFIM investigations at the MPIE are focused on ordered intermetallic phases such as NiAl, TiAl, and Fe₃Al where point defects and dislocations as well as phase and antiphase boundaries and precipitations are characterised. In atomic layer resolved measurements concentrations of antistructure atoms and site preferences of dissolved ternary alloying elements like Cr, Fe, V, Mo, Nb and Re in the different sublattices of ordered phases, such as NiAl and TiAl can be measured. In addition, atomic segregations of partly soluble elements at interfaces are detectable by APFIM.

Moreover, nanoscale precipitates can be investigated and their compositions can be determined.

The recently installed improvements of the APFIM facility are a new faster and easier software for computer controlled atom probe measurements and evaluation as well as a longer flight path which enables the detection of lighter elements such as C, B, and N and improves the signal-to-background ratio.

New conceptions and remodelling of rapid solidification facilities

J. Gnauk

During the reconstruction of the laboratory halls 5 to 7, the rapid solidification facilities were dismantled. Utilising this circumstance, the facilities are newly focused. Besides the installation of the levitation melting facility and the melt drop furnace, the instrumentation of the planar-flow-casting (PFC) facility will be completely renewed.

This is in order to determine quantitatively the kinetics of rapidly solidifying metallic melts. The experimentally recorded kinetic data are very important and will be used for thermodynamic calculations of the solidifying state far from the local equilibrium. However, comprehensive sets of non-equilibrium solidification data are not available. For



Fig. 15: In-rotating-liquid-spinning (INROLISP) facility.

this purpose, a high speed quotient pyrometer was set up into a specially constructed scanning unit, which controls the relevant section of the rotating wheel, where the solidifying ribbons undergo its solidification. With the pyrometer of a response time of 2 ms it will be possible to scan the whole section several times while the meltspinning process is running.

The In-rotating-liquid-spinning (INROLISP) facility will be used for continuous casting of thin metallic fibres of 30 to 150 µm in diameter (Fig. 15). It can also be employed as a shape-flow-casting (SFC) facility for direct continuous casting of wires with diameters of 1 to 3 mm. The complete instrumentation and the computer driven process control was rebuilt for this purpose. The figure shows a macro-photograph from the installed facility. It was equipped with a new controlling and timing system for the production of very thin fibres of diameters less than 50 µm in order to improve and for a more precise control and reproducibility of the process parameters. Also a new type of nozzles with a shorter total length will be designed and manufactured, to allow laser drilling of the outlet part inside the nozzle. By conventional mechanical drilling it is not possible to make precise outlet nozzles with exact dimensions and geometries.

Structure and physical properties laboratory

U. Brück

The laboratory for structure investigations is equipped with diverse X-ray goniometers operating at low, medium and high temperatures from 20 °C up to 1200 °C for X-ray analysis of coexisting phases in high-temperature structural materials including the precise lattice parameter determination. The newly installed facility is the „GrindoSonic“ for the determination of the elastic moduli of single crystals and polycrystalline metals, ordered alloys and ceramic materials (Fig. 16).

As the development of high temperature structural materials is a central topic in the Department of Materials Technology, the knowledge of the elastic stiffness at the application temperatures of the alloy is of great importance. The system is measuring the elastic moduli in steps of 1 K at different heating rates. Due to this accuracy, an additional aspect of this method is the determination of the temperatures of the first or second order phase transformations.

The measurement of the elastic modulus is performed dynamically using the impulse excitation technique (IET). The IET is based on the analysis of the resonance frequencies (flexural, torsional and



Fig. 16: „Grindo Sonic“ system for measurement of elastic moduli in the temperature range between 20 °C and 1200 °C.

longitudinal) of a test specimen after it was „impulse excited“ (= gently tapped). From the vibration, the resonance frequencies can be determined using an extraordinary precision device (the scatter of multiple readings approximates $\pm 0.01\%$) and are related to the stiffness, mass and geometry of the specimen. The relation is well known for crystallographically isotropic samples of uniform shape such as bars or disks possessing defined dimensions, thus making

IET a most accurate and very fast method to determine elastic moduli of isotropic materials (ref. ASTM E 1876 – 99, ENV 843-2). The instrument is equipped with a computer-controlled furnace allowing a fully automated determination of the elastic modulus in a temperature range from 20 °C up to 1200 °C. The measurements are performed in an inert gas atmosphere in order to avoid severe oxidation of the specimens.



PART II.

RESEARCH ACTIVITIES

| | |
|--|-----------|
| Inter-Departmental Research Activities | 47 |
| New Steels | 47 |
| Iron Aluminium Based Materials | 49 |
| Carburisation and Metal Dusting | 51 |
| Microstructure and Reactivity | 52 |
| Surface Mechanics and Adhesion | 53 |
| Numerical Modelling | 54 |
| | |
| Research Activities within the Departments | 57 |
| Department of Physical Metallurgy | 57 |
| <i>(P. Neumann, until May 2004;</i> | |
| <i>G. Sauthoff, May - Nov. 2004, provisional)</i> | |
| Department of Computational Materials Design | 61 |
| <i>(J. Neugebauer, since Nov. 2004)</i> | |
| | |
| Department of Interface Chemistry and Surface Engineering | 63 |
| <i>(M. Stratmann)</i> | |
| Department of Materials Technology | 77 |
| <i>(G. Frommeyer)</i> | |
| Department of Microstructure Physics and Metal Forming | 85 |
| <i>(D. Raabe)</i> | |
| | |
| Department of Metallurgy and Process Technology | 97 |
| <i>(A.R. Büchner, provisional)</i> | |
| | |
| Selected Scientific Topics | 99 |
| Development of a Thermodynamic Database for Ferritic Steels | 99 |
| <i>J. Balun, V. Knežević, G. Inden, P. Unucka, J. Houserova, A. Kroupa</i> | |
| DFT-Based Modelling of SiO ₂ Surfaces and their Interaction | 101 |
| with Water | |
| <i>A.T. Blumenau, P. Schiffels</i> | |
| Newly Invented High-Strength and Light-Weight TRIPLEX Steel | 105 |
| Exhibiting Exceptional Ductility by Shear Band Induced Plasticity (SIP) | |
| <i>U. Brück, G. Frommeyer</i> | |
| Understanding and Reducing of Spottiness at Twin Roll Cast Thin Strip | 109 |
| <i>A.R. Büchner</i> | |



| | |
|---|-----|
| Fundamental Studies on the Formation of Ultra-Thin Amorphous Conversion Films on Zinc Alloy Coatings <i>N. Fink, B. Wilson, G. Grundmeier</i> | 111 |
| Modelling of Laser Welded Ti–Al <i>J. Gnauk, R. Wenke</i> | 115 |
| Production of Nanostructures from Directionally Solidified Eutectics <i>A.W. Hassel, B. Bello Rodriguez, S. Milenkovic, A. Schneider</i> | 119 |
| Evolution of Near Surface Concentration Profiles of Cr during Annealing of Fe-15Cr Polycrystalline Alloy <i>E. Park, M. Stratmann, M. Spiegel</i> | 123 |
| Simulation Study on the Influence of Texture on Earing in Steel using the Texture Component Crystal Plasticity FEM <i>D. Raabe, F. Roters</i> | 127 |
| On the Mechanism of Mechanical Mixing and Deformation-Induced Amorphization in Heavily Drawn Cu-Nb-Ag <i>in situ</i> Composite Wires <i>D. Raabe, A. Schneider, K. Hono</i> | 131 |
| Inhibiting Delamination of Organic Coatings from Metallic Substrates: How to Design Inherently Stable Interfaces <i>M. Rohwerder, M. Stratmann, R. Hausbrand</i> | 135 |
| Development of a Non Local Dislocation Density Based Constitutive Law for Crystal Plasticity FEM with Special Consideration of Grain Boundaries <i>F. Roters, A. Ma, D. Raabe</i> | 139 |
| Simulation of Precipitation Reactions in Ferritic Steels <i>A. Schneider, G. Inden</i> | 141 |
| Three-Dimensional Atom Probe Studies of Phase Transformations in an Fe-Al-Ni-Cr Alloy with B2-Ordered NiAl Precipitates <i>A. Schneider, C. Stallybrass, G. Sauthoff, A. Cerezo, G.D.W. Smith</i> | 145 |
| Thermomechanical Treatment, Microstructure and Properties of Ultrafine Grained Steels <i>R. Song, D. Ponge, D. Raabe, R. Kaspar</i> | 149 |
| Precipitation Behaviour and Mechanical Properties of (Ni,Fe)Al-Strengthened Fe-Al-Ni-Cr Alloys <i>C. Stallybrass, A. Schneider, G. Sauthoff</i> | 153 |
| Theoretical and Experimental Investigations of Structure Type Variations of Laves Phases <i>F. Stein, M. Palm, J. Konrad, D. Jiang, G. Sauthoff</i> | 157 |
| Relation of Stress Anomaly and Order-Disorder Transition in Fe ₃ Al-Based Ternary and Quaternary Alloys <i>F. Stein, A. Schneider, G. Frommeyer</i> | 161 |
| Non-Destructive, <i>in-situ</i> Measurement of De-Adhesion Processes at Buried Adhesive/Metal Interfaces by means of a New Height-Regulated Scanning Kelvin Probe Blister Test <i>K. Wapner, B. Schönberger, M. Stratmann, G. Grundmeier</i> | 165 |
| Investigation of the Bainitic Phase Transformation in a Low Alloyed TRIP Steel Using EBSD and TEM <i>S. Zaefferer</i> | 169 |



Inter-Departmental Research Activities

New Steels

The development and characterization of new steels is one of the major fields of activity of the Institute. Four departments are involved in this field. The topics are: new steels with improved mechanical properties (strength, ductility, fracture toughness, creep resistance), impact resistance, and leaner chemical compositions with better recyclability. In addition, steels with very fine grained and stable microstructures, which can be formed superplastically at high strain rates, exhibit a high potential for applications. Apart from the bulk properties, the surface properties of new steels are of high importance in particular with respect to improved corrosion resistance and other functional characteristics.

The improvement of the creep-resistance of new martensitic/ferritic 12% Cr steels in power plants by precipitation of the WFe_2 Laves phase besides carbonitrides is a major task, which is worked on in the Physical Metallurgy Department by the High Temperature Materials Group (*Sauthoff, Knežević*). The respective alloy design is strongly supported by theoretical simulations of the Phase Equilibria and Transformation Group (*Inden*).

The Thermomechanical Processing Group (*Ponge*) in the Microstructure Physics and Metal Forming Department is designing innovative concepts of thermomechanical processing and employing these to achieve ultra fine-grained (UFG) microstructures in C-Mn steels with 0.15 to 0.3 %C. Another innovative steel project aims at fine-grained materials produced by warm deformation (*Storojeva, Song, Kaspar, Ponge*). A third project is centred on high-strength long products with improved toughness and fatigue properties (*Detroy, Kaspar, Ponge*).

The Innovative Steel Research Group of the Materials Technology Department has focused its activities on the development and characterisation of ultrahigh strength and ductile *super* TRIP steels. In the thermomechanically processed state these metastable austenitic/martensitic chromium-nickel/manganese-molybdenum steels exhibit flow stresses of the order of 1850 to 2000 MPa and true tensile stresses up to 3400 MPa with 25 to 30 % tensile ductility. The extremely high strength due to extensive work hardening stress exponent of about $n = 0.7$ –

is caused by severe martensitic $\gamma_{fcc} \rightarrow \alpha_{bcc}^{Ms}$

transformation, high dislocation density in the austenite and martensite, and dispersion hardening of nanosized special carbides. These unique *super* TRIP steels achieve almost the theoretical strength of ferrous alloys and the energy absorption in impact tests is outstanding. Because of their chemistry, the corrosion resistance is markedly improved compared to conventional TRIP steels (*Frommeyer*).

High manganese and aluminium lightweight steels with higher carbon content fulfil the requirements of new design concepts of the automotive industry because of their high strength of about 700 to 900 MPa, elongations to failure of 55 to 70 % and reduction in density of about 12 to 16 %. The high strength and ductility is due to a triplex microstructure consisting of an austenitic matrix, ferrite and nanodispersed κ -carbides. These steels show homogeneous shear band formation in tension providing the SIP (shear-band-induced plasticity) effect (*Frommeyer, Brück*).

Newly designed high-strength chromium-aluminium ferritic stainless steels containing about 6.5 to 7 mass% Cr and Al exhibit excellent corrosion resistance under environmental conditions and a considerable reduction in specific weight of about 10 %. These steels are studied with respect to microstructure - property relations and applications as lightweight steels used in modern transportation systems. Another important aspect is the use of these low cost steels with their excellent formability for the realisation of the space frame concept with steel in future automotive technologies (*Brück, Frommeyer*).

Beside the bulk properties of new steels, the surface properties deserve great attention. In particular, the high amount of residual inert oxides on the surface after reductive treatments is a problem of high technological importance and has been chosen as one of the focal points for research in the Interface Chemistry and Surface Engineering Department. An aim of the Molecular Structure Group is to understand the wetting behaviour of liquid zinc at partially oxidised surfaces (*Rohwerder*). Novel high-performance thermal pre-treatments are developed by the High Temperature Reaction Group (*Spiegel*). The Corrosion and Electrochemistry Group studies the corrosion properties and mechanisms of the regarded steels (*Hassel*). Special emphasis lays on understanding the relationship between



microstructure and reactivity. Microelectrochemical methods are employed in order to study the corrosion differences on or in the vicinity of welds and also different corrosion rates on single grains with different orientation. Two classes of steels from the Materials Technology Department of the MPIE are presently in the focus of corrosion investigations: high manganese TRIP/TWIP steels for automotive applications and FeCrAl ferritic steels as low cost stainless steels (*Hassel*).

Related Projects

Brokmeier, Frommeyer: Investigations on newly developed ultrahigh-strength quasi perlitic steels with extremely fine lamellar microstructure

Brüx, Brokmeier, Frommeyer: Characterization of the mechanical properties and microstructure evolution of modified high manganese TRIP/TWIP steels in dependence on temperature and strain rate

Brüx, Frommeyer: Investigations on deep and stretch forming operations of iron-aluminium-chromium light-weight steels

Frommeyer, Brüx: Correlations between microstructures, deformation and strengthening mechanisms of high-strength and supraductile TRIPLEX steels exhibiting pronounced shear band induced plasticity (SIP effect)

Frommeyer, Brüx: Development of new ultrahigh-strength SUPER TRIP steels and investigations on strengthening and deformation mechanisms

Frommeyer, Jiménez: Investigations on fine structure superplasticity and superplastic deformation mechanisms in ultrahigh carbon steels with aluminium and tin forming κ -carbides

Gnauk, Frommeyer: Modelling of superplastic bonding and superplastic forming processes

Hassel, Lill, Spiegel, Sauerhammer, Stratmann, Brüx, Frommeyer: Alloy development, investigation and improvement of the properties of newly developed high strength and supraductile TRIP/TWIP steels for reinforced and crash absorbing vehicle compounds

Hassel, Stratmann, Frommeyer: Corrosion performance of new class of FeCrAl light weight ferritic steels

Ponge, Kaspar, Detroy: High strength long products with improved toughness and fatigue resistance

Ponge, Kaspar, Song: Ultra fine grained steel produced by innovative deformation cycles

Ponge, Kaspar, Storojeva: Heavy warm rolling for the production of thin hot strips

Sauthoff, Inden, Schneider: Ferritic steels with maximum creep resistance



Iron Aluminium Based Materials

The joint research activity on iron aluminium alloys and iron aluminide based materials Fe-Al based alloys for short - currently includes about twenty projects, many of them joint projects of the four departments Materials Technology (*Schneider* (coordinator), *Frommeyer*), Physical Metallurgy (*Palm* (coordinator), *Sauthoff*, *Stein*), Interface Chemistry and Surface Engineering (*Hassel*, *Spiegel*), and Microstructure Physics and Metal Forming (*Zaefferer*, *Raabe*).

Because a sound knowledge on phase diagrams provides the basis for any material development a number of selected base systems are studied with respect to phase equilibria and phase transformations, e.g. the systems Fe-Al-Mo (*Eumann*, *Sauthoff*, *Palm*), Fe-Al-Zr (*Stein*, *Sauthoff*, *Palm*), Fe-Al-Ti (*Ducher**, *Stein*, *Viguier**, *Palm*, *Lacaze**; *: CIRIMAT, Toulouse), Fe-Al-Ta (*Risanti*, *Schneider*, *Sauthoff*), and Fe-Al-C-X (*Falat*, *Schneider*, *Sauthoff*, *Frommeyer*). In this context the actual distribution of the elements within the lattice in dependence of temperature and composition, i.e. ordering and the degree of order, is of vital interest, which has been studied for a number of Fe-Al-X systems by field ion microscopy (*Dege*s, *Schneider*, *Frommeyer*). A detailed account on the investigation of Fe-Al-Ni-Cr alloys by 3-dimensional atom probe is given as „selected scientific topic“ (*Schneider*, *Stallybrass*, *Sauthoff*, *Cerezo**, *Smith**; *: Dept. of Materials, Univ. Oxford). The effect of carbon and vacancies on anelastic relaxation in Fe-Al-X (X = Nb, Ti) alloys has been studied by mechanical and positron annihilation spectroscopy combined with radiotracer diffusion (*Stein*, *Golovin**; *: Institute for Materials, TU Braunschweig).

The above studies reveal that a variety of quite different microstructures can be produced within Fe-Al based alloys and it is therefore possible to vary the mechanical properties considerably by appropriate microstructural engineering. One focus lies on strengthening Fe-Al based alloys at high temperatures. Strengthening by precipitates has been investigated e.g. within the above mentioned studies on the Fe-Al-X (X = Mo, Zr, Ta, C) systems. In many cases these precipitates are Laves phases. In order to understand the deformation behaviour of respective alloys, Fe-Al polycrystals strengthened with a Zr-containing Laves phase have been investigated by high-resolution transmission electron microscopy before and after plastic deformation (*Wasilkowska**, *Bartsch**, *Stein*, *Palm*, *Sauthoff*, *Messerschmidt**; *: MPI für Mikrostrukturphysik,

Halle). Besides strengthening by incoherent precipitates of intermetallic phases or carbides also the possibility of generating coherent microstructures exists. Thus, novel ferritic superalloys can be produced which are described in another „selected scientific topic“ (*Stallybrass*, *Schneider*, *Sauthoff*). Strength may also be increased by ordering and this effect has been studied in detail for Fe-Al-Ti alloys (*Palm*, *Sauthoff*).

A prominent feature of Fe-Al based alloys is the anomalous behaviour of the flow stress with temperature. It has long been discussed that this is associated with the D0₃/B2 ordering transition, but a careful analysis of the mechanical properties combined with investigations of the ordering transition by differential thermal analysis showed no direct correlation as shown in another „selected scientific topic“ (*Stein*, *Schneider*, *Frommeyer*). Besides strength at high temperatures, brittleness at ambient temperatures is a concern for Fe-Al based alloys. Therefore, in a fundamental study, the brittle-to-ductile transition temperatures of binary Fe-Al alloys have been investigated (*Risanti*, *Dege*s, *Falat*, *Kobayashi*, *Konrad*, *Palm*, *Pöter*, *Schneider*, *Stallybrass*, *Stein*).

An important aspect for every material is the possibility of forming, about which little knowledge exists for Fe-Al based alloys. Therefore, the hot rolling behaviour (*Konrad*, *Schneider*, *Zaefferer*, *Frommeyer*, *Raabe*) and control of recrystallisation of wrought alloys (*Kobayashi*, *Zaefferer*, *Schneider*, *Frommeyer*, *Raabe*) have been studied.

Fe-Al based alloys are well-known for their excellent oxidation and corrosion resistance, although the underlying mechanisms are not well established. Therefore the initial stages of Fe-Al oxidation are studied by thermogravimetry and in-situ with a heating stage within a scanning electron microscope (*Pöter*, *Stein*, *Spiegel*). In a further study the effect of metal dusting is studied (*Bernst*, *Spiegel*, *Schneider*). Fe-Al-Cr alloys with Al- and Cr-contents between 6 and 7 wt. % show good electrochemical resistance in acidic environment. The corrosion behaviour and the nature and the composition of passive films formed on single grains of various Fe-Al-Cr alloys have been investigated with a scanning droplet cell (*Lill*, *Hassel*, *Stratmann*, *Frommeyer*).

To communicate and discuss the results of the aforementioned projects a discussion meeting was held at the MPIE on March, 9th 2004. Besides an invited introductory presentation by D. Morris, CENIM



Madrid, fourteen oral talks and eight posters were presented. The workshop attracted an audience of about 70 people, many of them from industry, demonstrating the large interest in Fe-Al based alloys. The proceedings of the discussion meeting will be published as a special issue of *Intermetallics* in 2005.

Related Projects

Deges, Frommeyer, Schneider: Effect of ternary alloying additions on mechanical properties and ductility of Fe₃Al-Based alloys

Frommeyer, Deges, Boehnke, Denkena* (*IFW Univ. Hannover)*: Machining of iron-aluminium-alloys: Mechanisms of chip formation and reasons for wear

Palm, Lacaze (CIRIMAT, Toulouse): Re-investigation of the Fe-Al-Ti system

Palm, Schneider, Frommeyer: Development of Fe-Al-based alloys

Sauthoff, Schneider, Risanti: Deformation behaviour of Fe-Al-Ta alloys

Sauthoff, Schneider, Stallybrass: Ferritic Fe-NiAl superalloys

Schneider, Frommeyer, Sauthoff, Krein: Microstructures and mechanical properties of Fe₃Al-based alloys with strengthening boride precipitates

Schneider, Palm, Frommeyer, Milenkovic: Determination of phase equilibria and directional solidification of Fe-Al-Nb alloys

Schneider, Spiegel, Bernst: Metal dusting of Fe-Al

Schneider, Zaefferer, Frommeyer, Raabe, Konrad: Investigations of microstructures and hot deformation behaviour of Fe₃Al-based alloys

Spiegel, Stein, Pöter: Initial stages and kinetics of oxidation of binary and ternary iron-aluminides

Stein, Golovin (Institute for Materials, TU Braunschweig): Investigations of internal friction behaviour in Fe₃Al-based alloys

Zaefferer, Schneider, Frommeyer, Raabe, Kobayashi: Optimisation of texture and microstructure of Fe₃Al-based alloys



Carburisation and Metal Dusting

The high temperature corrosion process, metal dusting, attacks conventional high temperature alloys in petrochemical plants. This corrosion process results in a detachment of metal particles being embedded in a carbon deposit (coke, see figure). Joint activities in this field are performed to understand the underlying mechanisms (*Schneider, Spiegel, Inden*). With this understanding new high-temperature materials being resistant against metal dusting can be developed. The central research activities on carburisation and metal dusting are focussing on investigations of the high-temperature reactions using classical methods such as thermogravimetry and also surface analytical techniques such as Auger electron spectroscopy (AES) and X-ray induced photoelectron spectroscopy (XPS) (*Spiegel*). Cross-section preparation for TEM

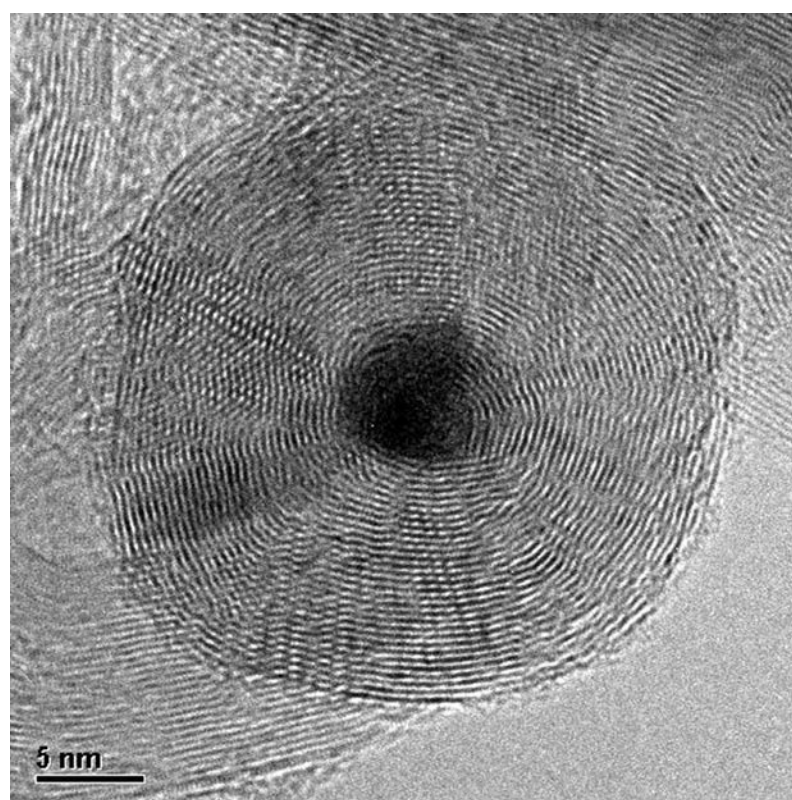
analyses of the reaction interfaces has been successfully tested. The materials under investigation are pure iron, iron aluminium and nickel-based alloys (*Schneider*).

Related Projects

Schneider, Grobert (Department of Materials, Oxford University, UK): High-resolution transmission electron microscopy, EELS and EDX studies of coke

Schneider, Inden, Bernst: Carburisation of diffusion couples

Schneider, Spiegel, Bernst: Metal dusting of iron aluminium alloys



High-resolution transmission electron micrograph depicting an iron-encapsulated graphitic carbon nanoparticle commonly found in coke. (N. Grobert, Department of Materials, Oxford University, UK).



Microstructure and Reactivity

Four groups from three departments of the institute are presently involved in the joint research activity on the relation between microstructure and reactivity: Interface Chemistry and Surface Engineering (*Hassel (coordinator), Spiegel, Stratmann*), Microstructure Physics and Metal Forming (*Ponge, Zaefferer, Raabe*), Materials Technology (*Schneider, Frommeyer*).

The correlation between microstructure and reactivity has gained more and more attention due to the progress in experimental techniques able to assign local reactivity differences to structural properties of the material. A detailed understanding of how the microstructure influences the reactivity may provide the possibility to control the reactivity in small areas. Hence, it would allow the implementation of new properties into a material by means of controlling its micro- or nanostructure.

A new class of FeCrAl light weight ferritic steels is investigated with respect to their corrosion behaviour. Some compositions display large differences in the dissolution speed of certain grains. The combination of a microstructure analysis as obtained from Electron Backscatter Diffraction EBSD followed by electrochemical investigations on single grains by means of a scanning droplet cell (SDC) demonstrated that the dissolution rate is 60% larger on (001) grains as compared to (111) grains (*Lill, Hassel, Stratmann, Frommeyer*).

TWIP/TRIP steels have recently attracted a significant industrial interest. Due to their extraordinary mechanical properties and their lower specific density a significant weight reduction of crash relevant parts can be achieved for applications in the automotive industry. Their microstructure can undergo critical changes e.g. within a weld or its heat influenced zone. Reactivity imaging is performed with scanning electrochemical techniques such as scanning Kelvin probe or SDC (*Lill, Hassel, Sauerhammer, Spiegel, Stratmann, Brück, Frommeyer*).

Nanotechnology became part of this central research activity in 2004 with the application of unidirectional solidification of eutectics. It produces fibrous or lamellar structures of two adjacent phases. With respect to their different chemical composition the reactivity differences are tremendous. In case of the quasibinary eutectic NiAl-Re each phase can be selectively inhibited, passivated etched or even

dissolved which opens a wide field of applications (details are described in the selected topic which is part of this report) (*Hassel, Schneider, Bello Rodriguez, Milenkovic*).

Grain orientation dependent phenomena i.e. nucleation of oxides and segregation of non-metallic elements are studied at high temperatures with focus on Fe-Cr, Fe-Al and model alloys (*Spiegel, Park, Poeter, Swaminathan, Parezanovic*). On iron, strongly different oxide nucleation rates and composition were found on (200) and (310) lattice planes. Degradations studies on native oxides and model oxide systems in aggressive environments (HCl, H₂O) are carried out and correlated to the chemical composition and electronic properties (*Spiegel, Asteman, Hassel, Lill, Park*).

The aim of another project is the joint investigation of single crystal plastic deformation and the electrochemical potential. A Fe-3%Si single crystal was deformed by a bending test. Such boundary conditions create a gradient of the plastic strain. This mechanical gradient corresponded very well to the observed changes of the electrochemical potential (*Schultze, Raabe*).

Related Projects

Hassel, Lill, Frommeyer, Stratmann: Corrosion behaviour of ferritic FeCrAl light weight steels

Hassel, Lill, Spiegel, Sauerhammer, Stratmann, Brück, Frommeyer: Alloy development, investigation and improvement of the properties of newly developed high strength and supraductile TRIP/TWIP steels for reinforced and crash absorbing vehicle compounds

Hassel, Schneider, Bello Rodriguez, Milenkovic: Production of nanowire arrays through directional solidification and their application

Schultze, Raabe: On the correlation of the plastic deformation and the electrochemical potential

Spiegel, Asteman, Hassel, Lill, Park: Stability of oxide scales

Spiegel, Park, Poeter: Initial stages of oxidation

Spiegel, Swaminathan, Parezanovic: Oxidation and segregation



Surface Mechanics and Adhesion

Surface mechanics and adhesion is a central research activity that considers the mechanical properties and forming behaviour of coatings on metals. The expertise of the Department of Microstructure Physics and Metal Forming (*Raabe*) in the understanding of forming operations, the mechanical properties of metal surfaces and the simulation of metal surfaces during forming is combined with the expertise in surface tailoring of metals of the department of Interface Chemistry and Surface Engineering (*Stratmann*). Within the Adhesion and Thin Films research group (*Grundmeier*), thin functional wear resistant and plasma polymer films with a thickness between 10 and 200 nm are deposited on model substrates. Especially, polymer/metal and organic/inorganic nano-composite as well as multilayer films are of interest. Recently, Ag-nanoparticle containing, thin Teflon like plasma polymer films have been synthesised.

The mechanical properties and adhesion of these films are then studied by means of the nano-indentation and nano-scratch technique. Simulation of the experimental data is done in close collaboration with Prof. Raabe's department. The nano-indentation of metal surfaces and metal coatings is simulated by use of crystal plasticity FEM (Finite Element Method), which is implemented into the commercial FEM software (MSC.Marc) by means of user subroutines. In this way, the full crystalline anisotropy (elastic and plastic) of the material and its develop-

ment (e.g. orientation change of the crystal) during the test are taken into account. For polymer coatings and their adhesion behaviour, suitable material laws have to be evaluated.

Moreover, the formability of surface layers is of common interest. Within the department of Prof. Stratmann, the focus is on the formation and reactivity of defects in thin interfacial films (*Rohwerder*) and on interfacial crack formations and disbonding during forming (*Grundmeier*).

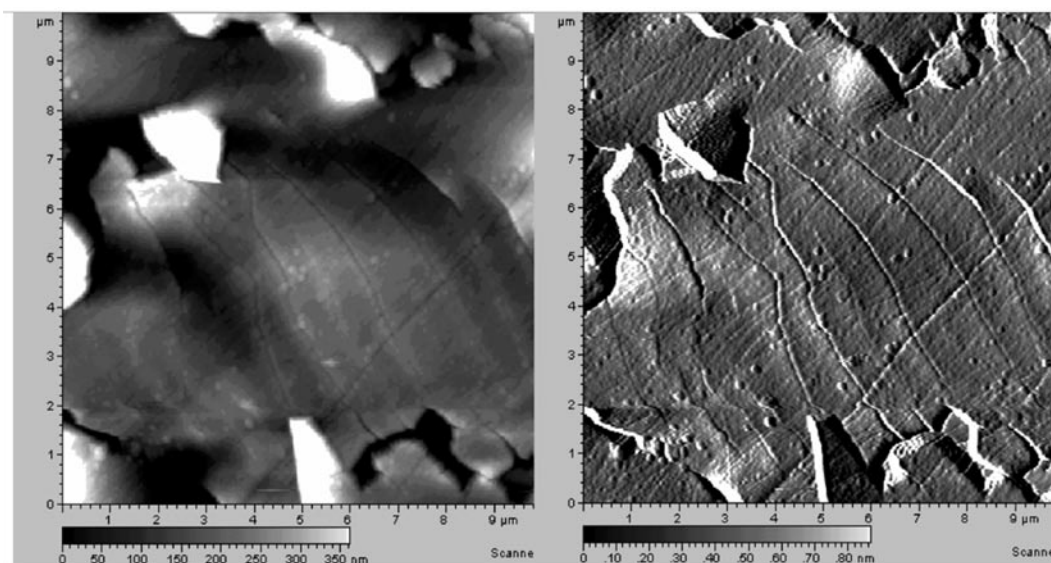
The complimentary activities in the department of Microstructure Physics and Metal Forming moreover focus on the simulation of the topologic development of the metallic surface (change of roughness etc.) during the forming process. Crystal plasticity FEM will be used to first simulate the uncoated material to be followed by a study on the influence of the coating on the surface development.

Related Projects

Baumert, Rohwerder: Forming of corrosion protecting plasma polymer films on steel sheet

Wang, Raabe, Grundmeier: Nanomechanical properties of functional multilayer and nanocomposite plasma polymer films

Yang, Ebbinghaus, Grundmeier: Nanomechanical properties of thin plasma polymers on soft and hard substrates



Plasma polymer-coated, mechanically polished zinc after 8 % linear stress was applied. a) Topography (z-range: 350 nm, scan range: 10 μm) and b) corresponding deflection image. (Stress direction: ↗)



Numerical Modelling

The departments of the institute put considerable effort into microstructure simulation, so far with emphasis on the individual perspectives of the respective working fields and in collaboration with the experimental groups of the respective departments. However, for the future it is planned to also couple the simulation efforts of the different research groups, e.g. in the field of forming of coated steel sheets (*Blumenau, Roters*).

In the department of Prof. Raabe, the group of Dr. Roters is developing a non local dislocation density based constitutive law, which can be used in classical Crystal Plasticity FEM as well as in the Texture Component Crystal Plasticity FEM developed by the group (*Roters, Ma*). As deformation gradients (non local model) are taken into account, the simulation of non homogenous deformation modes such as nanoindentation will profit from this extension of the constitutive model. Additionally the ability to calculate dislocation densities is important as input for successive simulations of recrystallisation and grain growth. These are simulated using the cellular automaton method (recrystallisation) and the Monte Carlo method (grain growth). The dislocation density (stored energy) is an important input for such simulations and can now be derived from crystal plasticity simulations together with the orientation information. The crystal plasticity simulations of nanoindentation will be extended to incorporate polymer coatings (*Roters, Zaafarani, Blumenau*). While models from literature will be used to simulate the polymer, the information about the metal polymer interface will be provided by the group of A. Blumenau.

The properties of metal/metal-oxide/polymer interfaces are calculated on an atomistic scale (*Blumenau*). In particular for the oxide/polymer interfaces on the one hand quantum mechanical effects play an important role for the bonding, on the other hand atomistic model structures have to be sufficiently large to give a good representation of real and relevant structures. Therefore ab-initio methods, Density Functional Theory (DFT) and more approximate methods such as density functional based tight binding (DFTB) are combined in multiscale approaches. The methods and codes applied are DFTB, developed and maintained at the University of Paderborn (Frauenheim), AIMPRO, a localised basis DFT-pseudopotential code developed in the UK (Jones, Univ. o. Exeter and Briddon, Univ. of Newcastle), and various commercial ab-initio/

quantum chemistry implementations. In the case of DFTB and AIMPRO, a close collaboration with the maintaining groups allows to modify the code according to the needs in oxide/polymer interface modelling. Results, such as the stable atomistic and electronic structures, will allow to analyse the nature of the bonding at the interface, model vibrational spectra, and more. Hence they will give deeper insight into adhesion and delamination phenomena. Furthermore parameters obtained in ab-initio modelling can be transferred to FEM-methods (*Roters*) to allow an ab-initio based FEM-modelling of coated metal sheets.

Phase equilibria in multi-component systems are calculated based on the so called CALPHAD approach (*Schneider, Inden*). For some alloy systems the thermodynamic parameters have to be optimised by assessing results of constitution experiments and also of ab-initio calculations. The numerical treatment of diffusion controlled phase transformations in multi-component systems is performed using the DICTRA software, which was developed in cooperation between the MPIE (*Inden*) and the KTH Stockholm (*Ågren*). The treatment is based (a) on the concept of sharp interfaces, (b) on local equilibrium at moving interfaces, (c) on thermodynamic driving forces obtained from the CALPHAD approach for computational thermodynamics, (d) on mobilities rather than diffusivities. It embraces isothermal, non-isothermal conditions and various geometries. In order to treat microstructure formation and the competition between growing phases, space may be subdivided into cells which are coupled by appropriate boundary conditions.

The calculation of phase and microstructure formation during solidification is done with a macroscopic approach, based on the generalised enthalpy method. Microstructure is calculated as averaged values for each volume element to describe its macroscopic behaviour. In contrast to other treatments for morphological evolution like the phase field method, the number of coexisting phases does not significantly influence the calculation effort. To perform these calculations, the phase equilibria have to be recalculated to be accessible in the needed HX representation. In addition to the CALPHAD approach, the given basic data is used to recalculate the phase diagram in this alternative way to be able to ignore phase boundaries and interface problems (*Gnauk, Wenke, Frommeyer*).



The behaviour of superplastic forming will be modelled in an FEM environment. Up to now, only isotropy is regarded. In combination with the crystal plasticity model of Roters, anisotropy could be included into the calculations (*Frommeyer, Gnauk*).

Related Projects

Joulaeizadeh, Grundmeier, Blumenau: Simulation of the chemical structure and adhesive properties of plasma grown metal oxide surfaces

Laaboudi, N.N., Rohwerder, Blumenau: Numerical modelling / lifetime prediction of delamination polymer coating disbonding and material degradation

Roters, Ma: Development of a non local dislocation density based constitutive law for crystal plasticity FEM with special consideration of grain boundaries

Roters, Zaafarani: Simulation of nanoindentation of polymer coated aluminium samples

Schneider, Inden, Eleno: Development of a thermodynamic database of high-temperature materials

Schneider, Inden, Strondl: Numerical modelling of steel transformations

Vakat



Research Activities within the Departments

Department of Physical Metallurgy

P. Neumann (until May 2004),

G. Sauthoff (May - Nov. 2004, provisional)

The macroscopic properties of steels are controlled to a large extent by their microstructure down to configurations and defects on the atomistic scale. These property-microstructure relationships have been studied in the department.

Steels with complex property profiles require the addition of many alloying elements. The determination of phase equilibria in such multi-component systems has been an important aspect of our studies. With the help of suitable models for the thermodynamic description of multi-component systems the phase equilibria were calculated numerically with high reliability. In this way the number of experiments, which are necessary to characterise the alloys can be reduced dramatically. The complexity of metallic alloy systems with their variety of different phases is an almost inexhaustible reservoir for new materials developments. However, such a complexity impedes their quantitative predictability. Therefore it has been an important task of the department to foster the knowledge of the thermodynamic description of the most important metallic alloy systems by using fundamental models of solid state physics as well as by experimental thermodynamic characterisation.

An outstanding example of this work is the development of a new thermodynamic database for ferritic steels which is now being used for supporting the development work on martensitic/ferritic creep-resistant steels for applications in conventional power plants at service temperature of 650 °C. In this database the element Ta was included in the phase descriptions of the intermetallic Laves phase and μ -phase for the first time. However, soon after completion new experimental results (Joubert) and ab initio calculations (Sluiter) were presented at the CALPHAD conference in May 2003 which showed that the usual three-sublattice description of the μ -phase is not appropriate and a five-sublattice description is mandatory with a four-sublattice version as acceptable simplification. In a cooperation with the Institute of Physics of Materials of the Czech Academy of Science in Brno ab initio calculations were performed. With these data the existing database could be updated and improved also with respect to the description of the Laves phase. This new database is the only one presently existing that

allows to calculate the existence of domains and solubility limits of the intermetallic phases. The scarce experimental data available are correctly reproduced. For details the reader is referred to the respective selected topic by *J. Balun et al.*

The kinetics of phase transformations in multi-component systems is even more complex than phase equilibria. This yields an unbelievable multiplicity of reactions. As an example, the reaction rate can be changed by orders of magnitude by changing the temperature during some heat treatment by a few tens of degrees or by adding small amounts of alloying elements below a tenth of a percent. Computer simulations helped to predict the development of transformations in time and allowed to determine the local distribution of elements and phases down to microscopic dimensions.

In particular, the precipitation reactions in model alloys of Fe-Cr-C, Fe-Cr-W-C, Fe-Cr-Si-C, and Fe-Cr-Co-V-C have been simulated in view of the already mentioned development of martensitic/ferritic steels for application at 650 °C. Important results on the competing precipitate reactions of the occurring stable and metastable phases have been obtained which allows for predicting the long-term evolution of the microstructures. This work is described in more detail in the selected topic by *A. Schneider and G. Inden.*

New demands - applications at higher temperatures, light weight constructions - require continuous development of new materials. As an example, the improvement of the thermodynamic efficiency of energy conversion is limited by the high temperature properties of materials with high enough toughness. In order to obtain a good combination of the creep resistance of ceramics and the toughness of metals, intermetallic phases are promising candidates. Aluminium or silicon forms dense oxide scales and thus provides a good oxidation resistance on respective alloys. Thus intermetallic alloys on the basis of the aluminides of titanium, iron and nickel and a number of silicides are most attractive for high-temperature applications. Such alloy systems offer a multitude of alloying possibilities and open a wide field for research, which has been focussed on

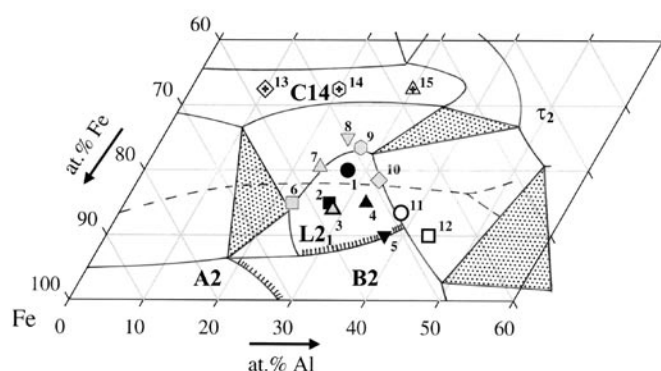


Fig. 1: Isothermal section of the Fe-rich part of the Fe-Al-Ti system at 900 °C with compositions of tested alloys 1 - 15 (A2, B2, L2₁, C14: phases with the respective structures; τ₂: τ₂ phase; second-order transitions are given as hatched lines). In addition the position of the eutectic trough for liquid + Laves phase + α Fe-Al-Ti solid solution is projected onto the isothermal section and given as interrupted line.

the design of novel materials with optimisation of strength, toughness and hot-corrosion resistance by control of alloy composition and phase distribution.

The work has been concentrated during the last two years on Fe-Al-base alloys which are highly promising for high-temperature applications because of their outstanding oxidation and corrosion resistance, comparatively high thermal conductance and low thermal expansion, strengthening through atomic ordering (with a transition from A2 structure, i.e. bcc disorder, to ordered D0₃ structure and B2 structure with increasing Al content) and manifold possibilities of precipitate hardening through ternary alloying.

Of particular interest is the Fe-Al-Ti system since the adding of Ti stabilises the D0₃ structure, which is then known as L2₁ structure, and produces Laves phase precipitates depending on the Ti content. Single-phase Fe-Al-Ti alloys with the Heusler-type L2₁ structure and two-phase L2₁ Fe-Al-Ti alloys with MgZn₂-type Laves phase or Mn₂₃Th₆-type τ₂ phase precipitates – see Fig. 1 – were studied with respect to hardness at room temperature, compressive 0.2% yield stress at 20 to 1100 °C, brittle-to-ductile transition temperature (BDTT), creep resistance at 800 and 1000 °C and oxidation resistance at 20 to 1000 °C. At high temperatures the L2₁ Fe-Al-Ti alloys show considerable strength and creep resistance which are superior to those of other iron aluminide alloys. Alloys with not too high Ti and Al contents exhibit a yield stress anomaly with a maximum at temperatures as high as 750 °C. BDTT ranges between 675 and 900 °C. Oxidation at 900 °C is controlled by parabolic scale growth. In view of the present results, the Fe-Al-Ti alloys on the base of the L2₁-ordered Fe₂(Fe,Ti)Al phase are promising for further development for high-temperature applications due to their improved strength at high temperatures in combination with a high oxidation resistance. The properties of these alloys, like those of other Fe-Al alloys, are controlled sensitively not only by the aluminium and/or titanium content, but

also by heat treatments which control the phase formation, atomic order in the phases and all other aspects of microstructure. This opens a wide range of possibilities for optimising L2₁-ordered Fe-Al-Ti alloys with respect to strength, ductility and oxidation resistance (M. Palm).

Various types of Laves phases can be precipitated in ternary Fe-Al alloys depending on the ternary alloying element. As is discussed in the selected topic by F. Stein, M. Palm and G. Sauthoff, Laves phases are the most frequent intermetallic phases at all and can crystallize in three different structure types. In many transition metal systems, two or three Laves phase polytypes coexist in equilibrium showing temperature, composition and/or pressure-dependent transformations. Existing models based on geometric and electronic factors fail in predicting the occurrence and structure type of Laves phases. The most striking example for this is the Nb-Co phase diagram. From detailed investigations of structure, stability and homogeneity ranges of Laves phases in selected binary and ternary systems and by an extensive inspection of literature data, some general rules for structure type variations of Laves phases have been derived.

A Laves phase with highest hardness and yield stress is obtained by alloying the intermetallic B2 phase FeAl with Ta. Fe-Al-Ta alloys with the ternary Laves phase Ta(Fe_{0.5+x}Al_{0.5-x})₂ have been studied experimentally with the objective of clarifying the effect of Laves phase precipitation and atomic ordering on the deformation characteristics of such Fe-Al-base alloys. The present study concentrates on the hardening effect of the Laves phase in ordered and disordered Fe-Al-Ta alloys with Al contents between 16 and 45 at.% showing the A2 disorder or the D0₃ or B2 order. Ta has a low solubility in Fe-Al alloys which is beneficial for slowing down precipitate coarsening. Small amounts of Laves phase together with atomic ordering increase the yield stress and affect ductility in a complex way – see Fig. 2. The alloys with 1% Ta exhibit a high oxidation resistance.

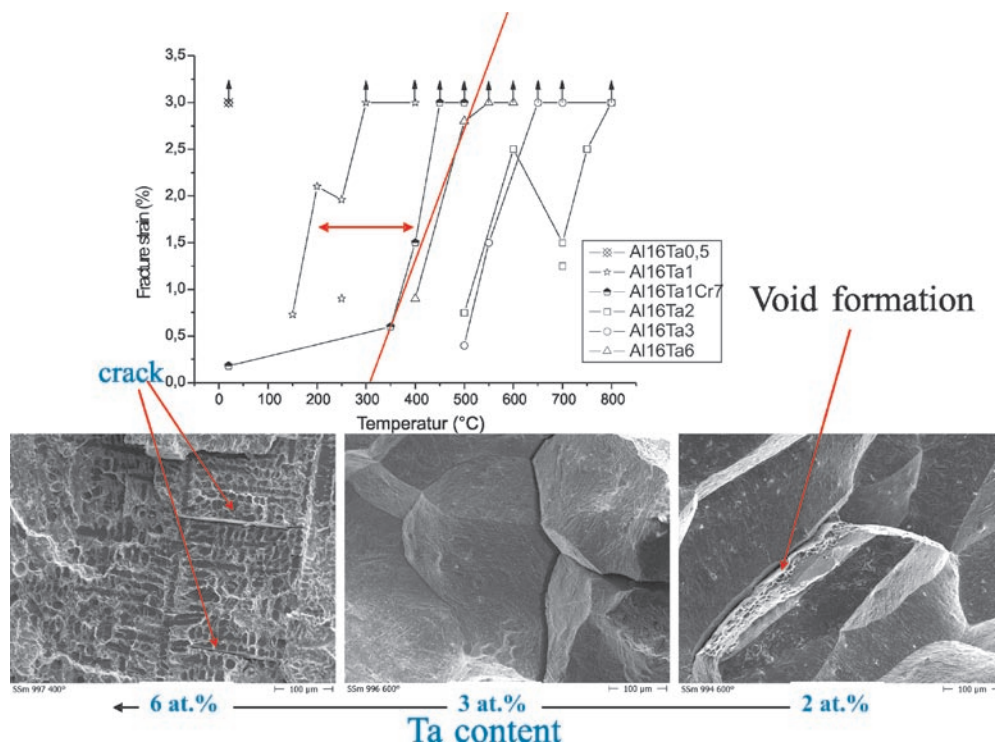


Fig. 2: Flexural fracture strain (4-point bending tests) as a function of temperature for disordered Fe-16 at.% Al alloys with various contents of Ta and Cr with scanning electron micrographs of fracture surfaces.

The continuing work aims at adjusting the Al and Ta content for an optimum relation of high-temperature strength and low-temperature ductility with maintaining a sufficient oxidation resistance (*D.D. Risanti, G. Sauthoff*).

Besides hardening Fe-Al alloys by the coarsely distributed incoherent Laves phase, there is the possibility of producing a fine coherent precipitate of the intermetallic NiAl phase. Strengthening through a homogeneous distribution of a second phase is a concept that is widely employed in high-temperature materials, the most prominent among which are nickel-based superalloys, which owe their high-temperature strength to finely dispersed Ni₃Al particles. It is shown that similar microstructures can be obtained in the Fe-Al-Ni-Cr system with ordered (Ni, Fe)Al precipitates in a ferritic matrix. These precipitates lead to higher levels of yield strength at elevated temperatures compared to conventional iron-base high temperature alloys. Thus the present Fe-Al-Ni-Cr alloys may be regarded as ferritic Fe-base superalloys. The results show that the investigated materials exhibit the highest yield strength after solution heat treatment and lower values after aging, indicating precipitation of fine particles during air cooling. The decrease of yield strength in the latter case was more pronounced for alloys with a high precipitate content than for leaner alloys. The details are described in the selected topics by *C. Stallybrass et al.* and by *A. Schneider et al.*

Apart from the work on the hardening of Fe-Al-base alloys, the development work on the martensitic/

ferritic 12%Cr steels is continued for increasing the creep resistance for applications at 650 °C. This is to be achieved through additional precipitation of the Laves phase besides the conventionally used carbides. Thus different types of precipitates, which block the movement of subgrain boundaries ($M_{23}C_6$, Laves phase) and dislocations (MX carbonitrides) and delay coarsening of the microstructure, are used for hardening. The aim is to produce a sequence of precipitates with differing kinetics using the slowly precipitating Laves phase for additional strengthening during coarsening and over-aging of $M_{23}C_6$. Additionally, various MX forming elements are used to determine the most effective combination of alloying elements for obtaining high amounts of finely distributed coherent or semicoherent particles with maximum strengthening effect. Cobalt and copper are used to achieve an initially 100% martensitic microstructure and moreover to slow down diffusion processes and to provide uniformly distributed nucleation sites for Laves phase precipitation. The results of long term creep tests have shown beneficial effects of Laves phase precipitation during high temperature exposure on the strengthening of W bearing 12%Cr martensitic/ferritic steels. Apparently, the addition of tantalum affects the Laves phase besides the effect on MX precipitation. The alloying with both vanadium and tantalum has further improved the creep strength. This is supported by ThermoCalc calculations which predict high amounts of MX carbonitrides precipitating in the solid state (at 650 °C). Only small amounts of Ti-MX carbo-

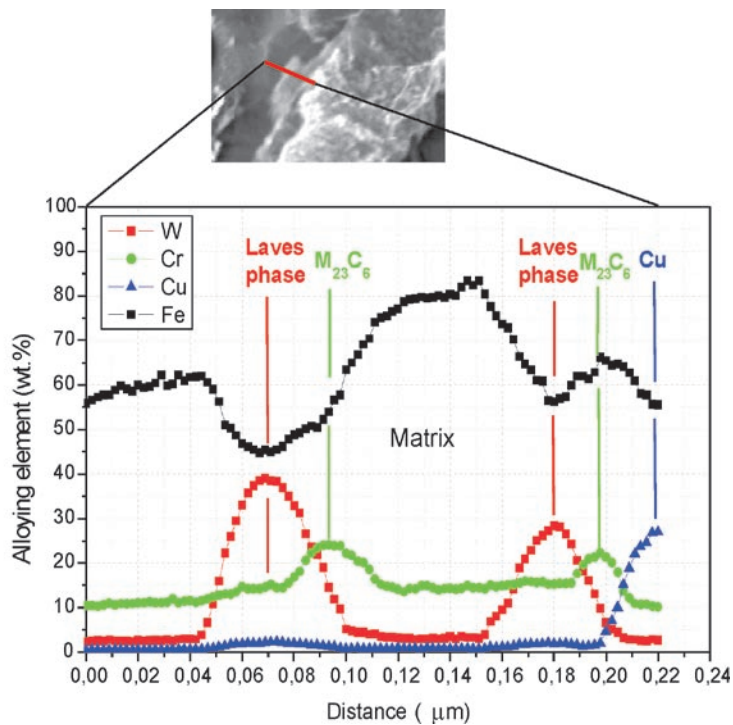


Fig. 3: Energy dispersive X-ray analysis line scan of a 11.9 wt.% Cr model steel with 4 wt.% W, 0.2 wt.% V, 4.5 wt.% Co and 1.0 wt.% Cu after annealing at 650 °C for 200 h.

nitrides can be precipitated as fine and semicoherent particles in the solid state. The partial substitution of Co by Cu (1 wt. %) has also shown positive effects on the creep properties (*V. Knežević, G. Sauthoff*).

Alloys to be studied with melting temperatures up to about 1850 °C have routinely been prepared by induction melting in ceramic crucibles under vacuum ($2 \cdot 10^{-5}$ mbar) or inert gas to obtain ingots of about 350 to 850 g (20 to 40 mm diameter and up to 200 mm length). Single crystals with up to 40 mm diameter and 130 mm length of alloys with melting temperatures up to 1700 °C have been grown in ceramic crucibles under vacuum ($2 \cdot 10^{-5}$ mbar) or inert gas using a modified Bridgman technique. The crystal orientations have been determined by laser light reflection at the etched crystal surfaces. An inductively heated levitation melting unit has been used for the preparation of small amounts (350 g maximum) of polycrystalline high-purity alloys with

high oxygen affinity with melting temperatures up to about 1900 °C with solidification in cold Cu moulds under vacuum ($2 \cdot 10^{-5}$ mbar) or inert gas as well as for the growth of long single crystals with continuous feeding. Alloys with higher melting temperatures (up to about 2200 °C) have been prepared by arc melting to obtain bars of about 80 g. The alloys have been heat treated at temperatures up to about 1600 °C in inert gas atmospheres or under vacuum.

The evolution of microstructures has been analysed by use of electron-probe microanalysis (EPMA), X-ray diffraction (XRD) at ambient and high temperatures, light optical microscopy, scanning electron microscopy (SEM), and transmission electron microscopy (TEM). In addition, phase transitions have been identified by high-temperature differential thermal analysis (DTA) and oxidation kinetics have been observed by high-temperature thermal gravimetry (both up to 1700 °C).

The mechanical behaviour has been analysed by computer-controlled testing in compression, bending and/or tension at temperatures in the range -180 - +1600 °C in air, inert gas or vacuum at deformation rates in the range 10^{-9} to 10^{-2} s⁻¹ with loads in the range 20 to 500 kN. Information on the local deformation behaviour has been obtained by computer-controlled microhardness testing, which supplies data not only on hardness of grains and phases, but also on elasticity and ratio of plastic and elastic work. With brittle materials indentation cracking occurs by hardness testing which allows toughness determination.

Two groups have contributed to the work of the department, i.e. the Phase Equilibria and Transformations Group till 31 December 2003 when Prof. Dr. G. Inden retired, and the High-Temperature Materials Group till 30 November 2004 when PD Dr. G. Sauthoff retires. The work is partially continued in Dr. A. Schneider's group in the Materials Technology Department.

Research Projects in Progress

High Temperature Materials

Sauthoff, Schneider, Knežević: Ferritic steels with maximum creep resistance: alloy development and long-term behaviour

Sauthoff, Schneider, Risanti: Deformation behaviour of Fe-Al-Ta alloys

Sauthoff, Schneider, Stallybrass: Ferritic Fe-NiAl superalloys

Phase Equilibria and Transformations

Inden, Balun: Development of a database for ferritic steels

Inden, Bernst: Effect of carbide-forming elements on the process of „metal dusting“

Inden, Zhang: Constitution of cementite



Department of Computational Materials Design

J. Neugebauer (since Nov. 2004)

In November 2004 Prof. J. Neugebauer, formerly University of Paderborn, had been appointed as director of a new department „Computational Materials Design“. Since the department will become operational only in March 2005 in the following only a brief discussion of its background and aims will be given.

The main expertise of the new department is the development and application of multiscale simulation techniques to describe materials properties and design. A key feature of these methods is that they are not restricted to a certain range of length and time scales but start on the most fundamental level – the atomic scale described by quantum mechanics – and go all the way up to the mesoscopic/macroscopic scale relevant for the application/design of the materials. A major advantage of this approach is that no experimental input is needed: It is free of any empirical or adjustable parameters and thus ensures an accurate description and a high predictive power on all scales. The activity of the new department will be focused on the following issues:

Method development: In order to bridge the various length and time scales atomistic methods have to be coupled/combined with meso-/macroscale approaches such as thermodynamics, statistical mechanics, or continuum theory. A main challenge which will be tackled is the development of methods which provide a highly accurate and numerically efficient scale coupling. To allow rapid development and implementation of these methods a fully modular and object oriented approach will be employed (see www.sfhingx.de).

Calculation of ab initio (parameter free) phase diagrams: Employing ab initio methods (density functional theory – DFT) the partition function and thus all thermodynamic potentials such as the free energy, the Gibbs free energy

are accessible. This approach provides the unique opportunity to directly derive temperature and pressure dependent phase diagrams for in principle any materials system. In a first step the accuracy of the underlying DFT functionals will be tested for elementary and binary materials by comparing with experimental data. In a second step this approach will be extended to allow a description of complex multi-component alloys.

Conformational studies: Based on multiscale methods equilibrium geometry, chemical composition and thermodynamic stability of extended defects such as dislocations and grain boundaries will be investigated. These studies will be used to get a deeper understanding of segregation effects and hardening. They also provide a firm basis to compute the dynamic behavior of dislocations and boundaries and thus allow a direct insight into the microscopic mechanisms determining the mechanical behavior of iron or steel such as strength, ductility or brittleness.

Nucleation theory: One of the key processes determining the microstructure and thus the mechanical behavior of materials is nucleation. To get a firm handle on this behavior it is crucial to understand and predict the size, shape, composition and density of the nuclei. However, an understanding and modeling of these features is still in its infancy. It is therefore planned to develop/apply methods which allow an efficient treatment of the solid/liquid interface and which provide an accurate estimate of the anisotropy of the interface energy. Based on these results parameters such as equilibrium shape, critical size, activation barriers will be calculated which give a direct handle in controlling grain size and are thus the key to study/fabricate nanocrystalline metals.

Vakat



Department of Interface Chemistry and Surface Engineering

M. Stratmann

Introduction

The department has its main focus on chemical reactions and physical properties of surfaces and interfaces with particular emphasis on increasing their stability and including functional properties into coatings on structural materials. Materials based on metals, polymers and metal/ceramic or metal/polymer composites are of interest. Scientific studies concentrate on degradation reactions such as aqueous corrosion, high-temperature corrosion, tribocorrosion and de-adhesion reactions with the aim of understanding their underlying physico-chemical reaction mechanisms. Based on this knowledge new and superior surfaces and interfaces are designed, characterized by their novel chemical composition, morphology and molecular and atomistic structure. Frequently, this requires surface modification techniques. The physico-chemical understanding of such technologies is among the main activities of the department.

The department includes approximately 65 people and among them more than 45 scientists. It is

engaged in more than 30 projects most of them in international collaboration. The experimental equipment is exceptional even on an international scale and allows performing state of the art science in surface and interface chemistry.

The structure of the department is summarized in Fig. 1. This structure includes three major lines:

- (1) **Scientific groups** as the most important part of the management structure. These groups are competence centres in various areas of science and they include specific experimental and theoretical knowledge. The scientific groups are largely integrated in the major departmental areas of scientific interests; however in parallel they also have their own specific and unique scientific goals.
- (2) **Laboratories** focus on the experimental techniques necessary for investigating surfaces and interfaces. They develop new and many times unique experimental set-ups

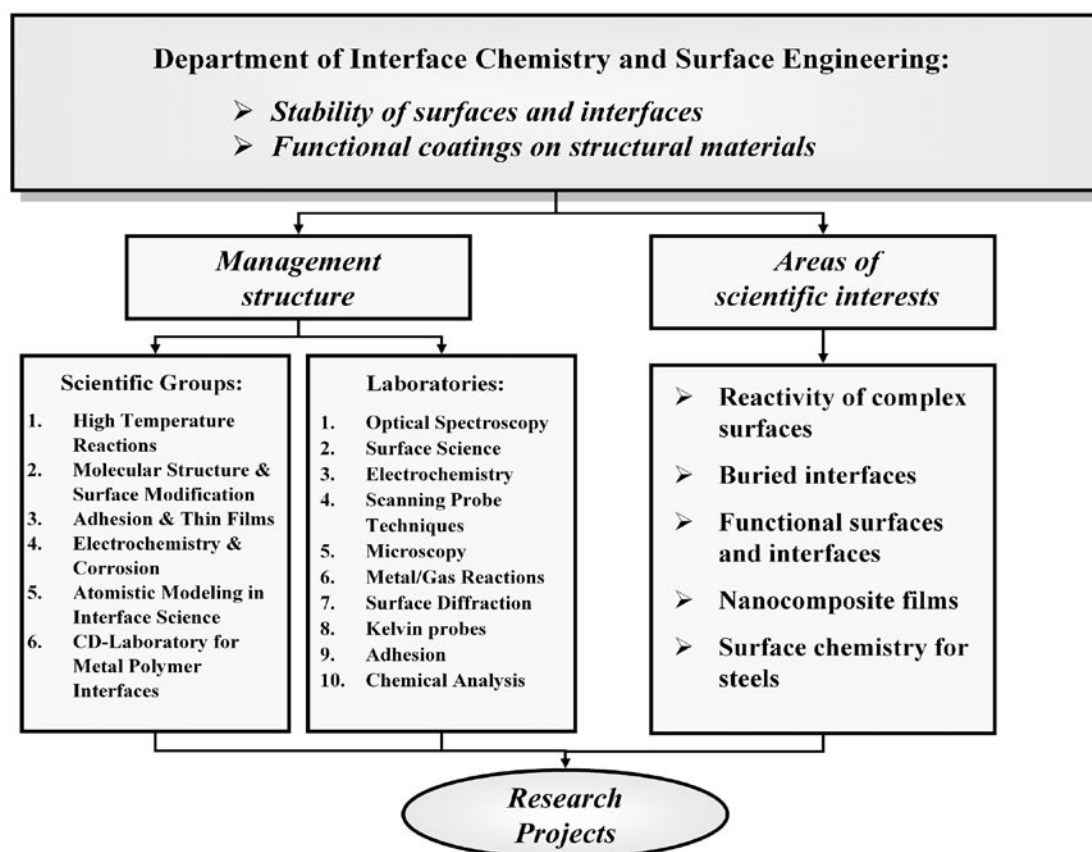


Fig. 1: Organization of the department.



which allow performing state of the art research projects. Obviously, strong links exist between the specific experimental knowledge of the scientific groups and some of the key laboratories.

- (3) The department has clearly defined **areas of scientific interest** which are common for almost all scientific groups and which define a scientific link between them. Indeed the long term goals on which the areas of scientific interests are based can be achieved only if the groups of differing scientific knowledge collaborate strongly. The collaboration is organized in projects typically financed either by stipends or by European or German funds.

The department is well integrated into the scientific structure of the institute. Major links include aspects of micromechanics of surfaces and interfaces (Prof. Raabe), the correlation between the reactivity of surfaces and their microstructure (Prof. Raabe), the corrosion stability of novel materials and the formation

of novel microelectrode arrays (Prof. Frommeyer) and the thermodynamic and kinetic simulation of surface reactions in particular for high temperature corrosion applications (Prof. Neumann). In future a very intense collaboration to the new Department of Computational Materials Design (Prof. Neugebauer) is expected as the atomistic scale of many experiments is very much in line with the computational expertise of this department.

Finally, it should be mentioned that the department is highly engaged in activities beyond the institute. The department coordinates a number of European research projects, it has attracted a *Christian Doppler Laboratory on Polymer/Metal Interfaces* financed by the Austrian Christian-Doppler-Society (Head of the CD-Lab: Dr. Guido Grundmeier, Industrial partners: Henkel Austria and voestalpine Stahl Linz) and based on its initiative the IMPRS „*Surmat*“ has been founded, which nowadays is a major source of international PhD students for the department.

Scientific Groups

High Temperature Reactions (M. Spiegel)

The group is specialized in the areas of

- high temperature corrosion including hot corrosion in melted salts
- stability and structure of thin oxide scales
- chemical vapour deposition

As the scale formed during continuous annealing of steel in reducing or oxidizing atmospheres

determines surface properties like wetting of liquid zinc, adhesion of corrosive salt particles or also the stability of buried interfaces it is of ultimate importance to scientifically understand the initial stages of oxide formation on pure metals and alloys. Whereas the formation of the first oxide monolayers on clean single crystal surfaces is well understood the influence of complex surfaces (grain orientation, grain boundaries) on crystal growth, the transition from 2D to 3D growth and the short term oxidation

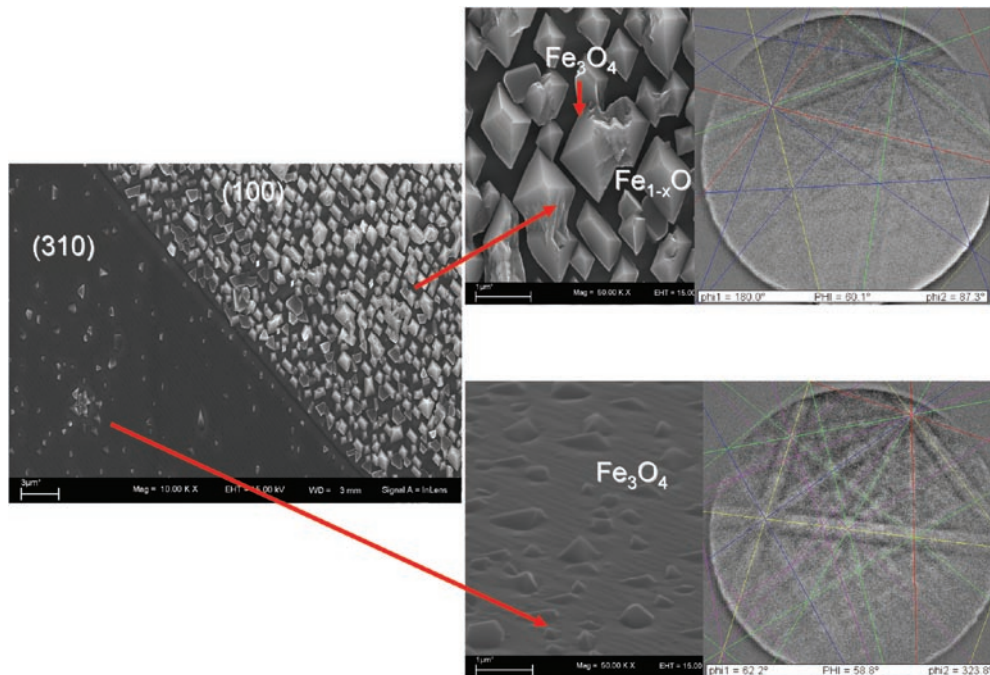


Fig. 2: In-situ study of initial stages of oxide growth including texture analysis of substrates and scales.



of alloys under kinetically controlled conditions are subject of considerable international activities. The group has established a number of unique experiments to follow these questions combining specialized reaction chambers within the UHV system of the department with the in-situ study of initial oxidation reactions in FE-SEM [1] (Fig. 2).

Research in High Temperature Corrosion is focused on molten salt and particle induced corrosion, where initial reactions between chloride particles and metal surfaces are studied. Kinetic and solubility studies of metals in molten salts are conducted in order to understand the rapid corrosion of alloys in the presence of ash deposits [2]. Mechanisms of oxide scale breakdown in corrosive gases such as HCl and H₂O are studied by means of thermogravimetry and mass spectrometry.

Molecular Structure and Surface Modification (M. Rohwerder)

The group's interests are focussed on

- semiconducting properties of surface oxide films
- elementary steps of electrochemically driven de-adhesion of polymers
- surface modification by organized monolayers

The electronic properties of the oxides formed during short term annealing define the rate of electron

transfer reactions (ETR) at the buried interfaces. Recent studies have demonstrated that intrinsically stable interfaces can be formed if the Fermi level within the oxide is tailored such that potential differences between defect and intact areas of the oxide vanish [3]. This finding, which is a breakthrough in interface chemistry, has triggered a number of very fundamental studies on the electronic properties of buried interfaces. These studies include the preparation of well defined oxide surfaces, the study of ETR on metal/polymer interfaces with a given charge distribution using charged monolayers and the study of the chemical interaction between the substrate and organic molecules using e.g. scanning probe techniques[4-6]. Interfacial potentials also dominate the reactions of conducting polymers or nano-capsules being present at the interface which all may be utilized to form self-healing interfaces (Fig. 3).

Another important topic within the group is the investigation of the fundamental steps of delamination on a molecular and nanoscopic scale, which involves the preparation of well defined model samples as well as the application of various scanning probe methods [4-6]. The role of nanoscopic defects at the interface, as they are e.g. formed by mechanical deformation of the substrate have been included in these fundamental studies [7].

The group is also quite active in the understanding of wetting phenomena of liquid zinc on oxide covered surfaces [8].

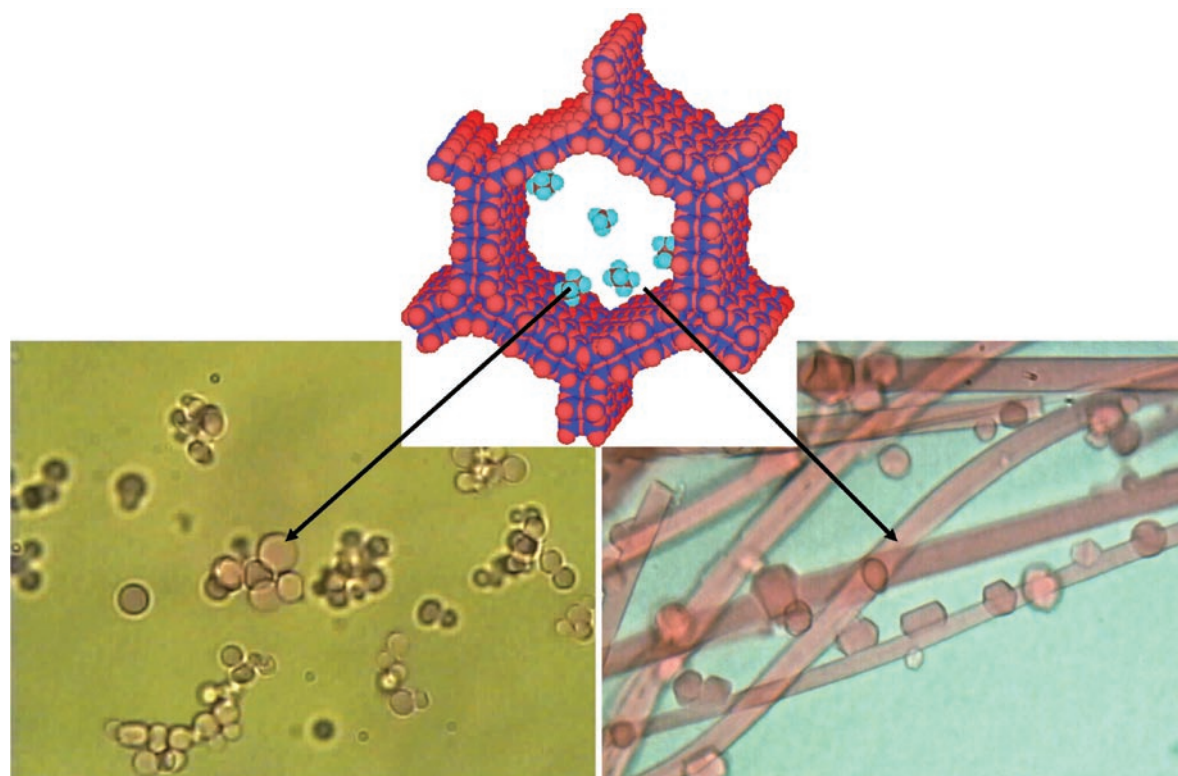


Fig. 3: Nanocapsules and nanofibers filled with inhibitors for self healing polymer coatings.

Adhesion and Thin Films (G. Grundmeier)

Topics of the group include

- fundamental aspects of adhesion
- interaction of low pressure and atmospheric cold plasmas with metal and polymer surfaces and tailoring of material properties by deposition of thin functional plasma polymers
- mechanisms of corrosion protection by means of pigment containing water borne latex coatings

interface. Very few techniques exist to analyse the transport phenomena of ions and water along polymer/metal interfaces in comparison to the bulk mobility. The group therefore focuses on optical techniques like ATR-spectroscopy and -microscopy in combination with isotope experiments to provide a detailed understanding of the mobility along interfaces. These results were successively supported by the application of the Scanning Kelvin Probe. It could be shown that the transport kinetics of water along polymer/metal interfaces is orders of magnitude faster than the bulk diffusion [9]. Furthermore, vibrational spectroscopy is applied for the study of the adsorption and adhesion of monomolecular layers by means of in-situ spectroscopy in external reflection (IRRAS) and in attenuated total reflection (SEIRA-ATR) as well as surface enhanced Raman spectroscopy (SERS) (Fig. 4) [10].

Tailoring of materials surface structures is done in various research projects and new surface modification techniques such as plasma processes are developed. In case of thin plasma polymer films, research focuses on the relation between morphology and chemical composition on the one hand and functional properties like permeability, mechanical properties, surface energy and wetting phenomena on the other hand [11-16].

Christian-Doppler-Laboratory for Metal/ Polymer Interfaces (G. Grundmeier)

In the first year the laboratory had its prime focus on the spectroscopic understanding of new advanced conversion chemistry on galvanized steel surfaces. Using in-situ and ex-situ optical spectroscopic techniques the formation and chemical composition of organic/inorganic hybrid films have been studied. The structure of the films could be correlated with their electrochemical and corrosion properties. Moreover, the grain orientation dependent film nucleation and the forming behaviour of thin film covered galvanized steel surface were studied. Parallel to this, new spectroscopic techniques (SEIRA-ATR) and AFM (for adhesion studies under potential control) were developed for the analysis of adhesion and de-adhesion mechanisms on surface modified metals.

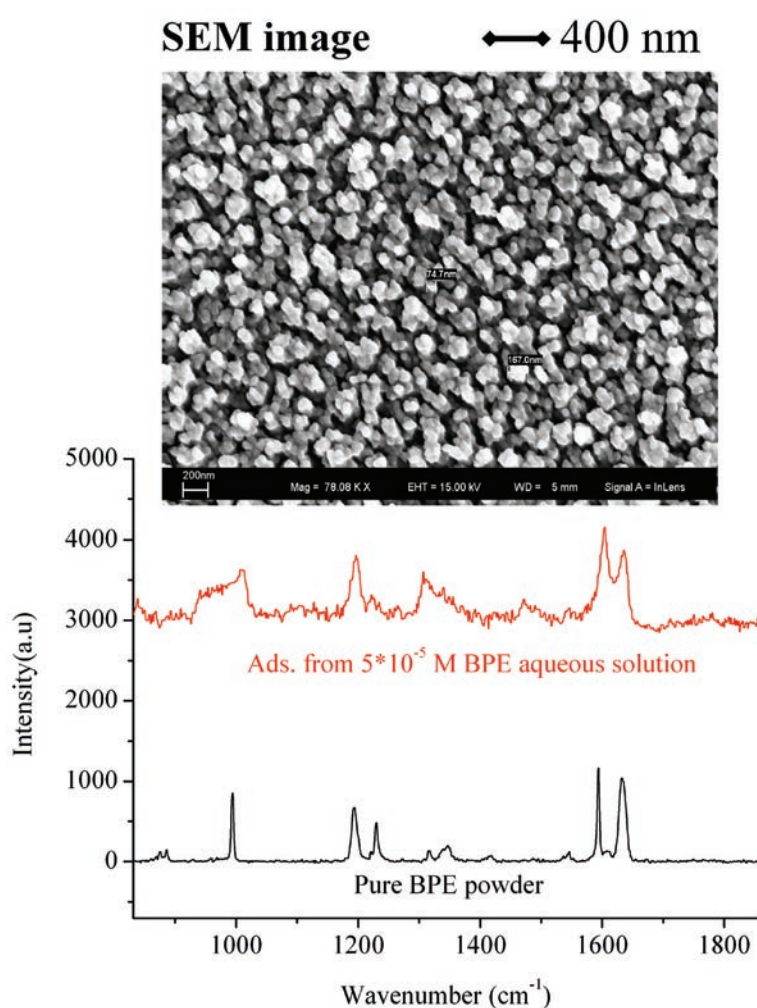


Fig. 4: Design of new SERS active substrates based on deposition of nanoporous plasma polymers and PVD of Ag and test of surface enhancement with *trans-bis-1, 4* (pyridyl)ethen (BPE)(Thesis: Guoguang Sun).

De-adhesion of organic polymers is in many cases triggered by chemical and electrochemical reactions which require the presence of water and ions at the

interface.



Electrochemistry and Corrosion (A.W. Hassel)

Major research areas are

- tribocorrosion and flow induced corrosion
- corrosion of novel materials
- nanostructured surfaces

The corrosion of materials is determined by the microstructure of the material. Therefore the group has developed techniques, which allow addressing individual parts of the surface using micropositioning systems [17, 18], identifying the microstructure using EBSD and finally analysing the local reactivity using home-made microelectrochemical devices [19]. This is used to understand the reaction kinetics of new complex materials like TRIP and TWIP steels or Fe-Cr-Al alloys, which are developed as cheap Ni-free stainless steels. A clear link between texture and local reactivity has been found which seems to correlate with the atomic density in the surface of a given crystal [20].

Microelectrodes are also used in multi-phase flow induced corrosion experiments which now allow the detection of single repassivation experiments after the impact of one particle on the surface [21]. The transients give direct insight into the repassivation kinetics of passivating surfaces but they also allow an understanding of the elementary steps of flow induced corrosion which are essential for stainless steels in many industrial systems [22,23].

Microstructure is not only important for the corrosion kinetics it also allows the development of a range of microelectrode array electrodes. Using the directed solidification of eutectic systems metallic nanofibers can be obtained in a metallic matrix which allow the preparation of a variety of nanostructured surfaces by etching and deposition techniques [24,25].

Atomistic Modelling in Interface Science (A.T. Blumenau)

This group has been established in autumn 2004. The group will essentially use ab-initio and DFT-based methods in order to understand interface phenomena on the molecular and atomistic scale in much more detail than it could be envisaged by sophisticated experiments only.

In the initial phase research will focus on the semi-conducting properties of thin oxide films, as they are dominating the kinetics of ETR, and on the chemical and electrical structure of metal/polymer interfaces. This will provide the theoretical knowledge necessary for an extensive modelling of de-adhesion reactions. The group will collaborate closely with the department of Prof. Neugebauer, sharing large scale computer hardware and software modules. Furthermore, a close interaction with the department's experimental groups will be established, in order to develop experiments which are defined on a scale suitable for DFT-based methods.

Laboratories

A number of laboratories are available within the department which include scanning probe techniques (AFM, STM, SKPFM), optical techniques (FT-IR, Raman, ATR, SEIRA, SERS, ellipsometry, UV-Vis), diffraction techniques (grazing incidence), UHV-techniques (AES, XPS, AES, TOF-SIMS, LEED, MBE etc.), analytical techniques (IC, ICP-OES), microscopy (FE-SEM including EBSD and EDX), electrochemistry (Kelvin probes, scanning Kelvin probes, CV, RDE, Impedance, high temperature electrochemistry etc.) and thermogravimetry coupled with mass spectrometry as well as high temperature furnaces with unique gas supply systems in order to simulate complex combustion environments.

In many circumstances besides commercial instrumentation unique experimental facilities have

been built up in the department during the reporting time; some major and internationally unique experimental developments are summarized below:

UHV-Laboratory

After four years of construction, the UHV laboratory could actually start operations in 2004. It contains a unified sample transfer system which allows transferring samples between the major UHV-system, a glove-box for electrochemical experiments and Kelvinprobe studies, the FE-SEM, the device which allows measuring contact angles at high temperatures (see below) and the SAM system (Fig. 5). XPS, TOF-SIMS and a high temperature STM system are integral parts of the UHV system which additionally

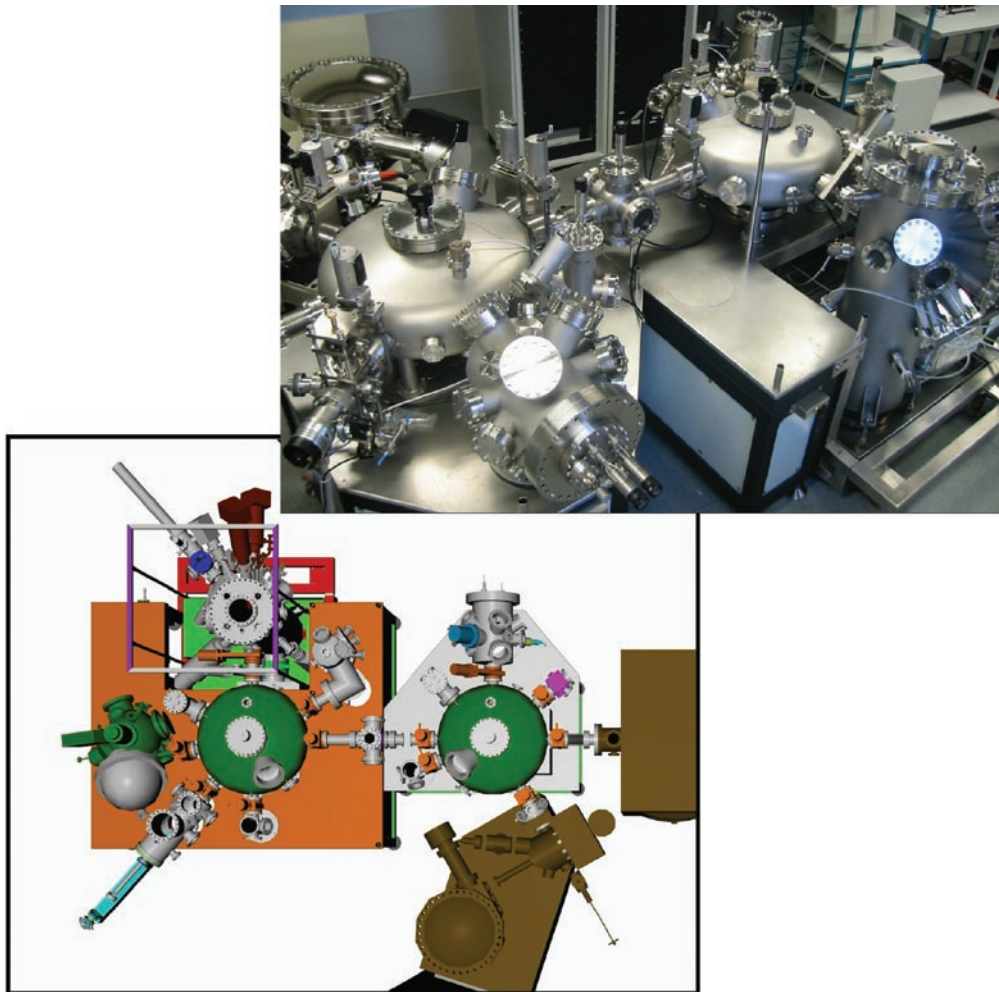


Fig. 5: The new UHV-lab of the department.

contains transfer units and chambers for high temperature oxidation, plasma-treatments, MBE and further surface characterisation. The system is used by all groups and represents the major instrumentation of the department.

High Temperature Contact-Angle Measurement under UHV Conditions

For the study of the interaction of liquid zinc with well defined and oxide covered steel surfaces a UHV system has been constructed, which allows to measure the dynamic contact angle at 500 °C in well defined atmospheres (Figs. 6 and 7). The base pressure of the system is low enough to avoid the oxidation of the liquid Zn-1%Al melt for the time of the experiment and as an additional unique feature it allows to spin off the liquid metal from the substrate after measurement of the contact angle with high rotation speed in order to obtain a newly formed interface. This interface is then transferred into the UHV system for further analysis without exposure to air.

3D-Scanning Kelvin Probe

A new scanning Kelvin probe has been constructed, which allows studying the height and the potential profile of the sample simultaneously by a double modulation technique. By this, the local resolution of the scanning Kelvin probe has been improved significantly (Fig. 8) and complex surfaces are now easy to analyse [26]. First studies include the filiform corrosion of aluminium and the mechanical-electrochemical de-adhesion of glues from metallic substrates using a blister test. Similar to stress corrosion cracking the de-adhesion rate depends in a non-linear manner as well on mechanical stress as on the electrochemical reaction rate.

Plasma Reaction Chamber for Fundamental Studies

A novel system has been established which enables the in-situ study of plasma-induced surface modifications (pulse, remote, vacuum and atmospheric plasma) by means of grazing incidence FTIR

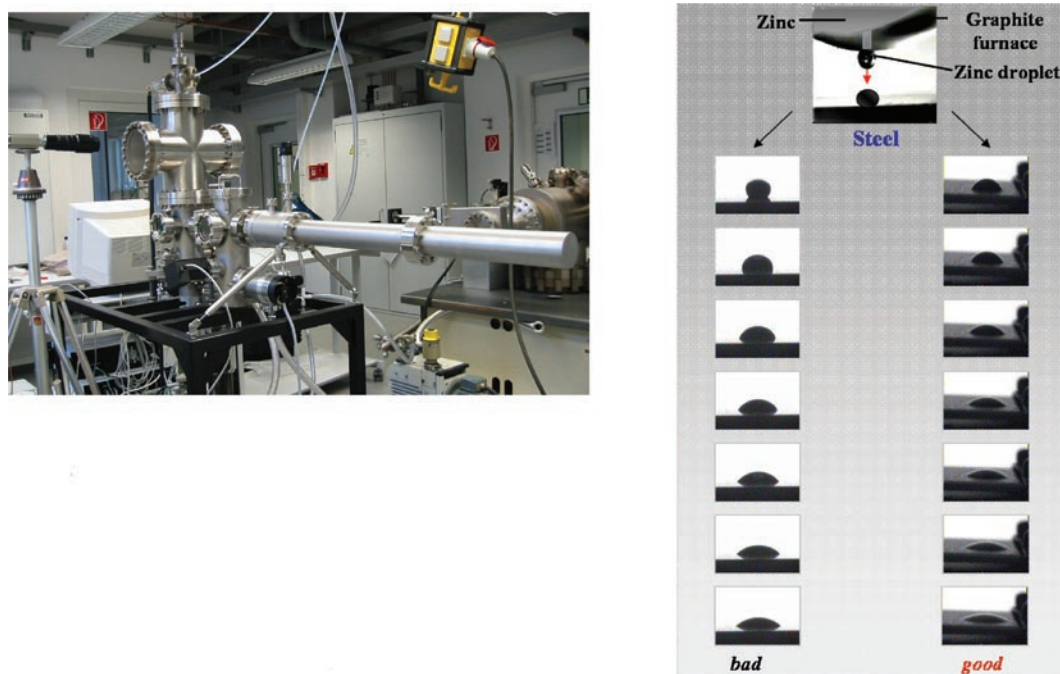


Fig. 6: UHV system for measuring contact angles of liquid zinc on technical surfaces and mesoscopic model surfaces.

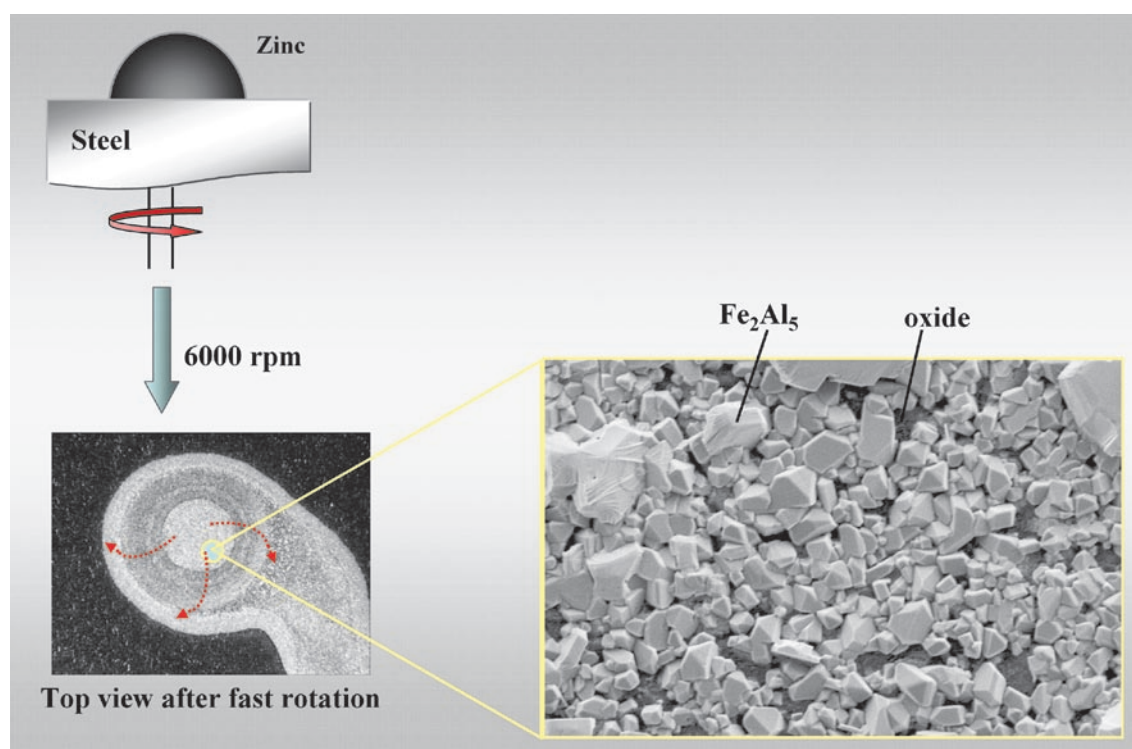


Fig. 7: Interfacial oxides and intermetallics after spinning off the liquid zinc droplets as shown in Fig. 6.

spectroscopy and a Kelvin probe. This unique set-up allows studying the electronic changes of passive layers on metals induced by the plasma and to correlate this electronic structure with the chemical composition (Fig. 9). The same system is also used to study the interaction of polymer surfaces with a plasma by which reactive centres are incorporated into the polymer film. Moreover, the important

question of ageing mechanisms of thin films can be studied by this system. Further developments will combine a magnetron sputter unit, a plasma source and advanced spectroscopy. In this system, novel nanocomposite and multilayer thin films will be prepared which are believed to be of importance for functional coatings with self repair or leaching properties and superior mechanical properties.

15*15 μm Cu dots on Aluminium, spacing 40 μm

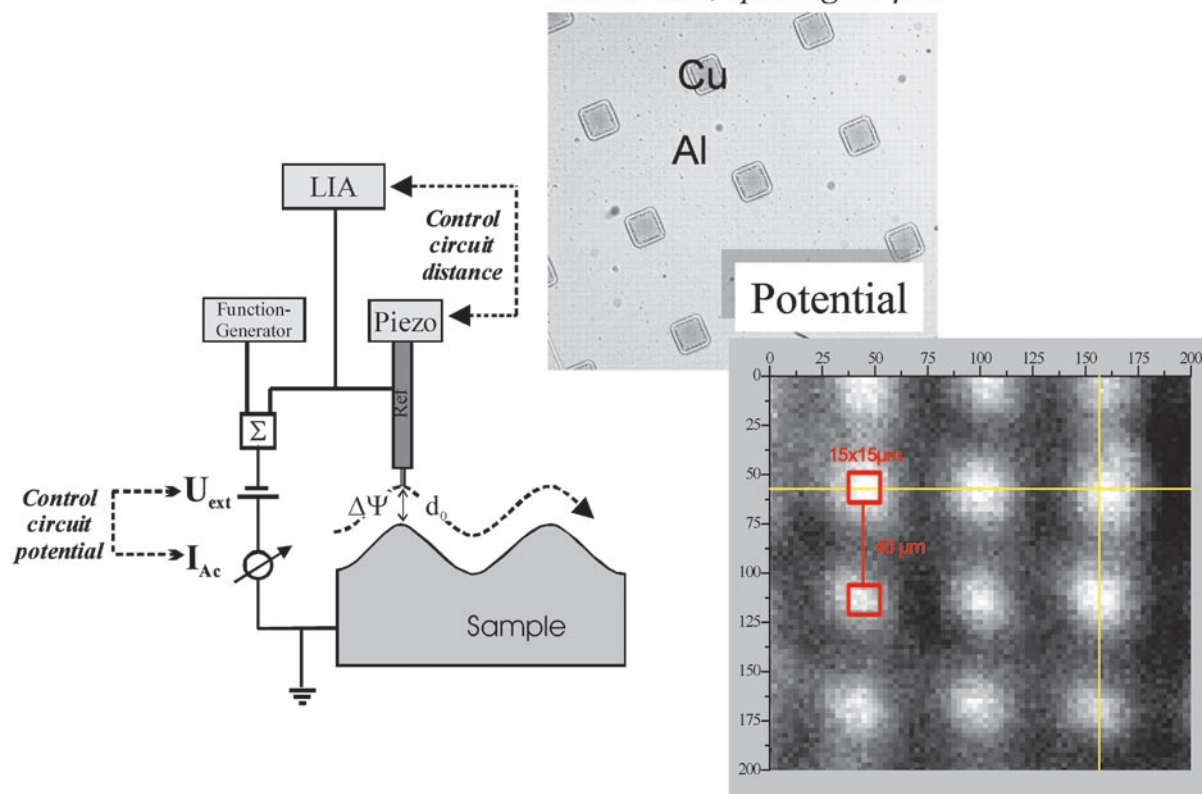


Fig. 8: Principal and spatial resolution of a new height regulated scanning Kelvin probe for corrosion and adhesion studies (K. Wapner, B. Schönberger, M. Stratmann, G. Grundmeier, *Journal of the Electrochemical Society*, in press).

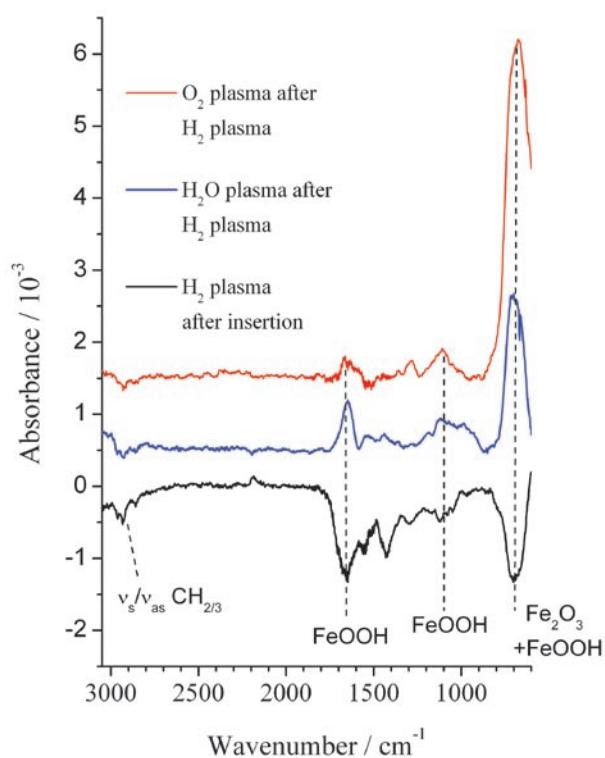


Fig. 9: In-situ IRRAS spectroscopy of plasma oxidation and reduction processes of ultra-thin passive films on iron (J. Raacke, M. Giza, G. Grundmeier, *Surface and Coating Technology*, submitted for publication).

FE-SEM for Studying Initial Stages of Metal/Gas Reactions

A commercial instrument (LEO) equipped also with EBSD has been modified to include a high-temperature reaction chamber. This chamber can be operated either at elevated temperatures for the in-situ study of crystal growth or oxidation on single grains or the chamber may be closed to study the metal/gas reaction at higher pressures even in the presence of reactive gases. First experiments have proven the capabilities of the instrument, which also allows correlating the grain orientation with the orientation of the oxides grown on the same grain. Therefore in one experiment a large set of data is obtained providing the full epitaxial relation between substrate and scale.

Microelectrochemistry and Flow-Induced Corrosion

This instrument combines the knowledge on the preparation of microelectrodes with a unique set-up to study the impact of individual particles. The microelectrode is kept under controlled electrochemical conditions and a jet of electrolyte containing the particles of interest is shot onto the surface with defined speed and momentum. A fast data-logging



system allows identifying single impacts and to follow fast transients which are due to passivation/corrosion of the sample after local removal of the passive film (Fig. 10). As the single events can later be analysed

by AFM techniques, a detailed analysis of the electrochemical transients is possible giving insight into the repassivation kinetics and the localized corrosion induced by the particle impact.

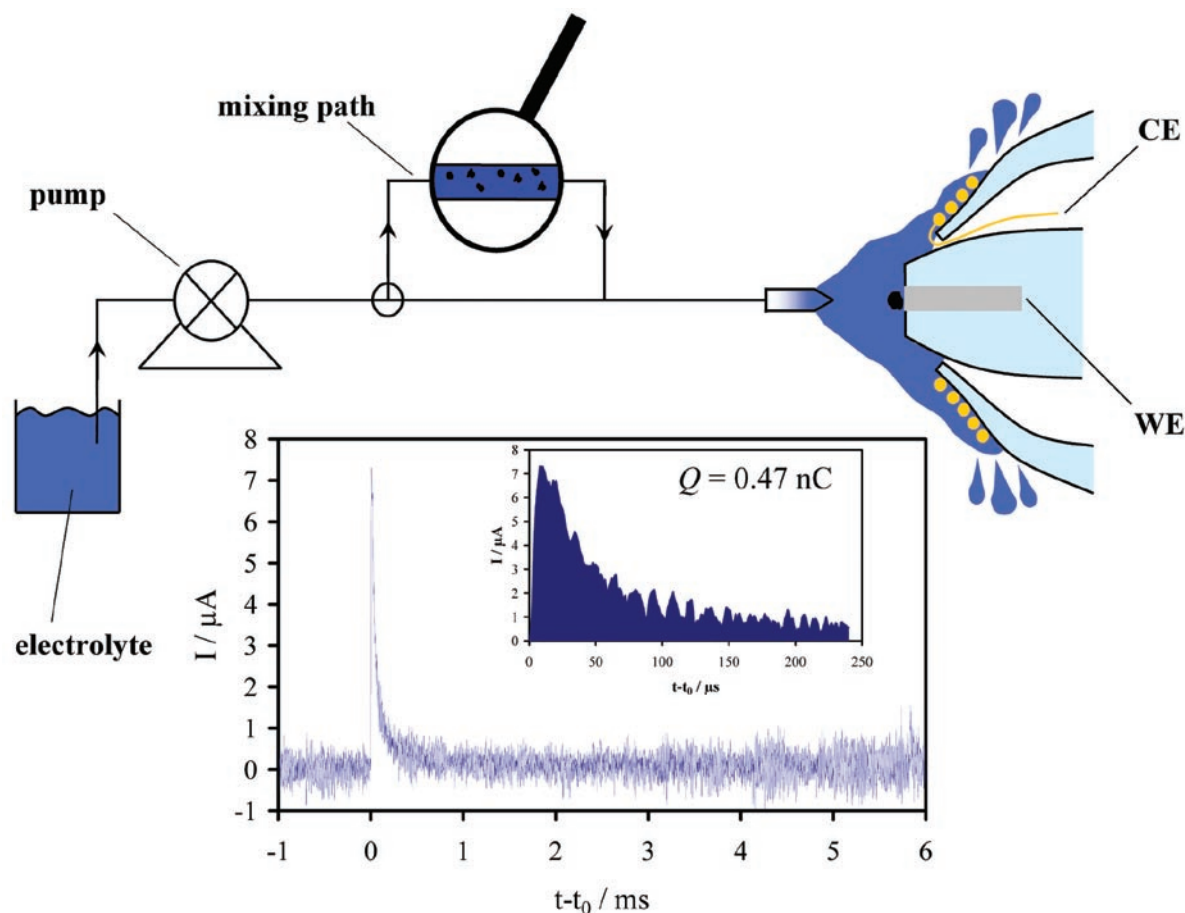


Fig. 10: Single impact of particles during flow induced corrosion and subsequent current transients of repassivation.

Areas of Scientific Interests

All scientific groups are horizontally linked by common areas of scientific interest:

Reactivity of Complex Surfaces

This area links all activities in the field of corrosion from aqueous corrosion to high temperature corrosion. Research in the past has either focussed on the reaction behaviour of poly-crystals with averaged rate laws or very few single crystal surfaces have been analysed with lack of any information regarding the influence of grain boundaries and high index surfaces.

The department has therefore put a considerable effort in experimental methods which allow a full description of the local reactivity even on complex surfaces. Investigations start on well defined single crystal surfaces using a high temperature STM-stage in the presence of pressures up to 10^{-4} mbar. These investigations aim at detecting the transition of 2D to 3D growth and the influence of surface segregation on the nucleation and growth of surface oxides. First studies have proven the tremendous influence of surface segregation on the nucleation density of oxides. Ongoing studies concentrate on the initial stages of alloy oxidation.



The next step focuses on the oxidation of pure metals and binary alloys in a high temperature reaction chamber situated inside a FE-SEM equipped with EBSD. These experiments have proven to be rather successful. Nucleation is not determined by the thermodynamic stability of the oxide phases but mostly by epitaxy relations between the grain and the oxide orientation. High nucleation density has been observed only on low index surfaces; additionally a clear preference in the oxide phases formed on different substrate grains is observed. Ongoing studies concentrate again on the oxidation of binary alloys. In these systems the initial stages of oxidation, the nucleation density of oxides, but in particular the 2D – 3D scale development depends on the possibility to form mixed oxide phases such as spinels (Fe-Cr-system) in comparison to oxide systems on alloys which do not show miscibility of oxide phases (Fe-Al system).

The last step makes use of the thermogravimetry available in the department on studies in a classical manner the initial stages of oxidation in high pressure environment. Microscopic and spectroscopic studies are performed as ex-situ experiments. The pressure gap will be overcome in future by using the high pressure chamber of the UHV-system of the department. This allows studying the initial stages of oxidation on well defined surfaces (single crystals) under high pressure oxidation conditions such that a direct comparison is possible to in-situ high temperature STM studies performed under low pressure reaction conditions.

Buried Interfaces

Buried interfaces are of continuing interest for all groups of the department. Research concentrates on the stability of such interfaces taking into account all relevant issues:

- Electrochemical reactions at the interface depend on the local potential gradient. Such gradients are modelled by the deposition of charged monolayers using Langmuir-Blodgett technique; the rate of ETR is subsequently studied by use of the Kelvin probe.
- The mobility of water and ions are studied with a variety of optical spectroscopic methods and the scanning Kelvin probe, which allows detecting a change due to charged dipoles at the interface. First results have shown a surprisingly strong dependence of the interfacial mobility on the interfacial structure.

- The rate of ETR at the buried interface depends – in the presence of passive oxides – strongly on their electronic properties. Inherent stable interfaces have been designed by optimising the oxide defect structure such that the work function of the oxide covered metal/polymer interface matches the work function of the freely corroding iron surface [4].
- The chemistry at the interface such as formation of chemical bonds or bond breaking reactions triggered by the reduction of oxygen are studied on a model interface using TOF-SIMS techniques. These studies give clear evidence of the oxidative degradation as a consequence of oxygen reduction.

Functional Surfaces and Interfaces

The department has a considerable interest in the study of new functional surfaces and interfaces. Part of this research is directly coupled to the studies on buried interfaces as they aim at the preparation of self healing interfaces which allow the detection of defects and the active repairs of such defects. Here conducting polymers are of prime interest. The potential jump which is associated with the change of the chemical state at the interface due to adhesion is used as a trigger to discharge the polymer which subsequently leads to the emission of cations used to block the interface electrochemically. Ongoing studies also concentrate on the use of nanocapsules embedded either in the polymer matrix or even within galvanically deposited zinc coatings.

A second part of the departmental work concentrates on the use of plasma polymers and plasma polymer nanocomposite and multilayer thin films. These films can be designed in a manifold manner with respect to chemical composition, morphology, surface energy barrier and mechanical properties. Research concentrates on the use of plasma polymers as ultra-thin interfacial barrier coatings for corrosion protection, as wear resistant coatings on polymers, as low energy easy to clean surfaces and as anti-bacterial nanocomposite films.

Finally PVD coatings are of considerable interest on steel and galvanized steel substrates. They are either used to form tailored oxides with a specific electronic structure or they are used for surface alloying. Surface alloying is regarded as the most interesting topic for the formation of patinas on steel and recent research concentrates in particular on the reaction mechanism of patina formation making use of spectroscopic and Kelvin probe methods.



Surface Chemistry for Steel Substrates

Steel surfaces are of particular interest for the department. Steel related projects cover the full range of surface treatments:

- Short time annealing is studied to understand the scale formation prior to galvanising in oxidizing and reducing atmospheres. The segregation of non-metallic elements is of particular importance.
- Hot dip galvanizing is determined by wetting of liquid zinc on the oxide covered surface and by interfacial reaction between the liquid bath and the substrate. Both phenomena are studied with unique instrumentation.
- Surface reaction between zinc alloys and the gas phase lead to semiconducting oxides; this is subject to extensive investigations.
- Cleaning of the surface, amorphous thin film formation based e.g. on zirconates and phosphates containing water based chemical solutions are studied in detail in particular with spectroscopic and microscopic techniques.
- The interaction of water born coatings and pigments with steel and galvanized steel surfaces is being studied in close collaboration with the chemical industry.
- Last but not least: corrosion reactions such as the tribocorrosion of stainless steels, the corrosion of modern TRIP and TWIP steels, the biological induced corrosion, the hot corrosion and the high temperature corrosion in aggressive atmospheres are investigated in close collaboration in different groups of the department.

References

1. Pöter, B.; Stein, F.; Palm, M.; Spiegel, M.: EUROCORR 2004, Sept. 12-16, 2004, Nice, France.
2. Ruh, A.; Spiegel, M.: Mater. Sci. Forum 461-464 (2004) 61.
3. Rohwerder, M.; Hausbrand, R.; Stratmann, M.: Steel Res. Int. 74 (2003) 453-458.
4. Rohwerder, M.; Frankel, G.S.; Leblanc, P.; Stratmann, M.: „Application of Scanning Kelvin Probe in corrosion science“, in: Methods for Corrosion Science and Engineering, F. Mansfeld, P. Marcus (eds.), Marcel Dekker, New York, *in press*.
5. Rohwerder, M.; Hornung, E.; Stratmann, M.: Electrochim. Acta 48 (2003) 1235-1243.
6. Ehahaoun, H.; Stratmann, M.; Rohwerder, M.: Electrochim. Acta, *in press*.
7. Baumert, B.; Stratmann, M.; Rohwerder, M.: Z. Metallkd. 95 (2004) 447-455.
8. Frenznick, S.; Stratmann, M.; Rohwerder, M.: Conf. Proc. GALVATECH 2004, p. 411-417.
9. Wapner, K.; Grundmeier, G.: Electrochim. Acta, *submitted*.
10. Wapner, K.; Grundmeier, G.: Adv. Eng. Mater. 6 (2004) 163-167.
11. Carpentier, J.; Thiemann, P.; Barranco, V.; Grundmeier, G.: Surf. Coat. Technol. 173-174 (2003) 996-1001.
12. Grundmeier, G.; Brettmann, M.; Thiemann, P.: Appl. Surf. Sci. 217 (2003) 223-232.
13. Thiemann, P.; Shirtcliffe, N.; Carpentier, J.; Stratmann, M.; Grundmeier, G.: Thin Solid Films 446 (2004) 61-71.
14. Barranco, V.; Thiemann, P.; Yasuda, H.K.; Stratmann, M.; Grundmeier, G.: Appl. Surf. Sci. 229 (2004) 87-96.
15. Barranco, V.; Carpentier, J.; Grundmeier, G.: Electrochim. Acta 59 (2004) 1999-2013.
16. Carpentier, J.; Grundmeier, G.: Surf. Coat. Technol., *in press*.
17. Hassel, A.W.; Lohrengel, M.M.: Electrochim. Acta 42 (1997) 3327-3333.
18. Hassel, A.W.; Seo, M.: Electrochim. Acta 44 (1999) 3769-3777.
19. Lill, K.A.; Stratmann, M.; Frommeyer, G.; Hassel, A.W.: 55th Meeting of the Int. Soc. Electrochem., Sept. 19-24, 2004, Thessaloniki, Greece.
20. Lill, K.A.; Stratmann, M.; Frommeyer, G.; Hassel, A.W.: Electrochim. Acta, *submitted*.
21. Akiyama, E.; Hassel, A.W.; Stratmann, M.: Proc. Asian Pacific Corr. Contr. Conf. 13 (2003) C02 1-8.
22. Akiyama, E.; Hassel, A.W.; Stratmann, M.: Electrochim. Acta, *submitted*.
23. Tan, K.S.; Hassel, A.W.; Stratmann, M.: Mater.-wiss. Werkstofftech., *accepted for publication*.
24. Hassel, A.W.; Bello-Rodriguez, B.; Milenkovic, S.; Schneider, A.: Electrochim. Acta, *accepted for publication*.
25. Hassel, A.W.; Bello-Rodriguez, B.; Milenkovic, S.; Schneider, A.: Electrochim. Acta, *accepted for publication*.
26. Wapner, K.; Schönberger, B.; Stratmann, M.; Grundmeier, G.: J. Electrochem. Soc., *in press*.



Research Projects in Progress

Adhesion and Thin Films

Ebbinghaus, Grundmeier: Analysis of Cr-species on zinc

Ebbinghaus, Grundmeier: Plasma polymer coatings on aluminium

Fink, Grundmeier: Adhesion, electronic structure and mechanics of thin amorphous films on reactive metals

Joulaeizadeh, Blumenau, Grundmeier: Simulation of the chemical structure and adhesive properties of plasma grown metal oxide surfaces

Popova, Grundmeier: Forming behaviour of corrosion protection primers

Raacke, Grundmeier: Tailored adhesion mechanisms in composite systems by means of chemical surface functionalisation

Roßenbeck, Grundmeier: Corrosion protection by water based polymer dispersions

Stromberg, Grundmeier: Amorphous zirconate thin films on metals

Sun, Grundmeier: Formation, structure and adhesion promotion of bifunctional organophosphonates at interfaces between model adhesives and metal oxide surfaces (SurMat)

Titz, Grundmeier: New surface chemistry for highly stable functional coatings

Wang, Grundmeier, Raabe: Functional plasma polymer nanocomposite films (SurMat)

Wapner, Grundmeier: Long-term stable high performance joints based on structural adhesives

Wilson, Grundmeier: Analysis of the growth of thin amorphous films on zinc coated steel

Yang, Grundmeier: Tailored thin film plasma polymers for surface engineering of coil coated steel

Atomistic Modelling in Interface Science

Joulaeizadeh, Grundmeier, Blumenau: Simulation of the chemical structure and adhesive properties of plasma grown metal oxide surfaces

Laaboudi, N.N., Rohwerder, Blumenau: Numerical modelling/lifetime prediction of delamination polymer coating disbonding and material degradation

Electrochemistry and Corrosion

Akiyama, Smith, Hassel: Detection of discrete and single impacts in particle induced flow corrosion

Bello Rodriguez, Milenkovic, Schneider, Hassel: Production of nanowire arrays through directional solidification and their application

Bonk, Wicinski, Hassel: Passive/active transitions in cyclic corrosion tests

Bruder, Hassel: New approaches in electrolytic cleaning of cold rolled steel sheets

Diesing, Hassel: Electronic tunneling in metal-insulator-metal contacts

Dinh, Widdel, Hassel: Microbiologically influenced corrosion of iron by sulfate reducing bacteria

Fushimi, Hassel: Electrochemical micromachining of Nitinol based shape memory alloys

Lill, Hassel, Sauerhammer, Spiegel: Corrosion and corrosion protection of TRIP/TWIP steels

Neelakantan, Hassel: Microstructural aspects of passivity and corrosion of NiTi

Makhynya, Hassel: Corrosion of stainless steels in biofuels

Mingers, Hassel: Delamination of thermal spray coatings

Mozalev, Poznyak, Hassel: Nanostructured aluminium tantalum composite oxides

Tan, Hassel: Design and Construction of a sub-micron indenter for tribological investigations

Yadav, Manthey, Hassel: High throughput screening of corrosion behaviour in combinatorial alloy development of patina forming steels

High-Temperature Reactions

Asteman, Spiegel: Materials for increased performance in sustainable fuel combustion

Cha, Spiegel: Mitigation of formation of chlorine-rich deposits affecting on superheater corrosion under co-combustion conditions

Parezanovic, Spiegel: Oxidation and segregation on high strength steels

Park, Spiegel: High temperature corrosion of alloys for flexible tubes

Pöter, Spiegel: Initial stages and kinetics of oxidation of binary and ternary iron-aluminides



Ruh, Spiegel: Optimisation of in-service performance of boiler steels by modelling high temperature corrosion OPTICORR

Sanchez-Pasten, Spiegel: Investigations on the high temperature corrosion of metallic materials under waste incineration conditions at temperatures of 300 to 600 °C

Skobir, Spiegel: European network surface engineering of new alloys for super high efficiency power generators

Srinivasan, Spiegel: Microscopic aspects of alloy oxidation

Molecular Structure and Surface Modification

Borodin, Rohwerder: Self-organization of alkane phosphonate monolayers

Ehahoun, Rohwerder: Adjustment and stability of charge distribution at the molecular monolayer/metal interface

Fischer, Rohwerder: Cellulose and cellulose derivatives: molecular and supramolecular design

Frenznick, Parezanovic, Rohwerder: A mechanistic study of wetting and dewetting during hot dip galvanizing of high strength steels

Hüning, Park, Spiegel, Rohwerder: Initial stages of high temperature oxidation investigated by VT-STM

Laaboudi, N.N., Blumenau, Rohwerder: Numerical modelling / lifetime prediction of delamination polymer coating disbonding and material degradation

Lyapin, Rohwerder: Fundamental aspects of corrosion and delamination behaviour of novel zinc alloy coatings and Zn- intermetallic phases

Michalik, Rohwerder: Development of electrically conductive polymer coatings for coil coated steel sheets

Müller-Lorenz, Rohwerder: Soluble salt contamination on blast cleaned surfaces and the effect on the durability of subsequently applied paint systems

Paliwoda-Porebska, Rohwerder: Release systems for the self-healing of polymer/metal interfaces

Rohwerder: Self-healing at cut-edge of coil coated galvanized steel sheet

Stempniewicz, Rohwerder: Intelligent self-healing by nano- and micro-capsules

Yan, Rohwerder: Fundamentals of SECPM and EC-STM of de-alloying

Vakat



Department of Materials Technology

G. Frommeyer

Scientific Concepts

The Department of Materials Technology consists of three groups which are related to several topics of the materials research within the MPIE.

The steel research represents a key topic which is performed under the supervision of G. Frommeyer in collaboration with U. Brück. The continuous casting and rapid solidification rate technology group, headed by J. Gnauk, has a strong relation to the ongoing activities in the Metallurgy Department. The development and characterization of new materials, guided by A. Schneider, has various interactions with several groups of different departments of the institute.

The fundamental material science and technologically oriented research activities are focused on the following major subjects:

- Innovative Steel Research
- Rapid Solidification Technology
- Nanoscopic Characterization of New Materials
- Refractory Materials for High-Temperature Applications

The characterization and modelling of microstructures and properties of new high performance materials, in particular novel steels possessing high strength, excellent formability and reduced specific weight for advanced design concepts of modern transportation systems, mechanical engineering and architectural structures are important tasks in the field of innovative steel research. These intentions rely on great challenges of modern steels with superior

properties in competition with other materials, specifically light-weight metals, such as aluminium, magnesium and related composites. Supplementary aspects are current economical and environmental requirements, like reduced fuel consumption and exhaust gases, saving of natural resources and an efficient scrap metal recycling.

Besides this, some important physical properties should be taken into account. These are the electrical resistivity and specific surface heat radiation capacity of heat resistance wires, superior hard magnetic properties – high coercive forces and energy products – of permanent magnets of high magnetic polarization, or soft magnetic behaviour of high-grade electric steels based on iron silicon used in transformer cores and rotating electric machines.

Fine-structure superplasticity in ultrafine-grained iron-based alloys, steels, and iron aluminides have been investigated over several years. The main tasks are the analysis of the governing deformation mechanisms and parameter studies for optimum superplastic forming procedures under high-strain-rate conditions.

In recently performed studies on superplastic high-strength ultrahigh carbon-aluminium steels with additions of chromium and tin it has been shown that the principal deformation mechanism is grain boundary sliding accommodated by dislocation climb controlled by enhanced chemical diffusion, specifically due to the solute tin atoms of high diffusivity [1,2].

Innovative Steel Research

One important aim of the innovative steel research concerning light-weight constructions is the development and optimisation of high-strength steels of reduced density and improved corrosion behaviour. Newly developed Fe-Mn-Al-C light-weight steels possess lower density of about 15 %, superior strength properties, and high tensile ductility in comparison with conventional deep drawing steels

due to their specific chemistry, microstructures, deformation and strengthening mechanism. These steels exhibit a triplex microstructure consisting of austenite, ferrite and nanodispersed $(\text{Fe,Mn})_3\text{AlC}$ κ -carbides. The morphology and distribution of these carbides are strongly influenced by the alloying elements; although the thermal treatment may significantly affect their mechanical properties.



Pronounced homogeneous shear-band formation causes Shear-band Induced Plasticity – SIP effect – and the high-strength properties are due to effective solid solution hardening and dislocation interactions in crossing shear bands. The extraordinary ductility and toughness even under impact loading promote high energy absorption at very high strain rates up to 10^3 s^{-1} . Actually, the innovative steel research group is focussing its interest on microstructure evolution in dependence on the alloying elements and the processing parameters. These factors are strongly determining the mechanical properties [3].

Another subject is the design and evaluation of new high-strength and wear resistant quasi perlitic steels with sufficient toughness and fatigue properties in the temperature range from -50 to $100 \text{ }^\circ\text{C}$. These properties are required for novel steels in modern railway transportation systems and power trains. Quasi eutectoid high strength and ductile high-carbon steels with aluminium and chromium additions have been developed which fulfil these requirements. The

steels possess an ultrafine lamellar perlite microstructure of Sorbit and Troostit morphology. The lamellar thickness of the modified cementite and the interlamellar spacing of cementite and α -ferrite are on the submicron level. These ultrafine perlitic steels show extremely high strength, sufficient ductility and fracture toughness at room and lower temperatures down to $-60 \text{ }^\circ\text{C}$.

The newly invented SUPER TRIP steels are based on thermomechanically processed metastable austenitic/martensitic microstructures of high dislocation density. These steels consist of medium concentrations of chromium-nickel/manganese-molybdenum and exhibit extremely high flow stresses, ultimate tensile strengths, and fairly large tensile ductility. These unique steels achieve almost the theoretical strength of ferrous alloys due to severe martensitic transformations, the presence of high dislocation densities in austenite and transformed martensite, and very effective dispersion strengthening due to nanosized special carbides.

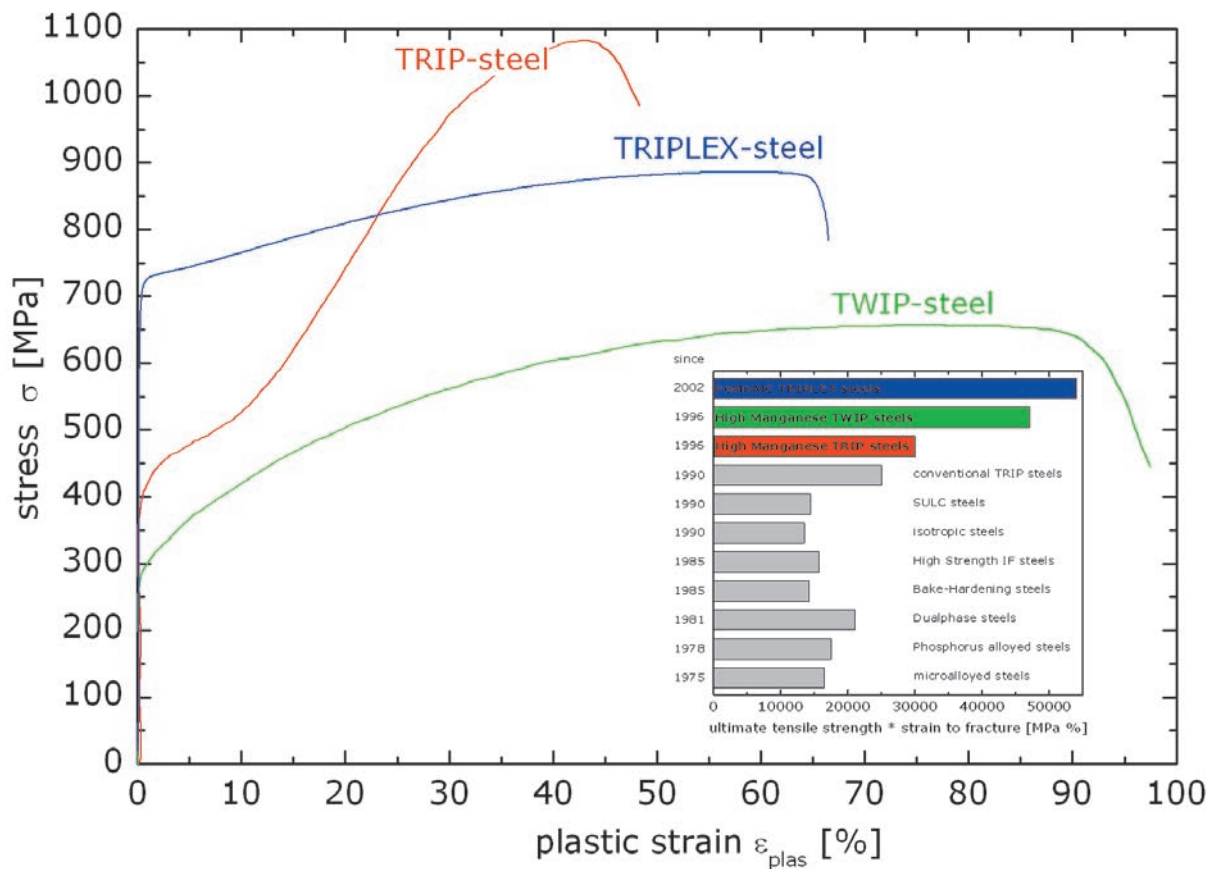


Fig. 1: Typical engineering stress strain curves of high manganese TRIP, TRIPLEX and TWIP steels.



Rapid Solidification Technology

The activities of the research group „rapid solidification technology“ are centered on the analysis and modelling of solidification processes in general and rapid solidification processes in particular. Technologies like near net shape casting or laser welding require suitable macroscopic solidification models to enlighten the process mechanisms and to supplement necessary experimental data. Experimental investigations on microstructures and physical properties of rapidly solidified materials as well as in-situ measurements of the governing process parameters (e.g. melt temperature, casting velocity cooling rate etc.) during solidification will sustain to confirm and refine conventional and newly developed models.

The modelling is carried out using conventional FEM methods as well as self developed thermodynamic libraries and experimental data. The calculations are based on the generalised enthalpy method, a single domain method for heat and solute transport, which allows the thermodynamic computation of coexisting multiple phases. This will be performed without an additional effort to calculate the transport phenomena. The model will be com-

pleted by a recalculation of the phase fraction under non-equilibrium conditions considering higher cooling rates far away from an expected local equilibrium close to a phase transitions. The model is applied to complex binary systems like Al-Ti and Al-Fe exhibiting intermetallic compounds. The extension of the model to a mathematical treatment of ternary systems is currently in progress.

Complementary to modelling, experimental investigations on rapid solidification rate process technology regarding e.g. near net shape casting are carried out. The planar flow casting (PFC) melt-spinning facility will be used for the measurement of kinetic solidification parameters as well as for the production of nanocrystalline or glassy ribbons. The in-rotation-liquid-spinning (INROLISP) facility is adopted to as-cast amorphous metallic fibres with 30 μm in diameter with excellent soft magnetic properties for the use in novel magnetic field sensors. The newly installed shape flow casting (SFC) facility for continuous casting of less ductile and non die-drawable alloys will be used to produce semi-finished wires with final diameters.

Nanoscopic Characterization of New Materials

The main topics of the Research Group „Nanoscopic Characterisation of New Materials“ are focused on the development and characterisation of novel materials for structural and functional applications. An important task of all projects is the understanding of the correlation between microstructures and mechanical properties. The evolution of the microstructure is investigated experimentally by microscopic and nanoscopic methods and predicted by computer simulations using the software Thermo-Calc and DICTRA. The materials under investigation are ordered alloys, such as Fe_3Al - and NiAl-based alloys, and ferritic steels.

Iron aluminium alloys with strengthening particles have been investigated with respect to potential high temperature applications. Studies on the constitution and on mechanical properties of various Fe-Al based systems were performed [4-16]. Computer simulations on phase equilibria and transformations serve

as predictive tools in order to lower the number of experiments.

The development of ferritic steels is based on experiments and computer simulations of thermodynamics and kinetics of phase transformations (collaboration with the department of Physical Metallurgy). The microstructural evolution and the effect of metastable precipitates on the growth kinetics of stable phases has been studied by means of computer simulations (DICTRA) [17].

In continuation of the previous activities on metal dusting, some materials have been tested to evaluate their high temperature corrosion behaviour under strongly carburising conditions [18-27]. It is suspected that iron aluminium-based alloys might possess a higher resistance to metal dusting because of the formation of a protective Al_2O_3 layer. Fundamental studies on the metal dusting of iron support the

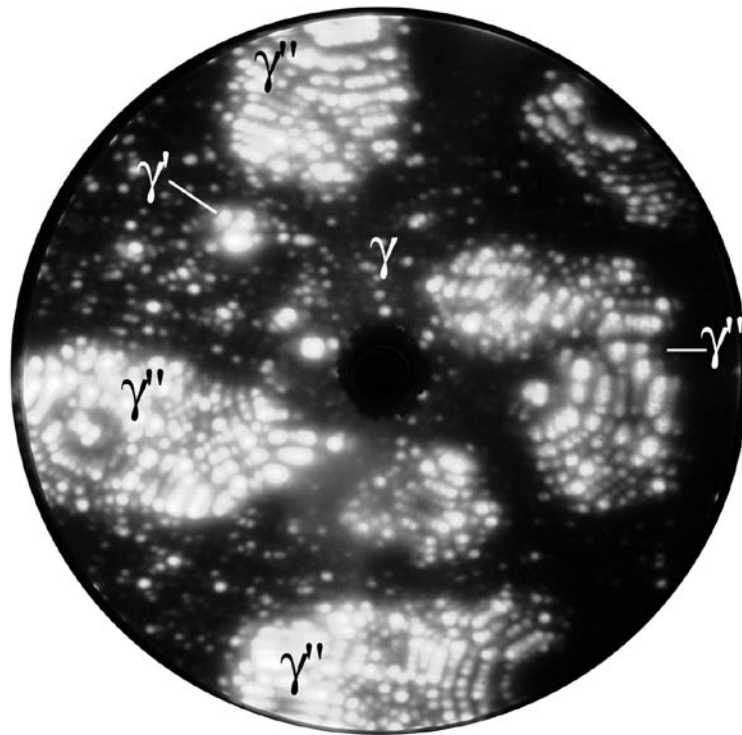


Fig. 2: Field ion microscopy (FIM) image of a nickel base superalloy showing one γ' precipitate (of about 4 nm in size) and several γ'' precipitates in the γ matrix with atomic resolution. The γ matrix appears darker than the precipitates due to its relatively high content of Cr which possesses a low evaporation field strength.

understanding of the more complex metal dusting corrosion of iron aluminium alloys.

Complementary to transmission electron microscopy (TEM) atom probe field ion microscopy (APFIM) is used for chemical analyses of interfaces, grain boundaries and antiphase boundaries in Fe-Al- and

NiAl-alloys and in steels. APFIM is also performed for investigating the site preferences of alloying elements in Ni-Al and Fe-Al alloys [28-32]. The 3-dimensional atom probe (3DAP) was used for nanoscopic analysis of steels and iron-aluminium alloys (collaboration with A. Cerezo, G.D.W. Smith, Department of Materials, Oxford University, UK) [33].

Refractory Materials for High-Temperature Applications

The new generation of energy conversion systems, such as internal combustion engines, jet engines, stationary gas turbines of power plants, and heating conductors require the application of high temperature or refractory materials with sufficient warm strength and creep resistance and excellent oxidation or hot gas corrosion properties.

One important class of materials are nickel- and cobalt aluminides alloyed with the refractory b.c.c. and h.c.p. metals Cr, Mo and Re. Quasi binary hypoeutectic and directionally solidified eutectic systems have been investigated with respect to mechanical properties, such as elasticity, solid solution hardening, fibre reinforcement, creep

strength and fracture toughness in view of atomic defects and microstructural features as well [34].

Among the investigated alloys the unidirectionally solidified fibre reinforced NiAl-(Mo,Re) eutectic composites possess optimum high-temperature strength and creep resistance up to 1250 °C. The chromium containing hypoeutectic material exhibits a good combination of strength and ductility up to 1150 °C. However, no tensile ductility at room temperature has been achieved up to now [35].

The influence of the high-melting point b.c.c. metals V, Nb, Cr and Mo and their site preferences on the temperature dependent mechanical properties and the superplastic behaviour at higher strain rates

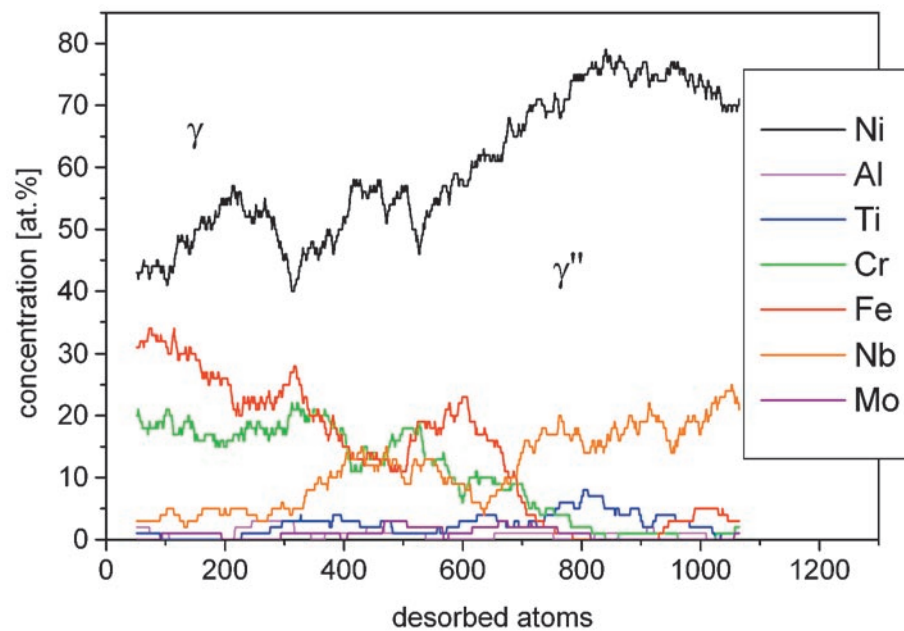


Fig. 3: Concentration profiles determined by atom probe (APFIM) showing the distribution of the alloying elements at the $\gamma - \gamma''$ transition.

on γ -TiAl base alloys have been studied. The site preferences were determined by high resolution APFIM and ALCHEMI analysis in collaboration with Vanderbilt University and Oak Ridge National Laboratory [36-38].

Quasi eutectoid titanium-transition metal alloys with ultrafine-grained microstructures consisting of titanium solid solutions, matrix grain size of about 0.5 to 0.7 micron, and a dispersion of intermetallic FeTi (B2 type of structure), Co_2Ti and Ni_2Ti (cubic complex E9_9 superlattice structure) particles of 0.2 to 0.3 micron in size exhibit superior strength properties and superplasticity at higher temperatures. In the coarse grained state the alloys reveal excellent creep resistance [39].

Advanced high melting point silicides with low density have been evaluated because of their potential applications at 1300 °C and above. The refractory titanium silicides Ti_5Si_3 and TiSi_2 with complex hexagonal D8_8 and orthorhombic C54 lattice structures exhibit superior physical and mechanical properties, such as high lattice energies and melting temperatures; high hardness, elastic stiffness and flow stresses; low densities and excellent creep and oxidation resistance. The complex lattice structures and the governing covalent bonding of these compounds cause a lack in ductility due to sessile superdislocations. The ductility and fracture toughness of the silicides have been considerably improved by adding aluminium to the refractory compounds and by producing nanosized grain structures. However, optimum creep strength at 1300 °C occurs in coarse grained silicides [40].

References

1. Frommeyer, G.; Jiménez, J.A.: Structural Superplasticity at Higher Strain Rates in Hypereutectoid Fe-5.5Al-1Sn-1.3C. *Metall. Mater. Trans.* (2004) *in press*.
2. Frommeyer, G.; Hofmann, H.; Löhr, J.: *Steel Res. Int.* 74 (2003) 338-343.
3. Brück, U.; Frommeyer, G.: In: *Proc. PLASTICITY 2003*, Quebec, Kanada; ed. A.S. Khan, Neat Press, Maryland, USA (2003) 169-172 (see also *selected scientific topics*)
4. Stein, F.; Schneider, A.; Frommeyer, G.: *Intermetallics* 11 (2003) 71-82 (see also *selected scientific topics*).
5. Schneider, A.; Falat, L.; Sauthoff, G.; Frommeyer, G.: *Intermetallics* 11 (2003) 443-450.
6. Schneider, A.; Sauthoff, G.: *Steel Res. Int.* 75 (2004) 55-61.
7. Stallybrass, C.; Schneider, A.; Sauthoff, G.: *Intermetallics*, *accepted for publication* (see also *selected scientific topics*).
8. Falat, L.; Schneider, A.; Sauthoff, G.; Frommeyer, G.: Mechanical properties of Fe-Al-M-C (M = Ti, V, Nb, Ta) alloys with strengthening carbides and Laves phase, *Intermetallics*, *accepted for publication*.
9. Kobayashi, S.; Zaefferer, S.; Schneider, A.; Raabe, D.; Frommeyer, G.: Slip system determination by rolling texture measurements around the strength peak temperature in a Fe_3Al -based alloy, *Mater. Sci. Eng. A*, *in press*.
10. Konrad, J.; Zaefferer, S.; Schneider, A.: *Mater. Sci. Forum* 467-470 (2004) 75-80.



11. Kobayashi, S.; Zaefferer, S.; Schneider, A.; Raabe, D.; Frommeyer, G.: Mater. Sci. Forum 467-470 (2004) 153-158.
12. Kobayashi, S.; Zaefferer, S.; Schneider, A.; Raabe, D.; Frommeyer, G.: Optimisation of precipitation for controlling recrystallisation of wrought Fe₃Al-based alloys, Intermetallics, *accepted for publication*.
13. Schneider, A.; Falat, L.; Sauthoff, G.; Frommeyer, G.: Microstructures and mechanical properties of Fe₃Al-based Fe-Al-C alloys, Intermetallics, *accepted for publication*.
14. Konrad, J.; Zaefferer, S.; Schneider, A.; Frommeyer, G.; Raabe, D.: Hot deformation behavior of a Fe₃Al-binary alloy in the A2 and B2-order regimes, Intermetallics, *accepted for publication*.
15. Risanti, D.; Deges, J.; Falat, L.; Kobayashi, S.; Konrad, J.; Palm, M.; Pöter, B.; Schneider, A.; Stallybrass, C.; Stein, F.: Brittle-to-ductile transition temperatures (BDTT) of Fe-Al alloys in dependence of the Al-content, Intermetallics, *submitted*.
16. Schneider, A.; Zhang, J.: Orientation relationship between a ferritic Fe-15Al matrix and κ-phase (Fe₃AlC_x) precipitates, Intermetallics, *submitted*.
17. Schneider, A.; Inden, G.: Simulation of the kinetics of precipitation reactions in ferritic steels, Acta Mater., *in press* (see also *selected scientific topics*).
18. Zhang, J.; Schneider, A.; Inden, G.: Corros. Sci. 45 (2003) 281-299.
19. Zhang, J.; Schneider, A.; Inden, G.: Corros. Sci. 45 (2003) 1329-1341.
20. Schneider, A.; Grabke, H.J.: Mater. Corros. 54 (2003) 793-798.
21. Schneider, A.; Zhang, J.: Mater. Corros. 54 (2003) 778-784.
22. Zhang, J.; Schneider, A.; Inden, G.: Mater. Corros. 54 (2003) 763-769.
23. Zhang, J.; Schneider, A.; Inden, G.: Mater. Corros. 54 (2003) 770-777.
24. Zhang, J.; Schneider, A.; Inden, G.: Corros. Sci. 46 (2004) 667-679.
25. Schneider, A.; Zhang, J.; Inden, G.: J. Corros. Sci. Eng. 6 (2004) Paper 87.
26. Zhang, J.; Schneider, A.; Inden, G.: J. Corros. Sci. Eng. 6 (2004) Paper 100.
27. Bernst, R.; Schneider, A.; Spiegel, M.: Metal dusting of binary iron aluminium alloys at 600 °C, Intermetallics, *submitted*.
28. Deges, J.; Schneider, A.; Fischer, R.; Frommeyer, G.: Mater. Sci. Eng. A 353 (2003) 80-86.
29. Fischer, R.; Frommeyer, G.; Schneider, A.: Mater. Sci. Eng. A 353 (2003) 87-91.
30. Deges, J.; Fischer, R.; Frommeyer, G.; Schneider, A.: Surf. Interface Anal. 36 (2004) 533-539.
31. Frommeyer, G.; Fischer, R.; Deges, J.; Rablbauer, R.; Schneider, A.: Ultramicroscopy 101 (2004) 139-148.
32. Deges, J.; Rablbauer, R.; Frommeyer, G.; Schneider, A.: Observation of Boron enrichments in a heat treated quasibinary hypoeutectic NiAl-HfB₂ alloy by means of APFIM, Surf. Interface Anal., *submitted*.
33. Schneider, A.; Stallybrass, C.; Sauthoff, G.; Cerezo, A.; Smith, G.D.W.: Three-dimensional atom probe studies of phase transformations in Fe-Al-Ni-Cr alloys with B2-ordered NiAl precipitates, *in preparation* (see also *selected scientific topics*).
34. Frommeyer, G.; Rablbauer, R.: Mater. Res. Soc. Symp. 753 (2003) 193-207.
35. Rablbauer, R.; Fischer, R.; Frommeyer, G.: Z. Metallkd. 95 (2004) 525-534.
36. Knippscheer, S.; Frommeyer, G.: In: Ti-2003, Science and Technology, eds. G. Lütjering, J. Albrecht, Wiley-VCH (2004) 2331-2338.
37. Uhlmann, E.; Frommeyer, G.; Herter, S.; Knippscheer, S.; Lischka, J.M.: In: Ti-2003, Science and Technology, eds. G. Lütjering, J. Albrecht, Wiley-VCH (2004) 2293-2300.
38. Frommeyer, G.; Knippscheer, S.: In: Ti-2003, Science and Technology, eds. G. Lütjering, J. Albrecht, Wiley-VCH (2004) 2249-2256.
39. Frommeyer, G.: In: Euro SPF 2004, Proc. Third European Conference on Superplastic Forming, eds. G. Bernhard, T. Cutard, P. Lours, Cépaduès-Editions, Toulouse (2004) 57-64.
40. Frommeyer, G.; Rosenkranz, R.: In: Metallic Materials with High Structural Efficiency, series II, eds O.N. Senkov, D.B. Miracle, S.A. Firstov, Kluwer Academic Publisher, Dordrecht, NL (2004) 146.



Research Projects in Progress

Rapid Solidification Technology

Frommeyer, Gnauk: Continuous casting of CrNi stainless steel and heat resistant Ni₃Al(B) and Al(Fe)Cr wires. Investigations on correlations between microstructures and solidification and cooling rates

Frommeyer, Gnauk: Thin strip and foil casting of heat resistant FeCr(Al) and Fe₃Al(Cr) alloys for catalytic converter systems.

Gnauk, Frommeyer: Continuous casting of soft magnetic fibres for new magnetic field sensors

Gnauk, Wenke: Macroscopic modelling of phase formation and microstructure evolution in aluminium-steel joining interfaces

Gnauk, Wenke: Modelling of phase and microstructure formation under non-equilibrium conditions of aluminium titanium laser welded seams

Gnauk, Wenke, Frommeyer: Numerical modelling of solidification processes

Innovative Steel Research

Brokmeier, Br x, Frommeyer: Investigations on the microstructures and properties of high carbon TRIP-steels manufactured by Direct-Strip-Casting

Br x, Frommeyer: Development and optimisation of crash resistant high carbon TRIP/TWIP-steels for automotive applications

Br x, Frommeyer: Optimisation of microalloyed deepdrawing lightweight steels based on iron-aluminium

Br x, Frommeyer, Meyer, Kr ger* (*TU Chemnitz):* Investigations on the deformation behaviour under high dynamical multiaxial load of supraductile TRIP/TWIP-steels

Deges, Frommeyer, Schneider: Effect of ternary alloying additions on mechanical properties and ductility of Fe₃Al-Based alloys

Frommeyer: Development of novel SUPER TRIP steels and characterisation of microstructure and properties

Frommeyer, Brokmeier: Investigations on microstructures and properties of quasi eutectic high carbon-aluminium steels with ultrafine lamellar perlitic

Frommeyer, Deges, Boehnke, Denkena* (*IFW Univ. Hannover):* Machining of iron-aluminium-alloys:

Mechanisms of chip formation and behaviour for wear

Frommeyer, Jim nez: Investigations on superplasticity in super duplex stainless steels and UHC light-weight steels and optimisation of superplastic forming at high-strain-rates

Gnauk, Frommeyer: Modelling of superplastic forming operations

Development and Characterisation of New Materials

Fischer, Frommeyer, Deges, Schneider: Structural characterization of high temperature NiAl-(Fe, Cu, Mo) alloys by using Atom Probe Field Ion Microscopy (APFIM)

Frommeyer, Knippscheer: Alloy design of new beta titanium alloys

Frommeyer, Rablbauer: Investigations on structural superplasticity and deformation mechanism in NiAl(Cr) based alloys

Frommeyer, Schneider, Deges: Effect of ternary alloying additions on mechanical properties and ductility of Fe₃Al-Based alloys

Hassel, Milenkovic, Bello Rodriguez, Schneider: Directionally solidified alloys as a source for nanostructured materials

Knippscheer, Frommeyer: Characterization of microstructures and mechanical properties of TiAl-based alloys modified with alloying elements of the transition metals

Palm, Lacaze (CIRIMAT, Toulouse): Re-assessment of the Fe-Al-Ti system

Palm, Schneider, Frommeyer: Development of Fe-Al-based alloys

Palm, Schuster (Univ. Wien): Re-assessment of the Al-Ti system

Palm, Stein: Stability of the microstructure, mechanical behaviour and oxidation resistance of lamellar TiAl + Al₂Ti alloys

Rablbauer, Frommeyer: Studies on creep behaviour of intermetallic NiAl-X(Cr, Mo, Re) alloys

Sauthoff, Risanti, Schneider: Microstructures and mechanical properties of Fe-Al-Ta alloys with strengthening Laves phase precipitates



Sauthoff, Schneider, Knežević: Ferritic steels with maximum creep resistance: alloy development and long-term behaviour

Sauthoff, Stallybrass, Schneider: Ferritic Fe-Ni-Al-Cr alloys with coherent B2-ordered NiAl precipitates

Schneider, Eleno, Frisk (SIMR, Stockholm), Sundmann (KTH, Stockholm): Re-assessment of the Fe-Al-Ni system

Schneider, Falat, Frommeyer: Thermodynamics and kinetics of phase transformations and coarsening processes in Fe-Al-M-C(M=Ti, Nb, V, Ta) alloys

Schneider, Frommeyer: TEM-investigations on antiphase boundaries and dislocation structures of ordered Fe₃Al based alloys

Schneider, Frommeyer, Ishda: Constitution investigations on metastable equilibria in iron rich ternary Fe-Al alloys

Schneider, Frommeyer, Sauthoff, Krein: Microstructures and mechanical properties of Fe₃Al-based alloys with strengthening boride precipitates

Schneider, Inden, Eleno: High temperature materials

Schneider, Inden, Strondl: Ferritic steels with maximum creep resistance: computer supported modelling of phase transformations

Schneider, Palm, Frommeyer, Milenkovic: Determination of phase equilibria and directional solidification of Fe-Al-Nb alloys

Schneider, Spiegel, Bernst: Metal dusting of iron aluminium alloys

Schneider, Strondl, Frommeyer: Production of Ni-base superalloys by electron beam melting

Schneider, Zaeferrer, Frommeyer, Raabe, Konrad: Investigations of microstructures and hot deformation behaviour of Fe₃Al-based alloys

Spiegel, Stein, Pöter: Initial stages and kinetics of oxidation of binary and ternary iron-aluminides

Stein: DTA studies of phase transitions in intermetallic systems

Stein, Dovbenko, Palm: Phase equilibria in the Co-Nb-Al system

Stein, Golovin (Institute for Materials, TU Braunschweig): Investigations on internal friction behaviour in Fe₃Al-based alloys

Stein, Konrad, Palm: Structure-type variations of Laves phases in the Co-Nb system

Stein, Palm, Sauthoff, Raabe, Kreiner, Grin* (*MPI-CPfS, Dresden), Leineweber, Mittemeijer (MPI-MF, Stuttgart), Fischer, Jansen (MPI-FKF, Stuttgart):* Experimental and theoretical investigations on the structure and stability of Laves phases

Strondl, Schneider, Frommeyer: Investigations on phase transformations in Ni-base superalloys and NiAl-(Cr) alloys

Wittig (Vanderbilt University), Frommeyer, Knipscheer, Bently (Oak Ridge Nat. Lab.): Site preference studies on TiAl(Cr, Cu, Mo, Nb) using ALCHEMI and APFIM



Department of Microstructure Physics and Metal Forming

D. Raabe

Scientific Concept

The department conducts research on the relationship between processing, microstructure, and properties of structural materials with emphasis on steels. Detailed characterization and basic understanding of microstructure evolution under complex thermomechanical history and boundary conditions and its relevance for the mechanical behaviour plays a key role in our projects. Particular pronunciation is placed on the integration of continuum theory and experiment (Fig. 1). Five research groups form the cornerstones of the department:

- Theory and Simulation (F. Roters)
- Diffraction and Microscopy (S. Zaefferer)
- Thermomechanical Processing (D. Ponge)
- Metal Forming (W. Rasp)
- Leibniz group on Biological Nano-Composites (D. Raabe)

The table shows the most important highlights of the five groups during the last two years:

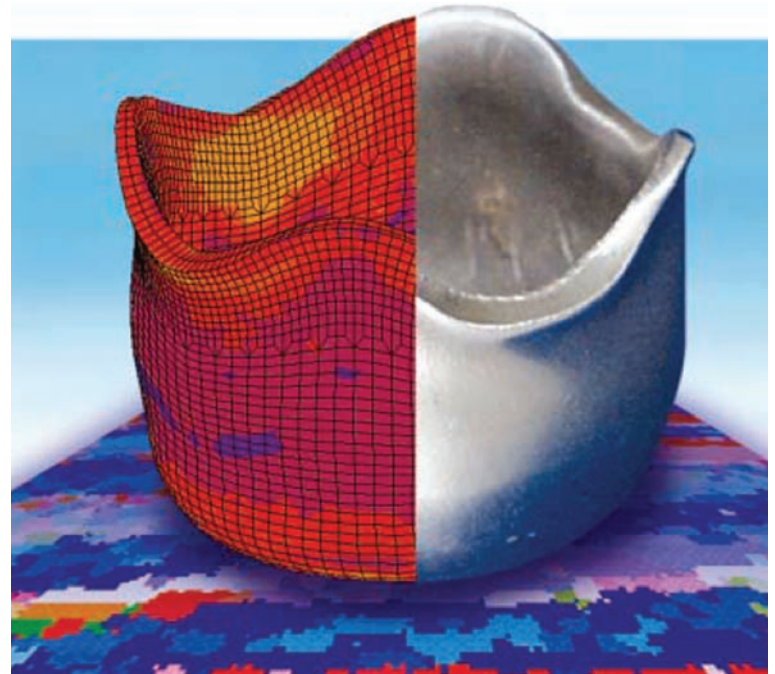


Fig. 1: Projects are characterized by a close integration of experiment and continuum simulation. The figure shows a Texture Component Crystal Plasticity Finite Element simulation.

| Research Group | Main Highlight in 2003 and 2004 |
|---|---|
| Theory and Simulation | crystal plasticity finite element methods for small scales (sub-grain scale) and for large scales (10^9 grains) |
| Diffraction and Microscopy | multiphase 3D EBSD nanotexture analysis via the integration of joint focussed ion beam and electron back scatter diffraction microscopy |
| Thermomechanical Processing | processing, microstructure, and properties of steels with ultrafine microstructures |
| Metal Forming | formability and properties of metals under hydrostatic pressure |
| Leibniz Group on Biological Nano-Composites | structure and properties of chitin-based biological nanocomposites |

Theory and Simulation (F. Roters)

Mission. The group for Theory and Simulation develops physically based models for the mechanical behaviour of materials. The Finite Element Method (FEM) is nowadays a standard tool for the simulation of the plastomechanical behaviour of materials. However the constitutive laws implemented in commercial FEM codes are usually too empirical to be predictive. The development of physically based constitutive models is, therefore, a key task in this field.

Recent highlight. The projects in the group Theory and Simulation in the past 2 years have focused on two topics, namely, the application of crystal plasticity theory to small scales and to large scales. The first group of projects (small scales) is concerned with the development of constitutive laws which root in dislocation dynamics and grain boundary mechanics. These laws can tackle small scale plasticity issues such as gradient and contact effects as well as interface mechanics [1-8]. The second area is the Texture Component Crystal



Plasticity FEM [9-12] which is a combination of the texture component method with the crystal plasticity FEM.

Microscopy and Diffraction (S. Zaeferrer)

Mission. The main mission of the Microscopy and Diffraction group consists in the experimental investigation of the microstructure and crystallographic texture in materials [13-19]. The focus lies on the investigation of local processes (Fig. 2). Therefore, the experimental methods comprise transmission and high resolution scanning electron microscopy (TEM and SEM) together with the corresponding diffraction techniques (transmission Kikuchi and spot diffraction in the TEM and backscatter electron diffraction (EBSD) in the SEM). For 3D EBSD investigations, a high-resolution, high-beam Zeiss Crossbeam XB1560 FIB equipped with a TSL EBSD system is available. Additionally, X-ray diffraction is used to measure textures and stresses.

Recent highlight. The most important current project in the group is the development of a novel multiphase 3D EBSD nano- and microtexture analysis method via the integration of joint focussed ion beam and electron back scatter diffraction microscopy. This is realized by using a Zeiss Crossbeam XB1560 FIB which is a combination of a high resolution SEM and a focussed ion beam (FIB)

microscope. While the SEM part is used to observe and analyse the sample, the FIB part serves to cut and structure the sample surface. One particular application will be 3D orientation microscopy by a cut-and-analyse serial section technique. To this end a surface is prepared by FIB and analysed by EBSD. Subsequently the next section is cut and observed again and so on. In this way, resolutions of about 50 nm in depth will be achievable and material volumes of about $50 \times 30 \times 30 \mu\text{m}^3$ can be investigated. Besides standard electron detectors the instrument is also equipped with a transmitted electron detector for the acquisition of scanning transmission electron images from thin foils which are made by FIB cutting.

Thermomechanical Treatment (D. Ponge)

Mission. The aim of the group for Thermo-mechanical Processing is the investigation of the relationship between the processing, microstructure, and mechanical properties of steels [20-24]. The characterization and the understanding of the mechanisms which guide the observed microstructures under complex thermomechanical history and boundary conditions and their relevance for the observed micro- and macromechanical behaviour is the key area of all projects in this group. Experiments are conducted by using a variety of casting and large scale forming devices, such as the 2.5MN hot compression machine.

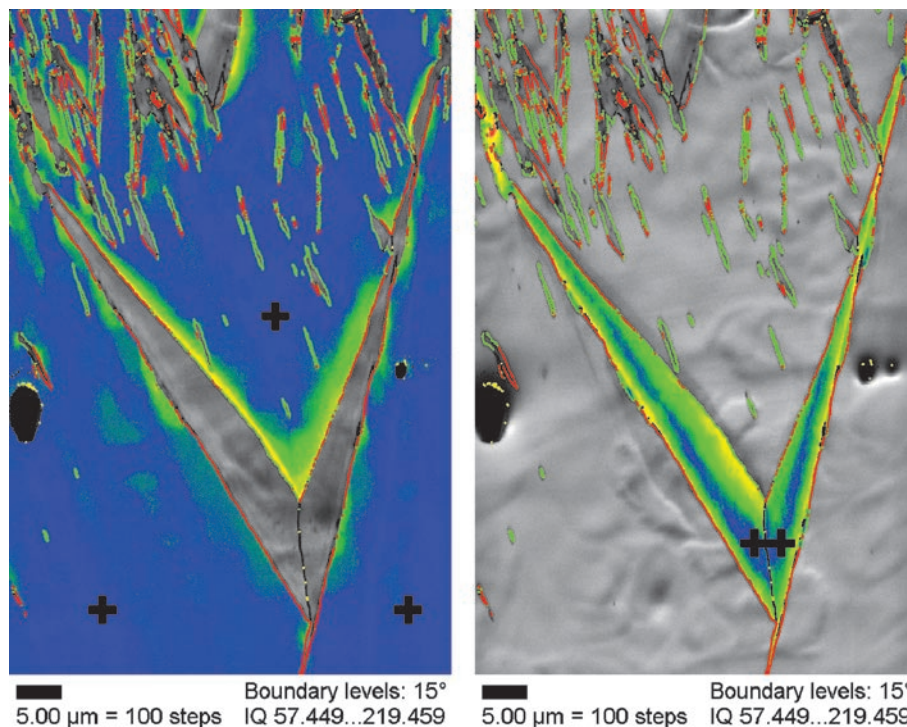


Fig. 2: Quantitative high resolution texture measurement on lenticular martensite. The color coding shows the orientation gradients before and inside of the martensite plates with a maximum misorientation of 10° . The data show strong orientation gradients only on one side of the martensite in the surrounding matrix. Inside the lenticular martensite the orientation relationship with the matrix changes systematically from Nishiyama-Wassermann to Kurdjumov-Sachs (Sato, Zaeferrer, unpublished data).



Recent highlight. Recent key projects in this group focus on steels with ultrafine grains [22,24,25]. Corresponding microstructures of plain C-Mn steels comprising fine ferrite grains and dispersed cementite particles have been achieved by controlled cooling and heavy warm compression. The grain boundary character distribution created in such steels was investigated by using electron backscattering diffraction (EBSD): The fraction of high angle grain boundaries was found to be approximately 60% in such materials.

Metal Forming (W. Rasp)

Mission. The main objective of this group is the analysis of forming processes with emphasis on hot and cold rolling [26,27]. Projects are based on mechanical and tribological fundamentals in order to study forming processes under the complex boundary conditions typically imposed by the workpiece-interface-tool system. Particular attention is given to a better understanding of the parameters that control the accuracy of the shape of formed parts and the appearance of the final surface.

Recent highlight. The key project in the Metal Forming group in the past two years was a study on the improvement of formability of brittle materials by a superimposed hydrostatic pressure. The experiments are performed by a simultaneous deformation of a brittle core material and a ductile shell. The deformation of the shell is a forward-extrusion process.

Leibniz Group on Biological Nano-Composites (D. Raabe)

Mission. The main objective of this new group is the basic study of natural crystalline composite materials that form the exoskeleton of arthropods. Particular attention is placed on the investigation of the structure and the mechanical properties of crustaceans, mainly of the homarus americanus (american lobster). This material is an excellent example of a bio-nano-composite with variable properties and substantial structural and mechanical anisotropy which manifests itself both, at the microscopic and at the macroscopic scale. As in most mineralized natural polymer tissues, the calcite components of the crustacean shell are associated with complex organic matrices which include proteins, glycoproteins, polysaccharides and lipids. The most important polysaccharide is the chitin, a cellulose-like biopolymer, one of the most abundant in nature that acts as a framework for the inorganic material.

Recent highlight. During the last year the newly established group, which is funded by the German research foundation DFG through the Gottfried Wilhelm Leibniz award, has been concerned with experiments for a better understanding of the structure of the exoskeleton of homarus americanus (lobster) and its relevance for the mechanical properties.

Spirit, Teamwork, Outreach

All projects in the department are pursued in a highly interdisciplinary manner. Our research style is characterized by a spirit of team work. Scientists in our department come from such different fields as theoretical and experimental physics, materials science and engineering, metallurgy, chemistry, theoretical solid mechanics, mechanical engineering, polymer physics, and polymer mechanics, i.e. communication is paramount to the success of the group. Projects are pursued in an atmosphere of mutual learning, inspiration, and interdisciplinary co-operation including in particular a steady exchange among theorists and experimentalists.

The working atmosphere within our department is dominated by an international flair bringing together young scientists from Brazil, Bulgaria, China, Egypt, France, Germany, India, Iran, Japan, Jordan, Korea, Russia, Spain, UK, and USA. This international orientation is also reflected by our main cooperation

partners outside the Max Planck Society, i.e. RWTH Aachen (Prof. Bleck, Prof. Gottstein), University of Clausthal (Prof. Bunge), DESY (Prof. Brokmeier), University of Göttingen (Dr. Klein), Carnegie Mellon University (Prof. Rollett), MIT (Prof. Radovitzky, Prof. Schuh), Technical University of Beijing (Prof. Mao), University of Lorena in Brazil (Prof. Sandim), and the National Institute for Materials Science in Japan (Prof. Hono).

Also, our department holds a strong position in the participation of senior female researchers in highly responsible and internationally visible leadership positions such as for instance Dr. Dorothee Dorner for the transformer steel research group, Dr. Patricia Romano for the biological microscopy initiative, Dr. Jeon Haurand for the FEM texture analysis group, Dipl.-Ing Alice Bastos for the nanotexture initiative, and Dr. Rongjie Song for the ultrafine grained steel projects.



Selected Interdisciplinary Key Projects

Consideration of Geometrically Necessary Dislocations and of Grain Boundary Mechanics in Crystal Plasticity Finite Element Simulations

Roters, Ma, Raabe, Gottstein (RWTH)

Crystallographic slip, e.g. movement of dislocations on distinct slip planes is the main source of plastic deformation in most metals. The crystal plasticity FEM combines this basic process with the Finite Element Method by assuming that the plastic velocity gradient is composed of the shear contributions of all slip systems. The dislocation model used in our approach is based on six main ingredients: 1) For every slip system mobile and immobile dislocations are distinguished. 2) The immobile dislocations are grouped into parallel and forest dislocations for each slip system. 3) A scaling relation between mobile and immobile dislocations is derived. 4) The Orowan equation is used as kinetic equation. 5) Rate equations for the immobile dislocation densities are formulated based on distinct mechanisms such as lock formation or annihilation. 6) Orientation gradients are described in terms of the dislocation density tensor. 7) We also introduce the mechanics of grain boundaries into the crystal plasticity FEM. While standard codes describe the

grain boundaries as kinematical discontinuities the new approach introduces an activation energy which captures the grain boundary resistance to slip penetration. Simulations are in excellent agreement with experiments.

Simulation of Micro- and Nanoindentation of Metallic Single Crystals with and without Polymer Coatings

Zaafarani, Ma, Roters, Wang, Nikolov, Raabe

This project is concerned with the investigation of nanoindentation mechanics (Fig. 3) using high purity single crystals with and without polymer coatings. Experiments are conducted on a Hysitron nanoindentation set-up using a conical indenter in order to avoid symmetries others than those of the crystals. Simulations are carried out by means of a 3D crystal plasticity Fe method which takes full account of crystallographic non-local gradient effects during the indentation.

Cellular Automaton Simulation of the Recrystallization Textures of IF Sheet Steels

Hantcherli (Ecole des Mines St. Etienne), Raabe

This project is a cellular automaton simulation study on the evolution of the recrystallization texture in a cold rolled interstitial free sheet steel (Fig. 4). The model is applied to experimentally obtained EBSD data. The dislocation density distribution for the driving force is approximated from the Kikuchi pattern quality of the EBSD data. Different models for nucleation and for the influence of Zener-type particle pinning are investigated.

Texture Component Crystal Plasticity FEM

Roters, Raabe

This project is about the mapping of texture functions into crystal plasticity FE simulations. Gauss-shaped texture components represent an ideal approach for including textures in FE models since they represent an excellent compromise between discreteness (spherical localization), compactness (simple functions), mathematical precision (excellent also of complex textures), scalability (the number of used texture components can be varied according to the desired exactness of the texture fit), conceptual simplicity (simple mathematical handling), and physical significance

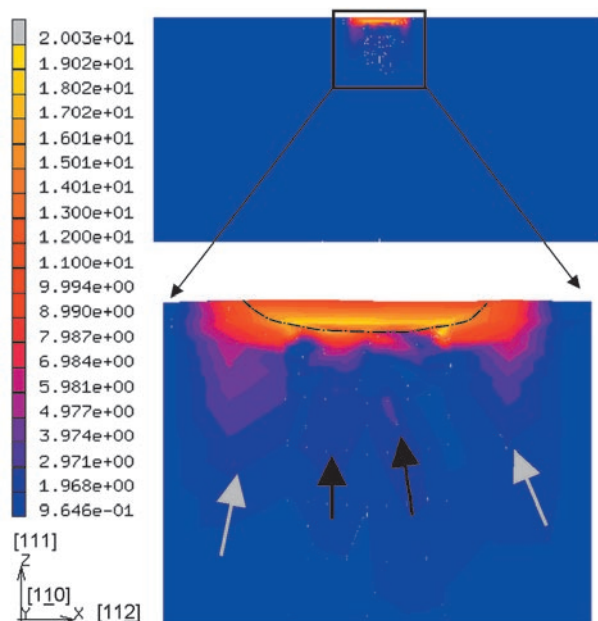


Fig. 3: Simulated distribution of the misorientations below a nanoindenter presented in the (110) cutting plane. The indents were simulated on the (111) plane of a Cu single crystal using a conical indenter. The color code shows the orientation change relative to the starting orientation. The dotted conus in the lower figure indicates the shape of the indenter.

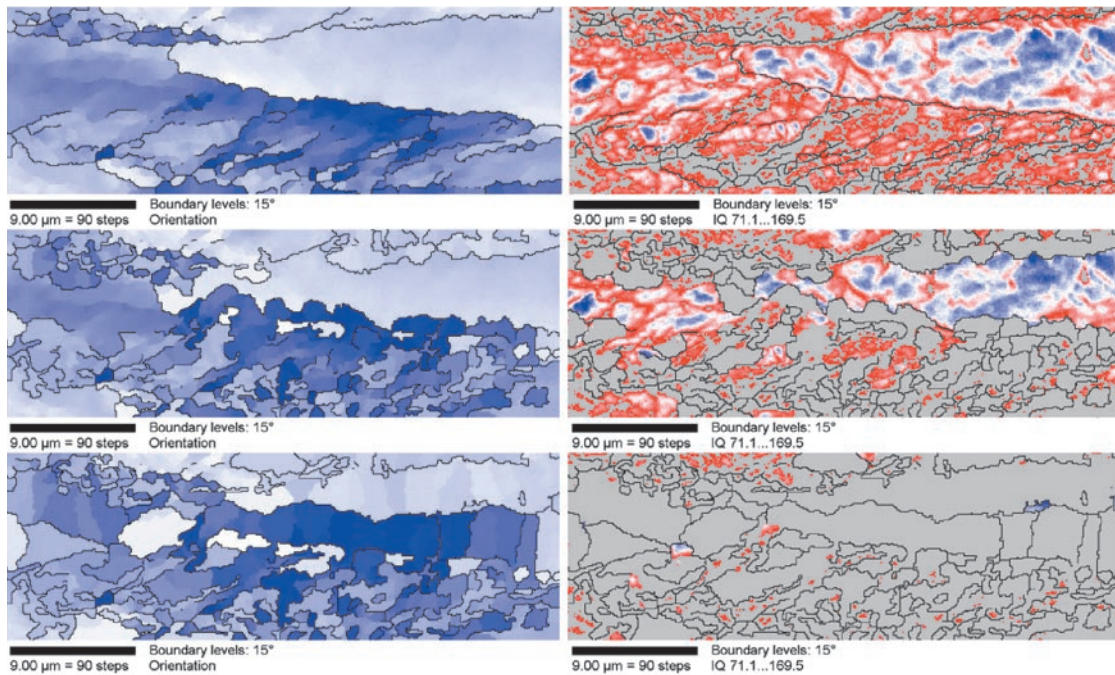


Fig. 4: Cellular automaton simulation results applied to EBSD starting data. Recrystallization microstructures after 30 vol.%, 65 vol.% and 99 vol.% . Left hand side: orientation map using the cube orientation as reference. Right hand side: dislocation density map (red = high, blue = low).

(components are linked to metallurgical mechanisms). The new method allows it for the first time to apply the crystal plasticity FE method directly to large scale forming problems under consideration of complete texture update. The method is tested and improved in cooperation with the German automotive industry.

Simulation of Scaling Effects in Nano- and Microscale Fluid Dynamics at Deformable Metal Surfaces

Varnik, Raabe

The aim of the project is a better microscale understanding of fluid dynamics in the vicinity of deformable metallic surfaces. Particular aspects are the investigation of scaling effects arising from changes in the topography of the metal due to plastic deformation relative to the properties of the fluid. Of importance is the transition from laminar to turbulent flow as a function of the surface roughness. Another aspect is the mechanical interaction between fluids and metallic surfaces, i.e. the microscale deformation of metals due to the local pressure exerted by the

fluid. A third area of interest concerns microscale fluid mechanics in confined regions, such as occurring when fluids are trapped between two rough metallic surfaces (Fig. 5) [28,29].

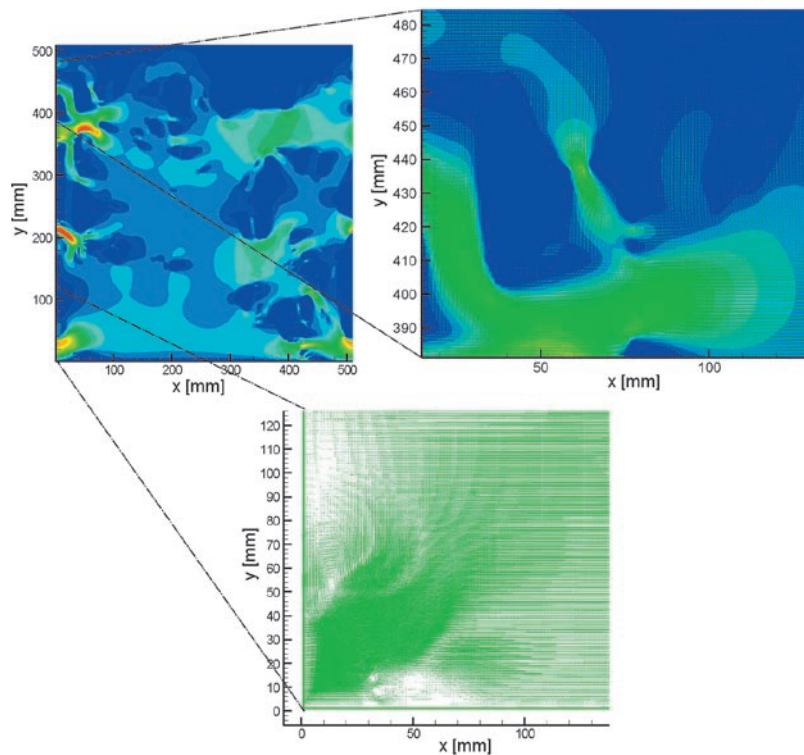


Fig. 5: A 2D example of the application of a Boltzmann lattice gas simulation for lubricant flow to measured roughness data of plastically deformed steel. The upper left figure shows the pressure distribution in the lubricant when compressed and redistributed in the experimentally determined obstacle (contact) field. The data show an in-plane view into the contact layer [28,29].

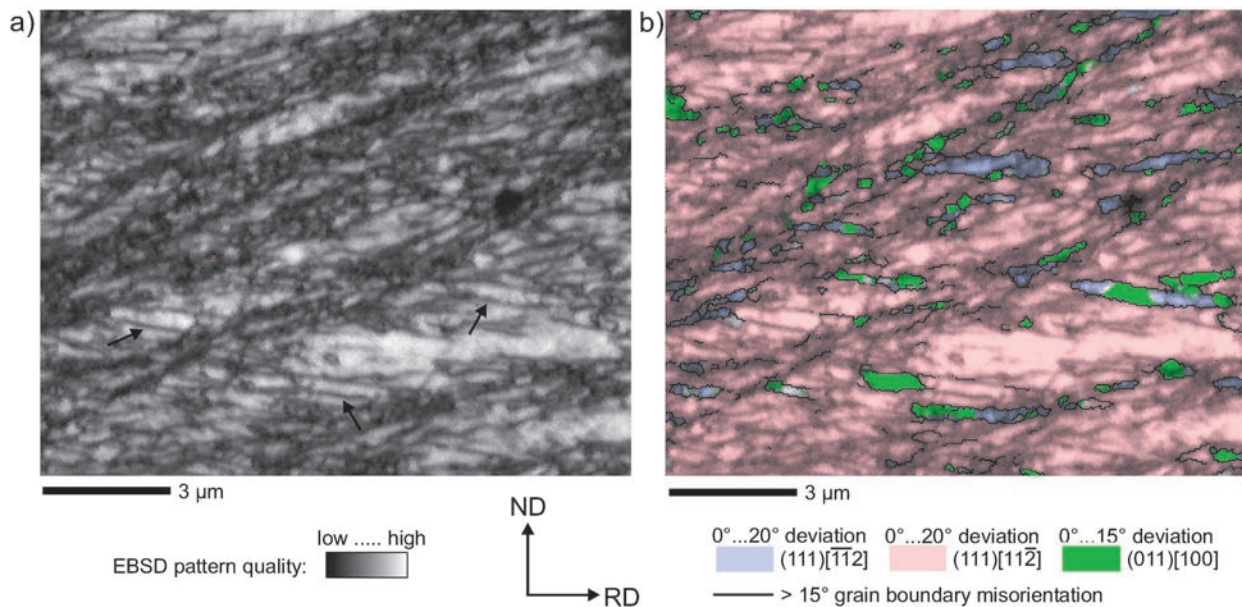


Fig. 6: Goss-oriented regions inside microbands in the 89% deformed FeSi singly crystal. a) EBSD pattern quality map. b) Same EBSD pattern quality map as in (a) combined with the corresponding crystal orientation (green = Goss).

Experimental Investigation and Simulation of the Deformation Behaviour of Bicrystals

Kuo, Dewobroto, Zaefferer, Winning (RWTH), Raabe

In this project Al bicrystals with $\langle 112 \rangle$ tilt boundaries and different misorientations are deformed in a channel die experiment in order to study the deformation at grain boundaries. Samples are characterized by strain measurements and microtexture mappings. The experiments are compared to crystal plasticity finite element simulations. It is observed that the 8.7° grain boundary does not show any orientation change in its vicinity which was interpreted in terms of free dislocation penetration. The 15.4° and 31.5° bicrystals showed orientation changes which were attributed to dislocation pile-ups [30].

Microband Analysis in Deformed FeSi Single Crystals

Dorner, Zaefferer

This project is about the deformation history of Goss grains during rolling. Single crystals with Goss orientation are rolled up to 89%. Most of the crystal volume rotates into the two symmetrical $\{111\}\langle 112 \rangle$ orientations. However, a small portion of the initial Goss component is still present, although the Goss orientation is mechanically unstable under plane strain loading. Two types of Goss-oriented crystal volumes prevail in the highly deformed material. We suggest that their origin is different. The Goss-oriented regions that are found within shear bands form generically during straining, whereas those that are found inside microbands prevail during cold rolling in the form of transition zones (Fig. 6).

Grain Boundary Characterization in Electrodeposited Nickel-Cobalt Nanocrystals

Bastos, Zaefferer, Raabe, Schuh (MIT)

The evolution of texture and the distribution of the grain boundary character in nanocrystalline polycrystalline metals are not fully understood. Detailed experimental studies at the grain scale in such materials have so far been limited by the required lateral resolution of the experimental techniques and by the presence of impurities, porosity, strain heterogeneity, and microstructure heterogeneity. In this project we investigate Nickel and Nickel-Cobalt samples with nano-sized grains (40 nm to 800 nm) produced by electrodeposition at MIT. The grain boundary character distribution, texture, and micromechanics are investigated by tensile tests performed within a high resolution scanning electron microscope. The Nickel and Nickel-Cobalt samples show a high fraction of twins and elongated crystals which may stem from growth selection during electrodeposition.

Microstructure and Texture of Ultrafine Grained C-Mn Steels and Their Evolution during Warm Deformation and Annealing

Song, Ponge, Zaefferer, Kaspar, Raabe

In this project we study the evolution of microstructure and texture of various C-Mn steels during large strain warm deformation and subsequent annealing. The process of grain subdivision during warm deformation is essential for the formation of ultrafine grains in such steels. Our work reveals

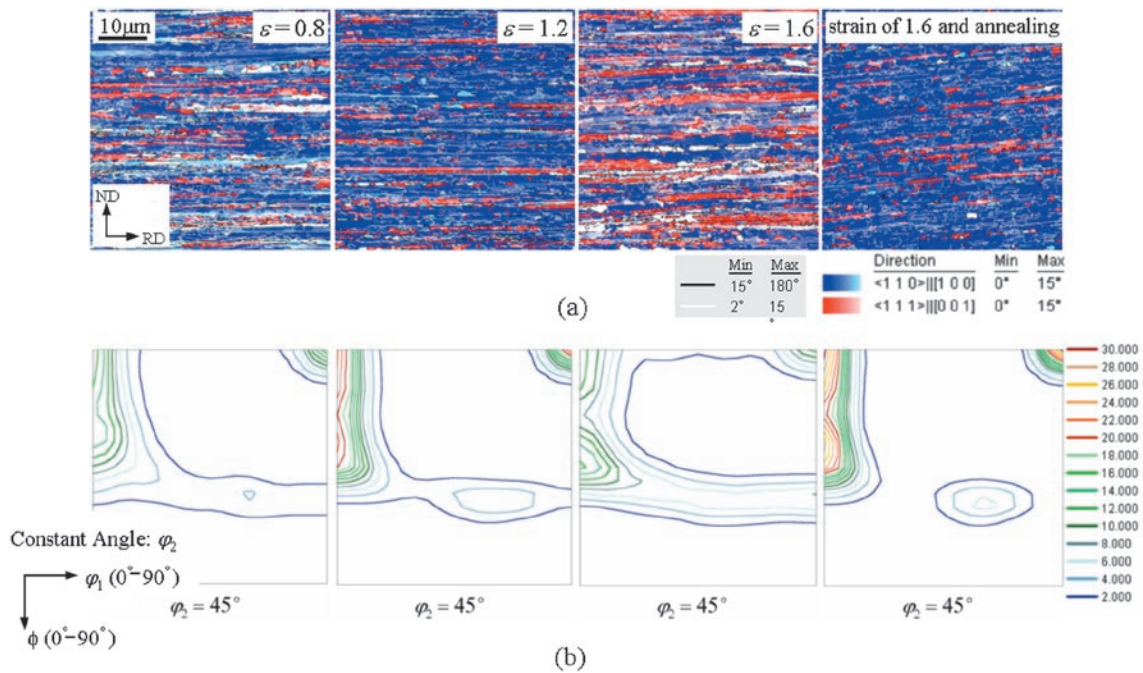


Fig. 7: Evolution of the crystallographic texture for a C-Mn steel during warm deformation and subsequent annealing at 823 K (each deformation step imposed a true strain step of 0.4 at a strain rate of 10 s^{-1}): (a) microtexture maps: α -fibre in blue and γ -fibre in red; (b) corresponding $\varphi_2 = 45^\circ$ sections through the orientation distribution function.

that pronounced recovery instead of primary recrystallization is required to obtain a large fraction of high-angle grain boundaries as a prerequisite for the development of ultrafine grains during warm deformation. Consistently, the texture of such steels observed after large strain warm deformation and subsequent annealing, consists primarily of the $\langle 110 \rangle \parallel \text{RD}$ texture fibre which indicates strong recovery (Fig. 7).

Micromechanics, Crystallographic Texture, Amorphization, and Recrystallization in Rolled and Heat-Treated Polymers

Jia, Chen, Godara, Raabe

This group of projects deals with texture, amorphization, and recrystallization in rolled and heat-treated semi-crystalline polymers. The change in crystallinity during rolling and heating is analyzed in terms of X-ray data (peaks and background) which are integrated over the entire pole sphere. This method eliminates texture effects in the analysis of crystallinity. The rolling texture typically consists of incomplete fibre textures which can be explained by shear on intralaminar shear systems. The X-ray analysis reveals that crystallinity drastically decreases during heavy rolling (Fig. 8). We observed that amorphization is a deformation mechanism which takes place as an alternative to intralaminar shear depending on the orientation of the lamellae. Sufficient heat treatment leads to the recrystallization of the amorphous material and to an enhancement of the original deformation texture [31].

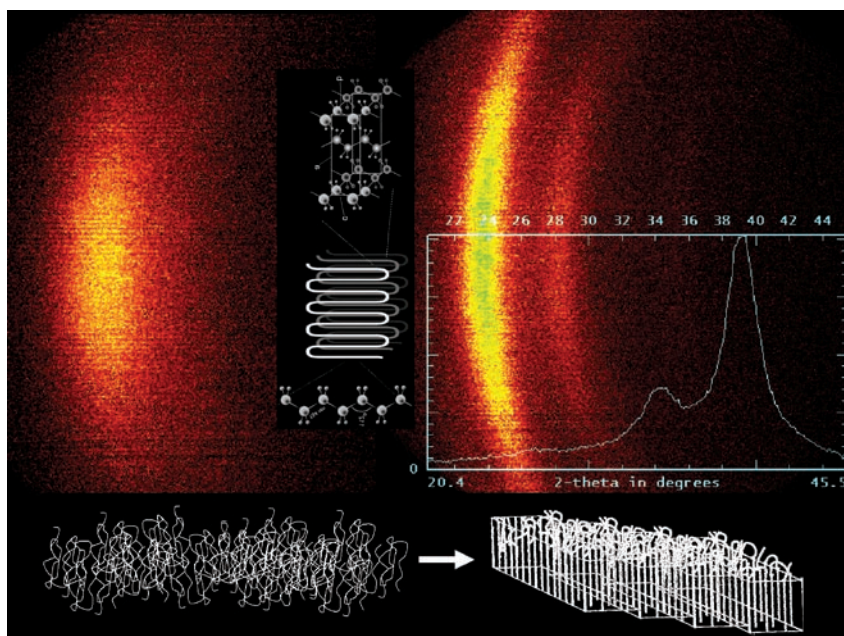


Fig. 8: Debye-Scherrer diagram taken from deformed polypropylene (PP) using $\text{Cr-K}_{\alpha 1}$ radiation at 40 kV and 40 mA.

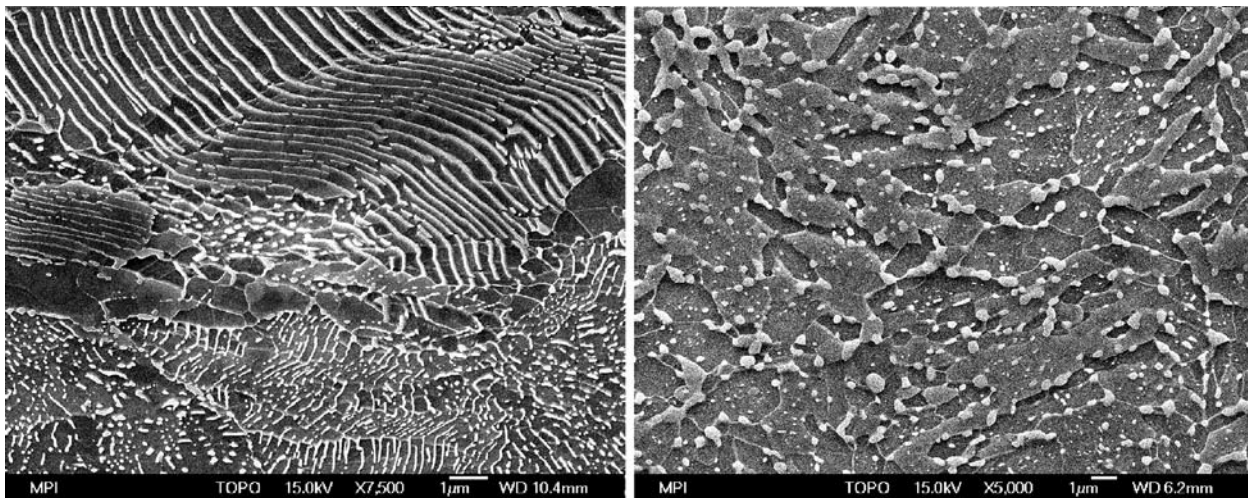


Fig. 9: Lamellar and globular forms of cementite.

Effect of Tramp Elements in High Strength SiCr Spring Steels

Barani, Kaspar, Ponge

This project deals with the optimization the critical contents of trap elements in high strength spring steels through thermomechanical processing. It aims to minimize the negative effects of P, Cu, and Sn on the properties of automotive springs. These elements may cause problems, namely, the temper embrittlement and the liquid copper embrittlement. In the project the rolling process and the heat treatment are investigated and the parameters are varied to improve the ductility and fatigue properties and maintain the required high strength level. The main interest is to avoid the above addressed embrittlement problems and to correlate the mechanical properties to the tramp element concentration and to the microstructure, i.e. to the austenite grain structure and the martensite morphology.

Heavy Warm Rolling for the Production of Thin Hot Strips with Improved Ductility

Ponge, Kaspar, Storjéva, Raabe

The project on heavy warm rolling for the production of thin hot strip aims to define processing parameters for rolling concepts in which a hot strip coil produced on a conventional hot strip mill is to be transferred to a single high reduction rolling stand (PonyMill) where a heavy warm reduction is imposed. For optimising the processing parameters the phase transformation behaviour is investigated for steels with 0.15, 0.35 and 0.67% carbon with and without austenite deformation (Fig. 9).

High Strength Long Products with Improved Toughness and Fatigue Resistance

Ponge, Kaspar, Detroy, Raabe

This project is about the thermomechanical treatment of high strength long products with improved toughness and fatigue resistance. It is the aim to identify suited medium carbon steel compositions in combination with corresponding processing strategies including thermomechanical treatment by avoiding quenching and tempering. The microstructural goal is to achieve a refined multi-phase structure (carbide-free bainite and acicular ferrite with a network of retained austenite) that exhibits the combination of high strength and improved toughness.

High Resolution EBSD Investigation of Deformed and Partially Recrystallized IF Steel

Thomas (TKS), Zaefferer, Friedel (TKS), Raabe

In this project the recrystallization behaviour of interstitial free steel is investigated by means of high resolution EBSD and TEM measurements. The deformed microstructure reveals three different microtexture groups which are characterized by their orientations and internal misorientations. The development of these regions during recrystallization has been observed (Fig. 10). Comparison of EBSD and TEM results indicates limitations of high resolution EBSD measurements concerning the observation of subgrain structures.

Correlations between Forming Limits, Equivalent Strain, Strain Path, and Surface Roughness

Wichern, Rasp

The objective of this project is to provide insight into the relationships between formability, strain, strain path, and roughness in sheet metals. A series

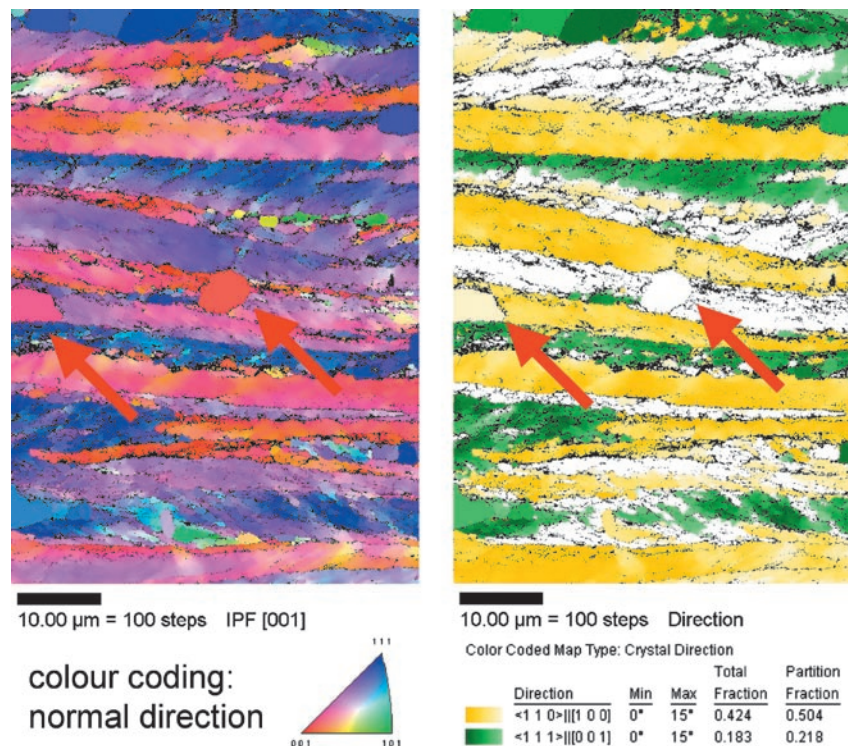


Fig. 10: EBSD results obtained from a sample annealed for 3 minutes up to a temperature of 680 °C. The red arrows point out two nuclei which do not belong to α - or γ -fibre. Additionally several nuclei with γ -fibre orientations can be seen in the upper part of the picture.

of sheet steel specimens is strained along different strain paths and the strain and roughness are measured at identical positions on the specimens. The analysis of roughness versus strain provides the roughening rate for the various strain paths. The highest roughening rates occur close to the plane-strain strain forming path, which has also the lowest forming limit. For uniaxial and biaxial strain paths the formability is larger, the rate of roughening smaller, and the total final roughness level higher as compared to the plane-strain strain path.

Structure and Mechanical Properties of the Cuticle of Lobster

Sachs, Romano, Servos (Univ. Düsseldorf), Hartwig (Univ. Düsseldorf), Raabe

The cuticle of lobster (*homarus americanus*) is a multilayer chitin-protein-based biological composite containing variable amounts of biominerals. Basically, the cuticle consists of the epicuticle, exocuticle and endocuticle. The epicuticle is an outer thin waxy layer providing a permeability barrier. The exocuticle and endocuticle are made up of chitin fibres arranged in lamellas of different thickness. Local variations in composition and structure of the material provide a wide range of mechanical properties. It can be either rigid serving as a highly protective exoskeleton or it can be flexible serving as a constructional element

as in articular membranes at joints. Consequently, the lobster cuticle is an excellent model of a versatile solution to structural and functional materials challenges. We conduct a systematic study on the correlation between the microscopic structure (Fig. 11) and composition of the lobster cuticle and the resulting local mechanical properties.

Smart Anisotropy of Biological Nano-Composites

Romano, Sachs, Al-Sawalmih, Klein (Univ. Göttingen), Bunge (Univ. Clausthal), Brokmeier (DESY), Raabe

Many biological materials such as encountered in the exoskeleton structures of mollusc and crustaceans form nano-composites with directional properties. Many of the basic ingredients in such structures, i.e. the various mineral components, the proteins, glycoproteins, polysaccharides, and lipids, may at least in part occur in crystalline form. These compounds are not distributed randomly in orientation space but they typically occur in a variety of preferred topological and orientations which are optimized with respect to the external mechanical boundary conditions. By using synchrotron X-ray wide angle analysis we conduct corresponding texture investigations on different biological materials and correlate them with the observed microstructures, mechanics, and electrical properties.

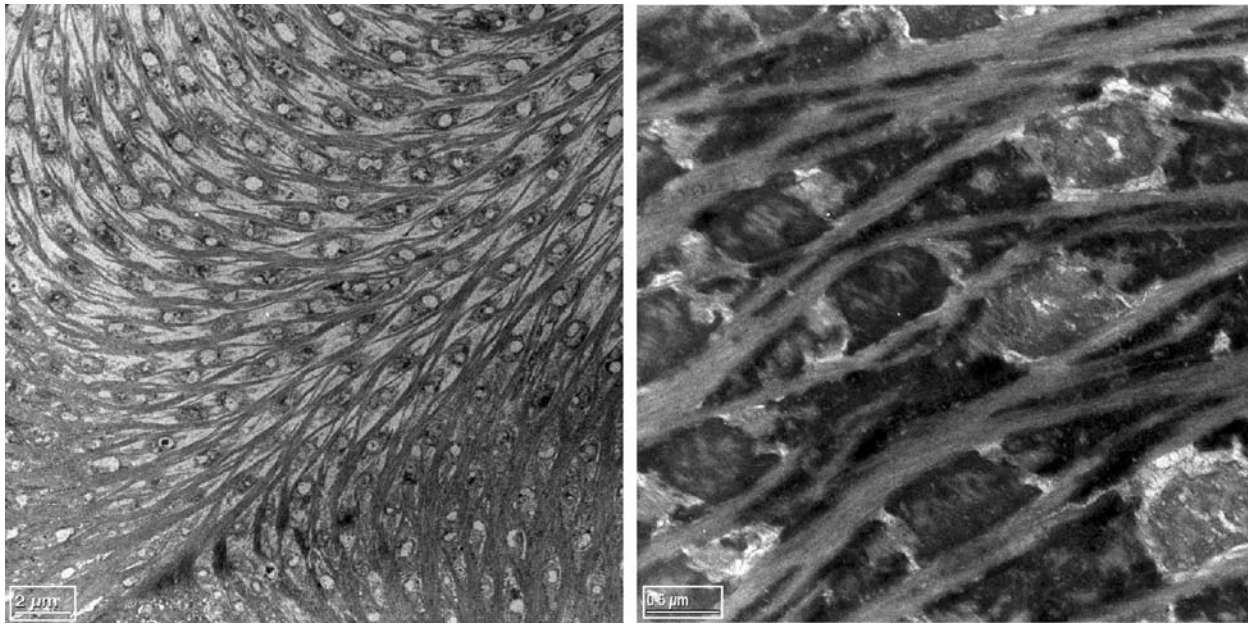


Fig. 11: TEM sections of 60 nm thickness of the cuticula of *homarus americanus* (lobster). The specimens were EDTA decalcified, NaOH deproteinized, treated by 2.5% Glutaraldehyde fixation, submitted to OsO_4 fixation and staining, and finally exposed to Uranyl Acetate staining (Servos, Romano, Raabe: unpublished data).

References

1. Roters, F.; Raabe, D.; Gottstein, G.: *Acta Mater.* 48 (2000) 4181.
2. Ma, A.; Roters, F.: *Acta Mater.* 52 (2004) 3603.
3. Roters F.: *Phys. Status Solidi (b)* 240 (2003) 68.
4. Wang, Y.; Raabe, D.; Klüber, C.; Roters, F.: *Acta Mater.* 52 (2004) 2229.
5. Zaefferer, S.; Kuo, J.-C.; Zhao, Z.; Winning, M.; Raabe, D.: *Acta Mater.* 51 (2003) 4719.
6. Raabe, D.; Zhao, Z.; Park, S.-J.; Roters, F.: *Acta Mater.* 50 (2002) 421.
7. Raabe, D.; Sachtleber, M.; Zhao, Z.; Roters, F.; Zaefferer, S.: *Acta Mater.* 49 (2001) 3433.
8. Raabe, D.; Sachtleber, M.; Weiland, H.; Scheele, G.; Zhao, Z.: *Acta Mater.* 51 (2003) 1539.
9. Raabe, D.; Roters, F.: *Int. J. Plasticity* 20 (2004) 339.
10. Zhao, Z.; Mao, W.; Roters, F.; Raabe, D.: *Acta Mater.* 52 (2004) 1003.
11. Raabe, D.; Zhao, Z.; Roters, F.: *Scr. Mater.* 50 (2004) 1085.
12. Raabe, D.; Klose, P.; Engl, B.; Imlau, K.-P.; Friedel, F.; Roters, F.: *Adv. Eng. Mater.* 4 (2002) 169.
13. Zaefferer, S.; Ohlert, J.; Bleck, W.: *Acta Mater.* 52 (2004) 2765.
14. Zaefferer S.: *Mater. Sci. Eng. A344* (2003) 20.
15. Wöllmer, S.; Zaefferer, S.; Göken, M.; Mack, T.; Glatzel, U.: *Surf. Coat. Technol.* 167 (2003) 83.
16. Chen, N.; Zaefferer, S.; Lahn, L.; Günther, K.; Raabe, D.: *Acta Mater.* 51 (2003) 1755.
17. Thomas, I.; Zaefferer, S.; Friedel, F.; Raabe, D.: *Adv. Eng. Mater.* 5 (2003) 566.
18. Zaefferer, S.: *Adv. Eng. Mater.* 5 (2003) 745.
19. Zaefferer, S.: *JEOL News* 39 (2004) 10.
20. Storojeva, L.; Escher, C.; Bode, R.; Hulka, K.: in: *IF STEELS 2003, Int. Forum Properties and Application of IF Steels*, Tokyo, Japan, ed. H. Takechi, Iron and Steel Institute of Japan (2003) 294.
21. Storojeva, L.; Kaspar, R.; Ponge, D.: *Mater. Sci. Forum* 426-432 (2003) 1169.
22. Song, R.; Ponge, D.; Kaspar, R.: *Steel Res.* 75 (2004) 33.
23. Storojeva, L.; Ponge, D.; Kaspar, R.; Raabe, D.: *Acta Mater.* 52 (2004) 2209.
24. Song, R.; Ponge, D.; Kaspar, R.; Raabe, D.: *Z. Metallkd.* 95 (2004) 513.
25. Song, R.; Ponge, D.; Raabe, D.; Kaspar, R.: *Acta Mater.*, *in press*.
26. Rasp, W.; Wichern, C.M.: *Steel Res.* 74 (2003) 300.
27. Filatov, D.; Pawelski, O.; Rasp, W.: *Steel Res.* 75 (2004) 20.
28. Raabe, D.: in: *Continuum Scale Simulation of Engineering Materials*, eds. D. Raabe, F. Roters, F. Barlat, L.-Q. Chen, Wiley-VCH, Weinheim (2004).
29. Raabe, D.: *Model. Simul. Mater. Sci. Eng.* 12 (2004) R13.
30. Zaefferer, S.; Kuo, J.-C.; Zhao, Z.; Winning, M.; Raabe, D.: *Acta Mater.* 51 (2003) 4719.
31. Raabe, D.; Chen, N.; Chen, L.: *Polymer* 45 (2004) 8265.



Research Projects in Progress

Theory and Simulation

Dorner, Chen (Col. School Mines), Raabe: 3D Potts Monte Carlo simulation of secondary Goss grain growth in FeSi steels

Hantcherli (Ecole des Mines St. Etienne), Raabe: Cellular automaton simulation of the recrystallization texture of an IF sheet steel under consideration of Zener pinning

Nestler (FH Karlsruhe), Thomas, Zaefferer, Raabe: Phase field simulation of subgrain coarsening applied to experimentally obtained TEM-microtexture data of subgrain arrays in an IF steel

Nikolov, Raabe: Constitutive modeling of amorphous and of partially crystalline polymer mechanics

Raabe: Cellular automata for recrystallization simulation

Raabe, Godara: Development and application of cellular automata for polymer crystallization

Raabe, Varnik: Boltzmann lattice gas cellular automata for microscale flow dynamics

Rollett (CMU), Zaefferer, Dorner, Chen (Col. School Mines), Raabe: 3D Potts Monte Carlo simulation of secondary Goss grain growth in FeSi steels

Roters: Development and application of the Texture Component Crystal plasticity FEM

Roters, Haurand: Influence of mesh geometry and boundary conditions on the simulation of texture development using the Texture Component Crystal Plasticity FEM

Roters, Ma: Development of a non local dislocation density based constitutive law for crystal plasticity finite element simulations

Roters, Ma: Strain and orientation gradients in steel at the grain scale

Roters, Ma, Raabe, Gottstein (RWTH): Consideration of grain boundary mechanics in polycrystal plasticity finite element simulations

Roters, Zaafarani, Nikolov, Raabe: Simulation of nanoindentation of polymer coated aluminium samples

Tikhovskiy, Roters, Raabe: Crystal plasticity FEM simulation of deep drawing of stainless steels

Varnik, Raabe: Simulation of scaling effects in nano- and microscale fluid dynamics at deformable metal surfaces

Zambaldi, Glatzel (Univ. Bayreuth), Ma, Roters, Raabe: Combination of cellular automaton and finite element simulations for recrystallization simulations

Zhao (MIT), Radovitzky (MIT), Roters, Raabe: Massively parallel 3D crystal plasticity finite element simulations

Diffraction and Microscopy

Bastos, Zaefferer, Schuh (MIT), Raabe: Textures of electrodeposit Nickel-Cobalt nanocrystals

Dorner, Zaefferer: Microband analysis in deformed FeSi single crystals

Dorner, Zaefferer, Günther(TKES), Lahn (TKES), Raabe: Secondary Goss grain growth in silicon steels

Jia, Godara, Zaefferer, Raabe: Micromechanics and textures of polyethylen and polypropylen

Kuo, Dewobroto, Zaefferer, Winning (RWTH), Raabe: Experimental investigation and simulation of the deformation behaviour of bicrystals

Mao (TU Beijing), Raabe: Texture of diamond

Sandim (Univ. de Lorena), Raabe: In-grain microtexture evolution in Niobium

Sandim (Univ. de Lorena), Zaefferer: Structure of shear bands in heavily deformed Titanium

Sato, Zaefferer: Investigation of orientation relationships in diffusional and martensitic phase transformations

Song, Ponge, Zaefferer, Raabe: Nano- and microtexture analysis of ultrafine grained steels

Song, Raabe: Nano- and microtexture analysis of gold wires

Yi, Zaefferer: Microscopic deformation mechanisms in Magnesium

Zaefferer: Texture analysis in multiphase steels

Zaefferer, Hirano: Recrystallization mechanisms in Ni₃Al alloys

Zaefferer, Kobayashi: Automatic scanning of phase states and phase diagrams by a multiphase EBSD method

Zaefferer, Ohlert (RWTH), Bleck (RWTH): Microstructural characterization of TRIP steels

Zaefferer, Raabe: 3D EBSD analysis by joint focussed ion beam and electron back scatter diffraction microscopy



Zaefferer, Schneider, Kobayashi, Frommeyer, Raabe: Optimization of texture and microstructure of Fe₃Al-based alloys

Metal Forming

Rasp, Filatov: Influence of deformation parameters in hot rolling on scale formation and ability for pickling

Rasp, Yusupov: Advanced modelling of lateral flow and residual stresses in flat rolling

Wichern, Rasp: Tribology tests for the characterization of cold-rolling oils

Wichern, Rasp: Improvement of formability by superposition of hydrostatic pressure

Thermomechanical Treatment

Ponge, Kaspar: Transformation behaviour of steel in the in-line hot rolling steel processing

Ponge, Kaspar, Barani: Effect of tramp elements in high strength SiCr spring steels

Ponge, Kaspar, Detroy: High strength long products with improved toughness and fatigue resistance

Ponge, Kaspar, Rasp, Elsner: Laboratory tests on optimizing process parameter of ferritic rolling deep drawable steels

Ponge, Kaspar, Song, Raabe: Ultra fine grained steel produced by innovative deformation cycles

Ponge, Kaspar, Storojeva: Heavy warm rolling for the production of thin hot strips

Leibniz group on biological nano-composites

Al-Sawalmih, Raabe: Electromagnetic properties of the lobster cuticula

Raabe, Al-Sawalmih, Klein (Univ. Göttingen), Brokmeier (DESY), Bunge (Univ. Clausthal): Texture and smart anisotropy of biological nano-composites

Romano, Servos (Univ. Düsseldorf), Sachs, Raabe: Optical and electron microscopy on chitin-based biological nano-composites

Sachs, Romano, Raabe: Structure and mechanical properties of the lobster cuticle

Zhang, Roters, Raabe: Mechanics of biological honeycomb structures



Department of Metallurgy and Process Technology

A.R. Büchner (provisional)

At present the institute is looking for a new head of department. Therefore, some topics of the Department of Metallurgy are not actively pursued now. Generally the Department of Metallurgy focuses on the fundamentals of steelmaking. The aims are both to optimise conventional process technologies as well as to support new lines of development. All technologies studied at the MPIE can contribute to reduce the number of process steps and to save cost and energy, and may be part of future concepts for new steel production lines. An important new technology is twin roll strip casting which has recently been adopted by the industry especially for the production of stainless steels and carbon steels.

Among the methods applied at the Department of Metallurgy, numerical modelling is a central tool. At the same time, various experimental studies are carried out using laboratory measurements and empirical data supplied by industrial partners. For further information on experimental equipment see chapter „Central Facilities“ in Part I.

In the field of thin strip casting, some special topics are outlined in the following.

Heat transfer in twin roll casting

Thiemann, Büchner

The central process of strip formation is the heat transfer between material and rolls. In this work the heat transfer was investigated experimentally in a laboratory twin roll caster and a special model mould. The observed quantities were heat transfer coefficient and heat flux density. The influencing parameters were: type of melt, material of substrate, roughness of substrate, velocity between melt and substrate, gas environment. The results coincide with the common model, where three parallel heat fluxes occur between solidified material and substrate, namely fluxes by radiation, through gas pockets, and over metallic bridges. In detail it was found:

The heat transfer coefficient increases: by 80% under He instead of air; by 15% if the substrate has a roughness of 1 μm instead of 7 μm ; by 15% in steel substrate instead of Ni or Cu-alloys.

Spottiness on twin roll strip

Büchner

A highly undesired feature of thin strip casting is the nonuniform temperature distribution of the strip leaving the rolls. This results from an inhomogeneous heat transfer between material and rolls in the range of the pool. Several detrimental consequences result therefrom. The final cooling from hot or colder spots leads to strongly different structure. Large internal stresses occur during cooling, and surface cracks are formed. Assuming that hot spots include pockets of liquid melt when the rolls are left, this leads to inhomogeneous shrinkage of the strip surface layers, and thus the surface is full of defects. An extensive experimental study under variation of roll material and roll velocity leads to the conclusion that spottiness depends on the temperature difference ($T_{\text{melt}} - T_{\text{roll}}$). The spottiness in case of LC-steel seems to vanish, if the roll temperature is about 400 °C.

Hot shortness in twin roll strip

Pötschke, Büchner

During casting and deformation certain limits of copper and tin are not to be exceeded in steel. One of the reasons is hot shortness due to selective oxidation of iron and resulting copper enrichment on the steel surface. A substantial experimental work has been done on this subject by the SIMR in Sweden. Together with literature these results were used to form a physical model which allows to determine a maximum copper content depending on the casting parameters strip thickness and oxygen content of the cooling atmosphere. Most of the copper is enriched on the steel surface if it is not transported into the scale. A critical copper layer thickness $d_{\text{Cu}} = 0.092 \mu\text{m}$ was calculated which is necessary to induce cracks of a depth of 0.2 mm. It is shown that for thin strip (high cooling rates) a significant higher copper content is tolerable than in the continuous casting line.

Hot rolled twin roll strip

Pötschke, Büchner

Thin strip of the low carbon steel grade DC 04 was cast on a laboratory twin roll caster and was subsequently in-line hot rolled in one step. The



microstructure is strongly influenced by the hot rolling parameters, namely temperature and logarithmic deformation. Good results were obtained by austenitic hot rolling which suppresses successfully the as-cast Widmannstätten like microstructure in favour of a homogenous polygonal grain. The results are analysed with respect to the temperature distribution in the strip during and after hot rolling and to the γ - α phase transformation temperature measured in a deformation dilatometer. In detail it was found that high hot rolling temperatures of 980 to 1050 °C and deformations above $\varphi = 0.3$ lead to a strong improvement of the microstructure over the entire strip thickness.

Cold rolled twin roll strip

Pötschke, Büchner

Copper influences severely the cold strip properties of thin strip. Twin roll casting experiments including

in-line hot rolling were conducted with LC-steel and varying copper contents (0-2.5 wt.%). Subsequently strip samples were descaled, cold rolled ($\varphi = 0.7$) and recrystallisation annealed. The cold rolled strip samples were batch annealed or continuously annealed and subsequently tested with respect to their texture and their mechanical properties. Copper above 0.5 wt.% strongly hinders the recrystallisation process so that the α -fibre created during cold rolling is not reduced. Above 0.8 wt.% copper the mechanical properties worsen severely so that they may not be used for deep drawing applications. Nevertheless higher copper contents as compared to continuous casting lines are allowed. Furthermore new options for steels are given with copper: For example martensite may be created with higher cooling rates than they are possible in thin strip. A large variety of properties can be obtained by appropriate subsequent annealing.

Research Projects in Progress

Near Net Shape Casting

Büchner: Thin strip casting of special steels for industrial application

Büchner: Considerations on construction of thin strip casting units

Pötschke, Büchner: Tramp elements Cu, Sn in thin strip

Pötschke, Büchner: In-line hot rolling in thin strip casting

Thiemann, Büchner: Heat transfer coefficient between material and rolls in twin roll strip casting

Thiemann, Büchner: Surface quality and solidification process



Selected Scientific Topics

Development of a Thermodynamic Database for Ferritic Steels

J. Balun, V. Knežević, G. Inden, P. Unucka*, J. Houserova*, A. Kroupa*

Department of Physical Metallurgy
(*IPM, Czech Academy of Sciences, Brno)

The binary systems Fe-Ta, Fe-Mo and Fe-W represent key-systems for the development of ferritic steels for application in 650 °C Ultra Super Critical Power Plants. In these steels a highly stable microstructure with initially 100% martensite is strengthened by different types of phases (e.g. $M_{23}C_6$, MX, Laves-phase, μ -phase). Recently, the Laves-phase and the μ -phase have attracted much interest since they are considered as potent candidates for strengthening provided size and distribution of the particles are within certain limits. The presently available thermodynamic description of those phases in the existing databases is not satisfactory for the following reasons:

- The element Ta is not included in the description of the Laves and μ -phase.
- The Laves-phase C14 is described as a line compound A_2B . However, experimental investigations show significant deviations

from stoichiometry. This is even more pronounced when it comes to the existence domains in ternary systems.

- The μ -phase is described by a three sublattice model $(A)_7(B)_2(A,B)_4$. According to this model the maximum theoretical solubility of element B is 46.16 at.%. Experimentally determined solubilities are far beyond that limit.

The three basic binary systems Fe-Ta, Fe-Mo and Fe-W were assessed on the basis of an improved description for both the Laves-phase and the μ -phase. For the Laves phase full solubility of the elements on the sublattices is allowed as expressed by the formula $(A,B)_2(A,B)$. The μ -phase is treated as a four sublattice phase $(A,B)_1(A,B)_2(A,B)_6(B)_4$. From a crystallographic point of view five sublattices should be distinguished. However, recent quantitative

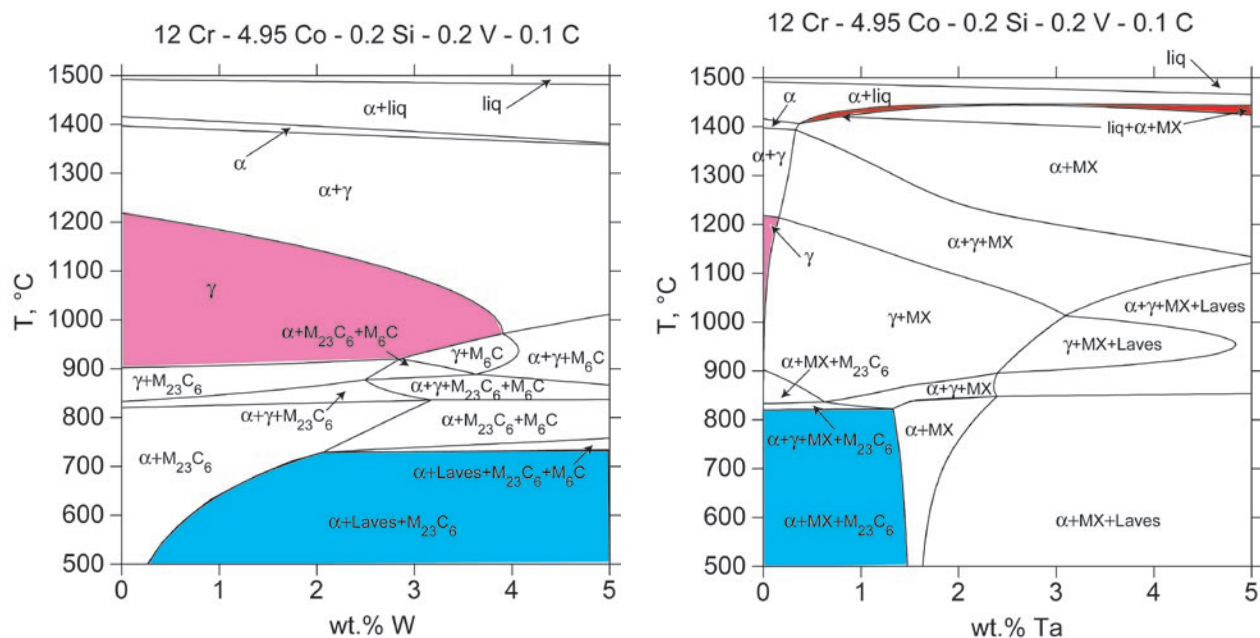


Fig. 1: Vertical section of the phase diagram of the systems Fe-Cr-Co-Si-V-C-X with X= W, Ta. The area of carbide precipitation within the liquid is shown in red. The area of pure austenite γ is marked as pink area, and the region of $M_{23}C_6$ + Laves phase is marked in blue. W alloys fulfil all requirements for ferritic steels: no carbide precipitation in the liquid, large domain of pure austenite and precipitation of carbides and Laves phase for creep resistance.

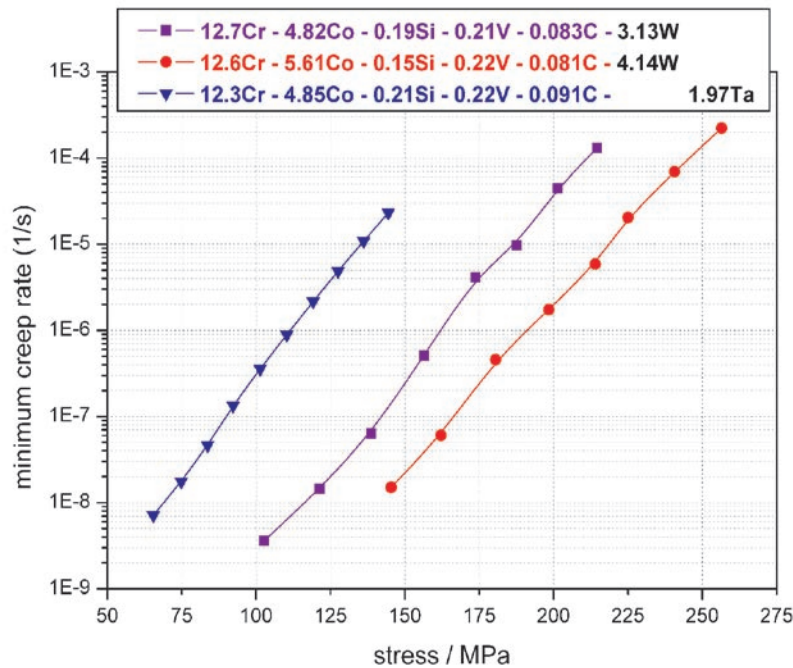


Fig. 2: Minimum creep rate in compression test at 650 °C. The W alloys are by far superior to the Ta alloy: the minimum creep rate is smaller than that of the Ta alloy by two to three orders of magnitude.

X-ray diffraction and ab initio calculations have shown that on two positions there is essentially only one component, such that these two can be subsumed to $(B)_4$. The numerical values of the thermodynamic parameters were optimized according to the CALPHAD method using the software PARROT. In view of the scarcity of experimental data available it was desirable to limit the number of parameters varied during optimization. For the Laves phase ab initio calculations could be performed providing the total energies of the so-called end members. The energies of the end members given by the pure components, A_2A and B_2B , were fixed to the values given by the ab initio calculations. The other two end members, A_2B and B_2A , were still varied and the optimized results could then be compared with the ab initio values. Very good agreement was obtained between the assessed values and the ab initio counterparts. This corroborates the reliability of the assessment.

These new data were successfully used in the current research focusing on new ferritic/martensitic steels for ultra high strength power plant components for temperatures at and above 650 °C and 300 bar. Critical issues are: no delta-ferrite at austenitization temperature, no carbo-nitride precipitation in the melt, creep resistance to be ensured by precipitation of carbides, mainly $M_{23}C_6$, M_6C , $M(C,N)$, and Laves phase. One route starts from alloys with Fe-12Cr-5Co-0.2Si-0.2V-0.1C-X, where X = W, Ta, Nb, Mo.

Fig. 1 shows the calculated vertical sections of the phase diagram with X = W, Ta. These calculations allow predicting whether the alloy system fulfils the requirements or not. In this instance it is immediately clear that alloys with W are good candidates for the kind of materials to be developed, while alloys with Ta (and similarly with Nb, Mo) are not because of carbo-nitride precipitation within the melt, too restricted possibilities for austenitization and subsequent carbide and Laves phase precipitation. These conclusions were fully confirmed by creep tests under compression. Fig. 2 shows the minimum creep rate as function of applied stress. For a given stress the minimum creep rate of alloys with W is two to three orders of magnitude smaller than that of the alloy with Ta.

In conclusion: Computational thermodynamics provides a very useful tool for designing and optimizing materials with given property profiles. The thermodynamic data also serve as input into kinetic calculations offering the possibility of predicting the stability of microstructures under complex service conditions. Existing limitations are not inherent to the method, they are essentially due to deficiencies in the thermodynamic descriptions of phases and lack of experimental data. These limitations can, of course, be overcome, and experimentally inaccessible data may be provided today by „ab initio“ techniques.



DFT-Based Modelling of SiO₂ Surfaces and their Interaction with Water

A. T. Blumenau, P. Schiffels*

Department of Interface Chemistry and Surface Engineering
(*Fraunhofer Institut für Fertigungstechnik und Angewandte Materialforschung, Bremen)

The development of new coatings or paints to protect metals in corrosive environments on the one hand and the tailored design of organic adhesives on the other hand are two of the major challenges in modern technology. In both cases many properties of the product are defined by molecular processes at the (metal)oxide/organic-phase interface. To open up the way for a cost-saving bottom-up-design of coatings and adhesives, a predictive atomistic modelling of the structure and properties of these interfaces is of utmost importance. In this context it is a first crucial step to model the oxide surface itself. And hence in this article we present a case study for surfaces of α -quartz (SiO₂) as model oxide surfaces and their interaction with water.

Computational methods. As representative atomistic structures will consist of several hundreds of atoms, in particular with respect to the perspective of modelling not just the oxide surface, but also its interaction with large organic molecules or whole interface structures, density functional theory (DFT) and methods based upon DFT are adequate tools in the computational modelling of interfaces. For systems of the given size, higher-accuracy methods will simply fail due to their computational complexity. In this work we focus on an approximate tight-binding approach to DFT, which allows to model even larger structures — or in dynamical simulations longer time

scales — than pure DFT. In this so-called DFT-based tight-binding (scc-DFTB) many integrals are calculated in advance using DFT and are then tabulated for future use to save computation time. The remaining energy contributions are approximated by a repulsive pair-potential, which is obtained in comparison with full DFT calculations on reference systems. For details see [1].

In this work the self-consistent-charge (scc) extension of DFTB is used. For validation purposes some of the structures discussed are additionally simulated using full DFT.

Surface structures of clean α -quartz surfaces.

In this paragraph we focus on ideal surfaces as they would be obtained in perfect vacuum when cleaving the crystal along crystallographic low-index planes (in this work in particular (0001)). To obtain atomistic models of these surfaces, a periodic 2x2x2 cell of bulk α -quartz in a feasible orientation is cut along the respective crystallographic plane. Then the two generated surfaces are separated (about 100 Å for DFTB models) to avoid any interaction between them. In other words the surface model consists of a periodic array of thin slabs with two surfaces each.

To give a better representation of a semi-infinite crystal with just one surface, one of the two surfaces in the model geometry is passivated by hydrogen as

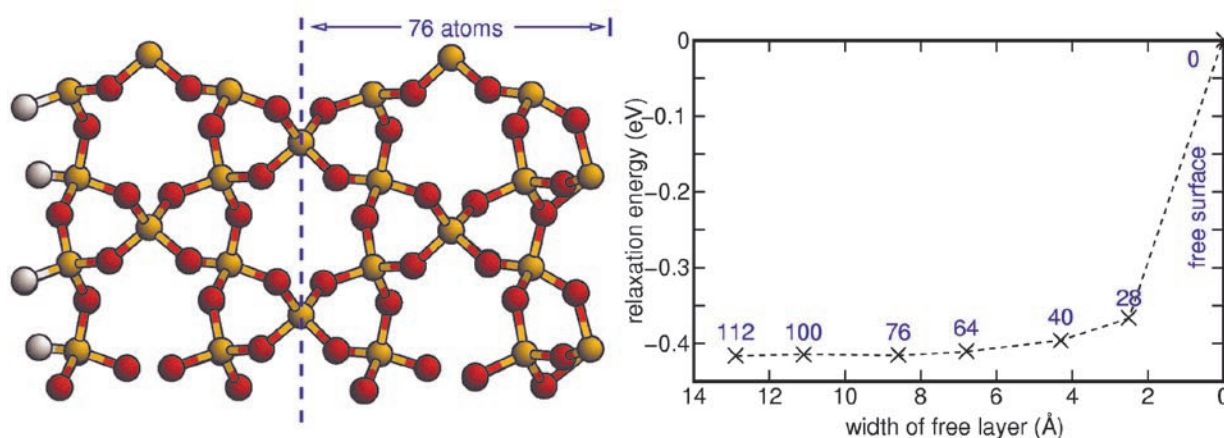


Fig. 1: *Left:* Structurally optimised $(10\bar{1}0)$ surface model (Si₄₈O₈₈H₈) projected along $[0001]$. 76 atoms closest to the free surface (right) were allowed to relax. *Right:* Relaxation energy per surface unit for different numbers of free atoms.



shown in Fig. 1. Our calculations show, that already two Si-layers away from the hydrogen passivation layer the charge distribution is almost the same as in ideal bulk material (less than 1% deviation in a Mulliken charge analysis).

In a second step, different surface structures and reconstructions are obtained from the starting geometries by randomising atom positions at the surface and optimising the structure energetically by applying the DFTB method. In this process it is advisable to constrain the atom positions close to the hydrogen passivated end of the model to their ideal bulk positions. This first of all ensures a better representation of ideal bulk material far away from the free surface to be investigated, and further has the advantage of speeding up the calculations. To investigate the effect of these bulk constraints, the model shown in Fig. 1 (left) has been optimised allowing different numbers of atoms close to the free surface to move in the relaxation process. Fig.1 (right) gives the corresponding relaxation energy. As can be seen, from 76 free atoms onwards (a layer of 8.6 Å) the energy difference becomes negligible and the energy converges towards -0.42 eV per surface unit cell for this particular surface.

Among the (0001) surfaces, one has to distinguish between „as-cut“ surfaces with a high density of dangling bonds, which are hence highly reactive, and the by far less reactive and reconstructed surfaces. Fig. 2 shows three examples of the latter, where all atoms are bulk-like coordinated. The dominating structural elements are (SiO)₃, (SiO)₄ and (SiO)₆ rings for A, B and C respectively. Reconstructions involving (SiO)₂ rings were found to be not stable in our simulation. Structure A and C are referred to as semidense and

dense since they are formed by respectively partially or fully merging the two topmost Si-layers into one surface layer giving a surface of high density [2]. Structure A and C have been studied in first-principle investigations before [2,3], the corrugated reconstruction B, however, has not been discussed in the literature before. It has a density similar to C. Table 1 shows the corresponding relaxation energies and relative formation energies of these surfaces found with the DFTB method and for comparison with less approximate DFT methods (CA-PZ and BLYP). As can be seen, all methods agree on structure C as

Table 1: Surface relaxation energies E_{relax} and relative formation energies E_{rel} (for stoichiometric growth) of the structures shown in Fig. 2. All energies are given in meV/Å². CA-PZ refers to the plane wave code CASTEP [4], using the parametrisation of Perdew and Zunger [6] with ultra-soft pseudopotentials and a 380 eV cutoff energy. BLYP refers to the Dmol³ program [6], using the BLYP parametrisation [7,8] with a double ζ -basis and polarisation functions.

| | | DFTB | CA-PZ | BLYP | Lit. [2] |
|---|-------------|------|-------|------|----------|
| A | E_{relax} | -122 | -131 | -86 | 40 |
| | E_{rel} | 41 | 59 | 63 | |
| B | E_{relax} | -108 | -122 | -71 | |
| | E_{rel} | 55 | 69 | 78 | |
| C | E_{relax} | -163 | -191 | -149 | 0 |
| | E_{rel} | 0 | 0 | 0 | |

the most stable reconstruction, followed by A and then C. Overall the relative energies are very similar comparing the different methods; and for the relaxation energy (the difference between the as-cut surface and the reconstructed surface) the DFTB values always lie between CA-PZ and BLYP, giving confidence in the applicability of DFTB in oxide surface modelling.

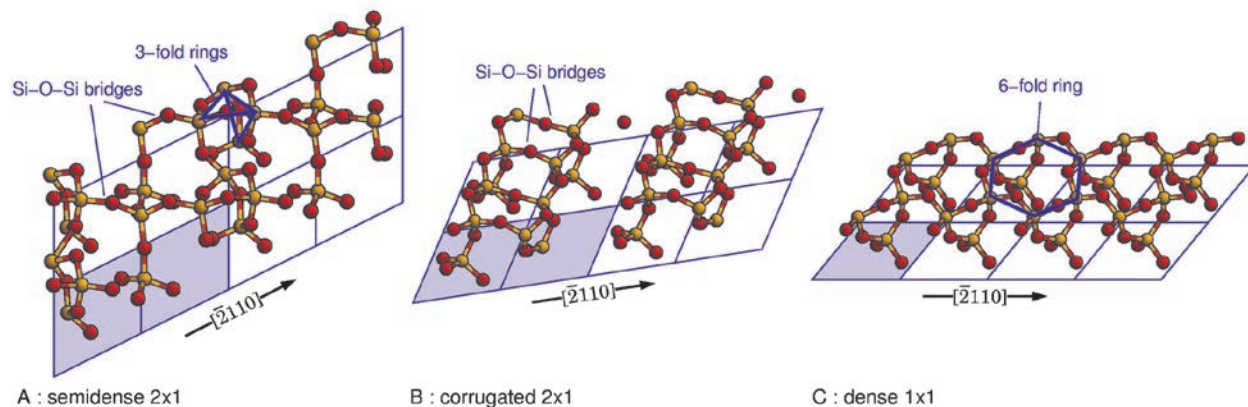


Fig. 2: Structurally optimised (0001) surface reconstructions **A:** A semidense 2x1 reconstruction consisting of Si O Si bridges and 3-fold rings. **B:** A corrugated 2x1 reconstruction with 4-fold rings. **C:** A dense 1x1 reconstruction (6-fold rings).

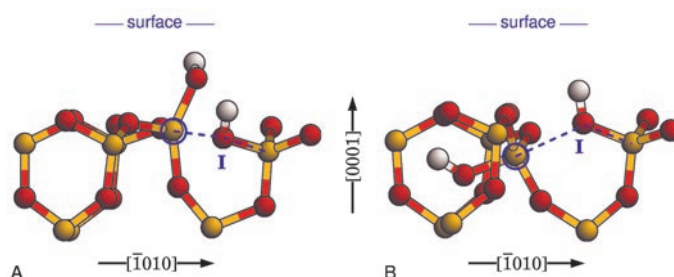


Fig. 3: Different structures of H_2O dissociatively „bound“ to the dense (0001) surface. The dashed blue lines indicate the former Si–O–Si bridges. As explained in the text, these configurations are not stable.

The interaction of water with dense (0001) surfaces. In principle the surface structure on the atomic scale will depend on the atmospheric environment, in particular on the presence of water. In earlier computational studies of highly reactive as-cut surfaces, water was found to strongly bond dissociatively to these surfaces [9]. The same was found using the DFTB method. Therefore in this paragraph we only present our results for the interaction of water with the most stable dense (0001) surface reconstruction of α -quartz (structure C).

As in this reconstruction all atoms are bulk-like coordinated, one would expect the surface to be passive. In order to bond a water molecule to the surface dissociatively, one of the Si–O–Si bridges has to be broken. Fig. 3 illustrates two possible configurations to then attach the proton and the OH-group. As expected, the reaction is strongly endothermic (by 0.9 and 0.4 eV per water molecule for A and B respectively). All other possible configurations give similar or even larger energies. In other words, with respect to water the ideal dense (0001) surface is found to be chemically rather inert.

However, within the vicinity of surface defects, water will most likely be adsorbed. One type of defect, which will always be present, are intrinsic point-like defects, in particular vacancies. The type of vacancy having the smallest effect on the bulk lattice or the fully reconstructed surface is the oxygen vacancy: Removing one oxygen atom results in two under-coordinated silicon atoms facing each other with a dangling bond at a distance of about 3 Å. With the length of a typical Si–Si bond being slightly less than 2.4 Å, only a small displacement is needed to form a strong Si–Si reconstruction bond. This is indeed observed in our DFTB calculations both in bulk α -quartz and also at the dense surface. Furthermore we find the vacancy to be most stable at the topmost surface layer of the dense reconstruction, with an energy difference of about 400 meV compared to a position in the bulk.

When a single water molecule reacts with a single oxygen vacancy at the surface, the largest energy gain can be achieved if the strain induced by the two displaced silicon atoms is released by breaking their common reconstruction bond. Whichever is bound to the first one of the Si atoms, proton or OH, will weaken the Si–Si bond. Once the remaining proton or OH approaches the remaining Si atom, the bond will finally be broken. Fig. 4 shows the lowest energy configuration, which gives a strong binding energy of 1.1 eV (DFTB).

Summary. The applicability of the DFTB method to oxide-surface related problems has been demonstrated in the case of SiO_2 by validation against full DFT approaches. As a first example application, the interaction of highly stable α -quartz surfaces with water molecules was studied. It was further shown that oxygen vacancies accumulated at the surface are preferred sites to initiate hydroxylation of passive dense surfaces.

Acknowledgements. The authors wish to thank T. Frauenheim (University of Paderborn) for kind support.

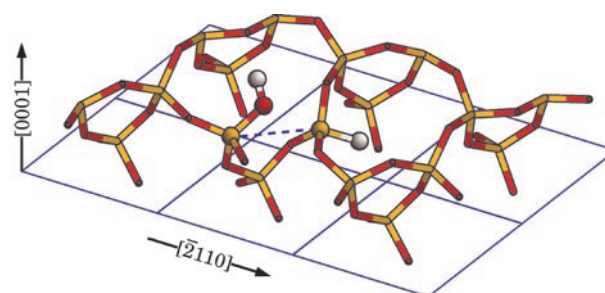


Fig. 4: A single water molecule bound dissociatively at an oxygen vacancy at the dense (0001) surface. The dashed blue line indicates the former Si–Si bond.



References

1. Frauenheim, T.; Seifert, G.; Elstner, M.; Hajnal, Z.; Jungnickel, G.; Porezag, D.; Suhai, S.; Scholz, R.: Phys. Status Solidi (b) 217 (2000) 41.
2. Rignanese, G.-M.; De Vita, A.; Charlier, J.C.; Gonze, X.; Car, A.: Phys. Rev. B 61 (2000) 13250.
3. Koudriachova, M.V.; Beckers, J.V.L.; De Leeuw, S.W.: Comput. Mater. Sci. 17 (2000) 182.
4. Segal, M.D.; Lindan, P.-J. D.; Probert, M.J.; Pickard, C.J.; Hasnip, P.J.; Clark, S.J.; Payne, M.C.: J. Phys. Condens. Mater. 14 (2002) 2717.
5. Perdew J.; Zunger, A.: Phys. Rev. B 23 (1981) 5048.
6. Delley, B.: J. Chem. Phys. 113 (2000) 7756.
7. Becke, A.D.: J. Chem. Phys. 88 (1988) 2547.
8. Lee, C.; Yang, W.; Parr, R.G.: Phys. Rev. B 37 (1988) 785.
9. De Leeuw, N.H.; Higgins, F.M.; Parker, S.C.: J Phys. Chem. B 103 (1999) 1270.



Newly Invented High-Strength and Light-Weight TRIPLEX Steel Exhibiting Exceptional Ductility by Shear Band Induced Plasticity (SIP)

U. Brück, G. Frommeyer

Department of Materials Technology

Requirements of the environmental policy and the automotive industry concerning weight reduction of vehicles, reduced fuel consumption and exhaust gas pollution imply the application of advanced structural materials with lower density and novel design concepts. Near austenitic or multi phase light-weight steels containing high manganese and aluminium contents fulfil these requirements due to their low density of about 6.5 to 7.1 g/cm³, high-strength of 700 to 1050 MPa and excellent formability. This novel class of high-strength steels ideally supplements the newly developed high-strength and supra-ductile TRIP and TWIP steels which achieve their extraordinary ductility and toughness by activating specific deformation mechanisms: **TR**ansformation Induced **P**lasticity and **TW**inning Induced **P**lasticity. In TRIPLEX steels intensive homogeneous shear band formation, the so-called **S**hear Band Induced **P**lasticity (SIP-effect) occurs during the deformation and enables the enormous formability even at high strain rates.

TRIPLEX light-weight steels revealing the SIP-effect are based on the ternary System Fe-Mn-Al. The structure of these steels is face-centred cubic (f.c.c.) at lower aluminium concentrations and medium manganese contents. Fig. 1 shows an isothermal section at 900 °C of the related Fe-Mn-Al phase diagram. With increasing aluminium concentration the microstructure is of dual phase consisting of austenite and ferrite. At higher manganese concentration additionally brittle β -manganese, which consists of a complex cubic unit cell, precipitates in the γ -matrix. With decreasing temperature the austenitic region will be closed up with lower aluminium and manganese concentrations. For stabilizing the austenitic matrix at room temperature and enhancing the aluminium solubility certain amounts of carbon are added. At low cooling rates or during aging at temperatures below 900 °C higher contents of carbon will cause a spinodal decomposition of the matrix into low carbon and carbon rich zones and subsequently the formation of

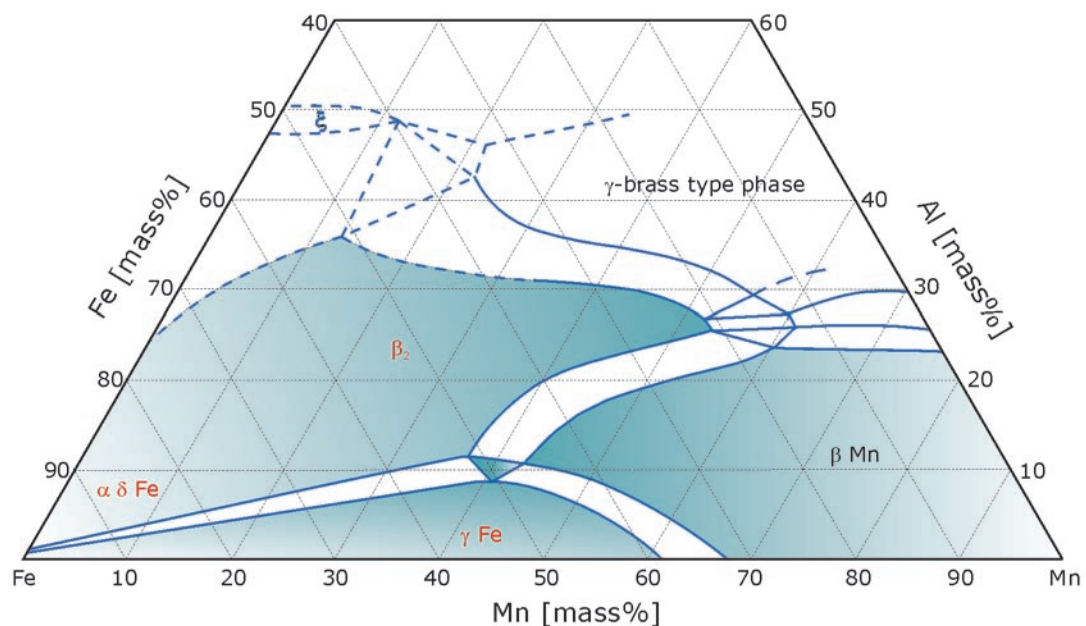


Fig. 1: Isothermal section of the ternary System Fe-Mn-Al at 900 °C.

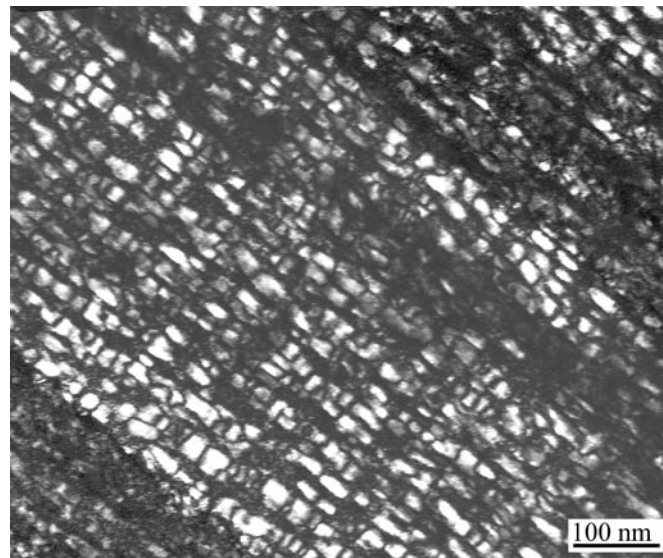


Fig. 2: TEM dark field image taken from the (110) κ -carbide superlattice diffraction peak of a κ -carbide containing air-cooled TRIPLEX steel.

perovskite structured $(\text{FeMn})_3\text{AlC}$ κ -carbides occurs [1]. The formation of the ordered phase $(\text{FeMn})_3\text{AlC}$ was identified in the X-ray diffraction pattern by asymmetrically broadened austenite diffraction peaks and by superlattice reflexes. TEM investigations reveal that the carbides form a three dimensional network of cuboide particles with a mean interparticle distance of about 30 nm. These are aligned along the elastically weakest [100] direction. For imaging the carbide morphology of the austenitic matrix the TEM dark field image of an air-cooled microstructure is displayed in Fig. 2 by using the (110) κ -carbide superlattice diffraction peak. The amount and distribution of these κ -carbides are strongly affected by the annealing procedure (temperature and time) and by the ratio of the aluminium to manganese plus carbon content.

At higher aluminium concentrations a volume fraction of 5-40 vol% ferrite remains in the austenitic matrix. This amount can be reduced by annealing the alloy in the austenite region [2] and by subsequent quenching to room temperature. After long term aging the brittle β -manganese phase starts to precipitate, whereas its volume fraction is increasing with proceeding aging time. This process reduces the maximum manganese concentration in TRIPLEX steels for sufficient formability. Likewise ferrite will be formed after long-term aging via the reaction: austenite \rightarrow κ -carbide + ferrite.

The density of high-strength steels with improved corrosion resistance can be lowered very effectively by addition of large amounts of aluminium [3]. Nevertheless, in binary ferritic iron-aluminium alloys the aluminium concentration is restricted to about 6.5 mass%. At higher contents the occurrence of the D0_3 -ordered phase drastically deteriorates the

formability. The reduction in specific weight of TRIPLEX steels is similarly caused by alloying the steel with the light-weight metal aluminium. At constant manganese content the density decreases approximately linear with increasing aluminium concentration. Dissolved aluminium atoms in the austenitic f.c.c. lattice lead to an additional reduction in specific weight due to their larger atomic radius ($r_{\text{Al}} = 0.143$ nm compared to iron $r_{\text{Fe}} = 0.126$ nm). The decrease in density of about 10% at high aluminium contents is solely caused by the lattice dilatation. Higher manganese contents ($r_{\text{Mn}} = 0.134$ nm) are also expanding the austenitic lattice and have a strong contribution to the reduced density. The maximum weight reduction at high aluminium and manganese concentrations amounts to more than 15%.

Due to the very effective solid solution hardening of aluminium the ultimate tensile strength of TRIPLEX alloys strongly increases with increasing aluminium content at constant manganese and carbon concentrations from 770 MPa to about 1050 MPa. The maximum tensile elongation of optimised TRIPLEX steels achieves more than 70 % at room temperature. Their enormous plasticity is caused by pronounced homogeneous shear band formation as shown in TEM investigations of deformed TRIPLEX alloys with high aluminium contents (Fig. 3) [4]. The extraordinary ductility even remains at low temperature of 77 K (-196 °C). Tensile tests performed at this temperature exhibit ultra high-strength of 1500 MPa and about 40 % strain to failure. In the temperature region between 150 °C and 300 °C the strength decreases very slightly caused by dynamic strain aging. Due to the high carbon content a pronounced Portevin-Le-Chatelier effect occurs

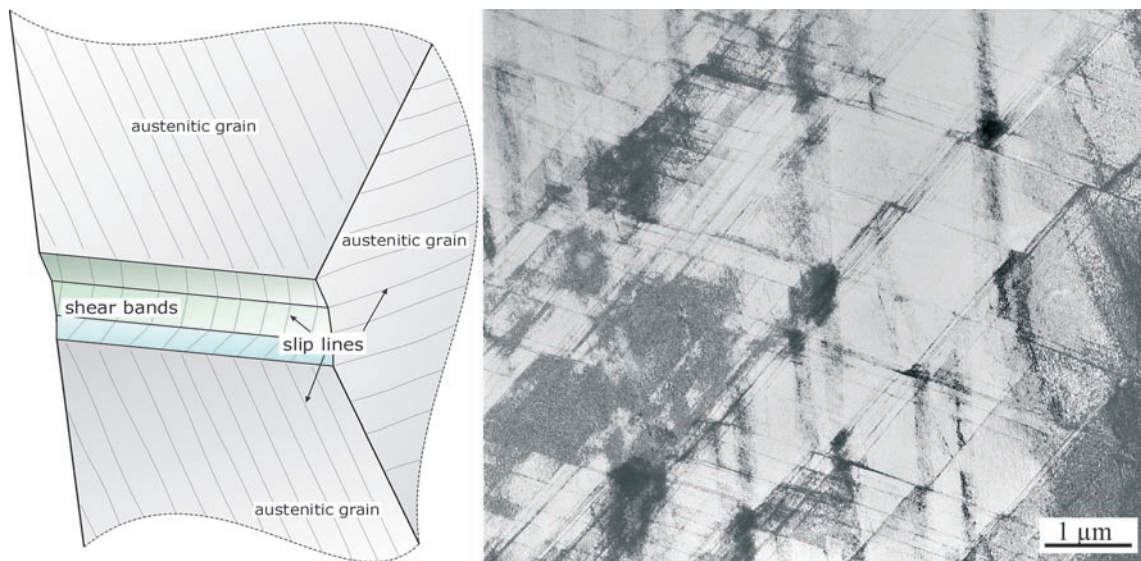


Fig. 3: Schematic drawing of shear band formation and TEM bright field image showing a deformed TRIPLEX steel with pronounced homogenous shear bands and twin planes.

which is detectable by the occurrence of serrations in the slope of stress-strain-curves. At a temperature of about 400 °C the ductility drastically decreases to the half value of the total elongation at 250 °C. X-ray diffraction patterns of deformed samples reveal the formation of ductility reducing κ -carbides during the quasi-static deformation process.

The ductility of TRIPLEX steels monotonically decreases with increasing strain rates. Nevertheless the total elongation still amounts to more than 45 % at the crash relevant strain rate of 10^2 s^{-1} . Simultaneously, the ultimate tensile strength increases to about 1100 MPa at $\dot{\epsilon} = 10^2 \text{ s}^{-1}$. Due to the extra-

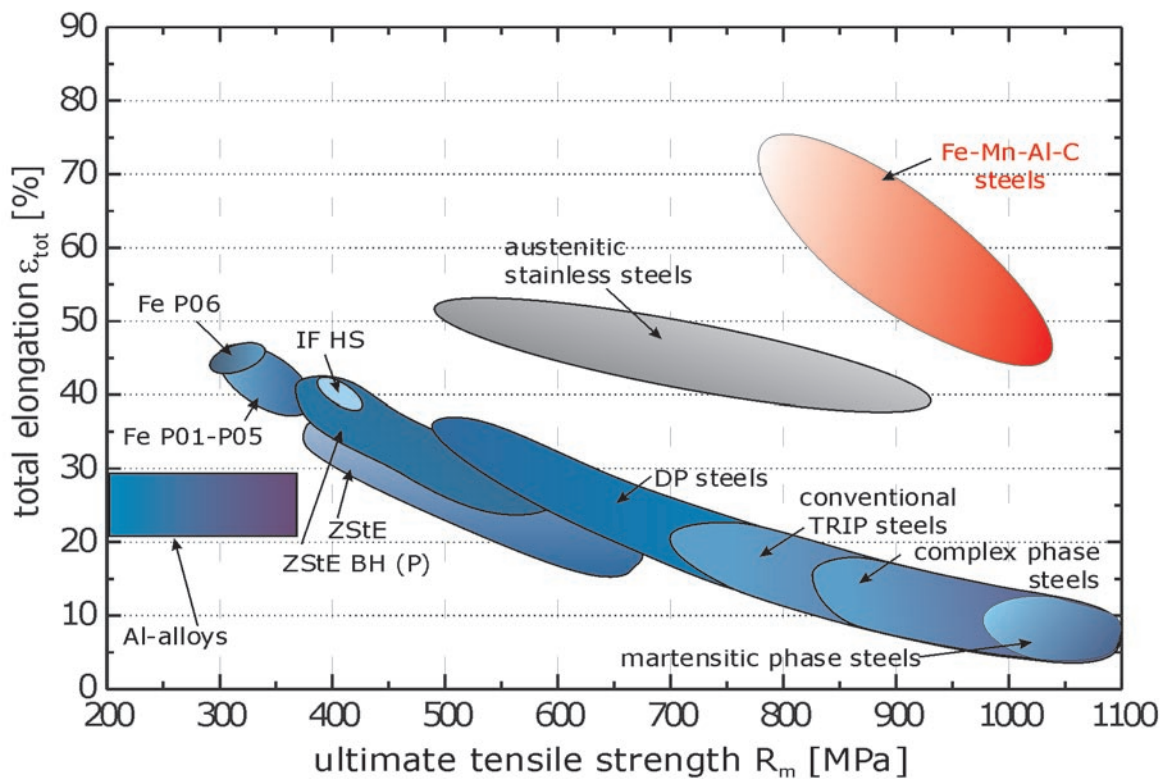
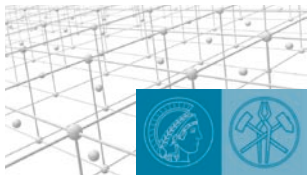


Fig. 4: Total elongation in dependence on the ultimate tensile strength of Fe-Mn-Al-C steels in comparison with other deep drawing qualities.



ordinary ductility at this high-strength level the specific energy absorption of TRIPLEX steels is about $E_{\text{spec}} \approx 0.45 \text{ J/mm}^3$, which is as twice as high as the specific energy absorption of conventional deep drawing steels.

In view of their lower density, enormous ductility, and toughness even at high strain rates and low temperatures, TRIPLEX steels are predestined for applications in advanced transportation systems and in mechanical engineering. A comparison of the mechanical properties with those of conventional deep drawing steels and aluminium alloys is presented in the total elongation vs. ultimate tensile strength diagram of Fig. 4. This comparison significantly displays that TRIPLEX steels represent a new

class of high-strength light-weight steels with superior mechanical properties.

References

1. Han, K.H.; Choo, W.K.: Metal. Trans. 20 (1989) 205-214.
2. Ishida, K.; Ohtani, H.; Satoh, N.; Kainuma, R.; Nishizawa, T.: ISIJ Int. 30 (1990) 680-686.
3. Ham, J.L.; Cairns, R.E.: Product Eng. 29 No. 52 (1958) 50.
4. Brück, U.; Frommeyer, G.: Proc. PLASTICITY 2003, ed. A.S. Khan, Quebec, Kanada (2003) 169 (ISBN 0-9659463-4-7).



Understanding and Reducing of Spottiness at Twin Roll Cast Thin Strip

A.R. Büchner

Department of Metallurgy and Process Technology

Twin roll casting of steel strip is studied since the eighties worldwide [1-3], and it is now on the border of industrial application [4-6]. Nevertheless, there are numerous special problems which have to be supported by basic research.

One of these problems is the inhomogeneity of heat transfer between strip and the rolls which leads to the well-known effect of spottiness, i.e. a non-uniform temperature distribution at the strip, see Fig. 1. The spottiness has several detrimental consequences. The structures from a hot or a colder spot may be strongly different. Several surface defects occur, when spottiness is present. It is also known, that the occurrence of hot spots causes surface cracks. Thus it is of use to study the spottiness effect. In this paper some experimental conditions are varied and their influences on spottiness are observed and discussed.

Experiments. Casting trials were carried out on a small laboratory caster, similar to that of Fig. 1. About 10 kg of LC-steel were cast with 16 or 25 cm/s in a thickness close to 2.2 mm. The material of the rolls, the roll roughness R_a and the Ti-content were also varied.

The result of the measurement was the heat transfer coefficient α . After [3] the heat flux density \dot{q} can be calculated from α .

One of the rolls was equipped with a thermocouple 1 mm beyond the roll surface, and therefrom good knowledge was available on the roll surface temperature. This is important, because the heat flux is caused by the temperature difference ($T_{liq} - T_{roll}$), acting as a driving force.

It was intended to judge the spottiness of all strips by measuring the surface temperature with a pyrometer. Unfortunately this pyrometer was too sluggish in reaction, and so no reference to the spottiness could be obtained by this method.

To obtain a quantitative measure of spottiness, three predicates of spottiness were defined by visual observation, see Fig. 2. To improve the objectivity of this procedure, three persons were involved and mean values were used.

Discussion. α , \dot{q} and spottiness predicates have a large experimental scatter; so only correlations using mean values can be studied. Clear quantities are obtained by using mean values corresponding to a roll velocity and a roll material. To investigate influences on the spottiness the means of spottiness degree were correlated to those of α or \dot{q} . No clear correlations were obtained thereby, as these correlations were depending on the roll velocity. A further correlation to the temperature difference ($T_{liq} - T_{roll}$) is given in Fig. 2 (T_{roll} in the sixth roll rotation; steady state of pool geometry nearly reached). This



Fig. 1: Demonstration of temperature spottiness in a laboratory twin roll caster; strip width 6.5 cm.

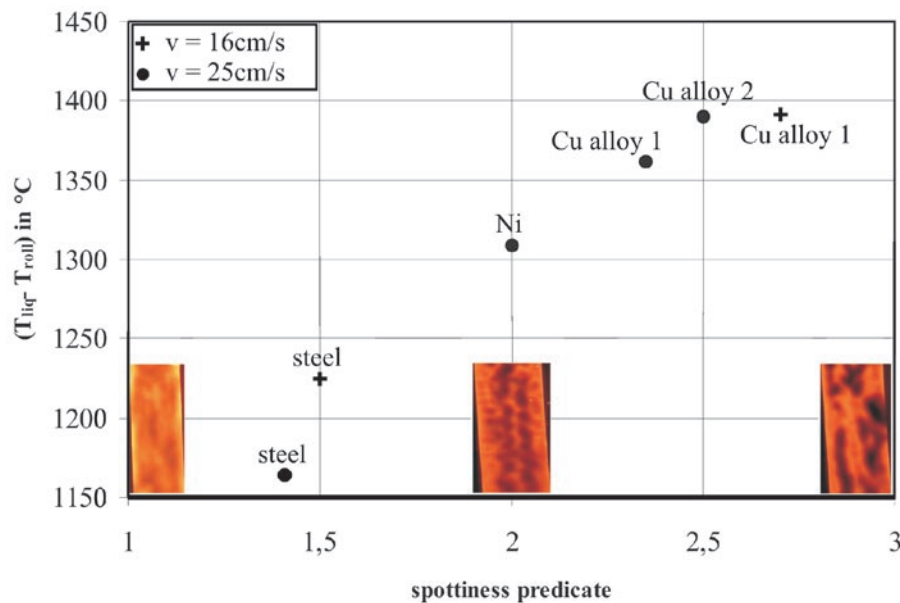


Fig. 2: Visual definition of spottiness predicates and correlation of these predicates with $(T_{liq} - T_{roll})$; material of rolls is indicated.

correlation is clear and unique, and it is independent of the roll velocity; it is also a very favorable one, as T_{roll} is a parameter which can be influenced intentionally in the experiment (what is not so simple for α and \dot{q}).

A qualitative understanding is underway, and it starts following to Fig. 3. During the growth of the solidified layer the first sublayer close to the roll gets colder, thus shrinking due to thermal effects. A bending occurs increasing the distance to the roll surface. Thereby the local value of α is reduced, and the further solidification is hampered. So at the place of this effect and at the end of the pool the solidification is not terminated, and a pocket of melt with a large amount of latent heat remains present. This place is seen during further cooling as a hot spot on the strip.

The occurrence of spottiness thus must be enhanced, when the mean α is reduced (due to gas pockets). The local \dot{q} is reduced because therefrom

the temperature difference over the solid layer ($T_{liq} - T_{low}$) and so the tendency for shrinking and bending is reduced. In total, \dot{q} will decrease if the driving force ($T_{liq} - T_{roll}$) is decreased.

The influence of the roll velocity on $(T_{liq} - T_{roll})$ is understandable, because T_{roll} (at the entrance into the pool) depends on the heat removal during the rest of roll rotation.

Conclusion. It was shown that under the experimental conditions used here the spottiness can be reduced or avoided by an elevated roll temperature, e.g. close to 400 °C. This can be achieved in the easiest way by using steel rolls instead of good heat-conducting Cu-alloy-rolls.

References

1. Birat, J.B.; Blin, P.; Jacquot, J.L.; Ribound, P.; Thomas, B.: In: Casting of Near Net Shape Products, eds. R.S. Carbonara, Y. Sahai, J.E. Battles, C.E. Mobley, The Metallurgical Society, Inc. (1988) 1-12.
2. Büchner, A.R.; Tacke, K.-H.: Stahl und Eisen 117 No.8 (1997) 47.
3. Büchner, A.R.: Steel Res. 68 (1997) 247.
4. Lindenberg, H.-U.: Conf. Proc. 15th Aachener Stahlkolloquium, RWTH Aachen, ed. R. Kopp (2001) 63.
5. Damasse, J.M.; Albrecht-Früh, U.: Steel World 7 (2002) 41.
6. Yamada, M. et al.: Proc. 4th Eur. Cont. Casting Conf., Vol. 2, Birmingham, UK (2002) 891.

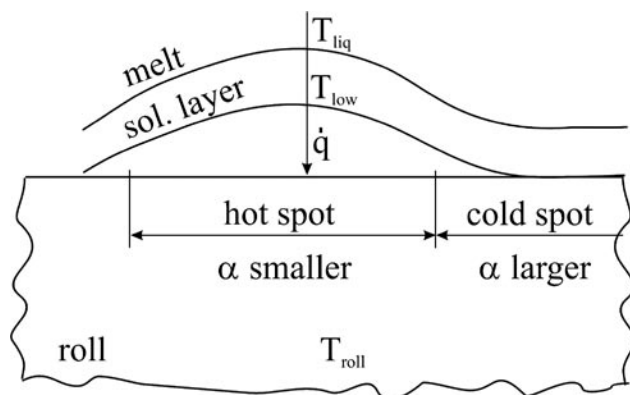


Fig. 3: Principle idea of spottiness interpretation; symbols see text.



Fundamental Studies on the Formation of Ultra-Thin Amorphous Conversion Films on Zinc Alloy Coatings

N. Fink, B. Wilson, G. Grundmeier

Department of Interface Chemistry and Surface Engineering

The development of environmental friendly conversion layers for both architectural and automotive applications has been the subject of increased research over the last decade as an alternative to carcinogenic chromate. The aim of this work is the study of chromate-free adhesion promoting thin layers on the surface of zinc coated steel in an effort to establish the interfacial reactions that are taking place and allow for improved chemistries to be implemented. Several techniques were used to get detailed information about the reaction states. FT-IRRAS and XPS were used to determine the effect both of cleaning on the pre-existing surface and the thickness of the layers produced after conversion treatment. In addition, atomic force microscopy (AFM) has been used to ascertain the impact that such treatments have on the surface morphology. Electrochemical methods have been used to investigate the chemistry occurring during the conversion process and to demonstrate the effectiveness of the new conversion layers at preventing delamination.

Thin films of conversion layer were deposited on to model substrates like polished pure zinc and non-skin passed hot dip galvanised (HDG) steel supplied by voestalpine (Linz, Austria). Samples with a size of 30 mm x 30 mm were cut from the supplied

substrate and subjected to a solvent cleaning process to ensure complete removal of any oils or surface contamination. In addition, alkaline cleaning of the surface (pH 13, 55 °C) was carried out to activate the surface for the subsequent conversion layer treatment that was based on phosphate chemistry. During alkaline cleaning several effects occur. One is the removal of organic contamination, coupled with the dissolution of the thin aluminium-oxyhydroxide layer on top of the HDG layer takes place. In addition zinc-oxyhydroxide is removed during the cleaning process and a new oxide layer of defined stoichiometry is formed. As a result of these processes during alkaline cleaning a change in topography is expected and was examined by means of AFM.

The typical reflection absorption infrared spectra of the alkaline cleaned non-skin passed surface, with solvent cleaned NSP as a reference, is presented in Fig. 1. The primary change that can be observed between the alkaline cleaned and solvent cleaned surfaces is a strong peak at 954 cm^{-1} . In the literature this peak position is known to correspond with Al-OH [1]. The negative nature of the absorbance recorded clearly illustrates that the alkaline cleaning process not only leads to the removal of any surface contamination but also results in dynamic surface etching and the removal of the thin aluminium layer

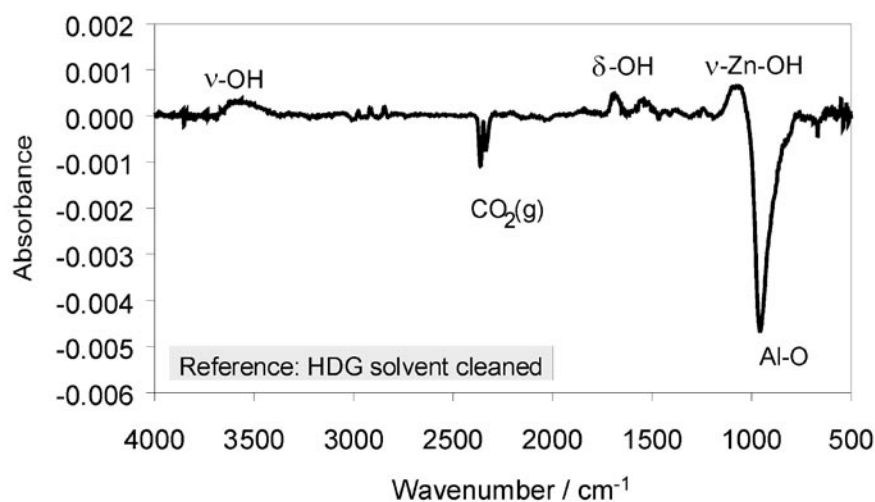


Fig. 1: Change in absorbance of the surface of non skin passed hot dip galvanised (HDG) steel recorded by IRRAS after 30 s alkaline cleaning (reference: solvent cleaned non skin passed HDG).

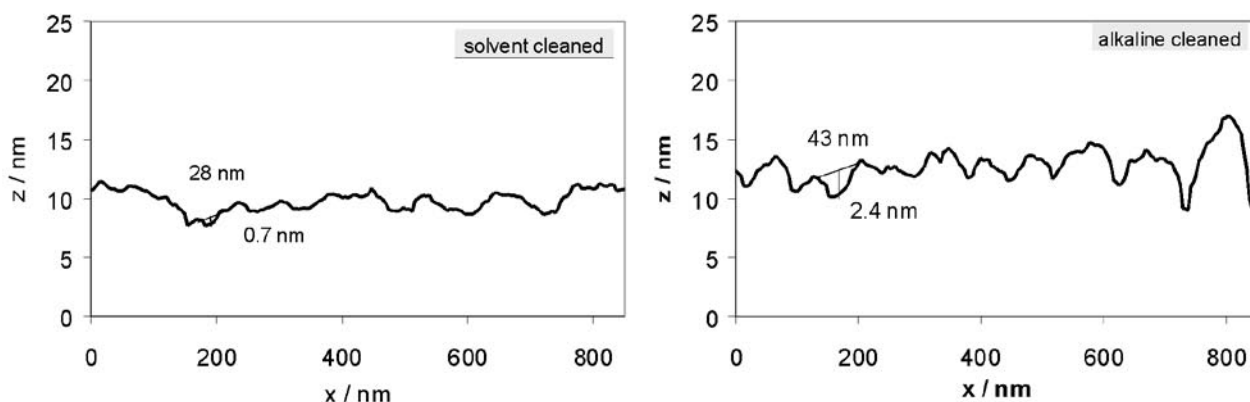


Fig. 2: Linescans taken from AFM topography images of non skin passed HDG before (left) and after 30 s alkaline cleaning (right).

present on the surface. In the case of the samples used here the thorough solvent cleaning already led to extremely low aliphatic carbon surface concentration, so that the CH_2 -peaks are almost negligible.

AFM measurements were performed on one single grain before and after the alkaline treatment of the surface to characterise the change in the surface morphology due to the cleaning process. Nanoscopic etch grooves have formed in the surface with a diameter of 30 to 40 nm and a depth of about 5 nm according to the AFM measurement. Thus the topographic measurement reveals that an increase in the actual surface area is induced by the alkaline cleaning step. The increase in the microscopic surface area can be estimated based on the assumption that a regular pattern of hills and valleys is given. This simple model would lead to a surface area increase of 100% due to the alkaline etching process.

Of course this might influence the later film formation process again which is also based on an etching step that triggers the film deposition since an increased microscopic surface area will lead to a larger change in the composition of the adjacent film forming electrolyte layer in the more macroscopic diffusion layer.

Effect of Conversion Solution Treatment. The initial states of conversion film formation on solvent cleaned HDG samples are analysed by means of high-resolution AFM (Fig. 3). The left topography image shows the surface after 5 s conversion solution treatment, here the initial state of film formation is underway. The right image shows the topography after 40 s of film formation, where an almost complete conversion layer with its different terraces is obvious.

The kinetics of deposition and surface coverage on the galvanised substrate as a function of im-

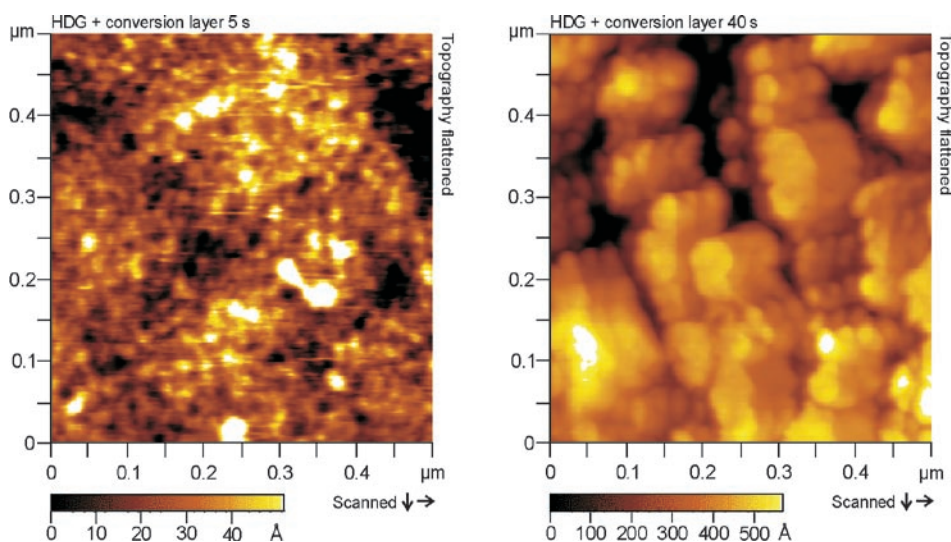


Fig. 3: AFM topography images of non skin passed, solvent cleaned HDG samples after different immersion times in the conversion solution (left: 5 s, right: 40 s).

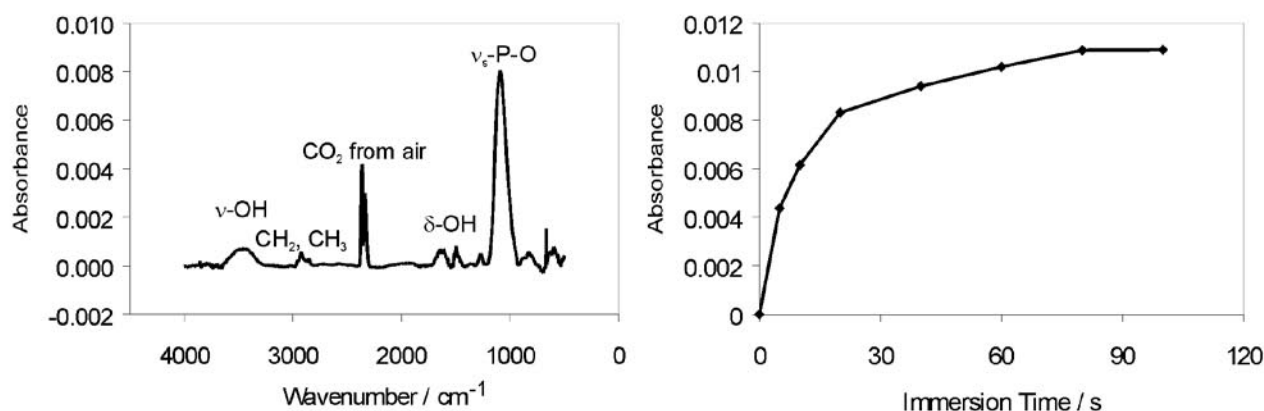


Fig. 4: (left) Typical FT-IRRAS spectrum of a HDG sample treated with phosphate conversion layer (left). Change in absorbance of the ν_s P-O phosphate peak (1092 cm^{-1}) with immersion time as measured by IRRAS (right).

mersion time in conversion layer solution were determined by a combination of FT-IRRAS and cyclic voltammetry. A distinct assignment of bands and their quantification can be given when a phosphate layer is deposited during the conversion process. In this case the absorbance of the symmetric stretching vibration of the phosphate bond (ν_s P-O) peak at 1092 cm^{-1} [2] was chosen as being representative of the levels conversion layer present on the surface and shows that maximum coverage is achieved after 60 to 80 s immersion (see Fig. 4).

Although the topography measured by means of AFM shows that the surface of the galvanised steel is completely covered after 40 s the amount of area that remains electrochemically active is unable to be determined solely by microscopic techniques. Hence, additional electrochemical measurements were carried out to determine the total amount of exposed zinc surface as a function of immersion time. The use of cyclic voltammetry (CV) allows the measure-

ment of the free zinc surface by evaluation of the oxidation peak area [3].

Fig. 5a) illustrates the changes observed in the cyclic voltammograms as a function of immersion time in phosphate containing conversion solution with alkaline cleaned HDG presented as a reference of the uncoated surface. The reduction and oxidation peaks are can be seen at -1.03 V and -0.9 V (vs. SHE) respectively and clearly illustrate a decrease to a maximum value with increasing immersion time. A plot of the normalized uncovered area of the anodic peak against immersion time is displayed in Fig. 5b). The results from this analysis of the CV data show how total surface coverage reaches a maximum of approximately 90%. Such results are in line with that observed by FT-IRRAS in that maximum coverage of the surface is obtained after 60 s.

Conclusions. Use of FT-IRRAS and cyclic voltammetry enables both the kinetics and surface coverage by conversion layers to easily followed and

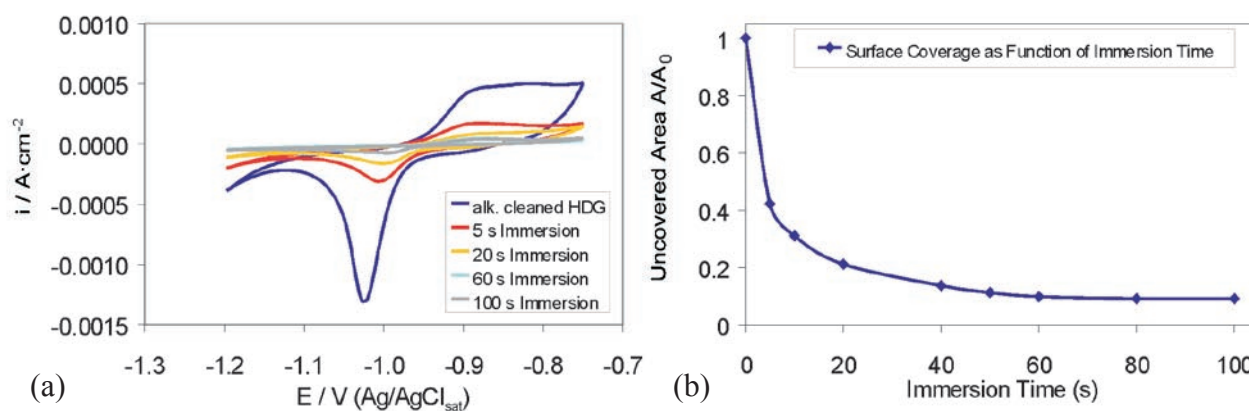


Fig. 5: (a) Cyclic voltammograms of samples subjected to different immersion times in phosphate containing conversion solution – alkaline cleaned hot dip galvanized steel as a reference sample; immersion times of 5, 20, 60 and 100 s respectively and (b) calculated free surface area plotted against immersion time.



rapidly assessed. AFM highlights the changes that occur on the nanometer scale as a result of both alkaline cleaning and conversion film formation processes. Alkaline cleaning results in an etching of the surface. In addition, topographic studies of film formation kinetics clearly show the formation and growth of the film from its initial state to an almost complete film with terraces after 40 s of immersion. The results show that ultra-thin conversion films can be characterised and optimized through the application of complimentary spectroscopic, microscopic and electrochemical techniques.

References

1. Nyquist, R.A.; Putzig, C.L.; Leugers, M.A.: Handbook of Infrared and Raman Spectra of Inorganic Compounds and Organic Salts, Academic Press, San Diego, CA (1997).
2. Steiner, G.; Sablinskas, V.; Savchuk, O.; Bariseviciute, R.; Jähne, E.; Adler, H.J.; Salzer, R.: J. Mol. Struct. 661-662 (2003) 429-435.
3. Losch, A. ; Schultze, J.W. ; Speckmann, H.D.: Appl. Surf. Sci. 52 (1991) 29-38.



Modelling of Laser Welded Ti–Al

J. Gnauk, R. Wenke

Department of Materials Technology

The prediction of phase and morphology formation, and the development of appropriate models have been intensively investigated over several years. The modelling of melting and solidification processes belongs now to a well established activity and the quantitative treatment of thermodynamic processes far away from the equilibrium state have been performed in several research groups [1-4].

However, thermal joining and specifically welding processes of different metallic materials, such as Al–Ti or Al–Fe etc., where various ordered phases with superlattice structures (intermetallics) will be generated, were not the central objectives of phase transformation and microstructure simulations up to now. Laser welding of such different materials show great potential applications in the aerospace and automotive industry, where the light-weight metals titanium and aluminium have a great impact on energy and weight saving in combination with the good heat resistance of Ti-alloys.[5] Major research activities on this focus are carried out in Japan [6] but also at TU-Clausthal [7] and at the „Bremer Institut für angewandte Strahltechnik“ (BIAS), whereby an intensive cooperation with the Department of Materials Technology exists.

Basic literature regarding the solidification phenomena can be found e.g. in the book of Kurz and Fisher [8]. Boettinger wrote an actual overview about modelling of solidification and microstructure evolution [9]. The research work presented in literature is concentrated mostly on modelling of phase and

microstructure formation at low cooling rates or local equilibrium at the liquid–solid interface. But also the modelling of high cooling rates and steep temperature gradients is carried out [4]. The majority of the research activities deals with binary or ternary two-phase systems. However, the formation of intermetallic phases is only rarely integrated into the model. Especially in the Ti–Al system, the modelling of the not yet completely known phase diagram is very difficult. Ongoing constitutional research improves the detailed knowing steadily. Only the micromechanical properties of γ -TiAl were modelled [10]. Moreover, there is a macroscopic approach for the formation of intermetallic phases of coated aluminium alloys [11].

This lack of research activities is due to the fact, that the constitution of titanium-aluminides regarding their crystal structures, superlattice- and microstructure morphologies is multifaceted and this deprives therefore a complete analysis. Nonetheless, important progress in the last years was made in this field [12-15].

To describe the heat and mass transfer in a macroscopic/mesoscopic model, various approaches are applied like the *phase field method* [16]. However, in this special case, the only suitable method is the *generalised enthalpy method*, developed by Tacke and Mackenbrock [17]. Here, the treatment of multiphase systems is much easier due to the single domain approach of the diffusive heat and mass transport than those of more conventional

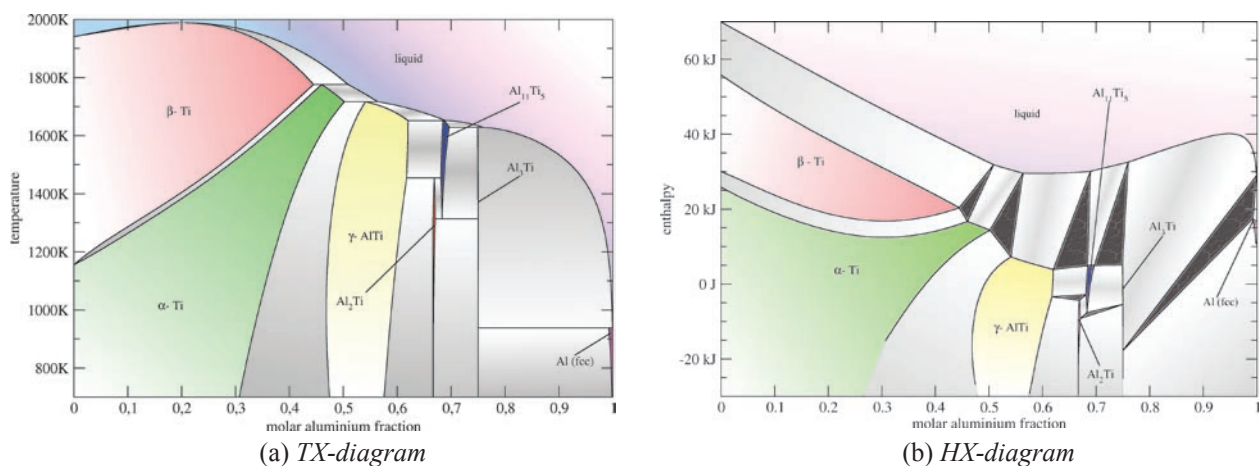


Fig. 1: Different representations of the Ti–Al phase diagram. The α_2 -phase is not yet implemented.



methods, based on the classical temperature-concentration-diagram.

Model details. The knowledge of the phase diagram is an essential part for the simulations. To be used with the generalised enthalpy method it was necessary to recompute the Ti–Al phase diagram in its HX representation. The thermochemical data and the phase describing models of the Gibbs free energy were taken from literature [18]. The non-ordered phases α -Ti, β -Ti, Al (fcc) and the liquid phase are calculated with a substitutional model where the atoms take random positions inside the lattice. Another model is applied to γ -TiAl and the Ti_3Al phase and describes phases with sublattices and preferred positions of atoms, allowing to recognize ordering. The stoichiometric phases Al_2Ti , Al_3Ti and $Al_{11}Ti_5$ are described by a model similar to the above mentioned sublattice model, except that only the stoichiometric composition is preferred. Indeed, this implementation allows concentrations beside the stoichiometric relation to consider, which slightly differs from the common line-compound definition.

With these thermochemical descriptions the chemical potentials can be calculated to define the phase boundaries. A multiphase region is present when the chemical potentials of each phase are equal. This condition is equivalent with the finding of a tangent for the two or three curves of the Gibbs energy of a two or three phase region. At the phase boundaries the enthalpies are calculated to form the shown enthalpy–concentration (HX-) diagram as can be seen in Fig. 1b.

For the simulation of the welding process, the diffusive heat and solute transport has to be calculated. Also phase transitions during solidification have to be taken into account. Common diffusive transportation models have to regard the classical Stefan problem to distinguish the different coexisting phases. Even the well established phase field method has to do it indirectly. Due to its single domain nature the problem can be ignored and no front tracking of phase boundaries is necessary if the generalised enthalpy method is used [19]. Fig. 1b clearly shows the advantage of the generalised enthalpy method. In contrast to the commonly used TX representation, where eutectic, respectively, peritectic three-phase regions are one-dimensional, here they become triangles, where every HX-pair determines a unique system state.

The diffusive heat and mass transport is described by the generalised flux Φ , defined by its flux density as

$$\frac{\partial \Phi}{\partial t} = -\text{div } \mathbf{J}_\Phi$$

This relation builds a linear system of conservation terms, which implements also the Soret and the Dufour effect for the cross terms between heat and solute diffusion. The driving forces are the temperature gradient for the heat flux and the gradient of chemical potentials for the material diffusion.

Taking the calculated values of the total enthalpy and concentration into account, the phase fractions, the partial enthalpies and the partial concentrations for each phase can be determined. This is done by a nonlinear equation system with fractional concentration, temperature and phase fractions as dependant variables and the total enthalpy H and concentration X of the system as parameters. A Newton-Kantorowitsch iteration now solves this system. If no solution is found e.g. for a local three-phase system, all subsystems will be generated, i.e. the equation systems of all possible two-phase pairs are solved and the one with the highest total entropy is selected. This process can be adopted easily to ternary or higher systems with more than three coexisting phases in local equilibrium.

The kinetic behaviour of phase formation is eminent to obtain necessary information on under-cooling, to calculate parameters like average dendrite tip growth velocity to determine the microstructure of the phase seam.

Two approaches are selected to calculate kinetic solidification phenomena. The most exact and very time consuming approach is the online calculation of the phases, using the constitutional model of the Ti–Al system. Here, the phase formation can vary between the normal equilibrium behaviour and the case of total solute trapping.

A second phase diagram for complete solute trapping, similar to the one shown in Fig. 1 can also be calculated as well as every state between the two border cases. Due to the fact, that this calculations are very time consuming, this model can not be used to calculate the phase formation in the complete macroscopic simulation.

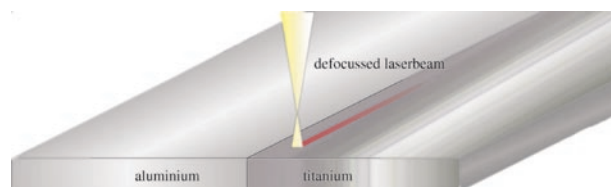


Fig. 2: Schematic drawing of a typical welding arrangement, butt joint, defocused laser beam on the titanium side.



The second approach can be performed much faster and is based on the assumption, that the phase transformation is delayed, depending on the actual cooling rate and the deviation from the respective equilibrium state, which generates a driving force to transform the phases. Here, some numerical kinetic parameters are needed, describing the delay of phase transformation between two phases. These kinetic coefficients will be derived by using the constitutional method described above, performing a numerical „experiment“ with controlled solidification conditions.

The model of microstructure is based on the theory of primary dendrite spacing, provided by Hunt and Kurz [8,20]. Here, the dendrite tip velocity is calculated as an average parameter, derived from the thermodynamic conditions during the simulation. In the particular case of directional growth of the intermetallic phase seam from the solid titanium into the molten aluminium it can be described easily by terms like $\lambda_1 = \sqrt{3\Delta T' R/G}$, where G denotes the interface temperature gradient dT/dz , R is the tip radius, and $\Delta T'$ the temperature difference between the root and the tip of the dendrite. In combination with the resulting phase fractions the microstructure of the phase seam can be predicted as a set of parameters like interdendritic constitution or the interdendritic spacings.

The model verification is an important part in the computer simulation field. A close and productive cooperation with the „Bremer Institut für angewandte Strahltechnik“ (BIAS), performing the laser welding of aluminium with titanium or steel for several years, allows to compare experimental results with the simulations.

In the ongoing investigation, two basic types of welding process are performed. One of this is that only the titanium is irradiated by a widened laser beam. The Ti remains solid at the interface, while the aluminium is melting, heated up by the heat conduction from the Ti side. Only diffusive transport phenomena are relevant here, fluid-dynamic processes do not have to be regarded (Fig. 2).

The other process is more difficult, because the titanium also melts at the interface adjacent to aluminium. More different phases will occur and also fluid-dynamic processes influence the distribution and mixture of the components, especially if a welding wire will be used. Both variants occur as butt and overlap joints.

Up to now, only the less complex variant (non fluid butt joint) is regarded in the simulations. In this case, as shown in Fig. 2, the sheets are fixed so that the face sides are forming a zero gap. The defocused laser is moved along the gap with an offset of about 4 mm on the titanium side.

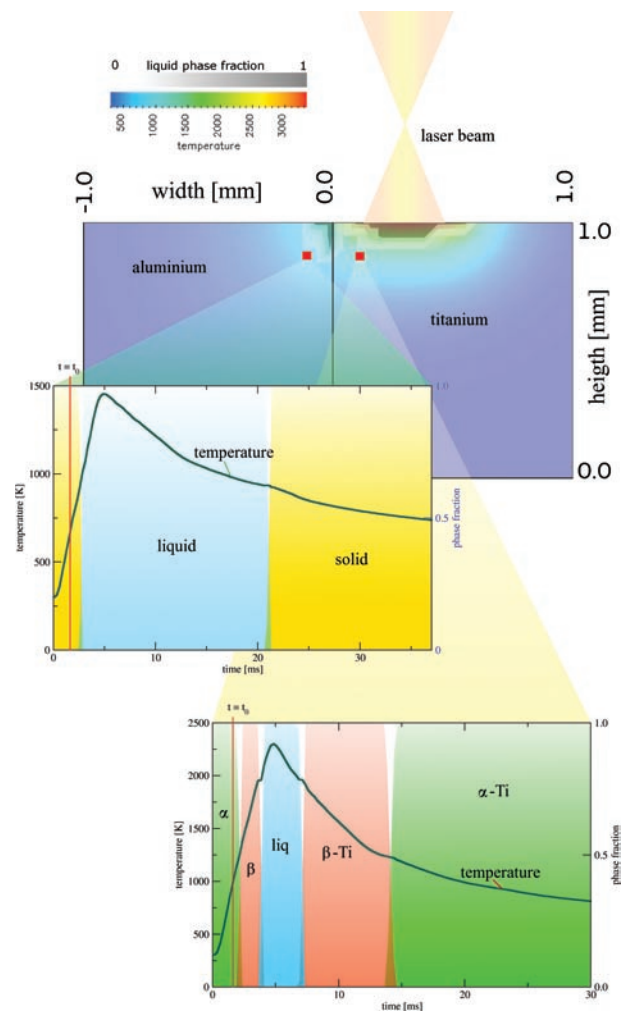
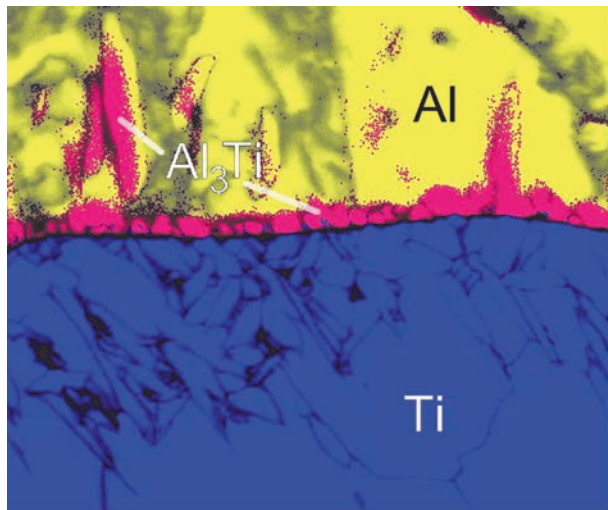


Fig. 3: Temperature – time – volume fraction dia-grams, showing the result of a typical simulation (1,6 ms after heating start, 4,5 kW laser defocused to 400 μm diameter, 300 μm offset to zero crack).

The simulation is carried out in a two dimensional grid, using a finite difference method and the discretised form of the generalised enthalpy method. Examined samples show that a short length scale is necessary to reproduce the phase seam. Furthermore, the interval of the time steps Δt is related to the length scale by $1/(\Delta x)^2$ due to the von Neumann stability criterion. As a result, a complete calculation of the grid would exceed the time limits. Therefore, a two stage procedure is necessary. The first run uses a large scaled grid to calculate the boundary conditions. In a second pass the real phase formation is computed within a much smaller length scale.

Fig. 3 presents a typical situation during the welding simulation. Above, the temperature profile of a cross section of the welded material is shown. Clearly visible is the effect of the strong difference in the thermal conductivities. The proceeding phase transformations are shown exemplarily for two different positions in the material at the bottom of



6.40 μm = 80 steps

Fig. 4: Combination of EDX and EBSD scans. The yellow area represents the aluminium phase, the α -titanium phase is blue marked. The resulting phase seam (red) consists in this case only of Al_3Ti .

Fig. 3. The cell at the aluminium side simply indicates the melting and solidification. Al_3Ti does not precipitate out in this distance from the interface. The Ti rich cell otherwise shows the α - β transition prior to melting and vice versa after the solidification.

For determining the very narrow phase seam in the laser welded samples, extensive microscopical characterisations are necessary. Besides the standard SEM, also TEM analyses were carried out. However, the check up of all provided samples will exceed the capacity of the TEM, and would be very time consuming. A combination of SEM examinations in combination with EDX and EBSD was carried out to examine a larger amount of samples. For this, the EDX and EBSD scans were performed simultaneously. The revealing phases were estimated by EBSD. Subsequently using EDX will help to distinguish crystallographic similar phases. Fig. 4 shows exemplarily the results of such a combined analysis. Clearly visible is the phase seam of Al_3Ti , grown from the titanium into the liquid aluminium.

References

1. Demetriou, M.D.; Ghoniem, N.M. et al.: Acta Mater. 50 (2002) 1421.
2. Glasner, K.: Physica D 151 (2001) 253.
3. Wang, G.X.; Prasad, V.: Mater. Sci. Eng. A, 292(2) (2000) 142.
4. Assadi, H.; Greer, A.L.: Mater. Sci. Eng. A 226–228 (1997) 70.
5. Schubert, E.; Klassen, M. et al.: J. Mater. Process. Technol. 115 (2001) 2.
6. Uenishi, K.; Kobayashi, F.: Intermetallics 4 (1995) S95.
7. Majumdar, B.; Galun, R. et al.: J. Mater. Sci. 32 (1997) 6191.
8. Kurz, W.; Fisher, D.: Fundamentals of Solidification. Trans. Tech. Publications, Aedermannsdorf, Switzerland (1984).
9. Boettinger, W.J.; Coriell, S.R. et al.: Acta Mater. 48 (2000) 43.
10. Marketz, W.T.; Fischer, F.D. et al.: Z. Metallkd. 90 (1999) 588.
11. Juffs, L.; Hughes, A.E. et al.: Micron 32 (2001) 777.
12. Knippscheer, S.; Frommeyer, G.: Adv. Eng. Mater. 1 (1999) 187.
13. Mishin, Y.; Herzig, C.: Acta Mater. 48 (2000) 589.
14. Djanarthany, S.; Viala, J.-C. et al.: Mater. Chem. Phys. 72 (2001) 301.
15. Reddy, R.G.; Yahya, A.M. et al.: J. Alloys Compd. 321 (2001) 223.
16. Cha, P.-R.; Yeon, D.-H. et al.: Acta Mater. 49 (2001) 3295.
17. Mackenbrock, A.; Tacke, K.-H.: Metall. Mater. Trans. B 27 (1996) 871.
18. Ansara, I.; Dinsdale, A.T.; Rand, M.H. (eds.): COST 507, Thermochemical database for light metal alloys, Vol. 2, European Commission (1998).
19. Mackenbrock, A.; Tacke, K.-H.: In: Modelling of Casting, Welding and Advanced Solidification Processes VII, ed. J.C.M. Cross, The Minerals, Metals & Materials Society (1995).
20. Hunt, J.D.: Mater. Sci. Eng. 65 (1984) 75.



Production of Nanostructures from Directionally Solidified Eutectics

A.W. Hassel¹, B. Bello Rodriguez¹, S. Milenkovic², A. Schneider²

¹Department of Interface Chemistry and Surface Engineering, ²Department of Materials Technology

The production of nanostructures is of great interest due to their broad potential for applications in optics, electronics and magnetics. Nanostructures have conventionally been manufactured by lithographic techniques [1], although such an approach only produces wires with a small aspect ratio. The production of **nanowires** has been carried out by template-directed synthesis involving either chemical or electrochemical depositions [2]. Both the template and the grown metal wires are *self organised nano structures* (SONS), which give the advantage of allowing the production of large numbers of similar nano-ordered systems. This is a prerequisite for a cheap and commercially competitive technique. The alternative route for the production of such SONS presented here is based on **directional solidification of eutectics**. Directional solidification has widely been used for the production of high purity single crystals [3]. It was first developed to produce single crystals of semiconductor materials and later applied to Ni based superalloys for high temperature services. In the

1960s and 1970s it was applied to eutectic alloys processing [4-7]. Research was initially focused on materials for high temperature structural applications, but it was soon broadened to non-structural materials for electronic, magnetic, and optical applications [8]. The advantages of producing *in-situ* composites by directional solidification of eutectics are as follows: it allows components to be produced from the melt in a single stage process; there is intrinsic thermodynamic stability and chemical compatibility between the matrix and the reinforcements; and the microstructure can be controlled by adjusting the solidification conditions. Directional solidification of eutectics yields highly ordered structures with lamellar or fibrous morphology depending on the system and the solidification parameters. The essential feature of eutectic solidification is that the two phases with different compositions crystallise simultaneously by the advance of a common interface into the melt at a constant temperature. The structure of the solidified eutectic is usually an intimate well-defined mixture of constituent phases.

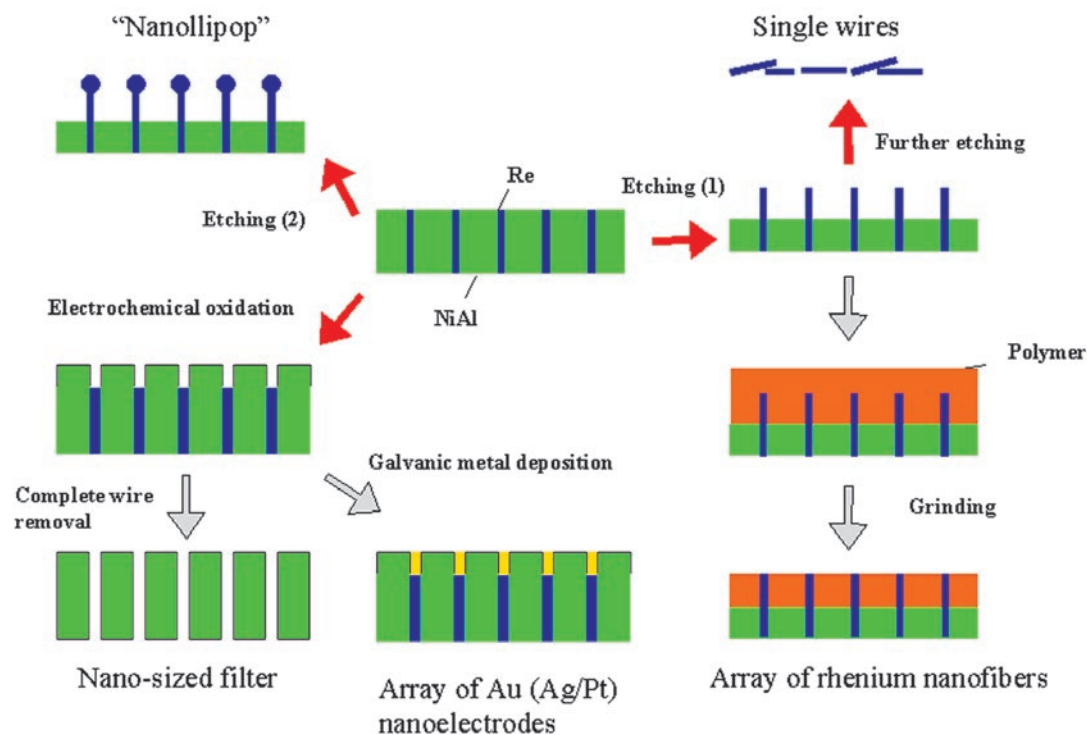


Fig. 1: Roadmap of the different processes employed and materials prepared such as nanowire arrays, nanowires, nanollipops, nanoelectrode arrays, nanopores and nanofilters (red arrows: experimentally realized, white arrows: work in progress).



In metals, where a large number of binary systems has been investigated, an amazing diversity of micromorphologies has been observed [9]. Hunt and Jackson [10] proposed that the eutectic morphology depends mainly on the entropy of fusion of the two phases. If both phases possess low entropy of fusion, the eutectic structure exhibits a regular morphology, which may be of fibrous or lamellar type. In the case of lamellar growth, two phases grow in the form of plates or lamellae, while in fibrous growth one of the phases grows in the form of fibres embedded into a continuous matrix of the other phase. Studies involving the directional solidification technique are numerous and versatile [11]. However, the authors are not aware of any work on using this technique in nanotechnology. In our approach, the idea is to produce fibrous eutectics with very fine and regular structures, in which elements such as rhenium, gold or platinum form the minor eutectic phase. Nanowires of these metals could therefore be obtained from such eutectics after selective etching of the matrix. For this process to occur, the second phase must be poorly soluble in the fibrous phase and show a different chemical behaviour. A nanodisc electrode array can be subsequently prepared by embedding the obtained metallic nanoelectrodes into a polymer and grinding until the wires are exposed (see Fig. 1). Such a material can be a beneficial electrode material e.g. for a sensor, if the distance between two wires is in the range of the diffusion hemisphere.

An alternative approach when using NiAl as a matrix is the electrochemical oxidation of the minor phase to a soluble compound- such as perrhenate in the case of rhenium. The use of neutral acetate buffer (pH = 6.0) results in a passivation of the matrix, wherein the Re phase is dissolved due to its oxidation to perrhenate. The vacancies left behind by the

dissolved rhenium fibres can then be filled with metals such as gold or platinum for the production of complementary nanoelectrodes arrays (Fig. 1). Whether or not the dissolution of the minor phase through the entire sample thickness can be achieved is not proven yet.

Formation of metallic nanowires by selective etching of the eutectic alloy. In order to produce optimal nanowires after etching of the eutectic matrix, fibrous eutectics with fine and regular structures must be considered. As in a large number of Al-Ni-X systems, the pseudobinary NiAl-Re section shows a eutectic reaction with a resulting fibrous morphology, being desired for the proposed approach. An alloy with 1.5 at.% Re was directionally solidified in a Bridgman furnace at the growth rate of 30 mm h^{-1} and temperature gradient of $\sim 40 \text{ K cm}^{-1}$. The resulting microstructure was fully eutectic consisting of a cell structure with a mean cell diameter of $\sim 500 \mu\text{m}$. Within the cells the Re fibres exhibited a mean diameter of 400 to 450 nm, while the mean inter-fibre spacing was 4 to 5 μm .

The selective dissolution of the matrix was achieved after digestion of the sample in a mixture containing HCl:H₂O₂. The concentration of both HCl and H₂O₂ yielded the total oxidation of the matrix, with the rhenium phase remaining in the solid, as confirmed after ICP-OES (inductively coupled plasma optical emission spectrometry) analysis of the treated sample [12]. This digestion procedure produced an anisotropic etching of the matrix, which displayed hexagonal pits located on the same or parallel axis (Fig. 2). However, after the etching not all the fibres exhibited the same shape, depending on their position and therefore, their exposure to the attacking medium. The digestion time was also found to play

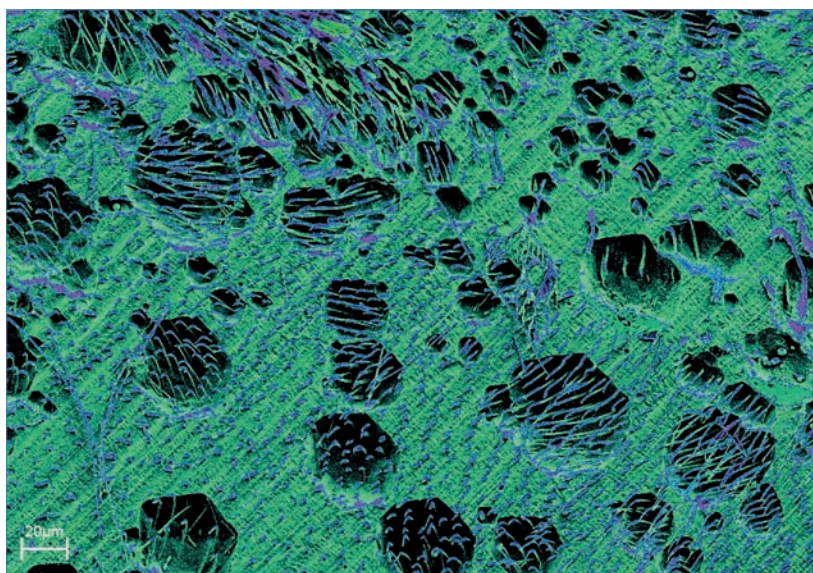


Fig. 2: Anisotropic etching observed for a NiAl-Re etched sample. The anisotropic etching of the single crystalline NiAl matrix (green) yields parallel aligned hexagonal etch-pits.

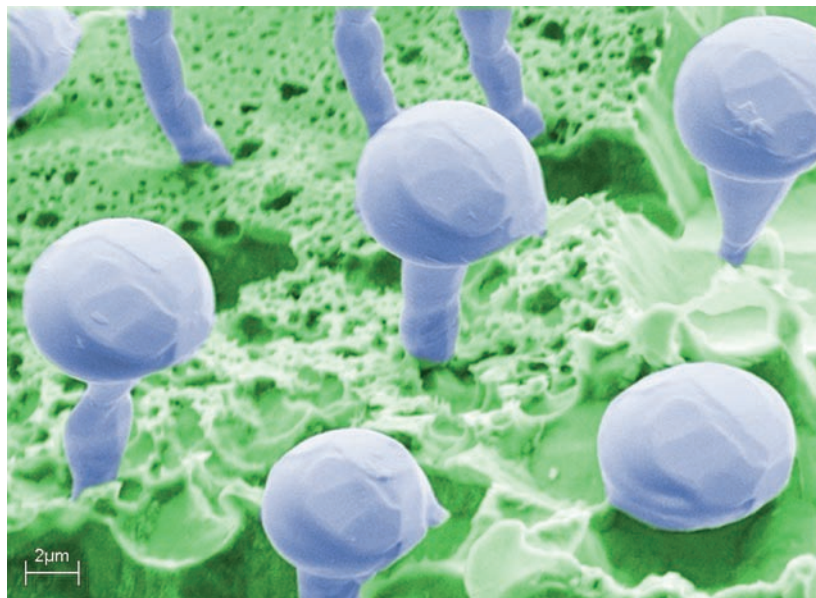
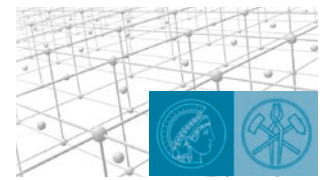


Fig. 3: „Nanollipops“ observed after attack of the NiAl-Re by $HCl:H_2O_2$. The identical habitus (identical facets) of the Re spheres on top of the nanowires prove that the wires are single crystals.

a significant role on the formation of fibres. Nevertheless, a dominant structure was found inside most of the pits originated by the chloride corrosion, which was mainly constituted by short fibres characterised by a prominent head (diameter $\sim 4 \mu m$), resulting in a final structure similar to a nanosize lollipop („nanollipop“, Fig. 3). EDX (energy-dispersive X-ray) analysis of these structures confirmed that they consist of pure rhenium.

All the „nanollipops“ presented identical features – resulting in each „nanollipop“ being a clone-image of either ones on the same plain. This effect suggested that their formation was linked to a sort of reaction that affected each structure at the same

magnitude. The suggested explanation is that the rhenium impurities in the NiAl matrix will be chemically oxidised to perrhenate once they loose galvanic contact to the metal. This leads to a significant local increase of the perrhenate concentration in the cavity which in turn allows a galvanic deposition of rhenium onto the bared Re nanowires. The larger space provided on the surface of the matrix may prevent this effect from happening outside the pits, thus originating mainly long and stretched fibres.

The production of rhenium nanowires via directional solidification also helped to determine their crystallographic nature. In an early work on single-phase materials, Jackson [13] distinguished between

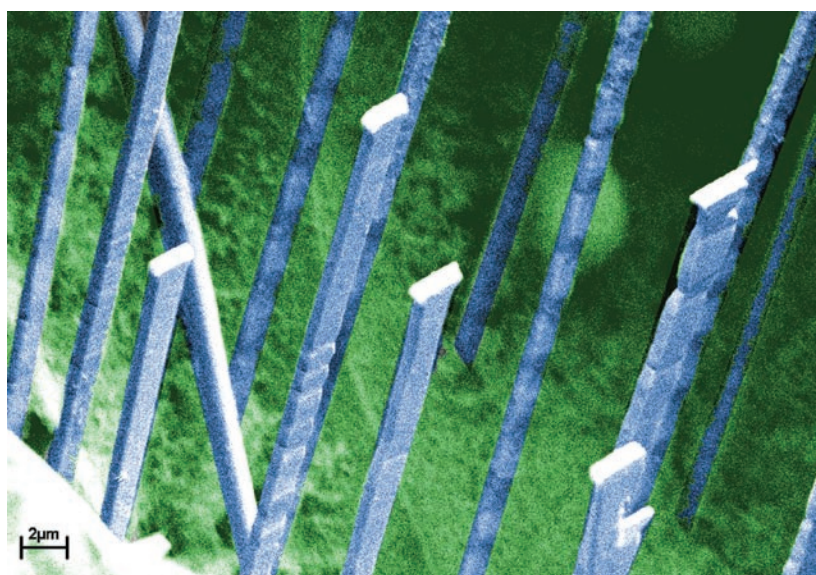


Fig. 4: Re fibres with a rectangular cross section. Re solidifies in a specific crystallographic relationship to the NiAl matrix to minimise the surface energy.

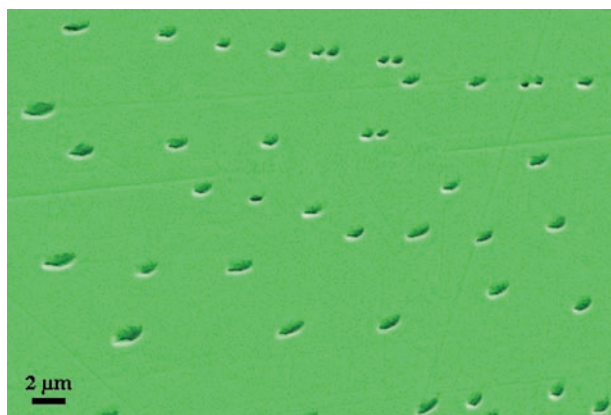


Fig. 5: SEM image of a polished NiAl-Re alloy after electrochemical oxidation at pH = 6.0. The NiAl is passivated (green) and the Re was oxidised and dissolved.

'non-faceted' phases that solidify with complete crystallographic isotropy via an atomically rough solid/liquid interface, and 'faceted' phases that have preferred crystallographic growth directions associated with atomically smooth solid/liquid surface facets. The presence of long fibres with rectangular shape, which are constrained with two perpendicular crystallographic directions (Fig. 4) clearly indicate the faceted nature of the Re phase.

Formation of nanopores by selective etching of the eutectic minor phase. An alternative procedure for the formation of nano-structures from the original NiAl-Re alloy is the selective dissolution of the minor Re phase in neutral acetate buffer. In such a medium, both Ni and Al would form oxides which then passivate the surface of the alloy. The spaces imbedded into the matrix could be filled up with alternative metals such as gold to produce arrays of nanoelectrodes.

The electrochemical behaviour of the NiAl-Re alloy in acetate buffer (pH = 6.0) displayed an anodic current which increased in the 0.5 to 1 V potential range. This increase was attributed to the formation of perrhenate. This assumption was confirmed after analysis of rhenium samples in acetate buffer at the same potential range; thus such analyses also showed maximal anodic current in the 0.5 to 1 V range. The SEM pictures taken after anodisation of the sample showed a relatively smooth surface with a high density of nanopores, possibly due to the dissolution of rhenium (Fig. 5).

According to the Pourbaix diagrams of Ni, Al, and Re in water at the studying pH (6.0) and potential range (-0.3 to 2 V), the aluminium and nickel oxides should be thermodynamically stable or kinetically stabilized, whereas the rhenium would predominantly be present in the form of soluble perrhenate [14]. This is in good agreement with the experimental observations.

Acknowledgements. The financial support of the Deutsche Forschungsgemeinschaft through the project *Production of Nanowire Arrays through Directional Solidification and their Application* within the DFG Priority Program 1165 *Nanowires and Nanotubes - from Controlled Synthesis to Function* is gratefully acknowledged.

References

- Schultze, J.W.; Bressel, A.: *Electrochim. Acta* 47 (2001) 3.
- Tsuji, M.; Hashimoto, M.; Nishizawa, Y.; Tsuji, T.: *Mater. Lett.* 58 (2004) 2326.
- Kurz, W.; Fisher, D.J.: *Fundamentals of Solidification*, Third Edition, Trans Tech Publications, Aedermannsdorf, Switzerland (1992) 305 p.
- Kraft, R.W.: U.S. patent 3,129,952 (1960).
- Cline, H.E.: *Metall. Trans.* 2 (1971) 189.
- Thompson, E.R.; Lemkey, F.D.: *Trans. Am. Soc. Met.* 62 (1969) 140.
- Gigliotti, M.F.X.: U.S. patent 4,292,076 (1981).
- Galasso, F.S.: *J. Met.* 19 (1967) 17.
- Gilgien, P.; Zryd, A.; Kurz, W.: *Acta Mater.*, 43 (1995) 3477.
- Hunt, J.D.; Jackson, K.A.: *Trans. Metall. Soc. AIME* 236 (1966) 843.
- Boettinger, W.J.; Coriell, S.R.; Greer, A.L.; Karma, A.; Kurz, W.; Rappaz, M.; Trivedi, R.: *Acta Mater.* 48 (2000) 43.
- Hassel, A.W.; Bello Rodriguez, B.; Milenkovic, S.; Schneider, A.: *Electrochim. Acta*, *accepted for publication*.
- Jackson, K.A.: in: *Liquid Metals and Solidification*, American Society for Metals, Cleveland, OH, USA (1958) 174.
- Pourbaix, M.: *Atlas of Electrochemical Equilibria in Aqueous Solutions*, Nat. Assoc. Corr. Eng., TX, USA (1974).



Evolution of Near Surface Concentration Profiles of Cr during Annealing of Fe-15Cr Polycrystalline Alloy

E. Park, M. Stratmann, M. Spiegel

Department of Interface Chemistry and Surface Engineering

Iron-chromium steels are of great importance for process industries and power plants. It is known that the passive oxide films on Fe-Cr alloys are composed of trivalent chromium oxide [1-5]. Because the surface oxide composition in the beginning of oxidation is dependent on the metal composition in the surface, the modification of the surface of Fe-Cr alloys to contain more Cr than in the bulk is advantageous for the formation of passive Cr-rich oxide film. This study investigated the surface chemistry of Fe-15 at.% Cr polycrystalline alloy after short-term heat treatments at 800 °C, the conventional heat treatment temperature for Fe-Cr alloys and stainless steels.

Experimental. The Fe-15 at.% Cr alloy was manufactured in the workshop of the MPIE. Experiments were carried out using a horizontal infrared-heating furnace with varied atmospheres. The composition of inlet gas was adjusted by mass flow controllers. The moisture was feeded using an oxal-acid-filled saturator and monitored by Moisture Analyzer. The oxygen partial pressure of the outlet gas was measured using a fuel-cell-sensor oxygen analyzer. The hydrogen and the nitrogen were ultra-high purity grade, and atmospheric air was used for

oxidation experiments. For all experiments, the dew point of the inlet gas mixture was -70.0 °C ($p_{H_2O} = 2.6$ vol. ppm).

Heat treatments in air – oxidation. The morphology of the surfaces of samples oxidized for different times at 800 °C in air is presented in Figs. 1 (a) to (f). The images were taken from the center of the grains. At first, the formation of round-shaped nuclei with diameter less than 100 nm was observed. The nuclei covered the surface within 30 seconds of oxidation. With increasing time, the nuclei grew and changed to polygonal grains. On the surface of O-90, the nucleation of a secondary oxide was observed. The secondary oxide nucleated between/on the former oxide grains and grew on their surface. It seemed that the newly formed nuclei grew or dissolved into the matrix oxide very quickly. Further oxidation resulted in the homogeneous layer composed of oxide grains with the size of 200 nm. The further change in the morphology with increase in the oxidation time was negligible. Figs. 2 (a) to (d) present the elemental compositions of the outer 100 nm of the surface layers of the samples, as obtained by XPS. The carbon on the initial surface disappeared, probably as CO₂ and CO during heating. The sur-

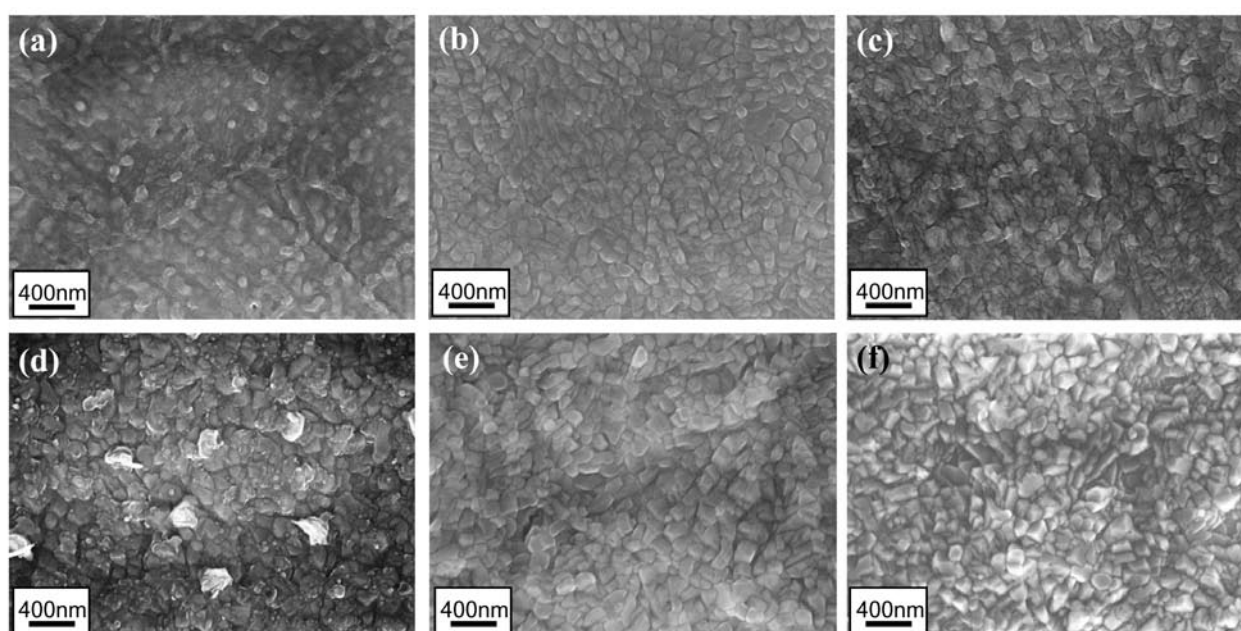


Fig. 1: Surface morphology of the samples oxidized for different times (sec.) in air. (a) O-0, (b) O-30, (c) O-60, (d) O-90, (e) O-120 and (f) O-300.

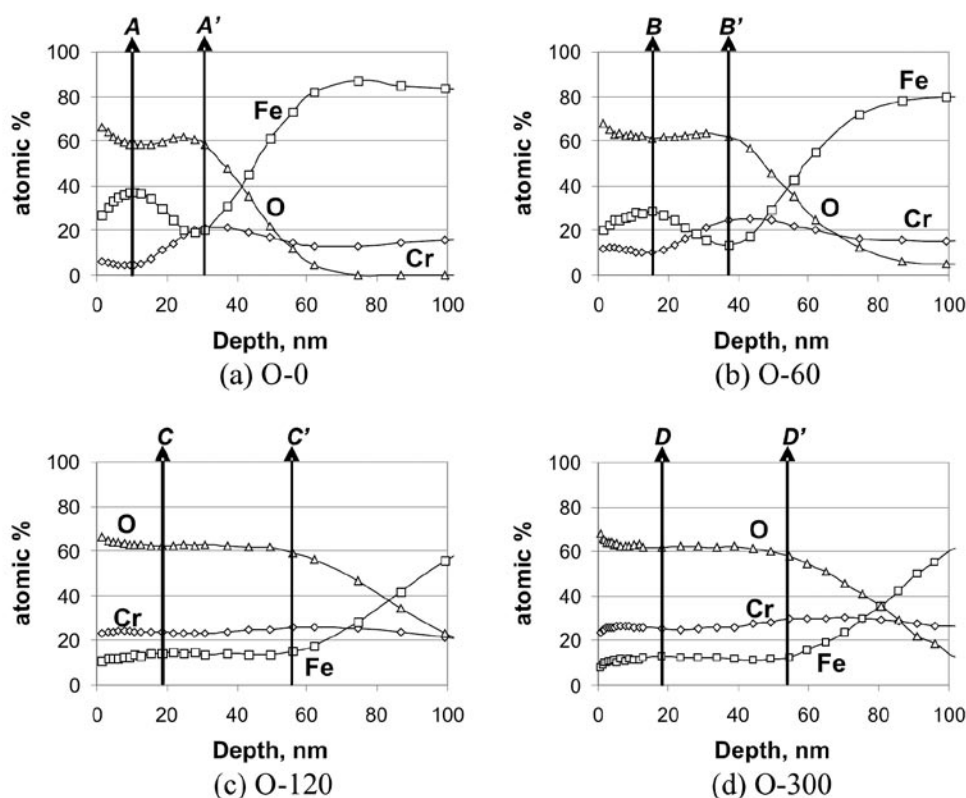


Fig. 2: Elemental depth profiles of the oxidized samples.

faces of the samples only contained Fe-Cr oxides. The oxidation started with the formation of a Fe-rich mixed oxide layer, representing the initial surface composition. The well-known duplex oxide layer outer Fe-rich oxide (*B*) and inner Cr-rich oxide (*B'*), formed in 60 seconds of oxidation. The duplex oxide layer transformed to Cr-rich mono-phase ((Fe,Cr)₂O₃) layer with increasing time. The transformation occurred by the enrichment of Cr in the former Fe-rich oxide layer and the nucleation/growth of the Cr-rich secondary oxide layer, as observed in the morphology (Fig. 1 (d)). In the period of *t* = 120 to 300 s, the Cr content in the mono-phase layer increased with time, while the changes in the thickness (Fig. 2 (c) and (d)) and the morphology (Figs. 1 (e) and (f)) were little. It implies that in the period *t* = 120 to 300 s Cr diffusing to the surface was consumed to reach an equilibrium phase composition in the oxide lattice without further nucleation and growth. The oxide in the interface of each sample, where the oxygen content starts to decrease (points *A'*, *B'*, *C'* and *D'*), was composed of Fe²⁺ and Cr³⁺. In the case of the sample O-60, the oxide composition in the interface (*B'*) represented the stoichiometric Cr-Fe spinel ratio, Cr:Fe = 2:1 for FeO·Cr₂O₃. The phase of the interface oxide should be spinel; however, it seemed to be with non-layer structure or in a metastable state only resulted from the decrease in the oxygen partial pressure with the increase in the depth, because it allowed Cr to diffuse through to the interface from the bulk.

In the experimental range, the transformation during the oxidation of the polished Fe-15 at.% Cr alloy at 800 °C is schematically summarized by Fig. 3. The block arrows represent the diffusion of Cr. In the beginning of oxidation, the reaction is controlled by the surface/interface diffusion of cations resulting in the formation of the Fe-rich oxide layer and the Cr-depletion zone as observed in the samples O-0 and O-60. With the increase in oxidation time, the former Fe-rich oxide is enriched with Cr and converted into the Cr-rich oxide mono-phase layer. The transformation combines the new nucleation observed in the sample O-90. It is noted that the enrichment of Cr in the surface oxide layer started when the surface was completely covered with the nuclei formed in the beginning (*t* > 30 sec.). It has been known that the formation of the nuclei on the surface causes the decrease in the oxygen partial pressure at the oxide/metal interface, resulting in the selective oxidation of Cr, and further the formation of Cr-rich oxide layer on the surface [1,2].

Heat treatments in N₂-H₂ gas mixtures – annealing. The effects of H₂ in the heat treatment atmosphere were examined by annealing samples in N₂-*x* vol.% H₂ (*A*-1 to *A*-4, *x* = 0, 1, 5 and 10, respectively) for 60 seconds at 800 °C. In thermodynamics, the phases evaluated from Fe-Cr-O system at 800 °C depend on the oxygen partial pressure and the Cr content. In application, the enrichment of Cr on the surface (i.e., Cr/Fe ratio

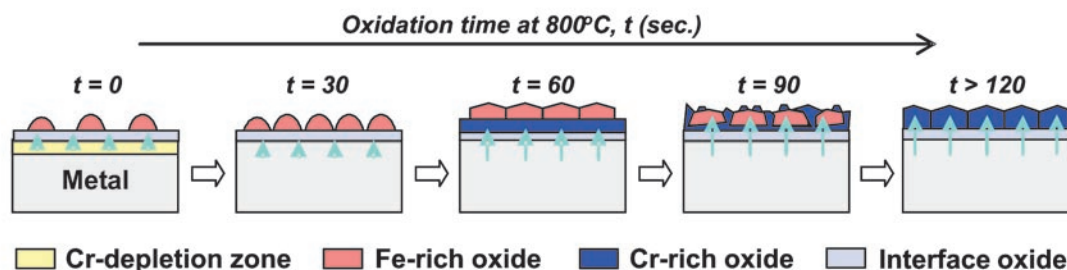


Fig. 3: Schematic model of the oxidation of the polished Fe-15at.%Cr alloy surface.

higher than 2.0) enlarges the Cr-rich corundum zone up to $p(O_2)$ as low as about 10^{-23} . It should be noted that the selective oxidation of Cr occurs when $p(O_2)$ is in the range between 10^{-27} and 10^{-18} at 800°C [6]. The equilibrium phase composition of each annealing atmosphere based on the oxygen partial pressure is $(\text{Fe,Cr})_2\text{O}_3$ and bcc-metal + Cr_2O_3 . The surface morphology of the samples after annealing is presented in Fig. 4. Although the characterization of each particle on the surfaces was not possible due to its fine size and the instrumental limitation, the increase in H_2 content in the atmosphere obviously decreased the size and the population density of oxide nuclei on the surface. The elemental depth analyses showed that carbon in the bulk segregated on the surface in case of the annealing in only N_2 , while decarburization occurred in the samples annealed in H_2 -containing atmospheres. A small amount of nitrogen was detected on top (10 nm)

surface of all samples. The peak position of N 1s in each sample shifted to the position of nitride, 398.5 ± 0.5 eV, implying the formation of Cr-nitride or Cr-N surface compound [7], however, there was little distinguishable differences in the nitride formation between samples annealed in different atmospheres. The top surface of the samples annealed in H_2 -containing atmospheres, A-2 to A-4, showed Cr^{3+} , Fe^{2+} and metallic Fe (no Fe^{3+}), resulting from the reduction of Fe^{n+} by hydrogen on the surface. The oxygen was in the form of O^{2-} throughout the whole analyzed depth.

The Cr_{total} to Fe_{total} atomic ratio and the oxygen content through the surface of each sample in logarithmic scale are presented in Figs. 5 (a) and (b). In all atmospheres, the annealing increased the Cr/Fe ratio due to the effects of heating and the co-segregation of Cr and N as expected from UHV

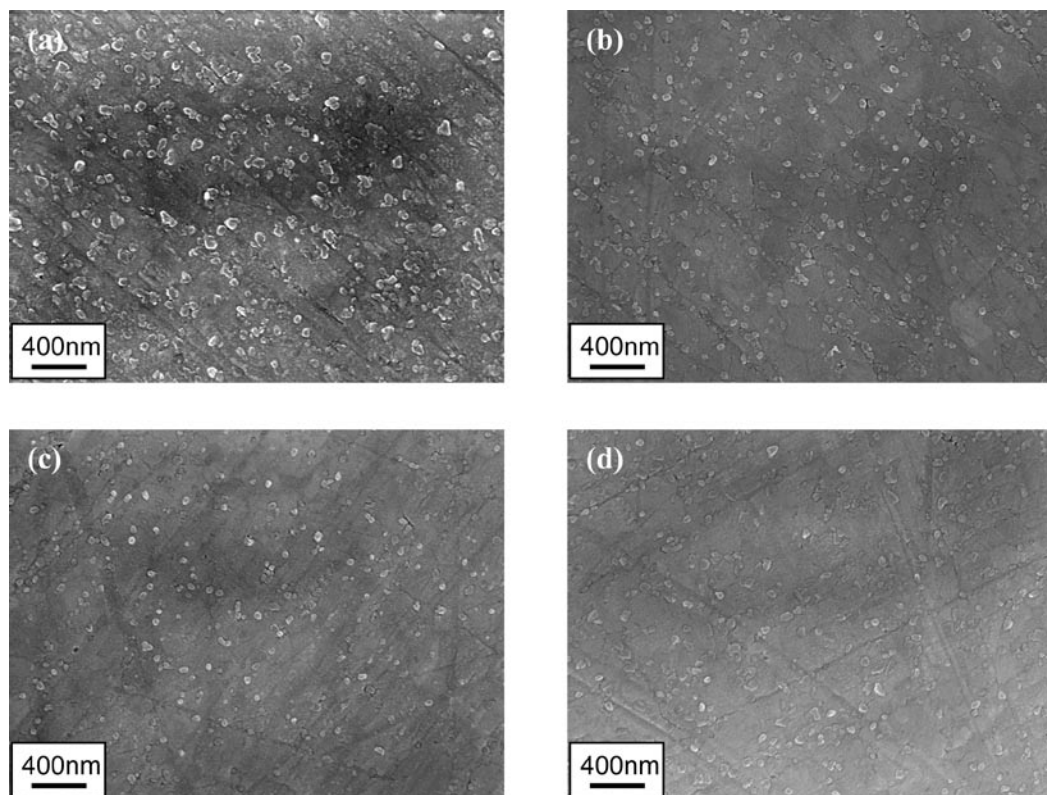


Fig. 4: Surface morphology of the samples annealed in different atmospheres. (a) A-1, in N_2 , (b) A-2, in N_2 -1% H_2 , (c) A-3, in N_2 -5% H_2 and (d) A-4, in N_2 -10% H_2 .

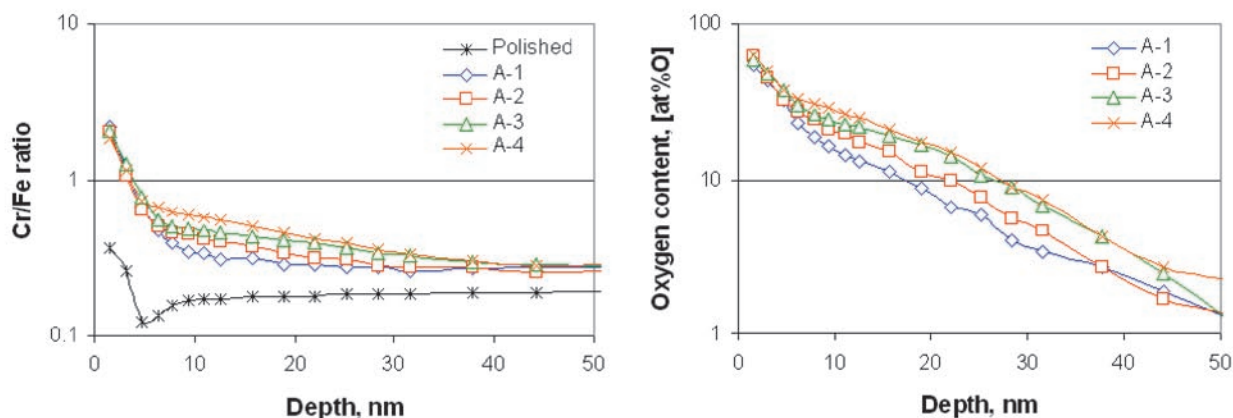


Fig. 5: Depth profiles of the annealed samples. (a) Cr_{total}/Fe_{total} ratio, (b) Oxygen.

studies in literature [7-13]. The addition and the increase in H_2 to the atmosphere further increased the Cr content of the sub-surface. The oxygen content also increased with the increase in the H_2 content in the atmosphere, which is in accordance with the Cr/Fe ratio. It is likely that the selective oxidation of Cr depends only on the Cr content, rather than oxygen partial pressure. (If there is enough oxygen to oxidize Cr, the transfer rate of oxygen is limited by the amount of Cr.)

The surface morphology of the samples (Fig. 4) and the elemental profiles (Fig. 5) suggest that the selective oxidation might have occurred as internal Cr_2O_3 formation with scattered nuclei of oxides on the surface, which is supported by the theoretical conditions for the internal oxidation i) the chemical affinity of oxygen for Cr is higher than that for Fe, ii) there is no passive oxide layer and iii) oxygen has higher permeability ($c_o D_o$) than that of Cr ($c_{Cr} D_{Cr}$) in bcc Fe-Cr alloy, i.e. $c_o D_o = 4 \times 10^{-11} \text{ cm}^2/\text{sec}$ (in bcc-iron at 800 °C [14,15]) and $c_{Cr} D_{Cr} = 4 \times 10^{-12} \text{ cm}^2/\text{sec}$ (in Fe-16Cr at 800 °C [16]).

This phenomenon that Cr diffusion is enhanced in the presence of hydrogen, can be explained by thermodynamics. Hydrogen in the experimental condition plays the following roles on the surface: i) decarburization under dissolution of Cr-carbides, especially of grain boundaries and ii) reduction of Fe oxides. While segregation of carbon was detected through the whole analyzed depth in the sample annealed in N_2 , the samples annealed in H_2 -containing atmosphere did not contain carbon except on the top surface ($z < 2 \text{ nm}$). In addition, iii) desulfurization on the surface is also expected, but could not be observed since the detection of sulfur was beyond the limitation of XPS analyses in this *ex-situ* experiment. These 'surface-clean-up' effects activate fast diffusion paths in the surface and near-surface, stimulating the outward diffusion of Cr to the surface for the segregation and further to the enrichment of Cr, and simultaneously, the inward

diffusion of oxygen through the surface resulting in the internal oxidation.

References

1. Kofstad, P.: High Temperature Corrosion, Elsevier, NY (1988).
2. Chattopadhyay, B.; Wood, G.C.: Oxid. Met. 2 (1970) 373.
3. Mathieu, H.J.; Landolt, D.: Corros. Sci. 26 (1986) 547.
4. Olsson, C.-O.A.; Landolt, D.: Electrochim. Acta 48 (2003) 1093.
5. McCafferty, E.: Corros. Sci. 42 (2000) 1993.
6. Turkdogan, E.T.: Physical Chemistry of High Temperature Technology, Academic Press, NY (1980).
7. Grabke, H.J.; Leroy, V.; Viehhaus, H.: ISIJ Int. 35 (1995) 95.
8. Abraham, F.F.; Brundle, C.R.: J. Vac. Sci. Technol. 18 (1981) 506.
9. Leygraf, C.; Hultquist, G.; Ekelund, S.: Surf. Sci. 46 (1974) 157.
10. Grabke, H.J.; Dennert, R.; Wagemann, B.: Oxid. Met. 47 (1997) 495.
11. Clauberg, E.; Uebing, C.; Grabke, H.J.: Surf. Sci. 433-435 (1999) 617.
12. Grabke, H.J.; Paulitschke, W.; Tauber, G.; Viehhaus, H.: Surf. Sci. 63 (1977) 377.
13. Suzuki, S.; Nakazawa, T.; Waseda, Y.: ISIJ Int. 36 (1996) 1273.
14. Swisher, J.H.; Turkdogan, E.T.: Trans. AIME 239 (1967) 426.
15. Bogdandy, L.; Engell, H.J.: The Reduction of Iron Ores, Verlag Stahleisen m.b.H. Düsseldorf (1970).
16. Bowen, A.W.; Leak, G.M.: Metall. Trans. 1 (1970) 2767.



Simulation Study on the Influence of Texture on Earing in Steel using the Texture Component Crystal Plasticity FEM

D. Raabe, F. Roters

Department of Microstructure Physics and Metal Forming

The shape anisotropy of cup drawn metallic parts is referred to as earing [1-10]. It is a characteristic phenomenon associated with the crystallographic texture and the resulting elastic-plastic anisotropy of metals. Sheet steels usually have pronounced textures which they inherit from the preceding processing steps such as hot rolling, cold rolling, and heat treatment. This short article reports about a set of studies on the direct application of crystal plasticity FE theory to the problem of large scale anisotropy prediction under consideration of the inherited material microstructure. For rendering the crystal plasticity finite element models more flexible with respect to the treatment of large polycrystalline entities Raabe and Roters recently introduced a texture component crystal plasticity finite element model [8,11,12]. The basic idea of this method consists in using a more effective way of describing the texture of macroscopic samples at each integration point, turning the FE-method into a texture component crystal plasticity finite element method.

The main challenge of integrating constitutive polycrystal plasticity laws into finite element approaches lies in identifying an efficient way of mapping a crystallographic texture which represents a *large* number of grains on the integration points of a finite element mesh. Such an approach must be formulated in a manner that still permits *texture update* in the course of the forming simulation. It is an important condition in that context that crystal plasticity finite element models require a *discrete* representation of the orientation distribution function at each integration point. For relatively small numbers of grains (less than 10^3 crystals) the discrete mapping of the texture on the mesh can be achieved by a one-to-one approach, where each Gauss point in the finite element grid is characterized by one crystallographic orientation. This method, however, is not suitable when meshing specimens which contain a much large number of grains such as in a typical steel sheet which is subjected to large scale metal forming operations.

The texture component finite element method is a novel approach in the context described above. It is a technique of approximating an initial orientation distribution function in the form of discrete sets of symmetrical spherical model functions and in

mapping these components on a finite element mesh. Model functions for textures have individual height and individual full width at half maximum as a measure for the strength and scatter of the texture component they represent. In the formulation used for this study they have the form of central functions, i.e. their scatter is isotropic in orientation space. The main task of this new concept is to represent sets of spherical Gaussian texture components on the integration points of a finite element mesh for a crystal plasticity simulation. This procedure works in two steps. First, the discrete preferred orientation g^c (centre orientation) is extracted from each of the

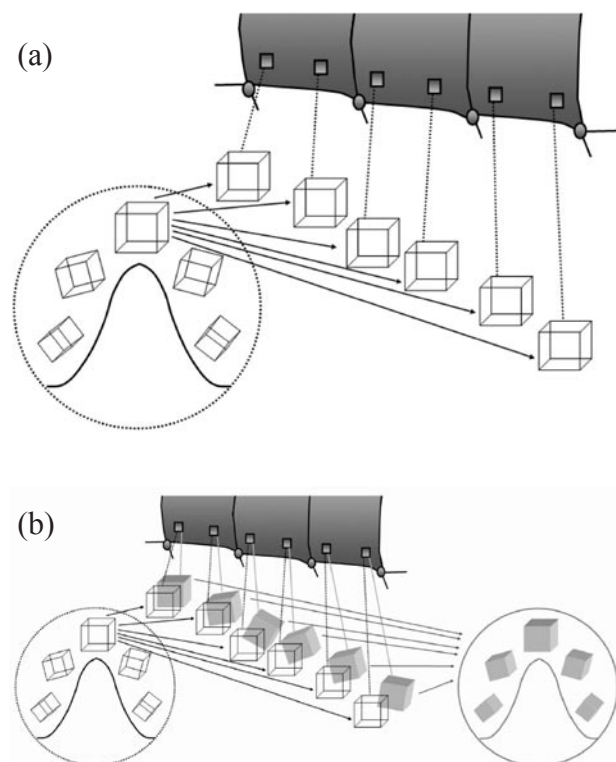


Fig. 1: Schematic presentation of the two steps required for mapping a texture component on the integration points. (a) In the first step the preferred orientation g^c (centre orientation) of each texture component is determined and assigned onto each integration point. (b) In the second step the orientations are re-oriented in such a way that their distribution reproduces the texture function which was originally prescribed in the form of a Gaussian texture component.

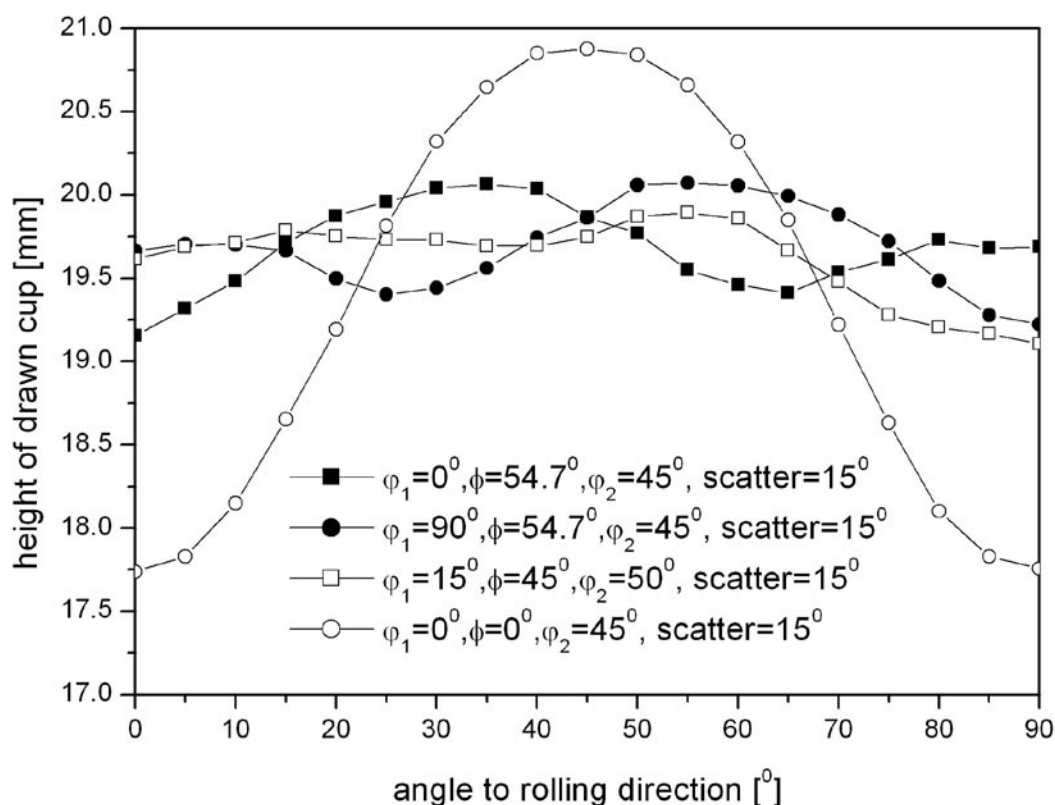


Fig. 2: Ear profiles of individual texture components with a scatter width of 15°.

texture components and assigned in terms of its respective Euler triple $(\varphi_1, \phi, \varphi_2)$, i.e. in the form of a *single* rotation matrix, onto *each* integration point. This step corresponds to the creation of a perfect single crystal. In the second step, these discrete orientations are re-oriented in such a fashion that their resulting overall distribution reproduces the texture function which was originally prescribed in the form of a Gaussian texture component. In other words the orientation scatter described initially by a texture component function is in the finite element mesh represented by a systematically re-oriented set of orientations, each assigned to one integration point, which reproduces the original spherical scatter prescribed by that component (Fig. 1).

This means that the scatter which was originally only given in orientation space is now represented by a distribution both, in real space and in orientation space, i.e. the initial spherical distribution is transformed into a spherical *and* lateral distribution. The described allocation and re-orientation procedure is formulated as a weighted sampling Monte Carlo integration scheme in Euler space. It is important that the use of the Taylor assumption locally allows one to map more than one preferred crystallographic orientation on each integration point and to assign to each of them an individual volume fraction. After decomposing and representing the initial texture components as a lateral and spherical single orien-

tation distribution in the mesh, the texture component concept is no longer required in the further procedure. This is due to the fact that during the subsequent crystal plasticity finite element simulation each individual orientation originally pertaining to one of the texture components can undergo an *individual* orientation change as in the conventional crystal plasticity methods. This means that the texture component method loses its significance during the simulation. In order to avoid confusion one should, therefore, underline that the texture component method is used to *feed* textures into finite element simulations on a strict physical and quantitative basis. The components as such, however, are in their original form as compact functions not tracked during the simulation. It must also be noted that the orientation points which were originally obtained from the components do not represent individual *grains* but portions of an orientation distribution function.

The finite element calculations were conducted by using MSC/Marc in conjunction with its user defined subroutine. An implicit crystal plasticity procedure was implemented and used for the time integration of the constitutive equations. Hardening of the ferritic low carbon body-centred-cubic steel was described in terms of a set of adjustable parameters, i.e. $\dot{\gamma}_0 = 0.001 \text{ s}^{-1}$ was used as reference value for the slip rate. The strain rate sensitivity parameter m was

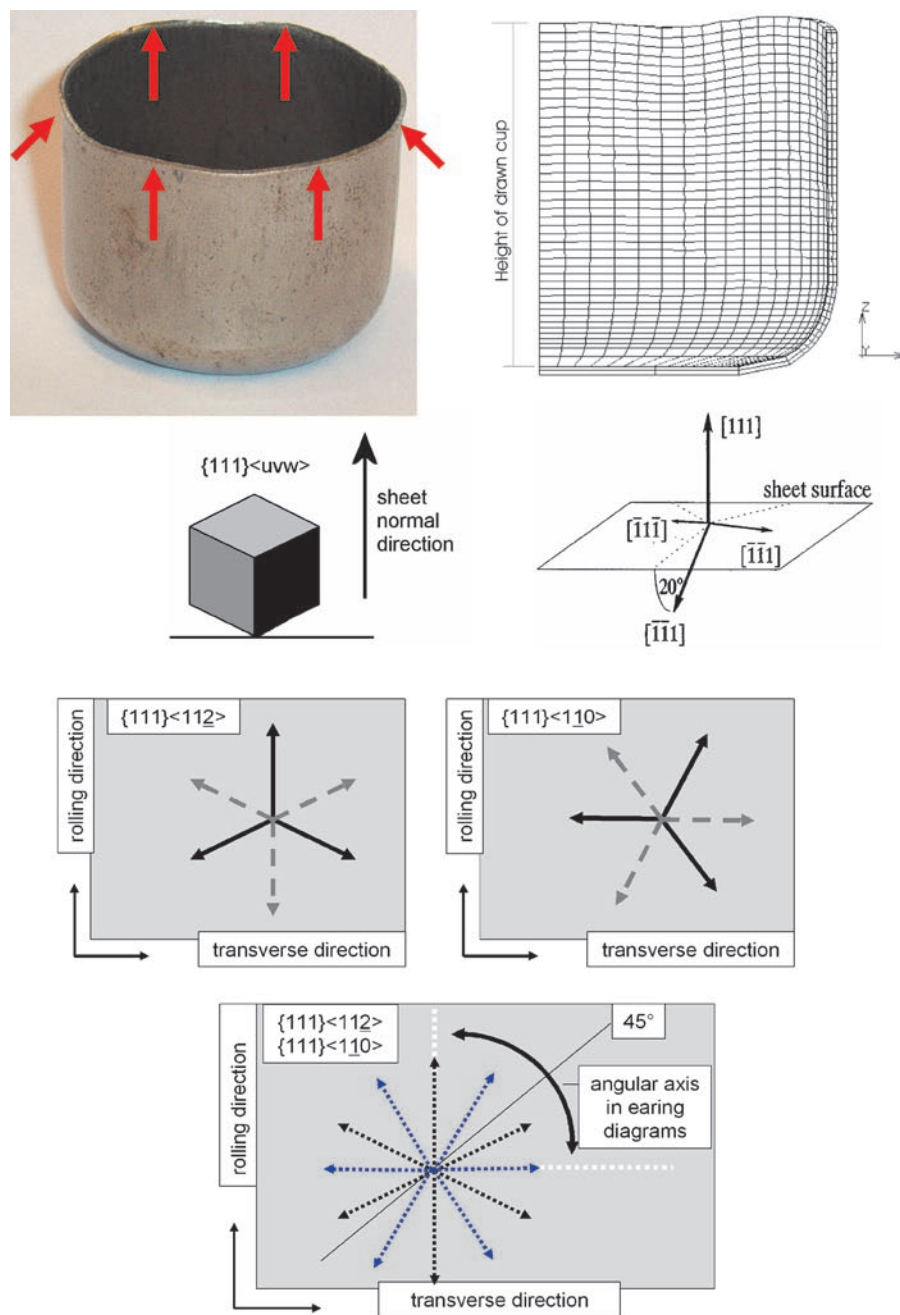


Fig. 3: Presentation of some important anisotropy and symmetry effects such as the projected $\langle 111 \rangle$ slip directions which are relevant for earing and cup drawing of body centred cubic steels. The figure also reveals that classical quadratic yield surface functions can not describe the shape anisotropy of steels since their typically strong $\{111\}$ textures entail a 6-ear drawing profile.

taken as 0.05. As hardening matrix parameters we used $q^{cp} = 1.0$ for coplanar slip systems and $q^{cp} = 1.4$ for non-coplanar systems. The components of the elasticity tensor (pure single crystalline Fe) were taken as $C_{11} = 230.1$ GPa, $C_{12} = 134.6$ GPa, and $C_{44} = 116.6$ GPa. The values of the slip system hardening parameters h_0 , a , and s_s , and the initial value of the slip resistance s_0 were taken to be $h_0 = 180$ MPa, $s_s = 148$ MPa, $a = 2.25$, and $s_0 = 16$ MPa.

The potential slip system families are the 12 $\{111\}\langle 111 \rangle$ and the 12 $\{112\}\langle 111 \rangle$ systems, Figs. 2-3.

References

1. Kocks, U.F.; Tóme, C.N.; Wenk, H.R.: Texture and Anisotropy - Preferred Orientations in Polycrystals and Their Effect on Material Properties, Cambridge University Press (1998).



2. Aretz, H.; Luce, R.; Wolske, M.; Kopp, R.; Goerdeler, M.; Marx, V.; Pomana, G.; Gottstein G.: *Model. Simul. Mater. Sci. Eng.* 8 (2000) 881.
3. Peeters, B.; Hoferlin, E.; Van Houtte, P.; Aernoudt, E.: *Int. J. Plasticity* 17 (2001) 819.
4. Van Bael A.; Von Houtte P.; Aernoudt E.; Hall F.R.; Pillinger I.; Hartley P.; Sturgess, C.E.N.: *Textures Microstruct.* 14-18 (1991) 1007.
5. Van Houtte, P.; Van Bael, A.; Winters, J.; Aernoudt, E.; Hall, F.R.; Wang, N.; Pillinger, I.; Hartley, P.; Sturgess, C.E.N.: *Proc. 13th RISO Int. Symp. Metall. Mater. Sci.: Modeling of Plastic Deformation and its Engineering Applications*, eds. S.I. Andersen, J.B. Bilde-Sorensen, N. Hansen, D. Jul Jensen, T. Leffers, H. Liholt, T. Lorentzen, O.B. Pedersen, B. Ralph, Riso Nat. Lab., Roskilde, Denmark (1992) 161.
6. Li, S.; Hoferlin, E.; Van Bael, A.; Van Houtte, P.: *Adv. Eng. Mater.* 3 (2001) 990.
7. Li, S.; Hoferlin, E.; Van Bael, A.; Van Houtte, P.; Teodosiu, C.: *Int. J. Plasticity* 19 (2003) 647.
8. Raabe, D.; Klose, P.; Engl, B.; Imlau, K.P.; Friedel, F.; Roters, F.: *Adv. Eng. Mater.* 4 (2002) 169.
9. Beckers, B.; Pomana, G.; Gottstein, G.: in: *Proc. Conf. on Constitutive and Damage Modeling of Inelastic Deformation and Phase Transformations*, ed. A.S. Khan, Neat Press, Fulton, MD (1998) 305.
10. Li, S.; Zhang, Y.; Gottstein, G.: *ISIJ Int.* 39 (1999) 501.
11. Raabe, D.; Roters, F.: *Int. J. Plasticity* 20 (2004) 339.
12. Raabe, D.; Zhao, Z.; Roters, F.: *Scr. Mater.* 50 (2004)1085.



On the Mechanism of Mechanical Mixing and Deformation-Induced Amorphization in Heavily Drawn Cu-Nb-Ag *in situ* Composite Wires

D. Raabe¹, A. Schneider², K. Hono*

¹Department of Microstructure Physics and Metal Forming, ²Department of Materials Technology (*NIMS, Tsukuba, Japan)

Binary and ternary metal matrix composites (MMC) consisting of Cu as matrix and a high melting bcc transition metal such as Nb or a fcc material such as Ag as a second and third phase, respectively, have attracted much attention. This is mainly due to two reasons: First, they are promising materials for robotics and high field magnet design [1-13] since after heavy deformation very high strength combined with good electrical conductivity can be achieved. Second, they serve as model composites for the investigation of fundamental mechanisms that determine the observed relations between microstructure and mechanical and electrical properties. For instance, in the field of mechanics, the Hall Petch type interaction of lattice dislocations with interfaces and the generation of geometrically necessary dislocations are considered as important mechanisms for the explanation of the enormous strength observed. In the field of electronics, the interaction mechanisms of conduction electrons and Cooper-pairs (in Nb) with the interfaces are assumed to mainly determine the resistive conductivity and the superconductivity of the bulk material.

In the last decades particular emphasis was placed on the investigation of binary Cu-Nb and Cu-Ag alloys. In the first case (Cu-Nb) the two constituents have negligible mutual solubility and form a quasi monotectic system. During casting the Nb solidifies with dendritic morphology (Fig. 1). Upon wire drawing the dendrites form into fibres the spacing of which continuously drops with increasing strain. Alloys consisting of Cu and 20% Nb reveal an ultimate tensile strength (UTS) of up to 2.2 GPa ($\eta = 12$). In the second case (Cu-Ag) the two constituents reveal a single immiscibility gap, leading to the formation of a simple eutectic equilibrium phase diagram with limited mutual solubility. Previous investigations on a Cu alloy containing more than 6% Ag have shown that this MMC consists of two phases, a Cu-rich solid solution and a Cu-Ag eutectic. During deformation the eutectic and the Cu-rich matrix form into lamellar filaments where the inter-lamellar spacing decreases with wire strain. An intermediate heat treatment leads to Ag precipitations. These can be used to increase the matrix strain and/or to form additional fibres during further drawing. After large wire strains

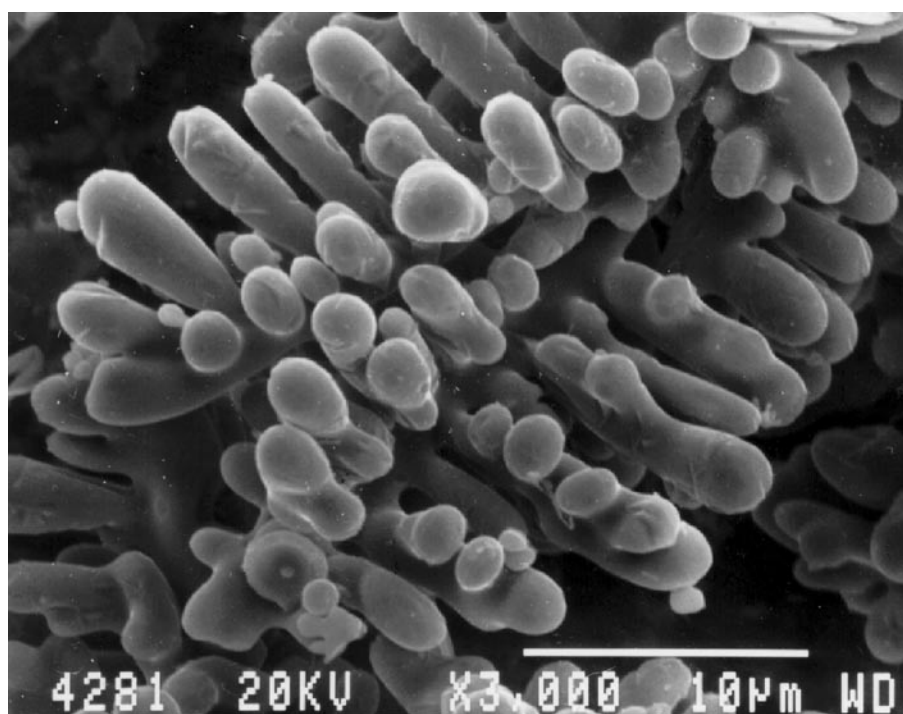


Fig. 1: Primary Nb dendrite in the as-cast state.

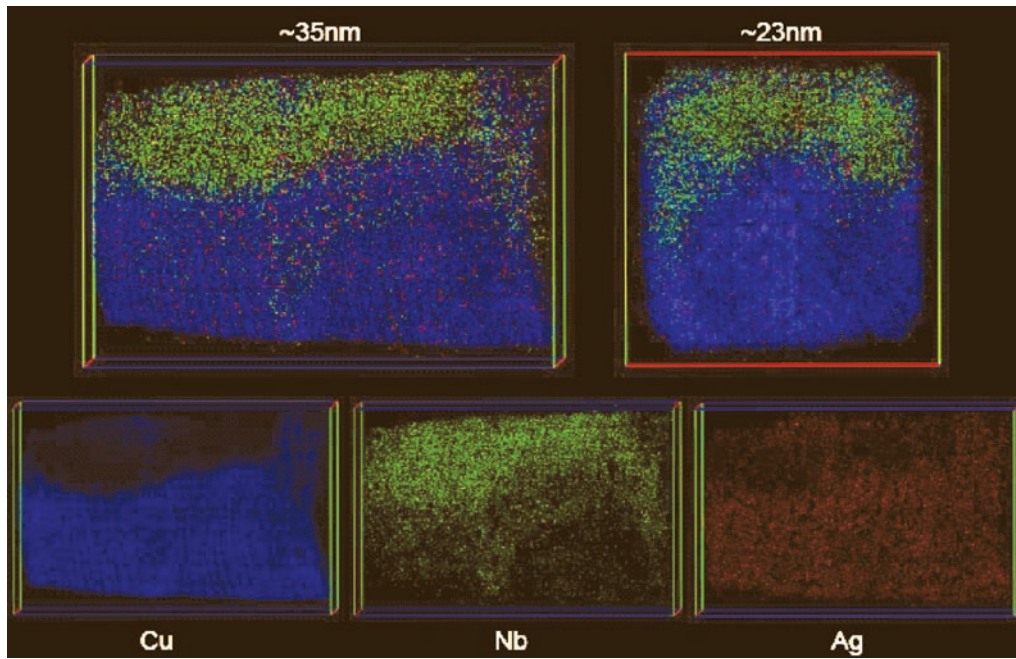


Fig. 2: Unpublished data (Hono, Raabe) obtained by 3D atom probe measurements on the elemental distribution of Nb, Ag, and Cu in a heavily wire drawn Cu-8.2%Ag-4%Nb alloy close to a Cu-Nb interface.

Cu-Ag MMCs reveal an UTS of up to $\sigma = 1.5$ GPa ($\eta = 10$).

As a logical consequence of these efforts on binary MMCs a new generation of ternary Cu-Ag-Nb composites was recently introduced [11-13] with the aim to combine the hardening effects of all three phases and the interfaces between them, and at the same time simplify the melting and forming process. The Cu-8.2% Ag-4% Nb alloy which is discussed in this article was melted in an induction furnace at a

frequency of 10 kHz and a power of 50 kW. All ingredients had an initial purity of at least 99.99%. Ingots of 18 mm diameter were cast under an Argon atmosphere at a pressure of $0.6 \cdot 10^5$ Pa. Since no experimental ternary phase diagram of Cu-Ag-Nb has been published, the binary phase diagrams of Cu-Nb and Cu-Ag had to be taken into account. According to the Cu-Nb system a melting temperature of at least 1500 °C is recommended for a Cu alloy with 4% Nb. However, due to the possibility

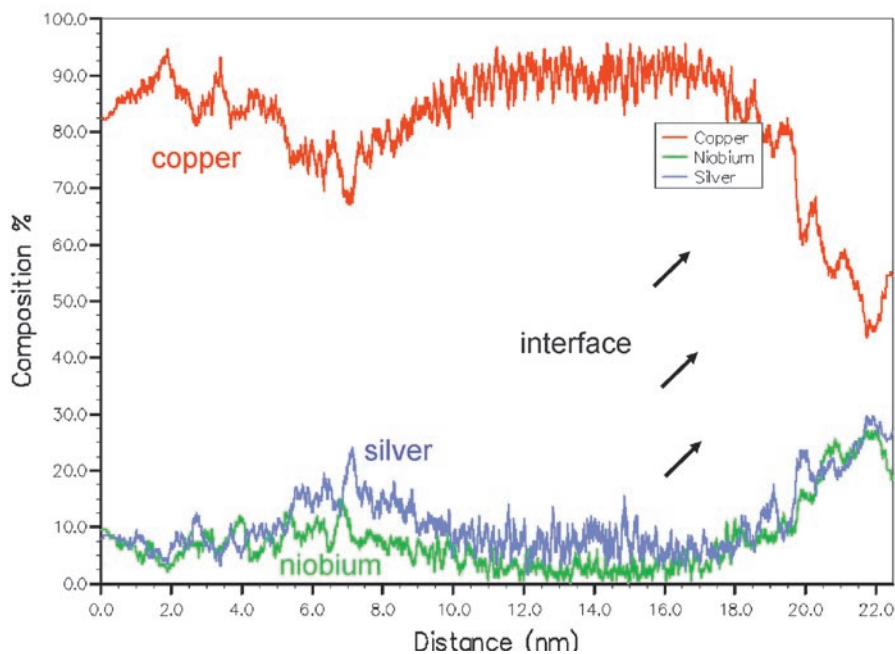


Fig. 3: Unpublished data (Schneider, Raabe) obtained by 3D atom probe line scan measurements on the elemental distribution of Nb, Ag, and Cu in a heavily wire drawn Cu-8.2% Ag-4% Nb alloy across an interface between the Cu matrix and the Nb fibre.

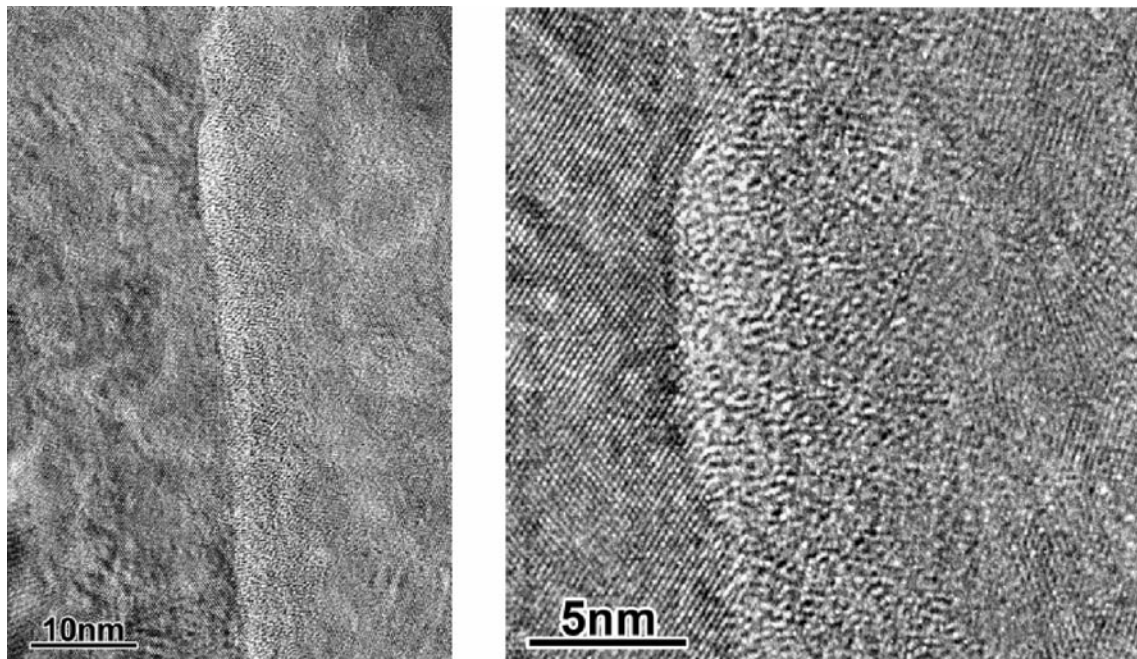


Fig. 4: Observation of solid state amorphization by large strain wire deformation (unpublished data by Hono, Raabe).

of a miscibility gap in the liquid phase due to the presence of foreign interstitials, a peak temperature of 1830-1850 °C was employed in order to assure complete dissolution of the Nb. For the cast, a crucible of high purity graphite and a preheated Cu mould were used. From the cylindrical ingots wires were produced by rotary swaging and subsequent drawing through hard metal drawing bench dies without intermediate annealing. The final diameter was 0.1 mm corresponding to a true strain of $\eta = 10.5$. Further processing details are reported elsewhere [11-13].

This article reports some of our recent ongoing work on a heavily wire drawn ternary Cu-8.2% Ag-4% Nb alloy placing particular attention on the investigation of two important aspects which are still unresolved. The first one is the mechanism of mutual chemical mixing among the different phases far beyond the values assumed by equilibrium thermodynamics. This effect leads to large non-equilibrium concentrations of foreign atoms in the respective other phases (Figs. 2,3). The second one is the partial loss of the crystalline structure (deformation-driven amorphization) observed after heavy wire drawing (Fig. 4) [14,15].

The changes in the mutual solubility are investigated via 3D atom probe measurements which were conducted at NIMS and at the University of Oxford. The structural observations were made by TEM at NIMS.

The data reveal that the deformation-induced chemical intermixing between the neighbouring phases exceeds the expected values by an order of magnitude.

We interpret the chemical intermixing in terms of a crawler-type mechanisms which is based on lattice dislocations which penetrate the interface between the Cu and the Nb (Fig. 5). This effect includes the assumption that lattice dislocations of the Cu matrix can penetrate the Cu-Nb and Cu-Ag interfaces, respectively, by the creation of residual interfacial misfit dislocations as required for the conservation of the total Burgers vector loop. This mechanisms may explain the mutual shearing of small portions

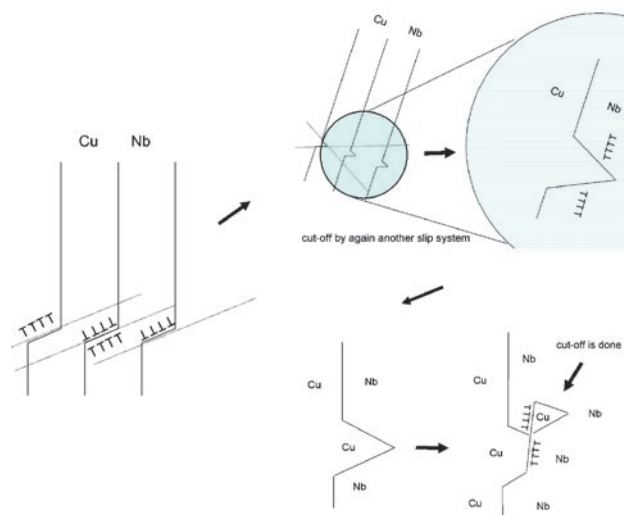


Fig. 5: Crawler-type dislocation mechanism explaining the deformation induced chemical intermix at the interfaces. This effect includes the assumption that lattice dislocations of the Cu matrix can penetrate the Cu-Nb and Cu-Ag interfaces, respectively, by the creation of residual interfacial misfit dislocations as required for the conservation of the total Burgers vector loop.



of material in a fine lamellar Nb or Ag filament by incoming dislocations from the Cu phase. The activation of a second slip system in the filament phase can then entail a cut-off effect as indicated by the schematical sketches in Fig. 5.

References

1. Spitzig, W.A.; Pelton, A.R.; Laabs, F.C.: Acta Metall. 35 (1987) 2427.
2. Raabe, D.; Heringhaus, F.; Hangen, U.; Gottstein, G.: Z. Metallkd. 86 (1995) 405.
3. Heringhaus, F.; Raabe, D.; Gottstein, G.: Acta Metall. Mater. 43 (1995) 1467.
4. Frommeyer, G.; Wassermann, G.: Acta Metall. 23 (1975) 1353.
5. Sakai, Y.; Inoue, K.; Maeda, H.: Acta Metall. Mater. 43 (1995) 1517.
6. Hangen, U.; Raabe, D.: Acta Metall. Mater. 43 (1995) 4075.
7. Raabe, D.; Heringhaus, F.: Phys. Status Solidi A 142 (1994) 473.
8. Raabe, D.; Hangen, U.: Acta Mater. 44 (1996) 953-961.
9. Raabe, D.; Hangen, U.: Phys. Status Solidi A 154 (1996) 715.
10. Trybus, C.; Spitzig, W.A.: Acta Metall. 37 (1989) 1971.
11. Raabe, D.; Mattissen, D.: Acta Mater. 47 (1999) 769-777.
12. Mattissen, D.; Raabe, D.; Heringhaus, F.: Acta Mater. 47 (1999) 1627-1634.
13. Raabe, D.; Miyake, K.; Takahara, H.: Mater. Sci. Eng. A 291 (2000) 186-197.
14. Raabe, D.; Hangen, U.: Mater. Lett. 22 (1995) 155-161.
15. Raabe, D.; Heringhaus, F.; Hangen, U.; Gottstein, G.: Z. Metallkd. 86 (1995) 405-422.



Inhibiting Delamination of Organic Coatings from Metallic Substrates: How to Design Inherently Stable Interfaces

M. Rohwerder, M. Stratmann, R. Hausbrand

Department of Interface Chemistry and Surface Engineering

From cars, airplanes and facades of buildings to encapsulation of microelectronic components, organic coatings are widely used as effective and versatile protection against corrosion. Some coating systems are able to preserve the functional integrity of the components for time scales up to decades.

However, due to internal or external defects such as imperfections at the interface, which may be caused by thermally induced strains or external loads, or scratches penetrating the coating, the protective properties may be negatively affected and the system degrades. In the worst cases, electrochemically driven delamination reactions start at these defects and proceed relatively fast into the intact polymer/substrate interface. This is possible since even though the organic coatings serve as an effective barrier layer, inhibiting access of ions and water to the substrate surface, under humid conditions there is always a certain uptake of water into the polymer, a prerequisite for the electrochemical reactions.

The fastest degradation reaction is the so called cathodic delamination. During this electrochemical delamination mode, a galvanic element forms between a defect in the polymer or at the buried interface, where the metal corrodes (anode), and the defect border, where oxygen is reduced at the buried interface (cathode) [1-4]. It is in particular the reactive side products of the oxygen reduction that lead to

the degradation of the interface and the consequent de-adhesion of the polymer from the substrate [1-4].

Since cathodic delamination is the fastest delamination mode, for an improved stability it is essential to suppress its underlying mechanisms.

One would assume that one logical approach for this would be to improve the stability of the bonds between organic coating and the substrate. However, even in the best case this just slows down the process and does not fully inhibit it. Another approach of course, would be to deposit an insulating inorganic layer between substrate and organic coating, which serves as a perfect barrier layer and on whose surface no electron transfer reactions are possible since it is insulating. The problem with deposited inorganic layers is that they are quite brittle and prone to be subject to defect formation (cracks, mechanical delamination), caused by external or internal stresses.

As we will see, the key for a truly inherently delamination resistant interface lies in the electronic properties of the native oxide at the polymer/substrate interface.

At the intact metal oxide/polymer interface the metal is in its passive (oxidized) state.

From the electrochemical point of view the corresponding electrode potential is more positive than the electrode potential of the corroding material (see

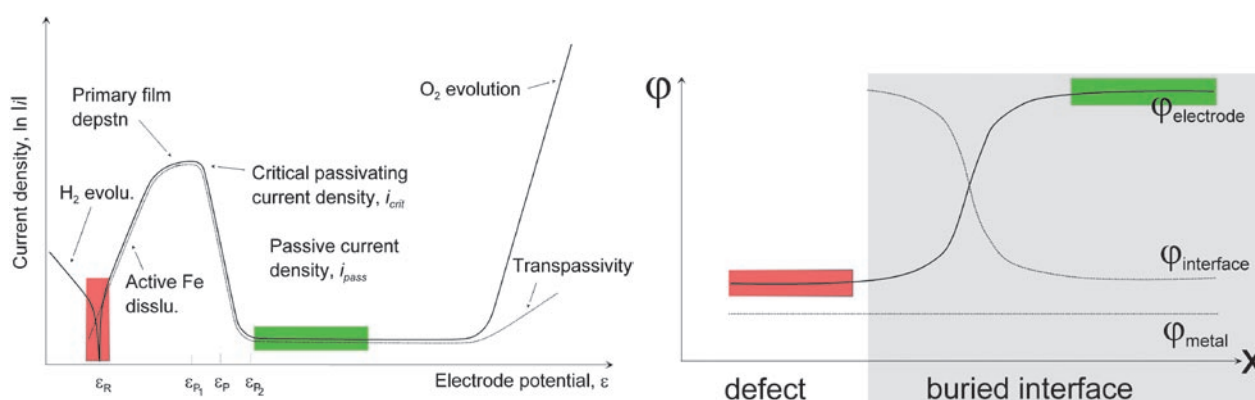


Fig. 1: a) Typical passivation behaviour of a metal, such as iron (see e.g. Kaesche: *Corrosion of metals*, 2003, Springer-Verlag Berlin). The passivation occurs through polarization from the active corrosion over a passivation peak. The potentials of the passive oxide are more positive than during active corrosion. b) Potential profile for an SKP scan from defect site of a coated metal to the intact interface (blue line). Since the Galvani potential in the metal is the same throughout the metal (straight dotted line), the Galvani potential of the organic side of the interface (curved dotted line) is at the intact interface (positive electrode potential) more negative than near the defect site (more negative potential).



Fig. 1a). This can also be seen in the potential profile of a delaminating sample in Fig. 1b. As expected, in the defect the potential is more negative than at the intact interface. The measurement of such potential distributions at the buried interface is only possible by use of the Scanning Kelvin Probe (SKP) technique, as described in the pioneering papers by Stratmann et al. ([1]). A prerequisite for the application of this technique is that the effect of other potential drops than the one at the coating/substrate interface (which determines the electrode potential at the interface) is eliminated by a suitable calibration process [1]. However, as will be discussed further below, concerning the effect of chemistry and structure of the polymer/substrate interface on the SKP measurement there is still work to do.

Now, how does this potential distribution affect the delamination behaviour? A first idea about the interplay between delamination and potential distribution can be obtained by considering the charge transport during cathodic delamination. For the cathodic delamination the electric circuit for the electron transport from the corroding defect to the oxygen reduction site at the delaminating buried interface is closed by predominant cation transport along the interface from the defect to the reaction site [1-4]. Only if the potential distribution is as shown in Fig. 1b, the migration of cations from the defect into the buried interface is promoted (the cations move from negative to positive potentials since the potential distribution in the organic side of the interface is inverse to the electrode potential (see also Fig.1b)). So to speak defect (anode) and intact interface (cathode) form a battery that drives cations from the defect into the intact interface by this potential gradient. This is also the reason why inhibitor anions in the defect cannot migrate into the buried interface (see e.g. [5]). Now, if the buried interface was electrochemically inert, i.e. no oxygen reduction possible, this ion migration would just result in interface charging and consequent cancellation of the potential differences and no delamination occurs. Unfortunately, in standard systems, such as polymer coated zinc, steel or galvanized steel, the

interfaces are not inert and oxygen reduction takes place, the flow of cations is kept up and delamination proceeds. This happens although in the initial stage oxygen reduction is inhibited at the intact interface, as can be seen from the electrode potentials measured with the SKP technique on the passive oxides of technical metals such as zinc and steel: the potentials are negative enough that they should allow oxygen reduction; since there is no anodic counter reaction at the intact interface, this potential can only be stable if the oxygen reduction is inhibited, otherwise it should drift to several hundreds of mV more positive values, as it is observed e.g. for noble metals such as gold (see below). Now, when comparing these potentials with the flat band potentials for the same oxides as measured by electrochemical methods it becomes obvious that the potentials of passive metal surfaces as measured with SKP are usually about 100 mV more positive than the flat band potentials of these surface oxide (e.g.: $\varphi_{\text{Fe,SKP}} \cong 0 \text{ V}_{\text{SHE}}$, $\varphi_{\text{Fe,flatband}} \cong -0.1 \text{ V}_{\text{SHE}}$; $\varphi_{\text{Zn,SKP}} \cong -0.55 \text{ V}_{\text{SHE}}$, $\varphi_{\text{Zn,flatband}} \cong -0.6 \text{ V}_{\text{SHE}}$).

The explanation for this is that since no corrosion can occur at the intact interface there is no counter reaction to oxygen reduction, and this results in an upward bending of the electronic band structure at the interface and thus in the formation of a depletion zone, inhibiting further electron transfer at the interface (Fig. 2a). This band bending results in higher electrode potentials as compared to the flat band case.

But if the electrode potential at the interface is pulled down by the Ohmic coupling to the defect (i.e. the Fermi level is shifted upwards), this band bending is lifted and electron transfer made possible (Fig. 2b). Thus, the oxygen reduction can take place and the interfacial bonds be destroyed: the cathodic delamination proceeds along the interface. This is the crucial mechanism behind cathodic delamination; it is the negative potential of the defect coupled to the buried interface that lowers the potential at this site and thusly turns the inert interface to a reactive one.

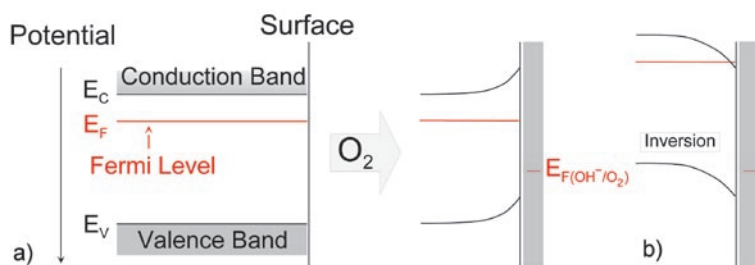


Fig. 2: a) Band bending on oxide surface in the presence of oxygen. The redox potential for the oxygen reduction is below the Fermi level causing electron transfer from oxide of oxygen. This results in an upward bending of the band structure and thus to the formation of a depletion layer until no more electron transfer is possible. b) Shifting up the Fermi level by negative polarization lifts the band bending and thus ETR is possible again.

This important aspect of the interplay between potential distribution along the interface, i.e. the potential difference between defect and intact interface, and delamination has never been discussed before; its crucial role for the delamination process has been neglected so far.

Now the idea is, that if the electronic properties of the metal oxide at the buried interface could be tuned in such a way that the corresponding potential is not longer more positive than that of the defect, then the above described mechanism cannot become effective; to the contrary, a coupling of a defect with a more negative polymer/oxide interface



would result in a lowering of the Fermi level and thus in increasing the band bending and the depletion zone. The hypothesis is that then cathodic delamination would be impossible.

How can this be achieved? For this it is helpful to call to ones mind that it is the position of the Fermi level that determines the electrode potential: the higher its position the more negative the potential. The position of the electronic band structures of semiconductors can be referenced to the standard hydrogen electrode (see e.g. [6]).

Most metals for technical applications such as iron or zinc form n-type semiconducting oxides. In view of the position of the conduction band of these oxides the SKP measurements imply that the Fermi level of their oxides are just below the conducting band level, i.e. these oxides are highly defective with a high donor density. This also implies that a significant upward shifting of the Fermi level, and thus a significant lowering of the potential, e.g. by further increasing the donor density will not be possible, because the possible position of the Fermi level is already at its upper limit. Since according to Fig. 1a the potential of the passive oxide is always higher than that of the defect, it seems not possible to achieve a potential inversion between defect and intact interface for pure metal substrates.

Now, the band gaps of the oxides of less noble metals are larger than the ones of more noble samples and since the native oxides of most practical metals are n-conducting with a high donor density,

their Fermi level is near the conduction band. Since the intrinsic Fermi level position, i.e. the mid position of the band gap, for most of these oxides is about the same [6, as a consequence the corresponding conduction band shifts up with increasing band gap and thus the electrode potentials of less noble metals are more negative than the ones of more noble metals.

Hence, for alloy substrates composed of less noble and more noble alloying elements the desired inversion of the potential difference is possible, if the defect corrodes more like the more noble component and the oxide at the intact interface is determined the one of the less noble component.

Because of their great technological and economic importance zinc alloys are an ideal system for the application of this hypothesis. One of the most interesting zinc alloys is the system Zn-Mg. Zn-Mg has been shown in earlier investigations to have excellent corrosion properties [7], as well in the painted as in the unpainted state. Since Zn is significantly nobler than Mg, and magnesium oxide is stable in alkaline environment as it prevails at the interface during cathodic delamination conditions, this alloy fulfils the necessary criteria required for a potential inversion between defect and intact interface. However, the fundamental aspects of the corrosion behaviour of the painted system, i.e. its delamination behaviour, have never been investigated in detail. Since it is important to correlate the delamination behaviour with the band structure of

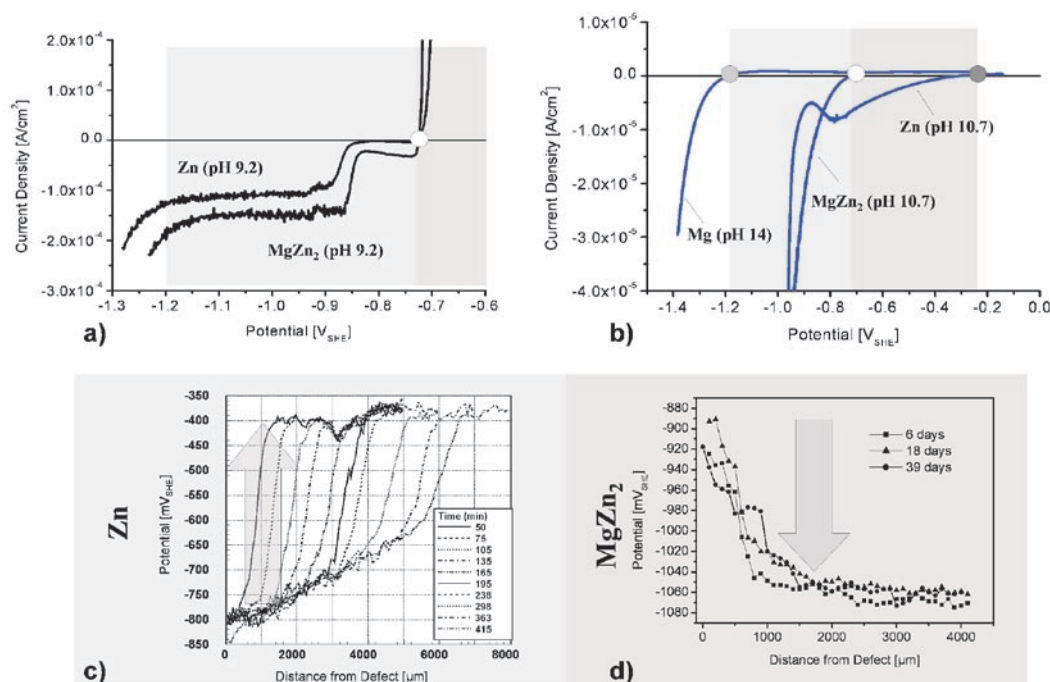


Fig. 3: a) Current/potential curves for Zn and MgZn₂ in chloride containing electrolyte (simulating the defect). Both materials corrode at the same pitting potential since due to selective dissolution of the Mg the MgZn₂ becomes similar to the Zn sample. b) Current/potential curves for Mg, MgZn₂ and Zn in chloride-free electrolyte at high pH (simulating the intact interface). Here all three materials passivate, first Mg, then MgZn₂ and then Zn. The potential of zero current (open circuit potential (OCP)) for Zn is considerably more positive than the corrosion potential in a), while for MgZn₂ this is not the case. The potentials of the polymer covered oxides are even a little bit more negative (see text). c) Resulting delamination behaviour for Zn and d) for MgZn₂.

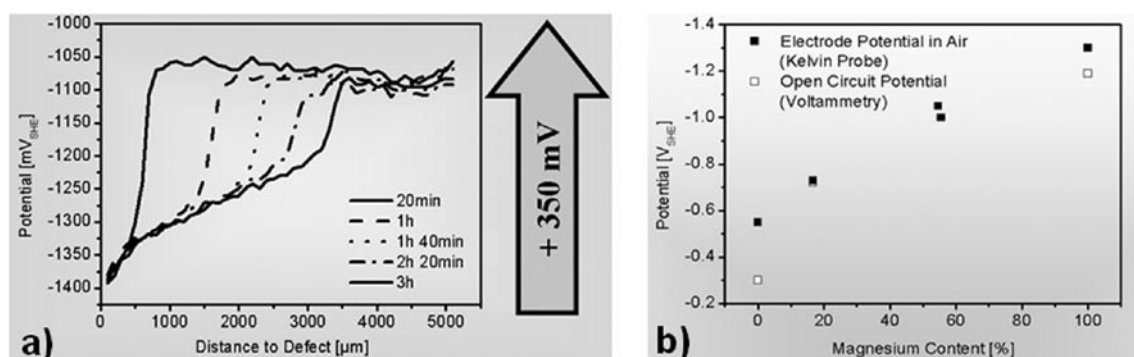


Fig. 4: a) Delamination behaviour of the same polymer coated $MgZn_2$, as in Fig. 3, but with Mg in the defect: the delamination is about three orders in magnitude faster, d) dependence of the OCP and the potential measured with SKP on Mg content in the oxide, obtained by different treatments.

the oxide and the corresponding potential, it was decided for this work to prepare samples of the pure intermetallic phase $MgZn_2$, which is the predominant phase found in the technical alloys. Preliminary results of this research have recently published [8]. In the following the results will be discussed in more detail in the light of the above described.

Fig. 3a shows that the corrosion potential in chloride containing solution of $MgZn_2$ is similar to that one of the more noble component, i.e. zinc; and Fig. 3b that the potential of the passive oxide is between that one of magnesium oxide and zinc oxide. This is exactly what is required for the potential inversion. Indeed, Fig. 3d shows that the potential of the defect is more positive than that of the intact buried interface and that the delamination velocity is extremely slow and most likely only anodic [8]; as postulated above, the potential is pulled up by the coupling to the defect. It is interesting to have a look at the delamination behaviour of the same system when brought into contact with a defect corroding at a potential more negative than that of the intact interface, e.g. pure magnesium. As can be seen from Fig. 4a in this case the delamination velocity is larger by about three orders of magnitude.

But the inversed potential difference should be promoting the observed anodic delamination, which is however a slow delamination mode. It might be speculated that if the potential difference were zero, there would also be no anodic delamination or at least an even slower one. Fig. 4b shows how the potential of the surface oxide can be tuned by different sample preparation. There might be a good chance that an adjustment to zero potential difference could be possible.

However, there are a number of problems to be solved yet. For instance, the oxide at the interface was found to change during long-term exposure which also slightly affects the potentials; the underlying processes need be understood. Also, the effect of the polymer/substrate bond on the electrode potential at the interface has been neglected in the above discussion. For the simple epoxy model polymer used in the work described here the effect

was quite negligible. However, comparative studies of Volta potentials obtained by SKP in dry and humid atmospheres on different metals coated by different polymers indicate that dipole moments of the bonds and of interfacial ordered water molecules may significantly alter the potentials [9,10]. In the view of the above, it also might be that the molecular structure (and the electric field gradient caused by interfacial dipoles) of the interface affects the electron transfer reactions, such as oxygen reduction, and thus the potential at which oxygen reduction is stopped. This effect is expected to be especially significant for noble metals, i.e. oxide-free metals or metals which form metal-like oxides. For some applications, e.g. in microelectronic components noble metals such as copper, silver or gold are used. Here, no band bending is possible; as the equivalent positive surface charging occurs. As first results from ongoing research indicate, the effect of the molecular structure at the interface has a significant effect on the resulting potentials.

References

1. Leng, A.; Streckel, H.; Stratmann, M.: Corros. Sci. 41 (1999) 547.
2. Leng, A.; Streckel, H.; Stratmann, M.: Corros. Sci. 41 (1999) 579.
3. Leng, A.; Streckel, H.; Hofmann, K.; Stratmann, M.: Corros. Sci. 41 (1999) 599.
4. Rohwerder, M.; Stratmann, M.: MRS Bulletin 24 (1999) 43-47.
5. Williams, G.; McMurray, H.N.: J. Electrochem. Soc. 148 (2001) B377-B385.
6. Hassel, A.W.; Schultze, J.W.: in : Encyclopedia of Electrochemistry Vol.4, eds. G. Frankel, M. Stratmann, Wiley VCH, Weinheim (2003).
7. Schuhmacher, B.; Wolfahrd, D.: in: GALVATECH 2001 Conf. Proc. (2001) 3.
8. Hausbrand, R.; Stratmann, M.; Rohwerder, M.: Steel Res. 74 (2003) 453-458.
9. Nazarov, A.P.; Thierry, D.: Protect. Met. 39 (2003) 55-62.
10. Nazarov, A.P.; Thierry, D.: Electrochim. Acta 49 (2004) 2955-2964.



Development of a Non Local Dislocation Density Based Constitutive Law for Crystal Plasticity FEM with Special Consideration of Grain Boundaries

F. Roters, A. Ma, D. Raabe

Department of Microstructure Physics and Metal Forming

As crystal plasticity is build on dislocation movement it is the aim of this project to introduce a constitutive model which is based on dislocation densities as internal variables into the crystal plasticity finite element formulation. As starting point we use a constitutive model for fcc materials recently developed by our group [1]. One special aspect of this approach is the explicit treatment of the mobile dislocation density. Following an idea presented in [2] we do not use an evolution equation for the mobile dislocation density but derive it from an energy optimisation procedure in the form of an instantaneous local equilibration.

A slightly modified version of this model was now implemented into our crystal plasticity finite element code. The modification concerns the treatment of the dislocation cell structure. As the simple stress averaging procedure used in our previous approach [1] for heterogeneously arranged cell walls and cell interiors is only valid for uniaxial load we do not distinguish between these two types of microstructure elements in the current version of the tensorial FEM implementation.

One major advantage of using a dislocation density based constitutive model approach as opposed to the conventional viscoplastic method is that more complex microstructural phenomena such as non-local strain gradient effects and the micromechanical effects associated with interfaces can be homogeneously incorporated into the constitutive law. Furthermore, owing to the strong path dependence of crystal plasticity and strain hardening, a physically based internal variable constitutive formulation has better predictive capabilities than empirical approaches.

The proper treatment of strain gradients gains particularly importance when conducting simulations at the subgrain resolution. Due to the compatibility constraints strain gradients are formed in the vicinity of grain boundaries and related interfaces. These gradients increase both the strength of the material and the hardening rate. In the framework of our new model they are accounted for by the so called geometrically necessary dislocations (GNDs). These dislocations increase the number of immobile dislocations and, therefore, result in both an increased strength and an increased strain hardening of the material.

However, the incorporation of geometrically necessary dislocations renders the FEM algorithm non local. This means that the integration of the constitutive equations at a given Gaussian point requires to include constitutive information from the neighbouring integration points for computing the lateral gradient terms. While in principle the gradients can be used as additional degrees of freedom in the FEM [3,4] their introduction is not straightforward in commercial FE solvers which we use for the implementation of our material subroutines. For this reason we have chosen an alternative way for realising the non local constitutive scheme. That is we split the FEM iterations within one time increment into two groups. Every even iteration (starting with 0) is solely used for data collection and every odd iteration is than used for the stress calculation and the update of the internal variables. By using this procedure it was possible to keep the integration scheme fully implicit in opposition to some other implementations which use simple forward integration for the GNDs (e.g. [5]).

The grain boundaries can be treated as additional obstacles to the motion of the mobile dislocations. Generally small angle boundaries and some special boundaries with a high degree of structural coherence are considered as being penetrable to dislocation motion, while non-special large angle boundaries are impenetrable to mobile dislocations. These properties must be translated into corresponding crystal plasticity finite element formulations: In a crystal plasticity FEM framework the various dislocation density classes are treated individually for each slip system. This implies that for each slip system the obstacle strength of the boundary can be different. We use the following thought experiment to illustrate the penetration process. A dislocation with a given Burgers vector \mathbf{b} and a given line segment \mathbf{s} located in crystal I is assumed to approach a grain boundary. On the opposite side of that grain boundary (i.e. in grain II) this exact dislocation configuration would not necessarily be mobile as the crystal orientation changes across that interface. However, one can identify that slip system in grain II which is closest to that of crystal I. If the dislocation would penetrate the boundary it could be transferred to that respective slip system. However, in order to obey the conservation of the lattice defect density it has to leave behind an additional dislocation line segment.



In general this segment would be immobile and trapped in or in front of the boundary. The energy for the creation of this additional dislocation segment can now be used as a measure for the obstacle strength of the boundary for the slip system considered. One advantage of this procedure is that the obstacle strength of the boundary may be different for each slip system. This implies that the overall effect of the boundary will depend on the applied load, as different slip systems will be activated for different loads.

The model is applied to the simulation of simple shear of Al bicrystals with different misorientations between the two abutting crystals. The corresponding experiments use a set-up as described in [6]. All three bicrystals have a straight symmetric $\langle 112 \rangle$ tilt boundary with a misorientation of 7.4° , 16° and 33° , respectively, i.e. the first is a small angle boundary, the second an intermediate one and the third a large angle boundary. The material parameters for the simulations were calibrated with the help of shear stress - shear strain curves obtained from single crystal experiments for both a phenomenological crystal plasticity model and the new dislocation density based constitutive description (Fig. 1). The results for the simulations of the simple shear of the bicrystals are shown in Fig. 2. The figures show the local distribution of von Mises strain. While the location of the grain boundary can be clearly seen in the experimental results, this is not the case for the simulations using the phenomenological crystal plasticity constitutive laws. Especially for the small angle boundary the empirical approach does not predict any influence of the boundary at all. In contrast, the non local dislocation density based model reproduces the experimental findings very well. The small deviations still found are probably due to differences in the exact boundary conditions of the experimental and the simulation set-up.

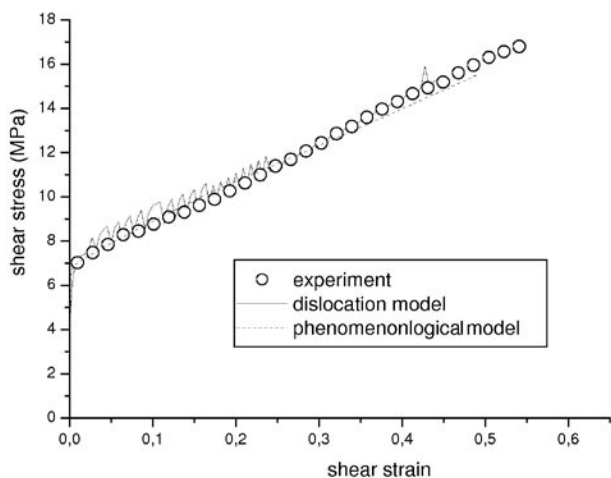


Fig. 1: Shear stress - shear strain curve from single crystal simple shear experiment used for calibration of model parameters.

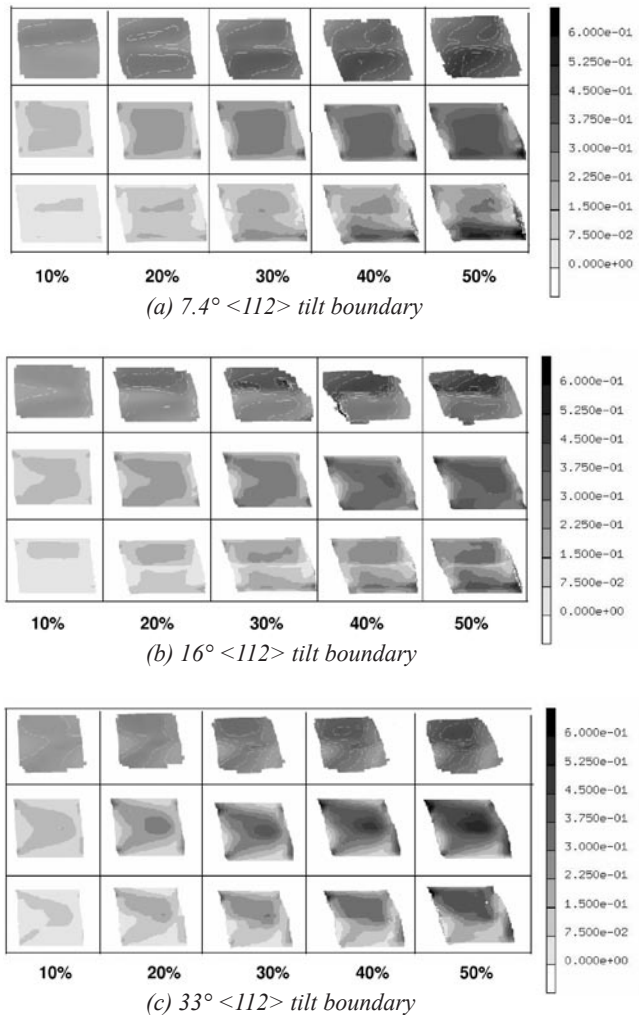


Fig. 2: Distribution of von Mises strain for bicrystal with (a) 7.4° , (b) 16° , and (c) 33° $\langle 112 \rangle$ tilt boundaries after different nominal shear strains. Top row: experimental results; middle row: simulation results using phenomenological crystal plasticity; bottom row: simulation using non local dislocation density based model.

The newly developed constitutive model has proven its strength in predicting the grain boundary effect on the local strain distribution. In the future it will be applied for the simulation of more complex crystal cluster arrangements.

References

1. Ma, A.; Roters, F.: Acta Mater. 52 (2004) 3603-3612.
2. Roters, F.: Phys. Status Solidi (b) 240 (2003) 68-74.
3. Evers, L.P.; Parks, D.M.; Brekelmans, W.A.M.; Geers, M.G.D.: J. Mech. Phys. Solids 50 (2002) 2403-2424.
4. Evers, L.P.; Brekelmans, W.A.M.; Geers, M.G.D.: J. Mech. Phys. Solids 52 (2004) 2379-2401.
5. Meissonnier, F.T.; Busso, E.P.; O'Dowd, N.P.: Int. J. Plasticity 17 (2001) 601-640.
6. Gardiner, J.C.; Weiss, J.A.: ASME J. Biomech. Eng. 123 (2001) 170-175.



Simulation of Precipitation Reactions in Ferritic Steels

A. Schneider¹, G. Inden²

¹Department of Materials Technology, ²Department of Physical Metallurgy

The development of a new generation of ferritic steels for application at service temperatures of 650 °C and higher requires the use of new alloying elements, of new composition ranges and also of new intermetallic phases. Long-term service is an important aspect leading to the requirement of highly stable microstructures at high temperatures. The development of such multicomponent materials is only feasible by making use of computational thermodynamics and numerical simulations of diffusion controlled phase transformations.

The precipitation reactions in model alloys of Fe-Cr-C, Fe-Cr-W-C, Fe-Cr-Si-C, and Fe-Cr-Co-V-C have been simulated. Remarkable results on the competition between stable and metastable phases have been found, and the long-term evolution of the microstructures could be predicted. Based on these results new ferritic steel alloys with optimised compositions and heat-treatments are being developed.

The present study is part of a project of development of new 12% Cr steels for application in 650 °C ultra super critical (USC) power plants in view of achieving a highly stable microstructure with initially 100% martensite which is strengthened by different types of phases ($M_{23}C_6$, MX, Laves-phase) [1-4]. A high creep resistance of these types of steels shall result from finely distributed precipitates in a tempered martensitic microstructure. The final microstructure is obtained by a two step heat treatment. First, an austenitisation treatment at temperatures around 1080 °C for sufficient time shall dissolve previously formed carbides. Alloy composition and type of alloying elements have to be chosen such that δ -ferrite does not form and primary precipitates (like MX nitrides) do not form in the liquid state. After austenitisation the alloys are air cooled to form 100% martensite. The final treatment is tempering at around 780 °C to form carbides and Laves phase in order to achieve good creep properties.

In order to establish a given microstructure by an adequate heat treatment it is important to know about the kinetics of transformation. This does not only apply to the formation of the microstructure, it also concerns its stability under long term service conditions at high temperatures, as e.g. at 650 °C in

the case of ferritic steels for power plants. Usually the discussion of the kinetics focuses on the evolution of stable phases only. However, there is no restriction imposed on metastable phases to prevent them from taking part in the kinetics. Of course, the metastable phases have to disappear eventually, but their temporary presence will strongly influence the kinetics of the other phases.

In this work the transformation kinetics is simulated using the software DICTRA [5]. Diffusion-controlled transformations are treated by DICTRA on the basis of the fundamental concept which is described in [6-11]. Applications of DICTRA are presented in [10-15]. The results obtained will show remarkable effects of competition between stable and metastable phases. This was also shown recently by Perez and Deschamps [16] for two-phase precipitation in low-carbon steels and by Bhadeshia et al. [17], [18] in various creep-resistant steels.

Precipitation of $M_{23}C_6$ in Fe-12Cr-0.1C. At first growth of $M_{23}C_6$ in a ternary Fe-12Cr-0.1C alloy (compositions in wt.%) shall be treated. The calculated isothermal section of the phase diagram of Fe-Cr-C at $T = 780$ °C (1053 K) is shown in Fig. 1.

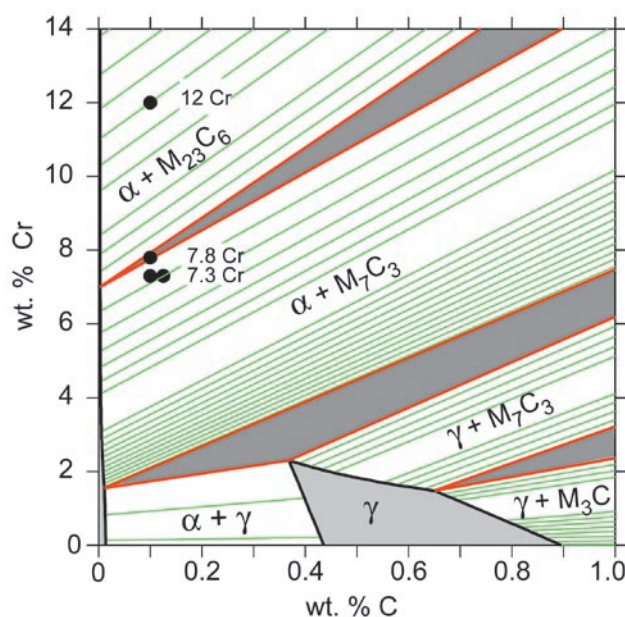


Fig. 1: Calculated isothermal section of the Fe-Cr-C phase diagram at 1053K. The points define the composition of ternary alloys being considered.

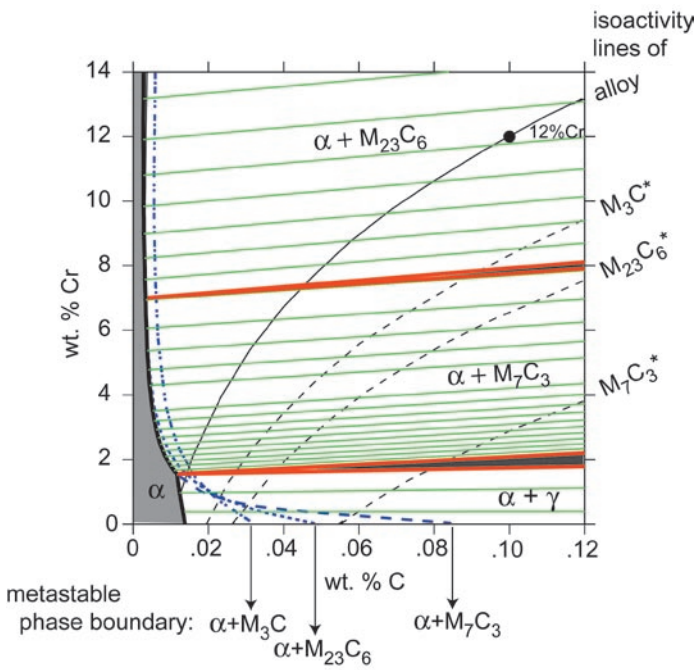


Fig. 2: Blow-up of the phase diagram Fe-Cr-C at 1053K showing the metastable extensions of the phase boundaries $\alpha + M_{23}C_6$, $\alpha + M_7C_3$ and of metastable $\alpha + M_3C$. The point defines the alloy Fe-12Cr-0.1C. The line through the point represents the isoactivity line for C in ferrite. Broken lines represent the isoactivity curves in ferrite corresponding to the C-activity of carbides M_xC_y with the same Cr/Fe ratio as in the alloy (the asterisk shall indicate this particular composition).

The composition of the alloy considered falls into the two-phase region α -Fe + $M_{23}C_6$. At this temperature and composition, $M_{23}C_6$ thus grows as a stable phase in ferrite. The boundary condition at the moving interface, called operating tie-line during the precipitation reaction, has to satisfy the condition that, for every diffusing species, the interface velocity obtained from the mass balance is the same. At first it has to be checked whether the growth of $M_{23}C_6$

is controlled by C- or by Cr-diffusion. In Fig. 2 the iso-activity line for C corresponding to the ferritic matrix, is shown together with C iso-activity lines of carbides with the same Cr/Fe ratio as in the alloy (the asterisk marks the special composition). If C-diffusion controls the reaction, i.e. if the growing carbide inherits the Cr-content of the matrix, the C-activity in the matrix must be higher than that in the growing carbide in order to force C to diffuse towards the carbide.

It can be seen from Fig. 2 that the C-activity in the matrix is lower than that of $M_{23}C_6^*$ and also that of any other carbide. Consequently, growth has to occur under Cr-diffusion control. During this regime the operating tie-line has to correspond to a C-activity close to that of the ferritic matrix in order to keep the C-flux small enough to fulfil the mass balance for Cr and C. The C-iso-activity line corresponding to the alloy intersects the phase boundary at a composition far within the metastable range of α -Fe + $M_{23}C_6$ (see Fig. 2). The variation of the the boundary condition at the phase interface with time is shown in detail in [10].

Competitive growth of stable and metastable carbides in Fe-12Cr-0.1C. When simulating the growth kinetics it is not sufficient to consider only stable phases. The driving force for nucleation of a metastable phase may be of the same order or even higher than that for the stable ones. Furthermore, the growth kinetics may be faster. For instance, it is possible that M_7C_3 nucleates simultaneously with the stable phase $M_{23}C_6$, grows to some extent and disappears eventually when the stable equilibrium is approached. The presence of such inter-mediate phases strongly influences the growth kinetics of the stable phases. This is illustrated in an example by means of a three cell calculation, allowing the simultaneous growth of $M_{23}C_6$, M_7C_3 and M_3C . The result of the simulation is shown in Fig. 3. Both

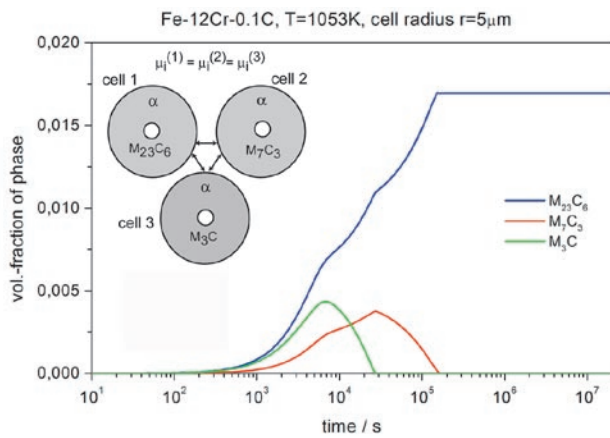


Fig. 3: Three-cell simulation of competitive growth of stable $M_{23}C_6$ and of metastable M_7C_3 and M_3C in Fe-12Cr-0.1C at 1053 K. The cell radii were 5 μm and the nucleus sizes were 1nm in each cell.

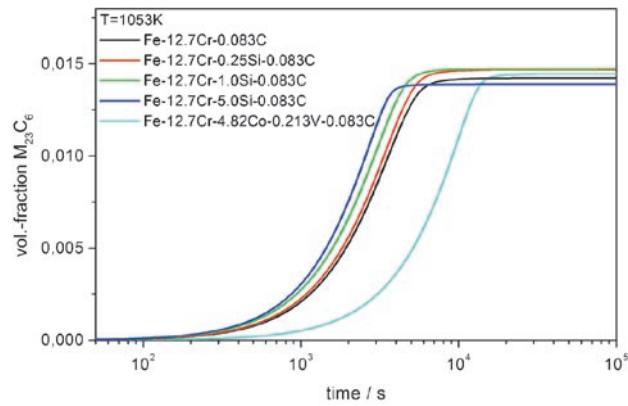
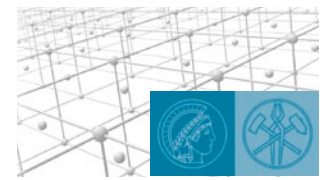


Fig. 4: Fraction of $M_{23}C_6$ phase formed during precipitation reaction at 1053 K in various ferritic steels. The simulations were performed for spherical cells of 5 μm in radius. The starting particle size was 1 nm.



metastable carbides appear at intermediate stages of the reaction.

Effect of additions of Si, Co, V, on the growth kinetics of $M_{23}C_6$ in Fe-Cr-C. In Fig. 4 volume fraction of $M_{23}C_6$ is plotted versus time for different ferritic steels with additions of Si, V and Co. The present thermodynamic databases assume no solubility of Si in $M_{23}C_6$ carbide. Consequently, $M_{23}C_6$ can only grow by pushing silicon ahead of the moving phase interface. This should lead to a slower kinetics compared to the case of no Si. However, the contrary is obtained in the simulation. This is due to the effect of Si on the activity in ferrite: Si increases both the C-activity and the Cr-activity. Since Cr diffusion controls the growth rate of $M_{23}C_6$ the accelerating effect comes from the increased Cr-activity in the Si-enriched ferrite matrix leading to a higher driving force for Cr diffusion towards the carbide. The boundary condition and the growth velocity are thus the result of a compromise between increased Cr-flux towards the carbide and Si transport away from the carbide. Obviously this leads to a slightly higher growth velocity. For Co the thermodynamic description allows for some solubility in $M_{23}C_6$ but it is very small. Therefore, most of the Co must be transported away in front of the growing particle. The addition of 4.82 wt.% Co to Fe-12.7Cr-0.083C reduces the growth kinetics significantly. V has practically no effect since $M_{23}C_6$ has sufficient solubility of V in $M_{23}C_6$ that it can take up the V-content offered by ferrite.

Precipitation of $M_{23}C_6$ and Laves phase in Fe-12Cr-3W-0.15C. In ferritic steels with W as alloying element, Laves phase plays an important role. The growth of $M_{23}C_6$ and Laves phase shall be simulated for a two step heat treatment: first annealing at 780 °C for 2 h, followed by annealing at 650 °C. This first heat treatment corresponds to the processing of high temperature ferritic steels, the second corresponds to the service condition. An Fe-12Cr-3W-0.15C alloy exhibits a two-phase equilibrium α -Fe+ $M_{23}C_6$ at 780 °C and a three-phase equilibrium α -Fe+ $M_{23}C_6$ + Laves phase at 650 °C. The simulation was performed with two spherical cells of radius 5 μ m. In Fig. 5 the calculated fractions of phases are plotted as function of time. The phase fractions are represented in both linear and logarithmic scaling in order to visualise details which cannot be seen in a linear representation. The 2 h treatment leads to the formation of $M_{23}C_6$ while the amount of Laves phase is negligibly small at this stage. The reduction in temperature from 780 °C to 650 °C after 2 h leads to a clear reduction in growth rate. This is due to the smaller mobilities. The driving forces for diffusion from the ferritic matrix to the precipitates are increased by the change in temperature. After about 6 days $M_{23}C_6$ has reached its equilibrium-volume fraction. The Laves phase grows very slowly. In the Laves phase

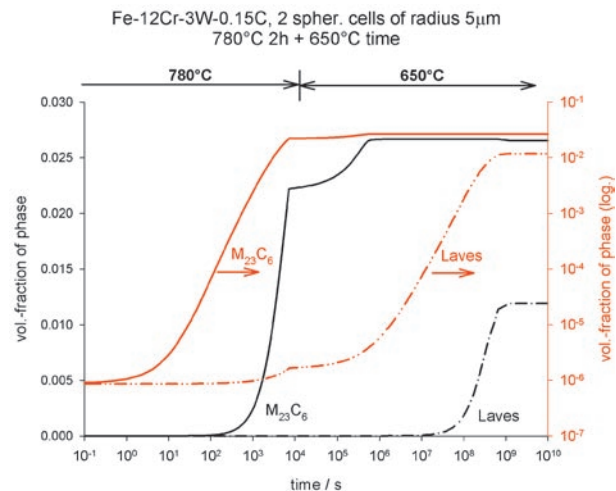


Fig. 5: Simultaneous growth of $M_{23}C_6$ and Laves phase (Fe,Cr)₃W in Fe-12Cr-3W-0.15C simulated for two coupled spherical cells of 5 μ m in radius. The simulation represents a heat treatment consisting of two steps: 2 h annealing at 780 °C and subsequent service condition at 650 °C for a given time. The phase fractions are plotted with linear (left) and logarithmic (right) axis.

the W-level is very high (33 at.%). Therefore, a high flux of W is required for the formation of Laves phase. The slow W diffusion leads to very slow growth such that equilibrium is reached only after about 10⁹ s or more than 10 years (see Fig. 5) for an average nucleus distance of 11 μ m (corresponding to 1 nucleus of Laves phase per two cells of 5 μ m radius).

Influence of cell size. It is to be emphasized that the kinetic behaviour of precipitation strongly depends on the cell size (or equivalently the average particle distance) which was arbitrarily fixed to a radius of 5 μ m in the cases discussed so far. The

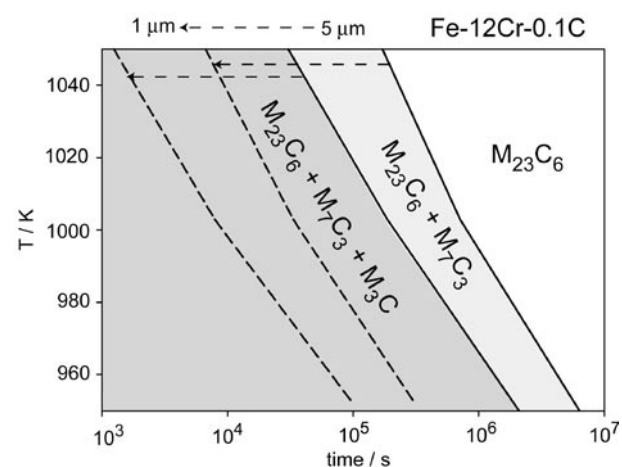


Fig. 6: Calculated time–temperature diagram of precipitation sequence. The solid lines delimit areas of existence of carbides if an average particle distance of 10 μ m (or cell radius 5 μ m) is assumed. The limits sensibly depend on the chosen cell size. The reduction of cell size from 5 μ m to 1 μ m shifts the limits by an order of magnitude as shown by the broken lines. This shows that such diagrams can only be used if the average particle distance is known.



cell size is particularly important when it comes to a comparison with experimental data. This can be discussed with respect to so-called „time–temperature precipitation sequence diagrams“. Such diagrams shall display the ranges in time and temperature where precipitates are observed experimentally. To show the effect of cell size the carbide precipitation sequence in Fe-12Cr-0.1C was calculated for two cell sizes and plotted as a carbide sequence diagram in Fig. 6. The limits of the existence domains of precipitates shift by more than an order of magnitude in time if the average particle distance is reduced from 10 μm to 2 μm .

References

1. Knežević, V.; Sauthoff, G.; Vilik, J.; Inden, G.; Schneider, A.; Agamennone, R.; Blum, W.; Wang, Y.; Scholz, A.; Berger, C.; Ehlers, J.; Singheiser L.: *ISI Int.* 42 (2002) 1505-1514.
2. Knežević, V.; Sauthoff, G.: in: *Proc. 7th Liège Conference on Materials for Advanced Power Engineering*, eds. J. Lecomte-Beckers, M. Carton, F. Schubert, P. J. Ennis, Forschungszentrum Jülich, Jülich (2002) 1289-1298.
3. Agamennone, R.; Blum, W.: in: *Proc. 7th Liège Conference on Materials for Advanced Power Engineering*, eds. J. Lecomte-Beckers, M. Carton, F. Schubert, P. J. Ennis, Forschungszentrum Jülich, Jülich (2002) 1161-1170.
4. Vilik, J.; Schneider, A.; Inden, G.: in: *Proc. 7th Liège Conference on Materials for Advanced Power Engineering*, eds. J. Lecomte-Beckers, M. Carton, F. Schubert, P. J. Ennis, Forschungszentrum Jülich, Jülich (2002) 1299-1310.
5. Borgenstamm, A.; Engström, A.; Höglund, L.; Ågren, J.: *J. Phase Equilibria* 21 (2000) 269-280.
6. Andersson, J.-O.; Ågren, J.: *J. Appl. Phys.* 72 (1992) 1350-1355.
7. Crusius, S.; Inden, G.; Knoop, U.; Höglund, L.; Ågren, J.: *Z. Metallkd.* 83 (1992) 673-678.
8. Crusius, S.; Höglund, L.; Knoop, U.; Inden, G.; Ågren, J.: *Z. Metallkd.* 83 (1992) 729-738.
9. Franke, P.; Inden, G.: *Z. Metallkd.* 88 (1997) 917-924.
10. Schneider, A.; Inden, G.: *Acta Materialia*, *in press*.
11. Schneider, A.; Inden, G.: in: *Continuum Scale Simulation of Engineering Materials: Fundamentals – Microstructures – Process Applications*, eds. D. Raabe, F. Roters, F. Barlat, L.Q. Chen, Wiley-VCH, Weinheim (2004) 3-36.
12. Inden, G.; Neumann, P.: *Steel Res.* 67 (1996) 401-407.
13. Inden, G.: *Entropie* 202/203 (1997) 6-14.
14. Inden, G.: in: *Thermodynamics, Microstructures and Plasticity*, eds. A. Finel et al.; Kluwer Acad. Publ. (2003) 135-153.
15. Inden, G.; Hutchinson, C.: in: *Proc. Symp. Austenite Formation and Decomposition*, eds. E.B. Damm, M.J. Merwin, ISS and TMS (2003) 65-79.
16. Perez, M.; Deschamps, A.: *Mater. Sci. Eng. A* 360 (2003) 214-219.
17. Robson, J.D.; Bhadeshia, H.K.D.H.: *Mater. Sci. Technol.* 13 (1997) 631-639; 640-644.
18. Fujita, N.; Bhadeshia, H.K.D.H.: *ISI Int.* 41 (2001) 626-640.



Three-Dimensional Atom Probe Studies of Phase Transformations in an Fe-Al-Ni-Cr Alloy with B2-Ordered NiAl Precipitates

A. Schneider¹, C. Stallybrass², G. Sauthoff², A. Cerezo*, G.D.W. Smith*

¹Department of Materials Technology, ²Department of Physical Metallurgy
(*Department of Materials, University of Oxford)

In the search for new high-temperature materials, iron aluminium based alloys show promising properties. The main advantage of Fe-Al alloys is their resistance to high-temperature oxidation and sulphidation which strongly depends on the Al content and is not yet tested for multicomponent systems. In order to improve strength and creep resistance of Fe-Al based alloys at high temperatures, novel alloys with intermetallic NiAl precipitates with B2 structure in a ferritic, disordered (A2) Fe(Al,Ni) matrix are being tested [1,2]. The appropriate combination of phases and optimisation of phase distribution leads to a selection of alloy compositions with relatively low amounts of Al. Consequently, the oxidation resistance becomes questionable. Further alloying with Cr improves the oxidation resistance without affecting the NiAl precipitation. The resulting microstructure with coherent NiAl precipitates in the Fe(Al,Ni,Cr) matrix is analogous to those of the Ni-base superalloys. Thus such Fe-Al-Ni-Cr alloys are considered as the basis for novel ferritic superalloys.

The ternary Fe-Al-Ni system is mainly characterised by a two-phase field between the f.c.c. solid solution of iron and nickel (γ) and the intermetallic Ni₃Al phase on the one hand and between the b.c.c. solid solution of iron and aluminium (α_1) and

the intermetallic B2-ordered NiAl (α_2) phase on the other. Thus alloying of Fe-Al alloys with Ni leads to precipitation of the intermetallic NiAl phase with B2 structure in a ferritic b.c.c. Fe(Al,Ni) matrix. Fig. 1a shows a pseudo-binary section from 97.5Fe-2.5Al to 48.75Ni-51.25Al (at.%) with the miscibility gap of the ternary Fe-Al-Ni system. It contains data from Hao et al. who investigated this miscibility gap in the ternary Fe-Ni-Al system by the diffusion couple technique [3]. The phase separation in an Fe-17.9Al-20.3Ni and in an Fe-17.7Al-11.2Cr-20.2Ni alloy was studied by Ghosh et al. by means of electron microscopy and also atom probe field ion microscopy [4]. They found that both alloys decompose by a spinodal mechanism when quenching from 1300 °C to room temperature.

In this work, the formation of the NiAl phase in an Fe-13.7Ni-17.9Al-9.8Cr (at.%) alloy during different heat treatments has been investigated using field ion microscopy (FIM), 3-dimensional atom probe (3DAP) analysis, differential thermal analysis (DTA), scanning electron microscopy (SEM) and transmission electron microscopy (TEM). Fig. 1b shows a section from 92.31Fe-2.41Al-5.28Cr to 45.3Ni-50.62Al-4.07Cr of the quaternary Fe-Al-Ni-Cr system. It shows a miscibility gap comparable to that of the ternary

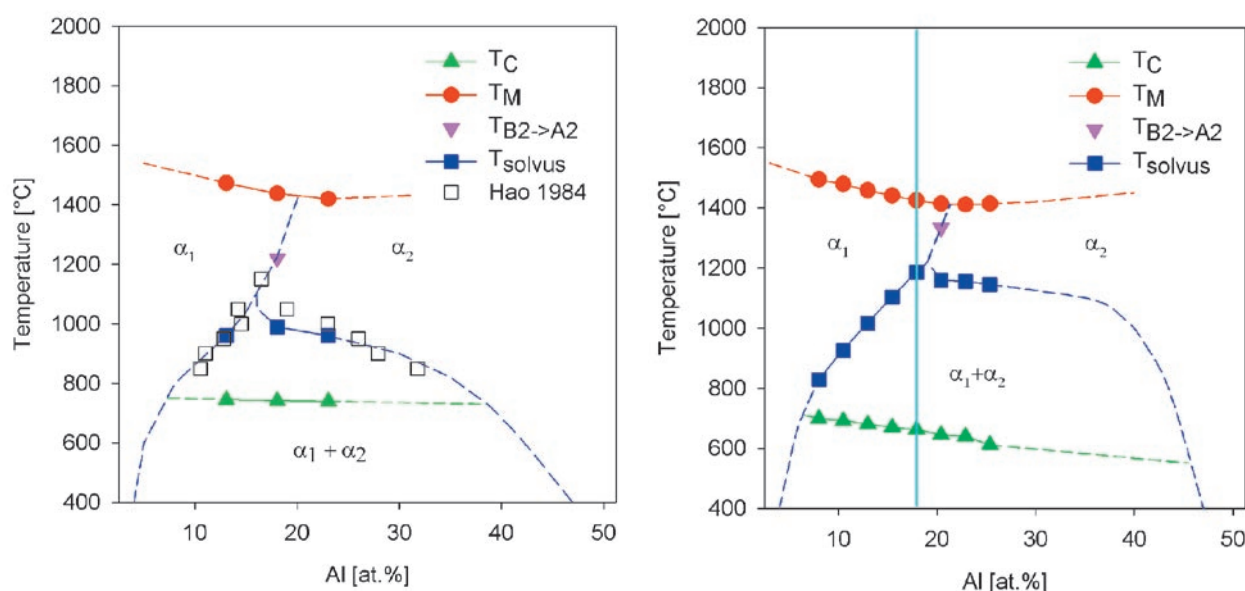


Fig. 1: a) Pseudo-binary section from 97.5Fe-2.5Al to 48.75Ni-51.25Al (at.%) showing the miscibility gap of the ternary Fe-Al-Ni system; b) section from 92.31Fe-2.41Al-5.28Cr to 45.3Ni-50.62Al-4.07Cr of the quaternary Fe-Al-Ni-Cr system.

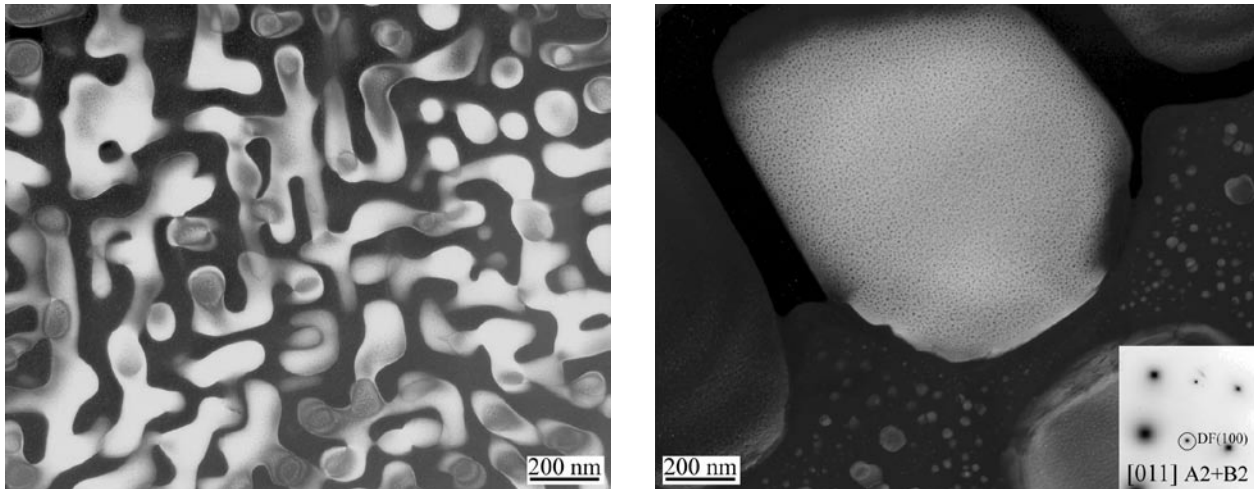


Fig. 2: Dark field TEM images of the Fe-13.74Ni-17.85Al-9.75Cr alloy (at.%): a) after solution treatment (ST) at 1200 °C for 24 h with subsequent air cooling (AC); b) after ST + AC followed by heat treatment at 900 °C for 100 h and AC.

system, but with different transition temperatures. The Curie temperatures change with varying alloy compositions due to the fact that the tie-lines are out of the section plane leading to a variation of the α_1 composition.

SEM and TEM studies revealed complex microstructures typical of spinodally decomposed systems (see Fig. 2a). The dark field TEM images of the Fe-13.74Ni-17.85Al-9.75Cr alloy show microstructures after solution treatment at 1200 °C for 24 h with

subsequent air cooling (Fig. 2a), and after solution treatment at 1200 °C for 24 h with subsequent air cooling, and heat treatment at 900 °C for 100 h with subsequent air cooling (Fig. 2b).

The spots in both phases – α_1 and α_2 – indicate the occurrence of three different precipitation reactions during cooling to room temperature after heat treatment. Apart from the formation of primary α_1 and α_2 phases, it was found by 3DAP investigations of the Fe-13.74Ni-17.85Al-9.75Cr alloy

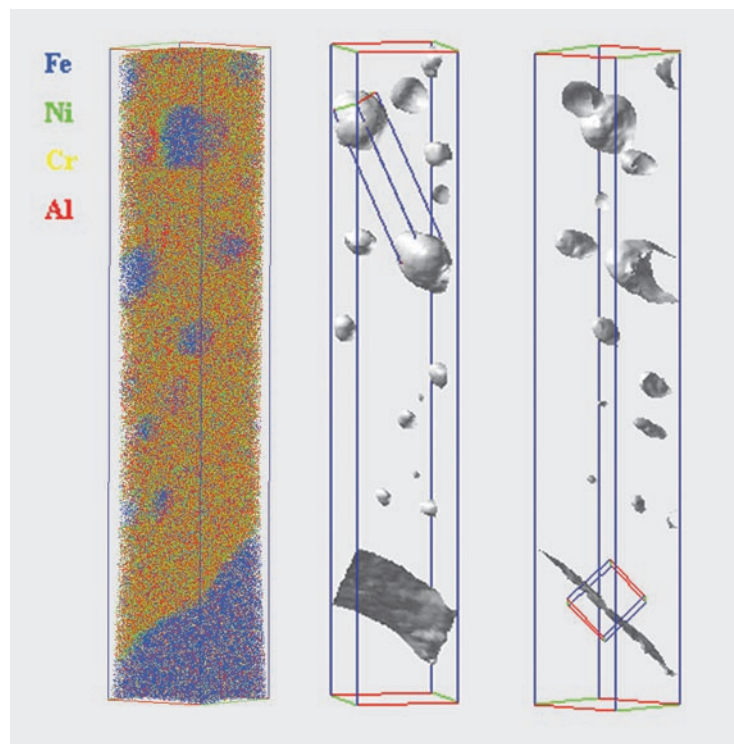


Fig. 3: a) Three-dimensional atom probe map from the Fe-13.74Ni-17.85Al-9.75Cr alloy (at.%) alloy after solution treatment at 1200 °C for 24 h with subsequent air cooling; b, c) Plots of the 50 at% Fe isosurface from two different viewing angles, also showing two different selected volumes, from which the composition profiles of Fig. 4 are taken (Box size: 17.25 nm (red) x 16.63 nm (green) x 96.96 nm (blue)).

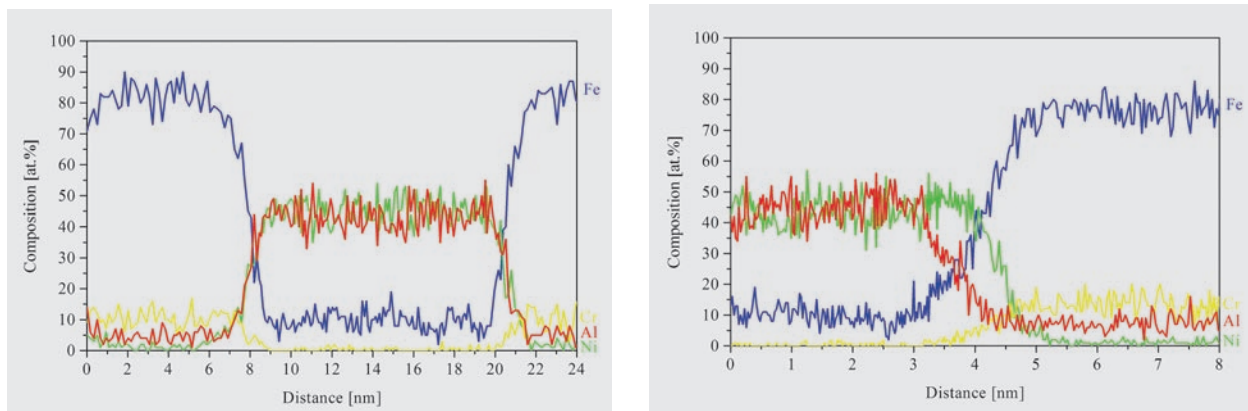


Fig. 4: Composition profiles (a and b) of the selected volumes shown in Fig. 3 b) and c), respectively (Fe-13.74Ni-17.85Al-9.75Cr alloy after solution treatment at 1200 °C for 24 h with subsequent air cooling).

(solution treatment at 1200 °C for 24 h with subsequent air cooling) that very small secondary α_1 precipitates grow in the primary α_2 phase (see Fig. 3). In the primary α_1 phase secondary α_2 precipitates could be identified. The composition profiles in Fig. 4 indicate that the phase separation within the miscibility gap proceeds by a process of nucleation and growth instead of spinodal decomposition. It is possible that the observed microstructure is at the later stages of spinodal decomposition when the final phase composition is reached. However, the observation of a distribution of precipitate sizes with compositions close to the equilibrium value, even

for the smallest precipitates, strongly suggests nucleation and growth.

Field ion microscopy (FIM) was used in this study to identify interesting areas for 3DAP analysis. Fig. 5 shows a FIM image of the Fe-13.74Ni-17.85Al-9.75Cr alloy after solution treatment at 1300 °C for 4 h with subsequent water quench. This particular image was taken after the 3DAP analysis. The dark area in the centre of the FIM image represents the B2-ordered NiAl (α_2) phase and the surrounding bright area stems from the α_2 matrix, as determined by atom probe measurement from the particular areas.

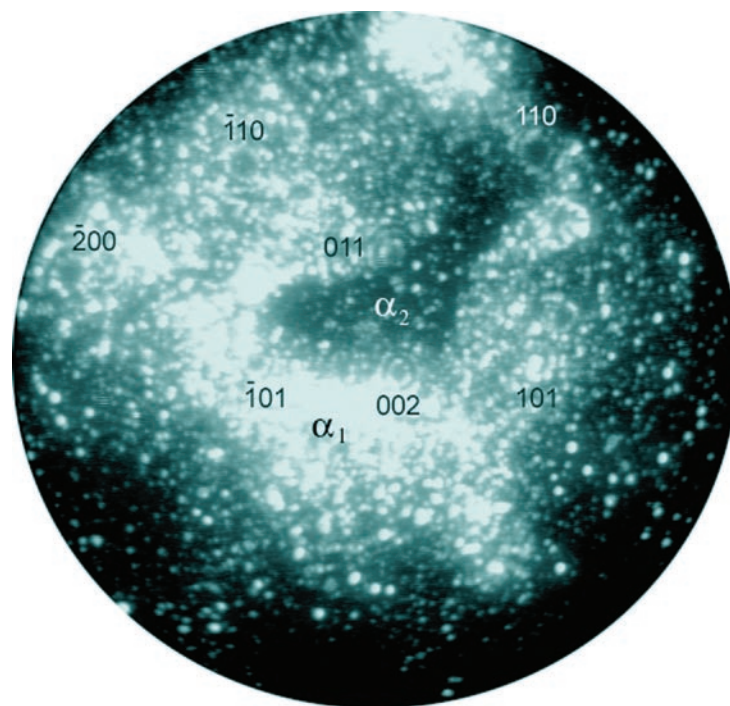


Fig. 5: FIM image of the Fe-13.74Ni-17.85Al-9.75Cr alloy after solution treatment at 1300 °C for 4 h with subsequent water quench. The dark area in the centre of the FIM image represents the B2-ordered NiAl (α_2) phase and the surrounding bright area stems from the α_2 matrix, as determined by atom probe measurement from the particular areas.



Conclusions. Three different precipitation reactions during cooling to room temperature after different heat treatments of an Fe-13.74Ni-17.85Al-9.75Cr alloy were identified using a combination of TEM and 3DAP. During the first reaction, larger scale α_1 and α_2 phases form. Very small secondary α_1 precipitates grow in the primary α_2 phase, whereas in the primary α_1 phase secondary α_2 precipitates could be identified. The composition profiles indicate that the phase separation within the miscibility gap proceeds by a process of nucleation and growth instead of spinodal decomposition.

References

1. Stallybrass, C.; Sauthoff, G.: Mater. Sci. Eng. A, *submitted*.
2. Stallybrass, C.; Schneider, A.; Sauthoff, G.: Intermetallics, *submitted*.
3. Hao, S.M.; Takeyama, T.; Ishida, K.; Nishizawa, T.: Metall. Trans. A 15 (1984) 1819-1828.
4. Ghosh, G.; Olson, G.B.; Kinkus, T.J.; Fine, M.E.: in: Solid-Solid Phase Transformations, eds. W.C. Johnson, J.M. Howe, D.E. Laughlin, W.A. Sofka, TMS, USA (1994) 359-364.



Thermomechanical Treatment, Microstructure and Properties of Ultrafine Grained Steels

R. Song, D. Ponge, D. Raabe, R. Kaspar

Department of Microstructure Physics and Metal Forming

Among the different strengthening mechanisms, grain refinement is the only method to improve both strength and toughness simultaneously. Therefore, ultrafine grained steels with relatively simple chemical composition, strengthened primarily by grain refinement, have a huge potential for replacing low alloyed high strength steels. The main benefits behind such a strategy are to avoid additional alloying elements, to skip complicated additional heat treatments like soft annealing, quenching and tempering, and to improve weldability owing to the reduced required content of carbon and other alloying elements when compared with high strength quenched and tempered steels [1,2]. A further high potential area of ultrafine grained steels is the domain of high strain rate superplasticity at medium and elevated temperatures.

In order to produce ultrafine grained C-Mn steels with a grain size of about 1 μm we developed new processing routes based on a large strain warm deformation. In contrast to other methods which are suitable only to produce ultrafine materials in very small quantities at the laboratory scale, the processing routes developed in this project are suited for the large scale mass production of ultrafine grained steels. In particular, a considerable effort was

made to understand the details of the evolution of microstructure and crystallographic texture during the large strain warm deformation and subsequent annealing treatment. The mechanical properties of the ultra fine grained steels were determined by tensile and impact tests. In the following we discuss our recent work on a plain C-Mn steel (0.22 mass% C, 0.21 mass% Si, 0.76 mass% Mn). Fig. 1 shows the processing route used for the thermomechanical treatment.

Without the large strain deformation the microstructure after the transformation is composed of ferrite with a mean grain size of 6.8 μm and lamellar pearlite. After finishing the complete processing as shown in Fig. 1 the microstructure consists of a ferrite matrix with an average grain size of 1.3 μm and globular cementite (Fig. 2). For the grain size determination by the linear intercept method only high angle grain boundaries with a misorientation angle of $\theta \geq 15^\circ$ were considered.

Fig. 3 shows the effect of the refinement of the microstructure due to the warm deformation on the yield stress and ductile-to-brittle transition temperature of the steel. It shows that it is possible to

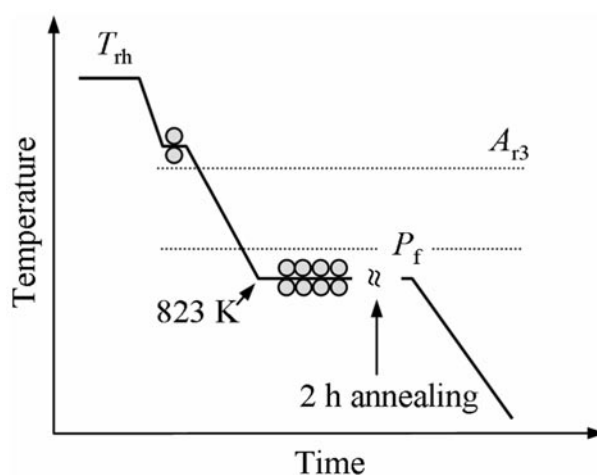


Fig. 1: Example of a large scale processing route to produce ultrafine grained steel. The samples were deformed 100 K above the A_{r3} -temperature in order to obtain a fine recrystallized austenite grain structure, cooled at a rate of 6.5 K/s down to 823 K to yield a fine ferritic-pearlitic microstructure without bainite and subsequently deformed by 4 passes each imposing a strain of 0.4. The industrial cooling was simulated by holding for 2 h at 823 K and a subsequent air cooling.

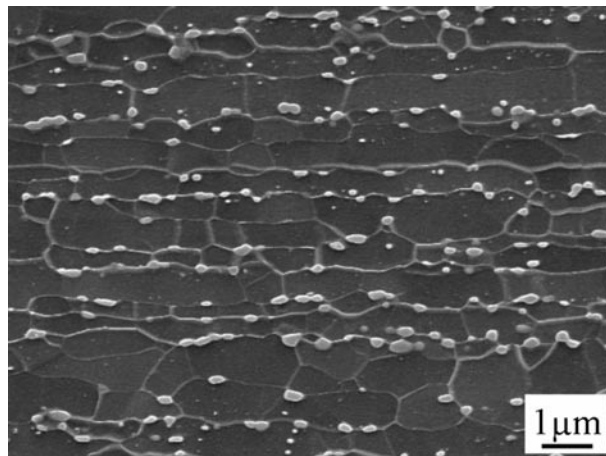


Fig. 2: Microstructure of the plain C-Mn steel after the processing given in Fig. 1.

obtain a considerable improvement of the mechanical properties in a plain C-Mn steel by an ultra grain refinement.

In order to introduce thermomechanical process routes for ultra grain refinement at large scales, it is essential to understand the mechanisms leading to this outstanding refinement of the microstructure during the warm deformation.

The main challenge of the thermomechanical process consists in the transformation of a microstructure with *coarse* initial ferrite and *lamellar* cementite into an *ultra fine* ferrite matrix with a uniform distribution of fine *globular* cementite. Therefore, an optimized warm deformation should lead to a rapid spheroidization of the cementite lamellae in the pearlite regions, a redistribution of cementite and in particular to the formation of new *high angle* grain boundaries in the ferrite matrix. A key point to reach these goals is a high density of lattice defects during the warm deformation. Because

static recrystallization during the interpass times would entail a significant reduction of the density of the lattice defects, it slows down the microstructural changes described above. In this case a complete cementite spheroidization for example is hardly possible.

By conducting a systematic study on steels with different carbon and manganese contents using different quenching strategies after intermediate strains in conjunction with a detailed characterization of the microstructure evolution it was possible to identify the governing mechanisms which determine the extreme grain refinement during the large strain deformation and the subsequent coiling [3-5]: Our study of the grain boundary character evolution by electron backscattering diffraction (EBSD) revealed, that during the warm deformation low angle grain boundaries are introduced into the grains. The misorientation of these new grain boundaries increases with increasing strain. This effect leads to

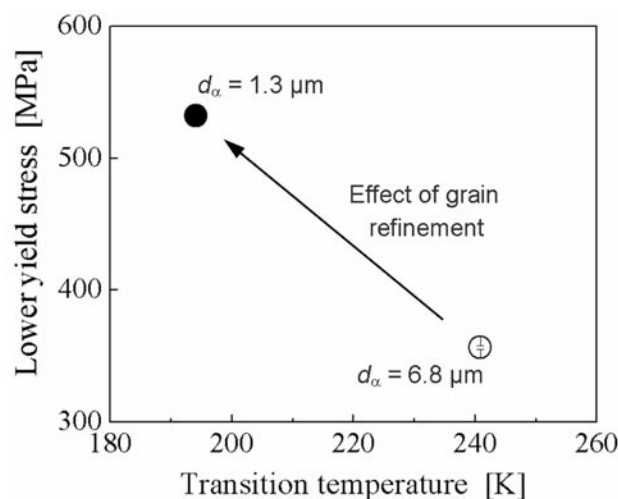


Fig. 3: Improvement of yield stress and ductile-to-brittle transition temperature by grain refinement.

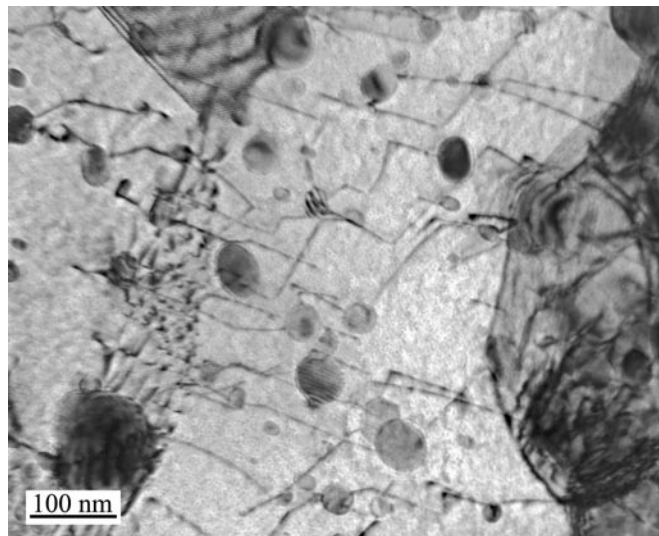


Fig. 4: TEM micrograph of the steel after the processing given in Fig. 1.

the gradual formation of new *high* angle grain boundaries. After a true logarithmic strain of 1.6 the fraction of high angle grain boundaries ($\theta \geq 15^\circ$) amounted to about 60% in this steel. A TEM investigation leads to the result that after the warm deformation and even after the coiling simulation the ferrite grains contain dislocations pinned by cementite particles (Fig. 4).

Together with the results of the texture development it can be concluded that during an optimized warm deformation a combination of continuous recrystallization and plastic deformation leads to the desired microstructural changes. During the coiling some additional microstructural changes can take

place: Controlled by some coarsening of the cementite particles an extended recovery leads to limited grain boundary migration. The result is a more equiaxed grain shape after the coiling process.

The main guidelines with respect to an industrial application of the methods described in this paper are as follows:

The process window for the warm deformation temperature should be limited to values where no recrystallization takes place during the processing. Otherwise the warm deformation is not efficient in refining the grains, spheroidizing the cementite lamellae, and redistributing the cementite. This

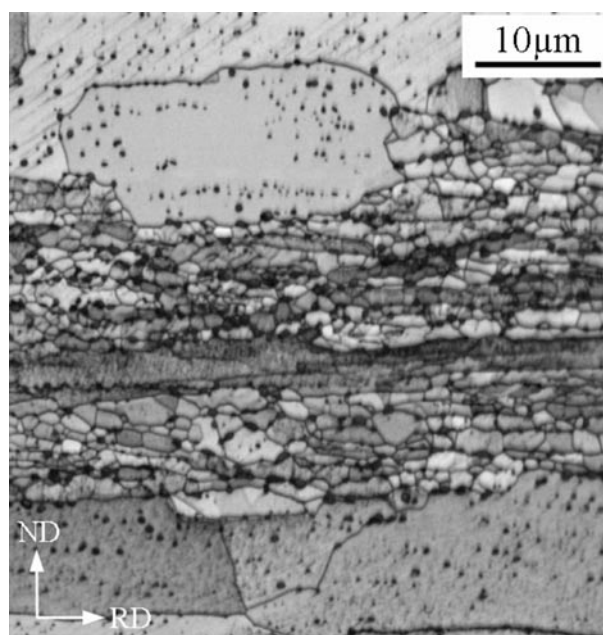


Fig. 5: EBSD image quality map of the steel after large strain deformation ($\epsilon = 1.6$) at 823 K and subsequent 2 h annealing treatment at 973 K.



applies also to the annealing temperature after the warm deformation. Fig. 5 gives an example of the effect of annealing for 2 h at a too high temperature of 973 K.

In steels with a higher carbon content recrystallization is suppressed by the high volume fraction of fine cementite particles even at higher temperatures, leading to a large process window. In steels with a lower carbon content correspondingly the process window is smaller. For a steel with 0.15 mass% C it is difficult in particular to obtain a homogeneous distribution of cementite after the processing.

References

1. Hodgson, P.D.; Hickson, M.R.; Gibbs, R.K.: *Scr. Mater.* 40 (1999) 1179.
2. Kaspar, R.; Distl, J.S.; Pawelski, O.: *Steel Res.* 59 (1988) 421.
3. Song, R.; Ponge, D.; Kaspar, R.; Raabe, D.: *Z. Metallkd.* 95 (2004) 513.
4. Song, R.; Ponge, D.; Raabe, D.; Kaspar, R.: *Acta Mater.* 2004; *in press*.
5. Storojeva, L.; Ponge, D.; Kaspar, R.; Raabe, D.: *Acta Mater.* 52 (2004) 2209.



Precipitation Behaviour and Mechanical Properties of (Ni,Fe)Al-Strengthened Fe-Al-Ni-Cr Alloys

C. Stallybrass¹, A. Schneider², G. Sauthoff¹

¹ Department of Physical Metallurgy, ² Department of Materials Technology

Nickel-base superalloys form an important group of high-temperature materials. Their development was driven by the need for materials with a high creep resistance at temperatures where austenitic steels are no longer sufficient, especially for the application in aircraft turbines. In order to achieve these high levels of creep resistance, they rely on a combination of solid solution and precipitate strengthening. The latter is achieved by a variety of phases, in particular by the L1₂-ordered Ni₃Al, known as γ' , which has a lattice parameter close to that of the fcc γ -matrix. Therefore, a homogeneous distribution of coherent γ' precipitates in a γ -matrix can be achieved. These alloys have reached an extraordinary degree of sophistication which makes operating temperatures of about 1100 °C, i.e. around 80% of the melting temperature, possible [1].

Compared to austenitic steels and Ni-base superalloys, ferritic materials generally offer better thermal conductivity, lower thermal expansion and lower density [2,3] – all of which are desirable properties for a high-temperature material. Their strength at temperatures above 600 °C is, however, insufficient for structural applications [4]. In the Fe-Al-Ni system, there is a miscibility gap between a ferritic, iron-rich phase and a B2-ordered (Ni,Fe)Al phase [5,6]. Since

the lattice parameters of both phases are nearly equal [7], microstructures similar to those of Ni-base superalloys can be realized. Chromium, which distributes mostly to the ferritic phase [8], is added because it reduces the aluminium content in the ferritic phase necessary to form a protective alumina scale [9]. The aim of this project is to investigate the precipitation behaviour and the effect of the (Ni,Fe)Al precipitates on the mechanical properties at elevated temperatures.

Precipitation behaviour. The miscibility gap in the Fe-Al-Ni system lies between the iron corner and NiAl. It extends up to a temperature of about 1100 °C [5,6]. The volume fraction of (Ni,Fe)Al-phase can be varied by changing the composition of alloys within the miscibility gap. Thereby, microstructures which consist mainly of the ferritic phase with (Ni,Fe)Al-precipitates can be obtained or vice versa. During air cooling from the solution treatment temperature of 1200 °C, precipitates with a size of around 50 nm form. TEM investigations of Fe-Al-Ni-Cr alloys revealed an additional fraction of (Ni,Fe)Al-precipitates within the ferritic matrix and Fe-rich precipitates within the 50nm (Ni,Fe)Al-phase, both with a size of around 5 nm [10]. When annealed at 900 °C within the miscibility gap, the precipitates coarsen with a

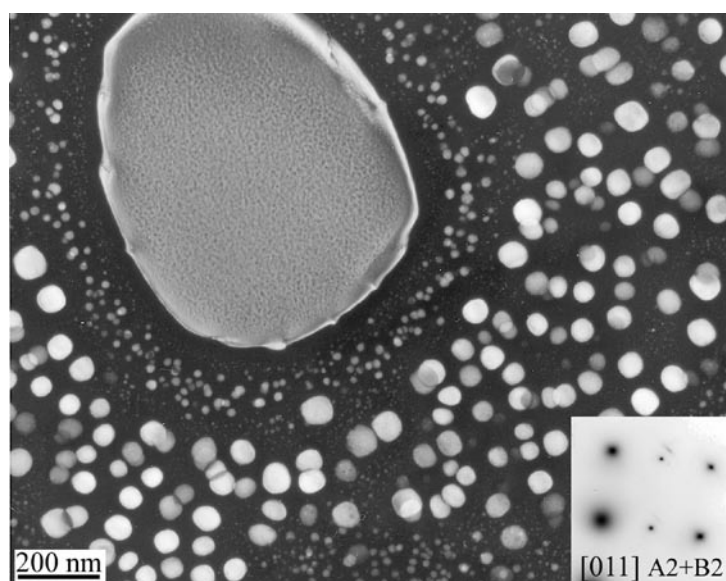


Fig. 1: Dark-field TEM micrograph of a Fe-Al-Ni-Cr alloy aged at 900 °C and air-cooled.



linear dependence between precipitate size and the cube root of aging time [11], as predicted by Ostwald ripening theory. In addition, secondary precipitates with a size around 50 nm and below form during cooling within the matrix and the primary (Ni,Fe)Al-phase due to decreasing solubilities for the elements

of the other phase [10]. Fig. 1 shows a coarsened (Ni,Fe)Al precipitate and secondary cooling precipitates of various sizes within the ferritic matrix. These secondary precipitates can be coarsened in a second aging treatment at a lower temperature. Within this project, a two-step aging treatment consisting of a primary aging step at 900 °C for 48 h followed by secondary aging at 750 °C for 300 h was investigated. TEM investigations showed that the 50 nm sized secondary precipitates were not present, but 5 nm precipitates were still observed. These are believed to form during cooling after the secondary aging step.

The difference in lattice parameter of both phases gives rise to an elastic stress field around the precipitates. The system minimizes the elastic energy by an alignment of the precipitates in the elastically soft directions [12]. The larger the difference in lattice parameters, the stronger is this tendency of the precipitates to align. The lattice parameters of both phases depend on their respective compositions. If a composition within the miscibility gap closer to the Al-corner is selected, then the lattice parameter misfit can be reduced. This is shown in Fig. 2 which compares the microstructures of a ternary Fe-Al-Ni alloy with that of a quaternary Fe-Al-Ni-Cr alloy, both with a composition based on the section $Fe_{0.975}Al_{0.025}-Ni_{0.4875}Al_{0.5125}$ and that of another quaternary alloy with a composition based on the section $Fe_{0.925}Al_{0.075}-Ni_{0.4625}Al_{0.5375}$. The volume fraction is similar in the three cases. The degree of anisotropy of the precipitate distribution decreases considerably from the ternary to the Al-rich quaternary alloy, as mirrored by the decrease in anisotropy of the Fourier spectra of the images. This coincides with a drop in the constrained lattice misfit from 0.27% to about 0.05%.

Mechanical properties. In compression tests between room temperature and 1000 °C [11], the 0.2% yield stress did not depend on the volume fraction of primary (Ni,Fe)Al-phase up to 600 °C, but on the volume fraction of secondary precipitates. Therefore, the highest yield stresses were observed after air cooling from the solution treatment temperature, where all precipitates are around 50 nm and below, and lower values were found after aging at 900 °C or 750 °C followed by air cooling. Depending on the heat treatment state, the yield stress at room temperature was between 832 MPa and 1052 MPa. It is believed that the secondary precipitates, which form during cooling from an aging treatment within the miscibility gap, contribute mostly to the strength at low temperatures, which was also reported for Ni-base superalloys [13]. The volume fraction of secondary precipitates, which depends on the composition of the matrix, should be roughly equal for all alloys, as long as their compositions lie within the miscibility gap at the temperature of aging. At higher temperatures, however, the secondary precipitates will themselves either coarsen or

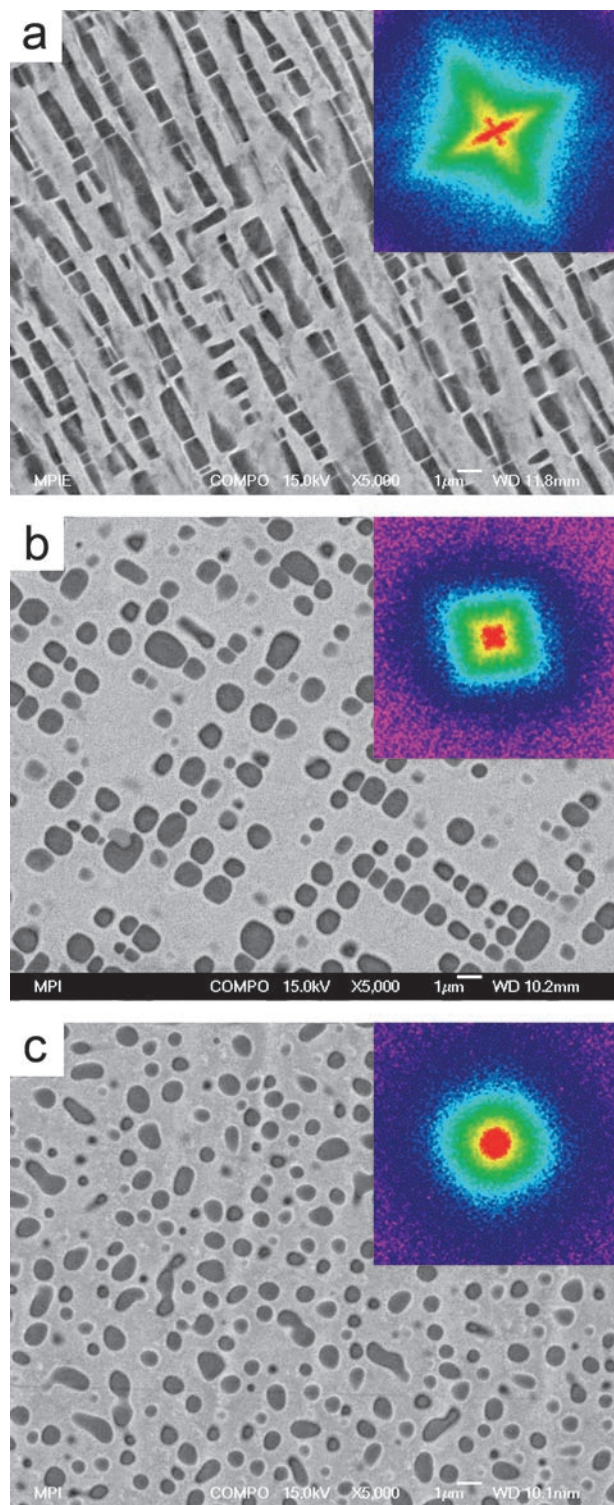


Fig. 2: SEM micrographs and Fourier spectra of a ternary Fe-Al-Ni alloy (a), a Fe-Al-Ni-Cr alloy with a composition based on the section $Fe_{0.975}Al_{0.025}-Ni_{0.4875}Al_{0.5125}$ (b) and a Fe-Al-Ni-Cr alloy with a composition based on the section $Fe_{0.925}Al_{0.075}-Ni_{0.4625}Al_{0.5375}$ (c).

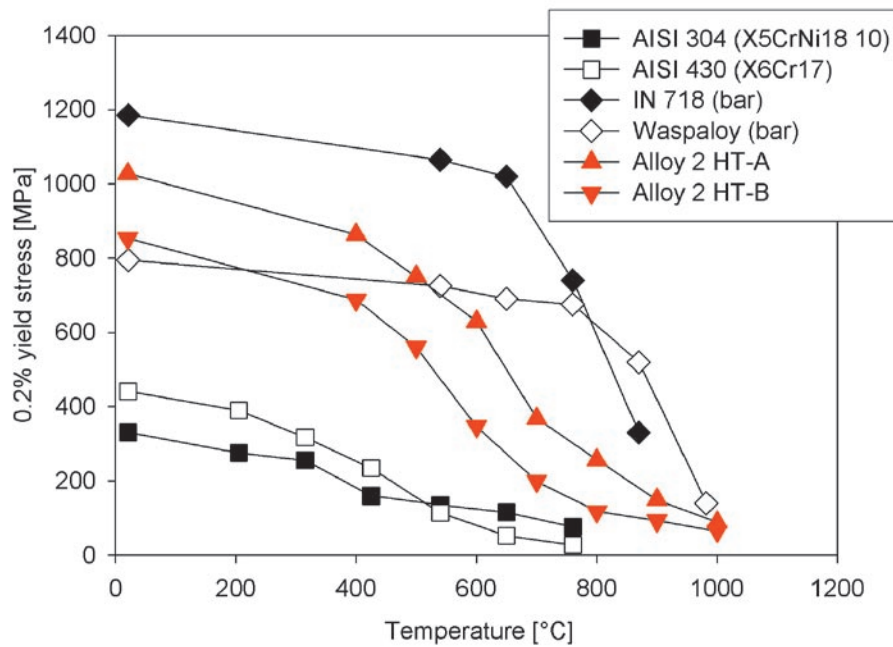


Fig. 3: Comparison of the 0.2% yield stress of alloy 2 (Fe 12.5Ni 21.5Al 10.0Cr) with 37 vol.% of (Ni,Fe)Al, tested after the solution treatment (HT-A) and after aging for 1000 h at 750 °C (HT-B), with other high temperature materials [2,3,15].

dissolve in the matrix and therefore will no longer contribute significantly to the strength. Now the primary precipitates take over. Above 600 °C, the yield stress was observed to increase with increasing volume fraction of the (Ni,Fe)Al-phase in all states of heat treatment. At 700 °C after the two-step aging treatment, the values for investigated quaternary alloys ranged from 121 MPa for alloys with a volume fraction of 9% to 224 MPa for alloys with a volume fraction of 37%. In Fig. 3, the yield stresses of several conventional high-temperature materials are compared to a Fe-Al-Ni-Cr alloy with 37 vol.% of (Ni,Fe)Al in two heat treatment conditions.

The two-step aging led to an increase of ductility. In four-point bending experiments, the temperature at which 4% of strain could be reached without traces of cracks on the tension side of the samples decreased from a range between 700 °C and >1000 °C in the solution treated condition down to between 400 °C and 500 °C. It is believed that this improved ductility is due to a lower volume fraction of secondary precipitates. The material tested had grain sizes of up to several mm. Further improvement of the ductility is expected if the grain size is reduced and the heat treatment is optimized.

Creep tests with a stepwise load increase were carried out in compression between 600 °C and 800 °C. The results of creep tests at 750 °C on alloys with between 9 vol.% and 37 vol.% of (Ni,Fe)Al after the two-step aging treatment are shown in Fig. 4. Up to 750 °C and within the range of investigated secondary creep rates, the dependence of the secondary creep rate of aged alloys on the stress

can be described by a power law if a threshold stress is introduced [14]. This behaviour is common in particle strengthened materials. The threshold stress increased with the volume fraction of precipitates. After two-step aging, threshold stresses between 32 MPa for the alloy with the low volume fraction and 73 MPa for the alloy with the high volume fraction of precipitates were observed at 750 °C [10]. In the solution-treated condition and at 800 °C, the creep behaviour deviated from this behaviour because the precipitate size is no longer stable during the experiment.

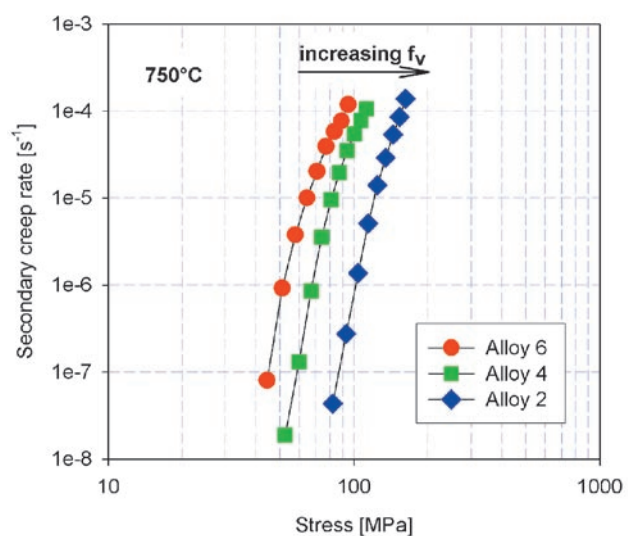


Fig. 4: Secondary creep rate versus stress of selected alloys tested at 750 °C after the two-step aging treatment with between 9 and 37 vol.% of (Ni,Fe)Al.



Conclusions. Understanding the precipitation process is essential for material development. Within the framework of this project, the evolution of the microstructure of ferritic alloys with (Ni,Fe)Al precipitates was investigated from the early stages of precipitation to coarsening. It was found that the constrained lattice misfit played an important role in the evolution of the microstructure, as it leads to particle interactions and an anisotropic distribution of precipitates. The constrained lattice misfit can be reduced and an isotropic particle distribution achieved by careful selection of the alloy composition within the miscibility gap.

The mechanical tests showed that the strengthening effect of (Ni,Fe)Al precipitates is significant. The yield stress above 600 °C and the threshold stress between 600 °C and 750 °C both depended on the volume fraction of (Ni,Fe)Al. The strength levels observed show that these alloys, which may be regarded as ferritic superalloys, have a potential for application up to 750 °C.

References

1. Durand-Charre, M.: *The Microstructure of Superalloys*, Gordon and Breach, Amsterdam (1997).
2. Rothman, M.F. (ed.): *High-Temperature Property Data: Ferrous Alloys*, ASM, Metals Park, OH, USA (1988).
3. High temperature, high strength nickel base alloys, Inco Limited, New York, NY, USA (1977).
4. Masuyama, F.: *Isij Int.* 41 (2001) 612-625.
5. Bradley, A.J.: *J. Iron Steel Inst.* (1951) 233-245.
6. Hao, S.M.; Takayama, T.; Ishida, K.; Nishizawa, T.: *Metall. Trans. A* 15 (1984) 1819-1828.
7. Calderon, H.; Fine, M.E.: *J. Met.* 35 (1983) 122-122.
8. Hao, S.M.; Ishida, K.; Nishizawa, T.: *Metall. Trans. A* 16 (1985) 179-185.
9. Tomaszewicz, P.; Wallwork, G.R.: *Corros.* 40 (1984) 152-157.
10. Stallybrass, C.; Schneider, A.; Sauthoff, G.: *Intermetallics*, *submitted*.
11. Stallybrass, C.; Sauthoff, G.: *Mater. Sci. Eng. A*, *submitted*.
12. Su, C.H.; Voorhees, P.W.: *Acta Mater.* 44 (1996) 2001-2016.
13. Beardmore, P.; Davies, R.G.; Johnston, T.L.: *Trans. Metall. Soc. AIME* 245 (1969) 1537-1545.
14. Gibeling, J.C.; Nix, W.D.: *Mater. Sci. Eng.* 45 (1980) 123-135.
15. Sims, C.T.; Stoloff, N.S.; Hagel, W.C. (eds.): *Superalloys II*, John Wiley & Sons, New York, NY, USA (1987).



Theoretical and Experimental Investigations of Structure Type Variations of Laves Phases

F. Stein¹, M. Palm¹, J. Konrad², D. Jiang^{1*}, G. Sauthoff¹

¹Department of Physical Metallurgy, ²Department of Microstructure Physics and Metal Forming
(*now at Katholieke Universiteit Leuven, Belgium)

Laves phases form the largest group of intermetallic compounds. Especially in the last ten years there is a renewed interest in Laves phases as they have become candidates for several functional as well as structural applications. The most prominent example for the first group of applications is the utilization of Laves phases as hydrogen storage materials especially in nickel-metal hydride batteries on the basis of the Laves phase $Zr(V,Mn,Ni)_2$. Moreover, they are candidates for magnetoelastic transducers ($(Tb,Dy)Fe_2$) and show promising superconducting properties ($(Hf,Zr)V_2$). In view of structural applications, Laves phases are attractive because of their high strength up to high temperatures. The principal shortcoming is their pronounced brittleness at ambient temperatures which has been tried to overcome by combining Laves phases with a ductile phase [1,2].

Laves phases have the general formula AB_2 and can crystallize in three different structure types: the cubic $MgCu_2$ type (C15), the hexagonal $MgZn_2$ type (C14), and the hexagonal $MgNi_2$ type (C36). The crystallographic structures of the three polytypes are closely related as is visualised in Fig. 1 [3]. They differ only by the particular stacking of the same four-layered structural units. As a consequence of this close relationship, the differences in total energies between the polytypes are generally very small and in many transition metal systems, two or three Laves phase polytypes coexist in equilibrium showing tem-

perature-, composition- and/or pressure-dependent transformations.

Geometric and electronic factors such as the atomic size ratio of the A and B atoms and their valence electron numbers are well known to affect the occurrence of a Laves phase and various simple models based on these factors have been developed aiming at a prediction of the stable polytype. In a recent review paper, we have critically assessed these factors. It could be clearly shown that the existing models and calculations fail in giving general predictions of the occurrence and structure type of Laves phases [4]. An example is shown in Figs. 2 and 3. In the ternary system Fe-Al-Zr, the binary Laves phases $ZrFe_2$ (cubic C15) and $ZrAl_2$ (hexagonal C14) form a continuous series of solid solutions with a threefold change of the stable polytype along the section $ZrFe_2$ - $ZrAl_2$ from C15 to C14 back to C15 and again to C14; see Fig. 2 [5]. Such multiple changes of the stable polytype have indeed been predicted in theoretical calculations as a function of the number of valence electrons, and an example is shown in Fig. 3 [6]. In the lower part of Fig. 3, the calculated stability ranges of the different polytypes are compared with experimental results for the above mentioned Fe-Al-Zr system and for the Fe-Al-Sc system [7]. Obviously, there is no good correspondence between experiment and theory, and a comparison between the two experimentally determined systems already shows that a description only on the basis of the number of valence electrons can not be successful.

In close cooperation with the Max-Planck-Institut für Chemische Physik fester Stoffe (Prof. Y. Grin, Dr. G. Kreiner) in Dresden, fundamental experimental and theoretical investigations on Laves phases in selected transition metal systems are currently performed in order to study problems concerning the occurrence and stability of Laves phases. In the framework of this cooperation, the series of Laves phases-containing systems Nb-X (X = Cr, Mn, Fe, Co) is investigated as the scarce information from the literature indicates that the phase diagrams of the systems of this series differ strongly from each other in the composition range of the Laves phases and at least in two of these systems (Cr-Nb, Co-Nb) more than one Laves phase polytype was observed.

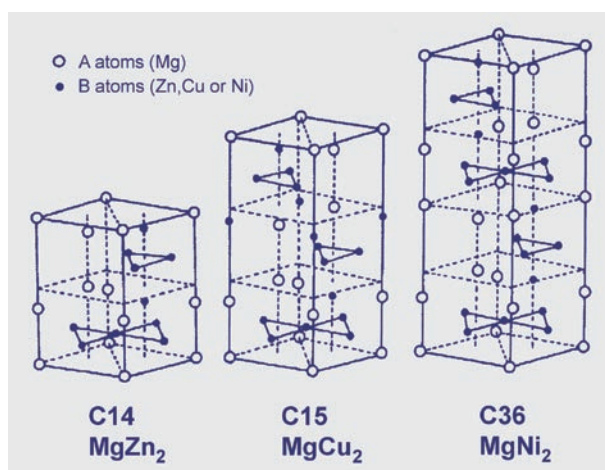


Fig. 1: The three polytypes of the Laves phase structure in a hexagonal setting (taken from [3]).

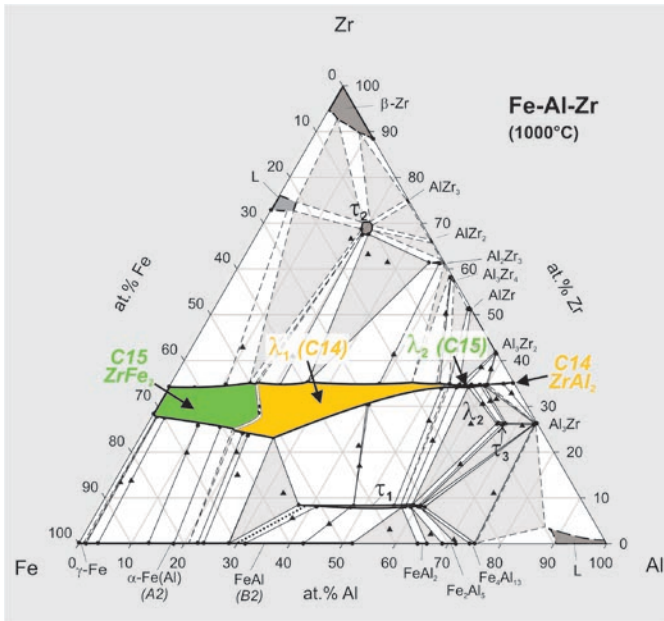


Fig. 2: Isothermal section at 1000 °C of the Fe-Al-Zr phase diagram showing the threefold change of the Laves phase polytype.

Perhaps the most interesting phase diagram is that of the Co-Nb system which was experimentally investigated in this institute. Some uncertainty exists in the literature concerning the phase diagram in the composition range of the Laves phase [8-10]. From detailed investigations of as-cast and heat-treated alloys of various compositions as well as diffusion couples by a combination of different experimental methods (electron-probe microanalysis (EPMA), differential thermal analysis (DTA), X-ray diffraction (XRD), and light-optical and scanning electron microscopy (SEM)), the phase diagram shown in Fig. 4 was established [11]. The co-existence of the three Laves phase polytypes C14, C15 and C36 in this system was confirmed. At and around the stoichiometric composition, the cubic C15 polytype is stable up to its congruent melting point at 1484 °C. Its homogeneity range is strongly extended to the Co-rich side reaching from 64 up to about 74 at.% Co. Besides the cubic C15 Laves phase polytype, the hexagonal C14 and C36 polytypes were found. Both occur at off-stoichiometric compositions, C14 near 64 at.% Co and C36 at 75 at.% Co (hence often designated as Nb₉Co₁₆ and NbCo₃, respectively), and both are stable only at high temperatures and in small homogeneity ranges. Both hexagonal polytypes form by a peritectic reaction from the melt, which can be clearly determined by DTA experiments. They decompose during cooling by eutectoid reactions into the cubic Laves phase plus NbCo (in case of the C14 polytype) or plus

Nb₂Co₇ (in case of the C36 polytype). Both eutectoid reactions are so slow that large amounts of the hexagonal Laves phases are maintained at room temperature after cooling and only dissolve after long-term heat treatments below the eutectoid temperatures.

Between the C14 and C15 Laves phase fields, a small two-phase field was detected by measuring concentration profiles in Nb/NbCo₂ (66.7 at.% Co) diffusion couples after heat treatments at 1280 and 1350 °C. For both temperatures, a step of about 1 at.% was observed in the concentration profiles measured by EPMA.

Diffusion couples which were composed of the cubic NbCo₂ Laves phase and pure Co and annealed at temperatures in the range between about 1100 and 1200 °C should contain the hexagonal C36 Laves phase besides the cubic polytype as can be expected from the phase diagram in Fig. 4. A respective concentration profile (Fig. 5) shows the steep concentration step between the Co(Nb) solid solution and the Laves phase with a composition typical for that of the C36 polytype. However, in contrast to the above diffusion couples with C14 and C15 Laves phase, no concentration step is visible which would indicate the transition from the C36 to the C15 Laves phase polytype. As the investigations of heat-treated alloys in the respective composition range had clearly proven the existence of the C36 Laves phase polytype, the two-phase field must be too narrow to be detected in the concentration profile (i.e. below

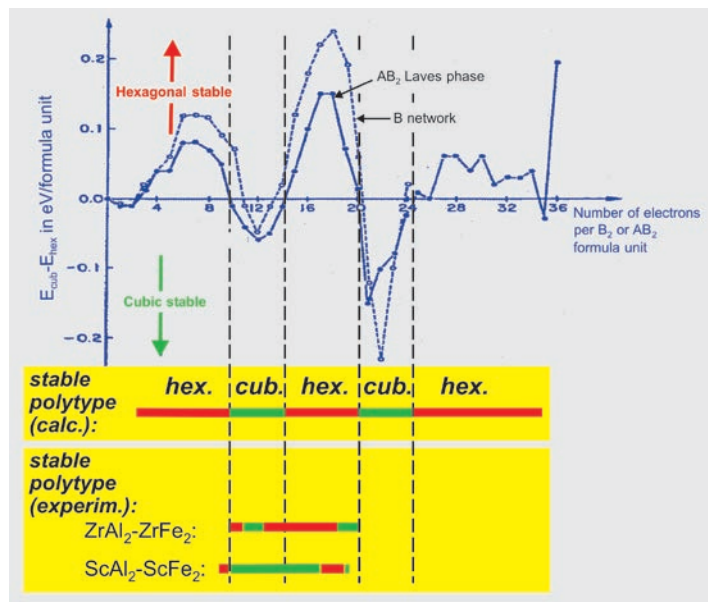


Fig. 3: Change of the stable Laves phase polytype as a function of the number of valence electrons per AB₂ formula unit as obtained from extended Hückel tight binding calculations [6], and observed structure changes in the Fe-Al-Zr (s. Fig. 2) [5] and Fe-Al-Sc [7] systems.

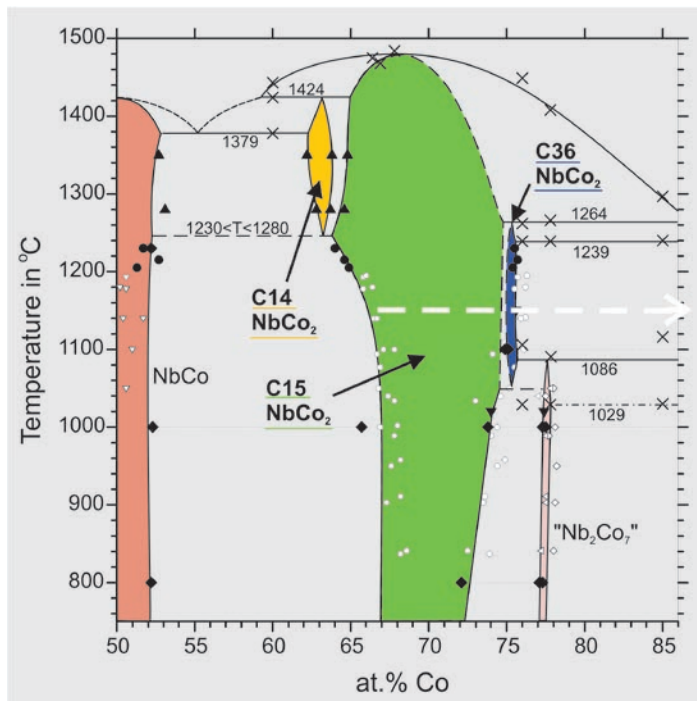


Fig. 4: Part of the Co-Nb phase diagram as obtained by EPMA on diffusion couples (black circles and triangles) and alloys of fixed compositions (diamonds) and by DTA (crosses) [11]. Earlier diffusion couple results from [9] (small white circles) are added. The white arrow indicates the diffusion couple shown in Fig. 5.

about 0.5 at.%) or C36 simply is not present in the diffusion couples. It is well-known that the formation of equilibrium phases may be hindered in diffusion couples due to kinetic reasons [12].

In order to solve this problem, the phases in the NbCo_2/Co diffusion couple were analysed in a high-resolution field emission scanning electron microscope equipped with a high-speed electron back-scatter diffraction (EBSD) system. A complete phase mapping across the phase boundaries in a strip $30\ \mu\text{m}$ wide was obtained by measuring with a step width of $300\ \text{nm}$. Fig. 6 shows the microstructure and colour-coded EBSD mappings of the phases (middle) and their crystallographic orientations (bottom). Four characteristic Kikuchi patterns measured in the different phase fields are added. The diffraction bands were indexed using the Hough transformation method. It can be clearly seen that the hexagonal C36 Laves phase has formed in a zone about $20\ \mu\text{m}$ wide between the C15 Laves phase and the fcc $\text{Co}(\text{Nb})$ solid solution. This result confirms that C36 NbCo_2 is an equilibrium phase of

the Co-Nb system as had been found in the investigation of heat-treated alloys of re-spective compositions, and it can be concluded that the extension of the two-phase field between the C15 and C36 Laves phase polytypes must be below about 0.5 at.%. In an earlier investigation of the Laves phases in the Fe-Zr system, we found a very similar behaviour concerning the occurrence of the different Laves phase polytypes [13]. Whereas the cubic C15 polytype exists at the stoichiometric composition and is stable up to its congruent melting point, the C36 polytype was observed at an off-stoichiometric composition and at high temperatures only. From detailed experimental investigations of the Laves phases as reported above for various systems and by critically assessing and evaluating a large number of phase diagrams reported in the literature with more than one Laves phase polytype, we found that the Co-Nb system shows a prototypic behaviour concerning the occurrence of Laves phases. In systems with two or three Laves phases, the C15 polytype always occurs at the stoichiometric composition and the hexagonal polytypes are only found at off-stoichiometric compositions and high temperatures. In some systems as e.g. Cr-Nb a temperature-dependent transformation of the Laves phase was observed. In these cases, the C15 polytype is always the low-temperature phase and the hexagonal polytypes occur at high temperatures. These and other general features of the polytypism of Laves phase are

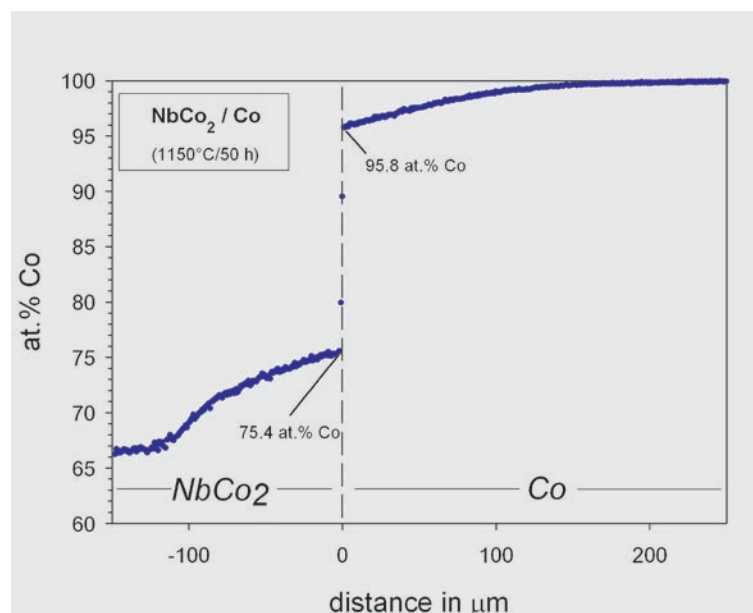


Fig. 5: Concentration profile measured by EPMA in a NbCo_2/Co diffusion couple which was annealed for 50 h at $1150\ \text{°C}$.

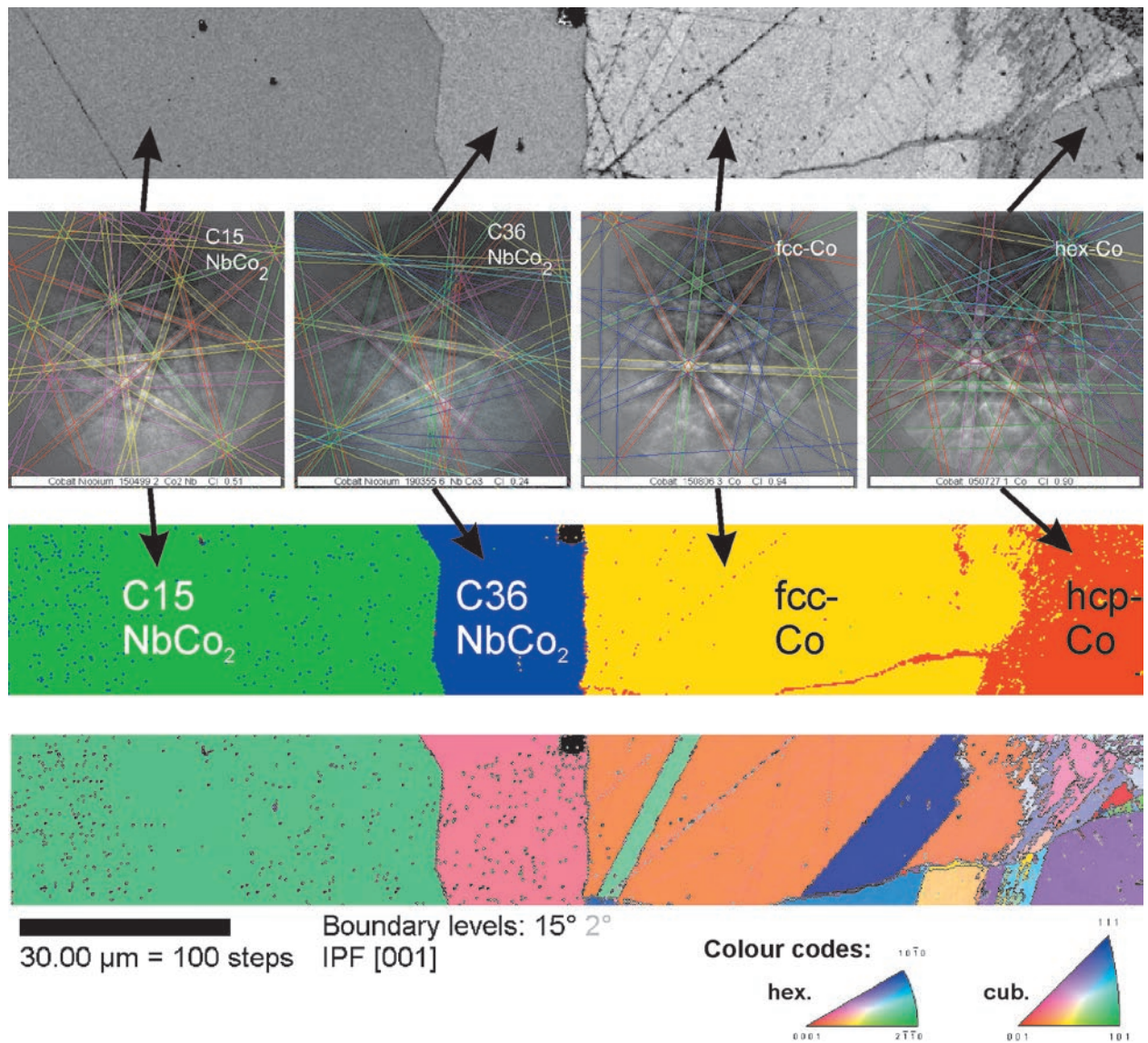


Fig. 6: Results of EBSD investigations of a NbCo_2/Co diffusion couple (50 h at 1150 °C) showing from the top to the bottom a micrograph of the microstructure, characteristic Kikuchi patterns of the four phases, and two colour-coded EBSD mappings of the phases and the crystallographic orientations, respectively

discussed in more detail in [14].

References

- Sauthoff, G.: Intermetallics, VCH, Weinheim, Germany (1995) 1-165.
- Sauthoff, G.: Intermetallics 8 (2000) 1101-1109.
- Kitano, Y.; Takata, M.; Komura, Y.: J. Microsc. 142 (1986) 181-189.
- Stein, F.; Palm, M.; Sauthoff, G.: Intermetallics 12 (2004) 713-720.
- Stein, F.; Sauthoff, G.; Palm, M.: Z. Metallkd. 95 (2004) 469-485.
- Johnston, R.L.; Hoffmann, R.: Z. Anorg. Allg. Chem. 616 (1992) 105-120.
- Dwight, A.E.; Kimball, C.W.; Preston, R.S.; Taneja, S.P.; Weber, L.: J. Less-Common Met. 40 (1975) 285-291.
- Massalski, T.B.; Okamoto, H.; Subramanian, P.R.; Kacprzak, L.: Binary Alloy Phase Diagrams, 2nd ed., ASM, Materials Park, OH, USA (1990).
- Sprengel, W.; Denking, M.; Mehrer, H.: Intermetallics 2 (1994) 127-135.
- Okamoto, H.: J. Phase Equilibria 21 (2000) 495.
- Stein, F.; Jiang, D.; Sauthoff, G.; Palm, M.: unpublished results, presented at TOFA 2004 (Discussion Meeting on the Thermodynamics of Alloys), Vienna, 12.-17.09.2004 (2004).
- Williams, D.S.; Rapp, R.A.; Hirth, J.P.: Thin Solid Films 142 (1986) 47-64.
- Stein, F.; Sauthoff, G.; Palm, M.: J. Phase Equilibria 23 (2002) 480-494.
- Stein, F.; Palm, M.; Sauthoff, G.: Intermetallics, *accepted*.



Relation of Stress Anomaly and Order-Disorder Transition in Fe₃Al-Based Ternary and Quaternary Alloys

F. Stein, A. Schneider, G. Frommeyer

Department of Materials Technology

Fe₃Al-based alloys belong to the most widely studied intermetallics for structural applications [1,2]. Their advantageous properties originate from their low density and excellent corrosion resistance in oxidizing and sulfidizing environments. At ambient and intermediate temperatures, Fe₃Al shows higher specific strength than other single-phase iron alloys and steels due to its ordered D0₃ superlattice structure [1] (Fig. 1). However, at about 550 °C the D0₃ structure transforms to a partially disordered B2 structure and at about 800 °C to a disordered A2 structure (Fig. 1). In parallel with the D0₃-B2 ordering transition, a sharp drop in the flow stresses occurs in the binary stoichiometric Fe₃Al compound having detrimental impacts on the material properties with regard to structural applications.

The addition of ternary alloying elements with the objective to increase the D0₃-B2 transition temperature T_c^{D03-B2} has already been studied and the results have been published in the literature [3-6]. Anthony and Fultz [4] found an approximately linear increase of the transition temperature with increasing solute concentration for a number of different metals (Ti, V, Cr, Zr, Nb, Mo, Hf, Ta, and W) with concentrations up to 4 at.%. The efficiency in raising T_c^{D03-B2} varies strongly for the different solutes. Whereas Cr additions have no significant effect, the addition of Ti results in a particularly strong increase of T_c^{D03-B2} of about 60 K/at.%. According to Anthony and Fultz [4], the efficiency of a ternary transition metal in increasing T_c^{D03-B2} is related to the difference of its metallic radius compared to that of Fe. Besides this atomic size mismatch effect, the valence electron concentration was proposed to be an important factor which affects the transition temperature [5,7].

The flow stress of Fe₃Al shows an anomalous increase at intermediate temperatures above about 300 °C up to a maximum between 500 and 600 °C. Beyond this temperature range a strong decrease in flow stress is observed. The occurrence of this flow stress anomaly is known for a long time [8,9]. However, its origin is not well understood up to now and several conflicting explanations have been proposed [10]. From the striking coincidence of the temperatures of the flow stress anomaly and the D0₃-B2 ordering transition, Stoloff and Davies [8] concluded that the flow stress is correlated with the degree of long-range order. In their paper published

already in 1964 they proposed a mechanism involving the transition from $\langle 111 \rangle$ superdislocation glide in the ordered D0₃ state to the glide of $\langle 100 \rangle$ dislocations in the partially ordered B2 state. However, the operating mechanisms which result in the anomalous increase of the flow stress at temperatures below the maximum were not clear. 34 years later Stoloff himself concluded in his reviewing paper on iron aluminides [2] that the anomalous behaviour of the strength increase still is not completely understood and seems to be controlled by a superimposition of several different mechanisms like cross slip of screw dislocations, antiphase boundary relaxation leading to dislocation drag, superdislocation climb locking, transition of dislocation type, or vacancy hardening [2,10]. Nevertheless, several authors still hold the opinion that the transition from D0₃- to B2-ordering is the governing factor for the anomalous behaviour [4,11-15].

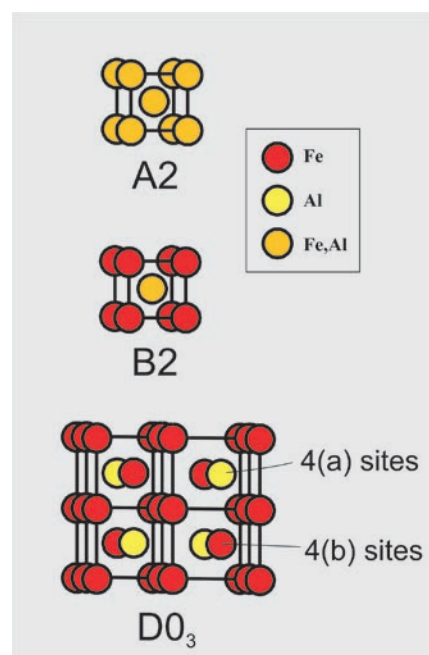


Fig. 1: Different cubic structure types of Fe₃Al. At temperatures below 550 °C, the structure is of the BiF₃ type called D0₃ in the Strukturbericht designation (space group Fm-3m). Between 550 and 800 °C, the 4(a) and 4(b) atom sites are no longer exclusively occupied by Al and Fe, respectively, but statistically by Fe or Al both with an occupation of 0.5 resulting in a CsCl-type B2 structure (space group Pm-3m). Above 800 °C, all atom sites are statistically occupied (0.75 Fe and 0.25 Al) resulting in a simple bcc A2 structure (W type, space group Im-3m).

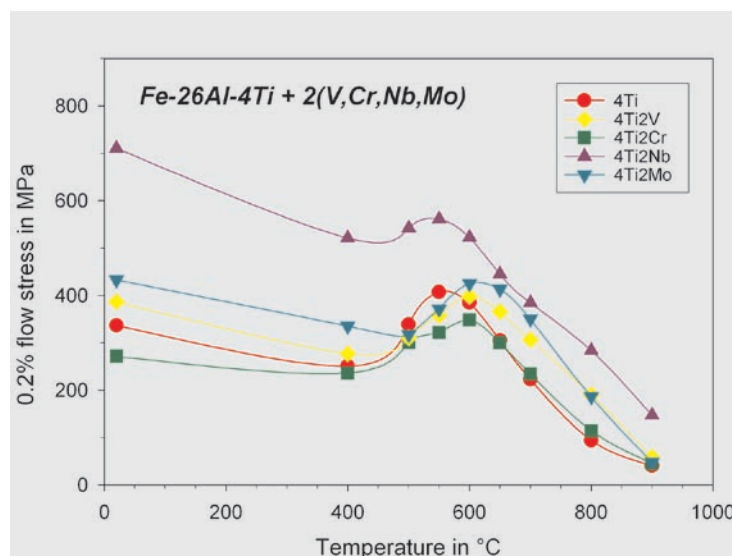


Fig. 2: Effect of the addition of 2 at.% V, Cr, Nb, or Mo to Fe-26Al-4Ti on the 0.2% compressive flow stress versus temperature curves.

In the present study, both the temperature dependence of the flow stress as well as the $D0_3$ -B2 transition temperature $T_c^{D0_3-B2}$ of various ternary Fe-26Al-X and quaternary Fe-26Al-4Ti-X alloys (compositions in at.%) with variable amounts up to 4 at.% of the transition metals X = Ti, V, Cr, Nb, and Mo were investigated. The most important aim of these studies was to establish whether there exists any correlation between the temperature of the flow stress maximum and $T_c^{D0_3-B2}$. Experimental details are given in [16].

The transition metals Ti, V, Cr, Nb, and Mo added to Fe_3Al are known to occupy the 4(b) sites of the $D0_3$ -ordered structure which are completely filled with Fe atoms in the binary alloy [3,7,4,5]. Therefore, the Fe content of the alloys was reduced by the respective amounts of added transition metals and the aluminium content was kept constant. The aluminium content of 26 at.% was chosen, because it is well known from the Fe-Al phase diagram [17] that the $D0_3$ -B2 transition at this composition is of second order. A two-phase field ($A2+D0_3$), which is present in Fe-Al with aluminium contents below the stoichiometric composition, should be avoided in order not to introduce an additional structure variant which might influence the temperature dependence of the flow stress.

Microstructure. The microstructures and chemical compositions of the alloys were characterized by light optical microscopy, transmission electron microscopy (TEM), and electron-probe microanalysis (EPMA). All alloys with the exception of those containing Nb form single-phase solid solutions. The solubility of Nb in the ternary as well as in the quaternary alloys was determined to about 0.8 at.% at 800 °C and 0.9 at.% at 1000 °C not depending on the Ti content (0 to 4 at.%). Therefore, investigated alloys with 0.5 at.% Nb

were single-phase, whereas the addition of 2 at.% Nb or more resulted in the formation of two-phase alloys containing precipitates of a $NbFe_2$ -based Laves phase. TEM investigations of selected alloys confirmed that the samples used for mechanical tests were completely $D0_3$ -ordered at temperatures below the determined $D0_3$ -B2 transition temperature. Homogenization treatments at 1200 °C yielded regular anti-phase-domain structures with small $D0_3$ domain sizes which significantly increased by subsequent annealing at temperatures below the $D0_3$ -B2 transition.

Flow stress anomaly. The anomalous increase of the flow stress at elevated temperatures between about 400 and 550 °C, which is well-known for binary Fe_3Al , was also observed for all investigated ternary and quaternary Fe_3Al -based alloys. Fig. 2 shows the temperature dependence of the 0.2% flow stresses of Fe-26Al-4Ti-2X alloys as an example demonstrating the effect of the alloying additions. The flow stresses were determined in compression tests performed with a constant deformation rate of $10^{-4} s^{-1}$. The temperature of the maximum of the flow stress anomaly of the ternary Fe-26Al-4Ti alloy shifts from 550 °C to about 600 °C for the Cr-, V-, and Mo-containing alloys. In case of the Nb-containing alloy, no shift is observed. It was found for all investigated ternary and quaternary alloys with different amounts and combinations of the alloying elements that the position of the flow stress maximum remains in the temperature interval between about 500 and 600 °C.

The precipitation of the Laves phase in the Nb-containing alloy obviously results in a significant increase of strength compared to that of the ternary Fe-Al-Ti alloy, whereas the other alloying additions show much less pronounced effects. From a comparison of an alloy containing 0.5 at.% Nb, which



is still single-phase, with two-phase alloys containing 2 or 4 at.% Nb, it follows that the strengthening effect in the Nb-containing alloy is a combined effect of precipitation hardening due to the Laves phase and solid solution strengthening due to Nb dissolved in the matrix.

The microstructure of the alloys has no effect on the shape and position of the flow stress anomaly. A comparison of as-cast samples and samples homogenized at 1200 °C with or without subsequent annealing for 168 h at 400 °C in the D0₃ region showed that the flow stresses are lowered by the D0₃-annealing probably due to coarsening of the anti-phase domains, but the shape and position of the stress maximum remain unaffected by the heat treatments.

Order-disorder transitions. The temperatures of the second-order D0₃-B2 and B2-A2 transitions as well as the solidus and liquidus temperatures T_{sol} and T_{liq} of the investigated alloys were determined by DTA (differential thermal analysis) experiments. Fig. 3 shows a typical heat flow vs. temperature plot, where the strong, first-order transformation from the solid to the liquid state as well as the less pronounced, second-order effects of the disordering transitions are clearly visible.

The temperature of the D0₃-B2 transition can be significantly increased by the alloying additions. The efficiency of the different transition metals added to the ternary Fe-26Al-4Ti alloy is about the same as in respective ternary alloys without Ti. In the range of studied compositions, the effect of two alloying additions on the transition temperature seems to be additive as long as no solubility limits are exceeded. The strongest increases of the transition temperature were obtained for Nb and Ti (about 62 and 57 K/at.%, respectively), V and Mo are less efficient (34 and

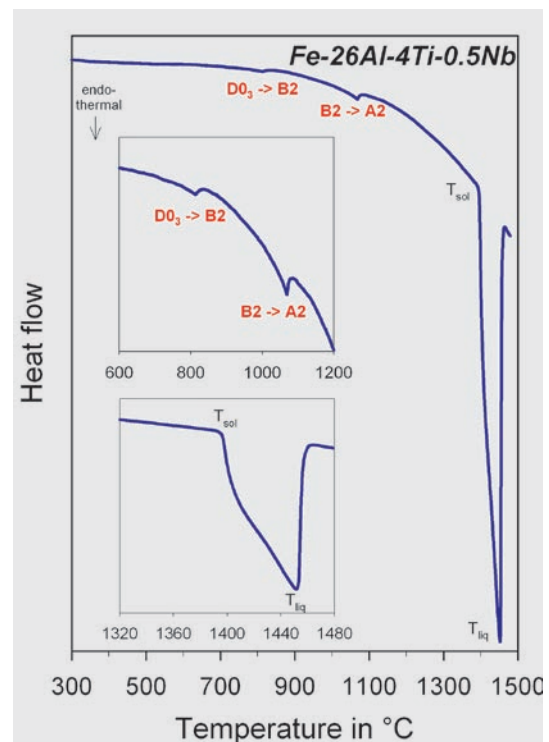


Fig. 3: DTA heating curve (10 K/min) of Fe-26Al-4Ti-0.5Nb showing the two second order transitions D0₃-B2 and B2-A2 and the strong, first-order reaction of melting.

36 K/at.%, respectively), and Cr additions show almost no effect. The B2-A2 transition temperatures of the single-phase alloys are affected by the alloying additions in a similar way as those of the D0₃-B2 transition. It is obviously that the mechanisms which shift the two transition temperatures to higher values must be closely related. Following the argumentation of Anthony and Fultz [4], the main reason for the increase of both transition temperatures should be the atomic size effect. Whereas Cr has almost the same metallic radius as Fe, the difference in the

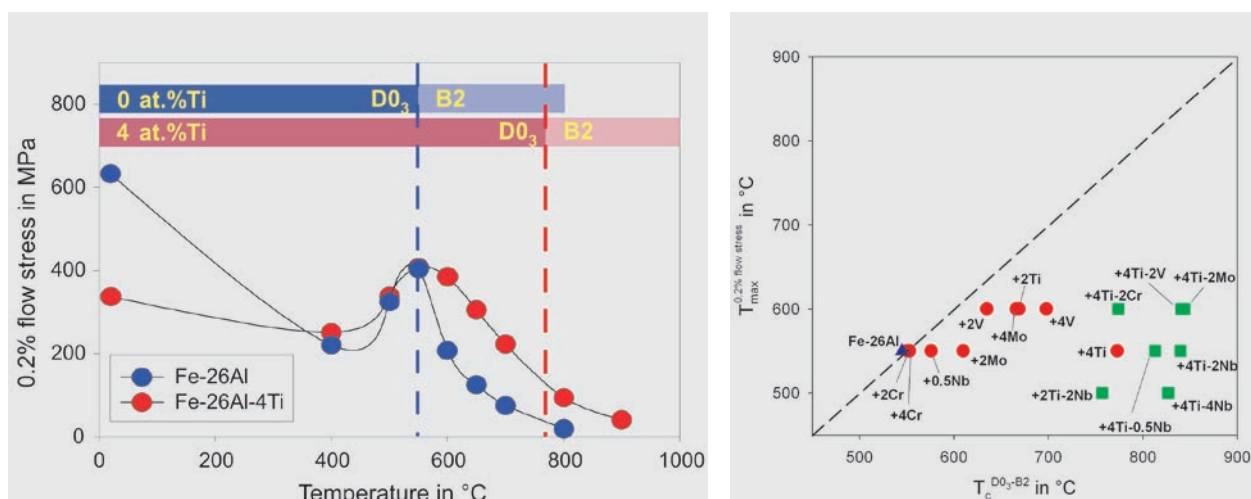


Fig. 4: a) Comparison of the stability ranges of the D0₃- and B2-ordered structure and the temperature-dependence of the 0.2% flow stresses of the alloys Fe-26Al and Fe-26Al-4Ti, and b) mapping of the D0₃-B2 transition temperatures versus the temperatures of the flow stress maxima.



metallic radii between Fe as host atoms and the other solutes increases in the order V, Mo, Ti, Nb, i.e. in the same order as their efficiencies in increasing the transition temperatures. Indeed, a plot of these efficiencies as a function of the metallic radius reveals an about linear relationship confirming the relevance of the atomic size effect.

Correlation between flow stress anomaly and structural transition temperatures. Fig. 4a shows the temperature-dependence of the 0.2% flow stresses of binary Fe-26Al and ternary Fe-26Al-4Ti together with the stability ranges of the $D0_3$ - and B2-ordered structure as obtained for these alloys by DTA investigations. It can be clearly seen that the order-disorder transition is shifted to significantly higher temperatures (from about 546 to 773 °C), whereas the position of the stress maximum remains unchanged at about 550 °C. In Fig. 4b, a plot of the temperatures of the maximum of the anomalous flow stress curves versus the $D0_3$ -B2 transition temperatures of all investigated alloys is presented. Obviously, there is no direct correlation between both temperatures. The same is true for the B2-A2 transition temperatures, since it has been shown that they are affected by the alloying additions in the same way as the $D0_3$ -B2 transition temperatures. Nb additions even result in a small decrease of the temperature of the flow stress anomaly while the critical temperatures of the structural transitions are increased. In many cases, as e.g. for the alloy Fe-26Al-4Ti-2Mo where the $D0_3$ -B2 transition temperature is about 250 °C higher than the peak temperature of the stress maximum, the strong decrease of the 0.2% flow stress nearly completely occurs in the temperature range where the $D0_3$ structure is still the stable one. These observations clearly prove that the disordering of the $D0_3$ structure can not be the governing mechanism for the observed anomalous behaviour of the flow stress.

References

1. Sauthoff, G.: Intermetallics, VCH, Weinheim (1995) 1-165.
2. Stoloff, N.S.: Mater. Sci. Eng. A 258 (1998) 1-14.
3. Fortnum, R.T.; Mikkola, D.E.: Mater. Sci. Eng. 91 (1987) 223-231.
4. Anthony, L.; Fultz, B.: Acta Metall. Mater. 43 (1995) 3885-3892.
5. Nishino, Y.; Kumada, C.; Asano, S.: Scr. Mater. 36 (1997) 461-466.
6. Nishino, Y.; Asano, S.; Ogawa, T.: Mater. Sci. Eng. A 234-236 (1997) 271-274.
7. Nishino, Y.: Mater. Sci. Eng. A 258 (1998) 50-58.
8. Stoloff, N.S.; Davies, R.G.: Acta Metall. 12 (1964) 473-485.
9. Morgand, P.; Mouturat, P.; Sainfort, G.: Acta Metall. 16 (1968) 867-875.
10. Morris, D.G.; Morris, M.A.: Mater. Sci. Eng. A 239-240 (1997) 23-38.
11. Vedula, K.: in: Intermetallic Compounds: Principles and Practice, Vol. 2, eds. J.H. Westbrook, R.L. Fleischer, Wiley, Chichester, UK (1994) 199-209.
12. Park, J.W.; Moon, I.G.; Yu, J.: J. Mater. Sci. 26 (1991) 3062-3066.
13. Park, J.W.: Scr. Mater. 41 (1999) 685-689.
14. Park, J.W.: Intermetallics 10 (2002) 683-691.
15. Song, J.-H.; Ha, T.K.; Chang, Y.W.: Scr. Mater. 42 (2000) 271-276.
16. Stein, F.; Schneider, A.; Frommeyer, G.: Intermetallics 11 (2003) 71-82.
17. Kubaschewski, O.: Iron Binary Phase Diagrams, Springer, Berlin, Germany (1982) 5-9.



Non-Destructive, *in-situ* Measurement of De-Adhesion Processes at Buried Adhesive/Metal Interfaces by means of a New Height-Regulated Scanning Kelvin Probe Blister Test

K. Wapner, B. Schönberger, M. Stratmann, G. Grundmeier

Department of Interface Chemistry and Surface Engineering

The Scanning Kelvin Probe (SKP) is an electrochemical technique that measures the electrode potential at metal/polymer interfaces and thereby detects changes in the buried metal oxide structure and variations of the interfacial ionic conductivity with high spatial resolution of about 50 μm . Thereby, one can distinguish between an ingress of ionic species into the polymer/metal interface, wet de-adhesion and a corrosive delamination [1]. The aim of this work is the combination of the SKP with a pressurized Blister Test (SKP-BT) that allows the application of a defined pressure on the metal halide electrolyte and thus on the adhesive. A defined adjustment of corrosive and mechanical load at the interface should lead to a better understanding of the interfacial degradation kinetics of structural adhesives used in corrosive environments. For the measurement of a spherical Blister Test sample with the SKP it becomes necessary to regulate the distance between the tip and the adhesive surface. Height regulating systems for the SKP have been

performed earlier with the usage of an additional external modulation voltage over the sample/tip gap [2], with the analysis of harmonics of the displacement current [3,4] or with the combination of a near-field microscope that controls the sample/tip distance [5,6].

For the measurement of corrosion reactions on adhesive/metal joints, it is necessary to work in normal pressure atmospheres with high humidity and to scan calibrated potentials on samples with tenth of millimetres size and adhesive layers of about 50 μm thickness. Due to this requirements, a new height regulating SKP (HR-SKP) was designed that principally works based on the addition of an external modulation voltage [7] (see Fig. 1). As the HR-SKP works at a small modulation voltage of about 300 mV, strong electric fields that might affect the physical conditions at the sample surface could be avoided. Thus, a real simultaneous measurement of the sample topography and the Volta potential becomes possible.

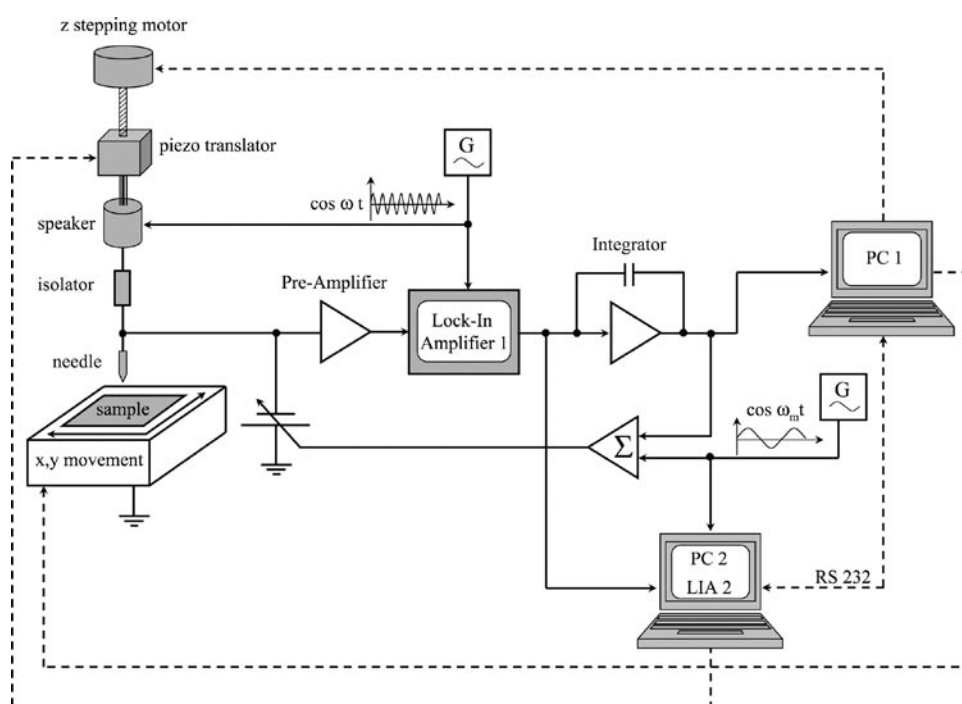


Fig. 1: Schematic of the height-regulating SKP.



The basic theory and experimental description of a Scanning Kelvin Probe has been extensively discussed by Stratmann and co-workers. For a parallel plate capacitor with the sinusoidal plate separation:

$$d(t) = d_0 + \Delta d \cos \omega t \quad (1)$$

with d_0 = average distance of the parallel plates, d = vibration amplitude, ω = angular frequency of vibration, and assuming $\Delta d \cos(\omega t) \ll d_0$, the amplitude of the current demodulated at frequency ω with a Lock-in Amplifier (LIA) is:

$$I(t) = (\Delta\Psi + U_0) \varepsilon \omega A \frac{\Delta d}{d_0^2} \quad (2)$$

with $\Delta\Psi$ = Volta Potential difference, U_0 = compensation Voltage, $C(t)$ = capacitance, ε = permittivity of inter electrode medium, A = area. The measurement of the Volta Potential is performed by zeroing the Kelvin current respectively its amplitude with the compensation voltage:

$$\text{if } I(t) = 0 \Rightarrow \Delta\Psi = -U_0 \quad (3)$$

For the height regulation, the d.c. compensation voltage is modulated with an additional sinusoidal a.c. voltage U_m :

$$U(t) = U_0 + U_m \sin \omega_m t \quad (4)$$

Thus the Kelvin current is given by:

$$i(t) = \frac{d}{dt} \{(\Delta\Psi + U(t)) \cdot C(t)\} \quad (5)$$

The demodulation is now done with two LIA's, one working at the frequency ω_m of the needle vibration and the second working at the frequency ω_m of the additional modulated voltage. Again, assuming $(\Delta d \cos \omega t) \ll d_0$, the current amplitudes measured by the LIA's are:

$$I_\omega = (\Delta\Psi + U_0) \varepsilon \omega A \frac{\Delta d}{d_0^2} \quad (6)$$

$$I_{\omega_m} = U_m \varepsilon A \omega_m \frac{1}{d_0} \quad (7)$$

Eq. (6) which is used for the potential measurement is identical to eq. (2), thus the Volta potential measurement is not affected during the measurements with height regulation.

The modulated current as in eq. (7) is proportional to $1/d_0$ and can be directly used for the height regulation control circuit. For the measurement with a constant tip/sample distance, I_{ω_m} is measured at the desired distance and then kept constant by movement of the piezo unit, though also the topography of the specimen can be measured by recording the piezo position.

Fig. 2 shows as an example the measurement of filiform corrosion on polymer coated aluminium alloy. The HR-SKP topography map of a filament grown from the artificial defect at about $y = -250 \mu\text{m}$ (not included in the scanned area) is shown in the left part of the figure. It can be seen that the tail of the filament has a height of about $6 \mu\text{m}$ whereas the head is about $10 \mu\text{m}$ high. The shape of the filament head is close to a hemi-sphere, comparable with the

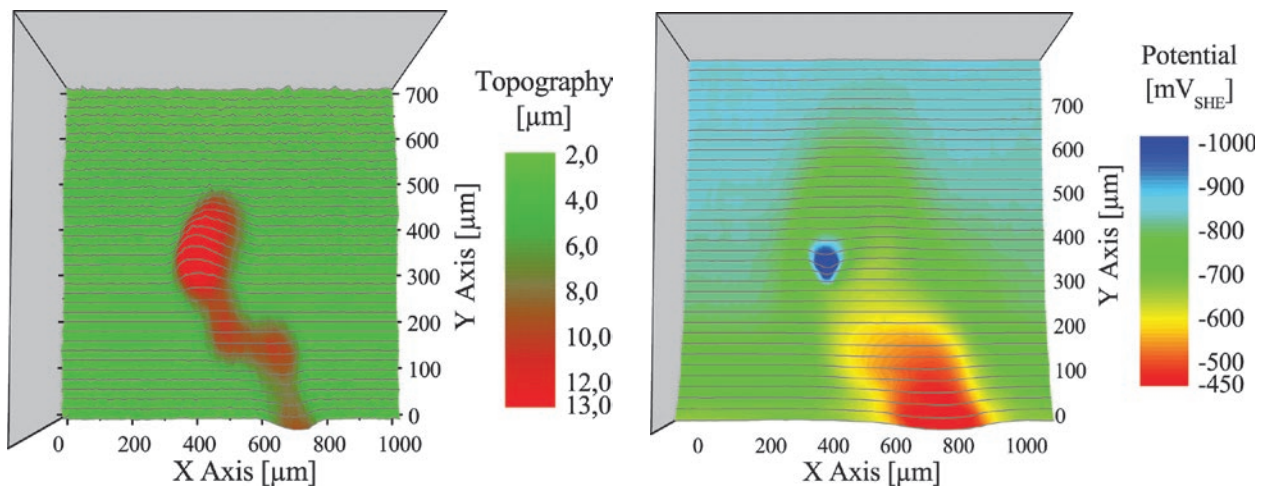


Fig. 2: Simultaneous measurement of height distribution and potential above an active filiform on polymer coated aluminium alloy as measured by the HR-SKP.



shape of a blister. This can be easily explained by the above described mechanisms of the filament growth: with regard to the mechanism of an anodic undermining, the head is filled with an electrolyte which is additionally under an elevated pressure due to osmotic forces or possibly due to the generation of hydrogen gas, whereas the tail of the filament is dry and filled with amorphous corrosion products. The HR-SKP potential map, which is shown in Fig. 2b, corresponds well to the SKP potential maps that have been reported by other authors, the filament tail has a potential about 150 mV higher than the passive state of the intact specimen. This can be interpreted with regard to the formation of aluminium-oxide/-hydroxide corrosion products and additionally the occurrence of reduction reactions, such as oxygen reduction, that possibly take place in the tail. The active part of the filament head, where the anodic reaction of active metal dissolution takes place, has accordingly a potential of about 500 mV lower than the intact area. The broad potential distribution in comparison to the narrow height distribution indicates a process that damages the polymer/metal interface prior to the actual de-adhesion process. This observation became only possible with the simultaneous height and potential measurement.

For the Blister Test experiment (Fig. 3), a pure iron sample was coated with a hot-curing two-component epoxy adhesive in dry nitrogen atmosphere. The specimen was hardened in a sandwiched geometry under a defined mechanical pressure and finally one side of the joint was removed by chemical etching, leaving a homogeneous adhesive film of about 50 μm thickness on the substrate. A hole of 1 mm diameter was prepared from the backside of the iron sample to the adhesive layer and filled with 0.5 M sodium chloride solution. The electrolyte was pressurized via a gas vessel whose pressure can be varied between 0 and 4 bar.

The initiation of a progressing cathodic delamination at the iron/epoxy interface can be observed in the electrode potential, while the measurement of the blister profile only reveals a slight increase of the height of the blister. A lift-off of the adhesive does not occur due to the low applied pressure on the blister.

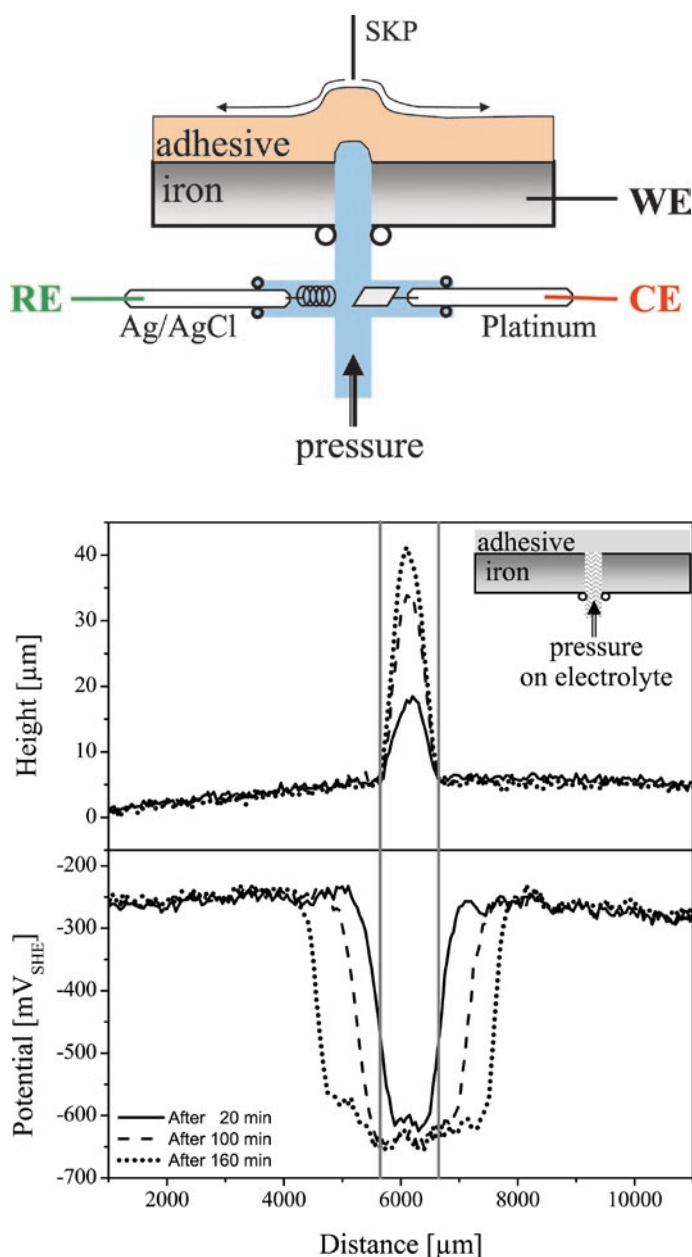


Fig. 3: a) Set-up of a HR-SKP Blister Test; b) measurement of a pure iron sample coated with an epoxy adhesive, with 0.5 M NaCl @ 500 mbar in the blister (defect potential: $-600 \text{ mV}_{\text{SHE}}$).

Recently, a potential control of the defect was introduced, so that the electrode potential in the blister hole can be controlled.

Acknowledgements. The financial support from the Bundesministerium für Bildung und Forschung is gratefully acknowledged.



References

1. Grundmeier, G.; Schmidt, W.; Stratmann, M.:
Electrochim. Acta 45 (2000) 2515.
2. Bonnet, J.; Soonckindt, L.; Lassabatere, L.:
Vacuum 34 (1984) 693.
3. Baumgärtner, H.: Meas. Sci. Technol. 3 (1992) 237.
4. Mäckel, R.; Baumgärtner, H.; RenJ.: Rev. Sci.
Instrum. 64 (1993) 694.



Investigation of the Bainitic Phase Transformation in a Low Alloyed TRIP Steel Using EBSD and TEM

S. Zaefferer

Department of Microstructure Physics and Metal Forming

Low alloyed steels with transformation induced plasticity (TRIP) are complex multiphase steels. After a heat treatment consisting of an intercritical annealing in the α - γ -two phase region, controlled cooling to bainite formation temperature and holding for a certain time at that temperature the microstructure consist of ferrite, metastable austenite and bainite [1]. During straining the austenite transforms further into martensite which leads - if the transformation occurs gradually with increasing strain - to strong hardening and consequently to large uniform elongation and high tensile strength. The most important parameters for a good TRIP effect are the proper stabilisation and the homogeneous distribution of austenite in the microstructure. A homogeneous austenite distribution is obtained during the intercritical annealing (and, in case, by appropriate hot or cold deformation). The stabilisation of austenite is achieved by a sufficiently high carbon content which is forced into the austenite during the bainitic phase transformation: the steel is alloyed with Si and Al in the 1-percent range. Both elements have very small solubility in cementite and lead to the fact that the bainite transformation occurs without formation of cementite. As a result the carbon is pushed out of the advancing bainite into the austenite. Temperature and duration of the bainitic annealing determine the amount of carbon that is pushed into the austenite and its distribution inside the residual austenite grains.

Optimisation of the TRIP effect requires a good knowledge on the effect of thermomechanical treatment on microstructure formation. High resolution electron backscatter diffraction (EBSD) mapping in the scanning electron microscope offers an almost ideal tool to observe all necessary details of the microstructure: fcc and bcc phases can be readily distinguished with a resolution of approximately 50 nm. Orientation relationships (OR) between austenite and ferrite can be determined, which gives important hints on the phase transformation mechanism. Furthermore, information on lattice defect density and orientation gradients created by geometrically necessary dislocations can be obtained which allow to conclude on the microstructure formation mechanisms. Nevertheless, for the observation of smallest

microstructures, for example fine bainite lamellae, and for very precise OR measurements, both, the spatial and angular resolution of EBSD are not sufficient. In these cases, electron diffraction in the transmission electron microscope (TEM) is used as complementary tool.

The present work briefly describes a model – developed on the basis of EBSD and TEM observations – for the formation of the bainitic microstructure in a low alloyed TRIP steel. A much more detailed presentation of the subject has been recently published [2].

Results and Discussion. The investigated steel (composition (wt.%) C 0.2, Mn 1.4, Si 0.5, Al 0.7) was cold rolled and then heat treated by intercritical annealing at 803 °C, cooling to and holding at a bainitic transformation temperature of 400 °C for 200 s [3]. It is important to note that the material completely recrystallised before phase transformation. Fig. 1 shows an orientation map of a small section of the material. Hatched areas correspond to austenite (fcc), the other areas have bcc structure but it cannot immediately be decided whether they are ferrite or bainite. The grey shading inside of the centre grain indicates the angular deviation of the crystal orientation with respect to some reference orientation in the centre of the grain (max. deviation 4°). Surprisingly, the grain does not show a uniform orientation as it would be the case for a recrystallised grain. Instead, only a small area in the centre has a constant orientation while the rest shows quite strong orientation gradients. At some places (marked by arrows) the orientation gradients lead into a diffuse boundary of 1 or 2° misorientation with a small subgrain of bcc structure. This subgrain has a sharp Kurdjumov-Sachs (KS) OR to the neighbouring austenite grain (that means, parallel planes and directions in the neighbouring α - and γ -grains are the following: $(111)_\gamma \parallel (011)_\alpha$ & $[110]_\gamma \parallel [111]_\alpha$).

A similar area has been investigated by TEM. This microstructure, together with phases and some misorientations, is shown in Fig. 2. From these and other TEM observations it was concluded that the areas marked „B“ in Figs. 1 and 2 correspond to bainite which consists in the current material of

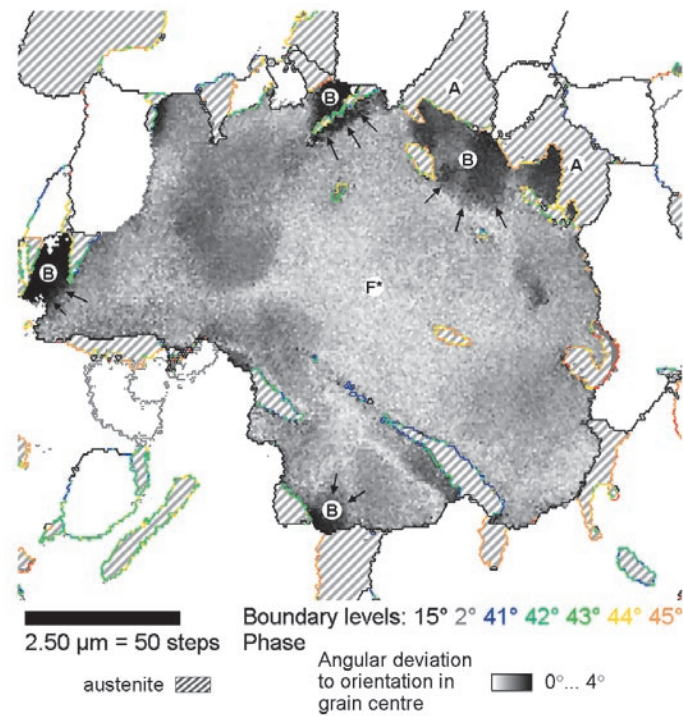


Fig. 1: Crystal orientation map obtained by EBSD showing one ferrite grain (marked F) and its surrounding austenite (A) and bainite (B) grains. The grey value of the ferrite grain corresponds to the misorientation of a given point to the orientation in the centre of the grain. α - γ phase boundaries are coloured according to their misorientation angle from 41° (dark blue) to 47° (red). The Kurdjumov-Sachs orientation relation corresponds to a misorientation of 42.85° (green).

approximately 100 nm thick lamellae of ferrite and austenite phase which are in sharp KS OR with each other. Fig. 3 presents a model of this structure. In Figs. 1 and 2 the lamellae are observed from the plate plane. The α -lamellae almost have the same orientation as one of the neighbouring ferrite grains (the grain marked F*). This grain observes an only approximate KS OR with the austenite inside of the bainite (and thus has a small angle grain boundary with the bainitic ferrite lamellae).

From all observations a model for the microstructure formation was developed which is displayed in Fig. 4 and briefly described in the following. Before annealing, the material has a pearlitic-ferritic microstructure. During intercritical annealing austenite grains nucleate with an approximate KS OR from parent ferrite grains. The austenite grains grow but do not completely consume their parents. During cooling now the ferrite grains grow again on the expense of their austenite neighbours but without (or with only little) nucleation of new grains. γ and α grains thus keep their original OR. The increasing carbon content at the transformation front leads to increasing stresses which are released by the formation of dislocations. The latter create the orientation variations observed in Fig. 1. When reaching the bainite transformation temperature the carbon diffusion in the ferrite can no longer keep up with the speed of the advancing plane transformation front. A possible explanation for the formation of the lamellar bainite is that the plane wave front now develops instabilities as it is known, for example, from the pearlite formation or from dendrite formation during the liquid–solid phase transformation. Additionally it is assumed that the reconstructive transformation (which does not require a sharp KS OR) changes into a displacive one which requires a sharp KS OR [4] and a clearly defined habit plane. The change from a relaxed to a sharp KS OR is responsible for the observed small angle grain

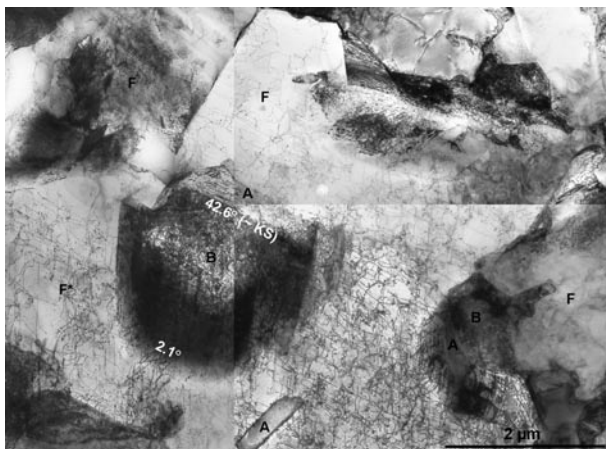


Fig. 2: TEM microstructure showing the surrounding of one bainite grain. Bainite occurs dark because of the overlap of several very thin lamellae of $\gamma\gamma$ and α . Some misorientations with the surrounding ferrite (F) and austenite (A) are marked as well.

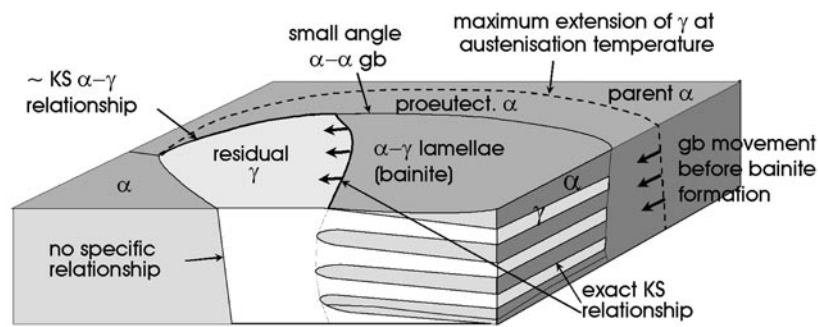


Fig. 3: Model of the structure of bainite in the investigated steel. The positions of boundaries with a sharp and relaxed KS orientation relationship and with small angle misorientation are marked.

boundary between ferrite and bainitic ferrite. Nevertheless, also bainite grows in a continuous process without nucleation of new grains.

Conclusions. In the investigated low alloyed TRIP steel bainite consists of thin lamellae of ferrite and austenite. The microstructure is formed by formation of γ -grains with a KS OR with the parent ferrite grains during intercritical annealing. During the subsequent cooling these grains shrink again without nucleation of new α -grains. The transformation first occurs reconstructive into ferrite and then, at lower temperature, displacive into bainite. Since α and γ grains observe already an approximate KS OR also the bainitic transformation does not require nucleation but just a slight orientation adjustment in order to realise a sharp KS OR. It should be mentioned that the usual TTT diagrams cannot be used to determine

the correct cooling process for the material because the missing nucleation event for ferrite formation leads to the disappearance of the ferrite nose. The formation of some proeutectoid ferrite during cooling therefore cannot be avoided.

References

1. Bleck, W.: Proc. Int. Conf. on TRIP-Aided High Strength Ferrous Alloys, Gent (2002) 13-23.
2. Zaefferer, S.; Ohlert, J.; Bleck, W.: Acta. Mater 52 (2004) 2765-2778.
3. Ohlert, J.: PhD Thesis, RWTH Aachen (2003).
4. Bhadeshia, H.K.D.H.: Mater. Sci. Eng. A 273-275 (1999) 58-66.

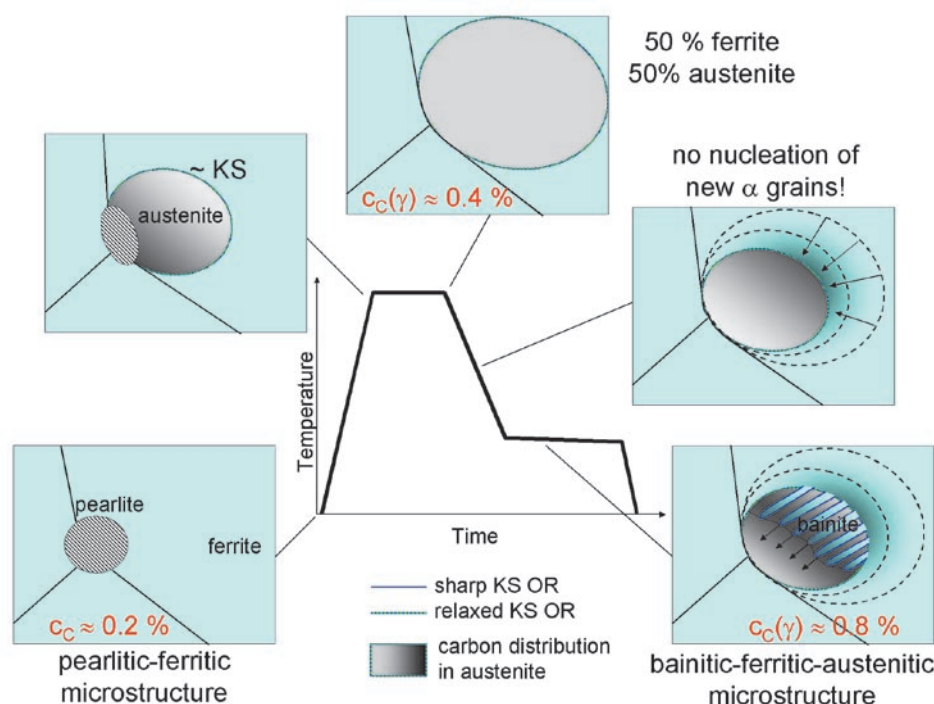


Fig. 4: Scheme of the formation of the bainitic-ferritic-austenitic microstructure during heat treatment. The grey value in the grains corresponds to the carbon distribution inside of the austenite grains. Green-blue broken lines mark grain boundaries with a relaxed KS-orientation relationship, solid blue ones (between the α and γ constituents in bainite) such with a sharp KS OR.



PART III.

GENERAL INFORMATION AND STATISTICS

| | |
|---|-----|
| Boards, Scientific Members, Heads of Departments, and Scientists at the Institute | 175 |
| Scientific Honours | 179 |
| Participation in Research Programmes | 180 |
| Collaborations with Research Institutes and Industrial Partners | 183 |
| Patents and Licenses | 188 |
| Conferences, Symposia, and Meetings Organized by the Institute | 189 |
| Institute Colloquia and Invited Seminar Lectures | 191 |
| Lectures and Teaching at University | 195 |
| Oral and Poster Presentations | 196 |
| Publications | 208 |
| Doctoral and Diploma Theses | 219 |
| Budget of the Institute | 221 |
| Personnel Structure | 222 |
| The Institute in Public | 224 |



Boards, Scientific Members, Heads of Departments, and Scientists at the Institute

Supervisory Board

(in 2004)

GRUSS, Peter, Prof. Dr., München
(chairman)
AMELING, Dieter, Prof. Dr.-Ing., Düsseldorf
(vice-chairman)
BELCHE, Paul, Dr., Eisenhüttenstadt
HEINKE, Rüdiger, Dr.-Ing., Wilnsdorf
JARONI, Ulrich, Dr.-Ing., Duisburg
KAISER, Gert, Prof. Dr., Düsseldorf
KREBS, Hartmut, Staatssekretär, Düsseldorf
LANZER, Wolf, Dr. mont., Duisburg
LINDENBERG, Hans-Ulrich, Dr.-Ing., Duisburg
RAUHUT, Burkhard, Prof. Dr., Aachen
SCHWICH, Volker, Dr.-Ing., Salzgitter
WARMUTH, Ekkehard, Dr., Berlin

Scientific Advisory Board

(in 2004)

LANDOLT, Dieter, Prof. Dr., Lausanne/Schweiz
(chairman)
KÖSTERS, Kurt, Dr. techn., Linz/Austria
(vice-chairman)
DREWES, Ernst-Jürgen, Dr.-Ing., Dortmund
GOTTSTEIN, Günter, Prof. Dr., Aachen
HAGEN von, Ingo, Dr.-Ing., Duisburg
HOUTTE van, Paul, Prof. Dr., Heverlee/Belgium
KURZ, Wilfried, Prof. Dr., Lausanne/Switzerland
LINDENBERG, Hans-Ulrich, Dr.-Ing., Duisburg
MARTIN, Georges, Prof. Dr., Gif-sur-Yvette/France
NIX, William D., Prof. Dr., Stanford/USA
SCHWICH, Volker, Dr.-Ing., Salzgitter
De WIT, J.H.W., Prof. Dr., Delft/The Netherlands

Scientific Members of the MPG at the Institute

NEUGEBAUER, Jörg, Prof. Dr. (since Nov. 2004)
NEUMANN, Peter, Prof. Dr. (until May 2004)
RAABE, Dierk, Prof. Dr.-Ing.
STRATMANN, Martin, Prof. Dr.

External Scientific Member:

HILLERT, Mats, Prof. Dr., Stockholm/Schweden

Emeriti:

ENGELL, Hans-Jürgen, Prof. Dr.-Ing.
NEUMANN, Peter, Prof. Dr. (since June 2004)
PAWELKSKI, Oskar, Prof. Dr.-Ing.
PITSCH, Wolfgang, Prof. Dr.



Directors and Heads of Departments

| Name | Date of Appointment | Status as of 01-01-2005 |
|----------------------------------|---------------------|---------------------------------|
| FROMMEYER, Georg, Prof. Dr.-Ing. | 01-01-1983 | head of dept. |
| NEUGEBAUER, Jörg, Prof. Dr. | 11-01-2004 | director |
| NEUMANN, Peter, Prof. Dr. | 11-21-1980* | director, retired on 05-21-2004 |
| RAABE, Dierk, Prof. Dr.-Ing. | 07-01-1999 | director |
| STRATMANN, Martin, Prof. Dr. | 01-01-2000** | director |

*chief executive from 11-01-1990 to 05-30-2002

**chief executive since 06-01-2002

Scientists at the Institute

(departments in alphabetical order)

Computational Materials Design

Neugebauer, Jörg, Prof. Dr.rer.nat. (*head of department*, since 11-01-2004)

Grundmeier, Guido, Dr.-Ing. (*group head*)

Hassel, Achim W., Dr.rer.nat. (*group head*)

Hausbrand, René, Dr.rer.nat. until 08-31-2003

Hüning, Boris, Dipl.-Phys.

Interface Chemistry and Surface Engineering

Stratmann, Martin, Prof. Dr.rer.nat. (*head of department*)

Kawakita, Jin, Dr. (*guest*, Japan), since 08-01-2004

Khalil, Ahmed, M.Sc. (Egypt), since 07-15-2004

Asteman, Henrik, Dr. (Sweden), since 02-15-2004

Klüppel, Ingo, Dipl.-Chem. (*guest*), since 07-01-2004

Akiyama, Eiji, Dr. (*guest*, Japan)

Li, Yuanshi, Dr. (China), until 03-31-2004

Barranco, Violeta, Dr.-Ing. (Spain), until 02-29-2004

Liu, Xiao, Fang, Dr. (China), 10-01-2003 to 03-31-2004

Baumert, Birgit, Dipl.-Phys., since 09-01-2004

Lill, Kirsten, Dipl.-Chem.

Bello-Rodriguez, Belèn, Dr. (Spain), since 04-01-2004

Lyapin, Andrey, Dipl.-Chem. (Russia), since 09-01-2004

Blumenau, Alexander, Dr.rer.nat. (*group head*), since 09-01-2004

Michalik, Adam, Dipl.-Ing. (Poland)

Bonk, Stephan, Dipl.-Phys., until 10-31-2003

Neelakantan, Lakshman, M.Sc. (India), since 06-28-2004

Borodin, Sergiy, M.Sc. (Ukraine), since 08-03-2004

Paliwoda, Grazyna, Dipl.-Chem. (Poland)

Büttner, Angela, Dr.rer.nat., since 10-15-2003

Park, Eung Yeul, Dr.-Ing. (South Korea), 05-01-2003

Cha, Sung-Chul, Dr.-Ing. (South Korea)

Parezanovic, Ivana, M.Sc. (Serbia and Montenegro)

Ehahoun, Hervé, Dr.rer.nat. (France)

Pöter, Birgit, Dr. rer. nat., since 10-01-2003

Fink, Nicole, Dipl.-Chem., since 04-15-2003

Popova, Vesselina, Dipl.-Chem. (Bulgaria), since 05-01-2004

Frenznick, Sascha, Dipl.-Ing., until 07-31-2004

Raacke, Jens, Dr.rer.nat.

Fushimi, Koji, Dr. (Japan), until 07-31-2003

Rohwerder, Michael, Dr.rer.nat. (*group head*)

Giza, Miroslaw, Dipl.-Phys., since 08-01-2003



Ruh, Andreas-Christian, Dipl.-Min.
Sanchez Pasten, Miguel, Dipl.-Chem. (*guest*, Mexico)
Satori, Hassan, Dr. (Maroc), since 08-15-2003
Sauerhammer, Björn, Dr.rer.nat.
Swaminathan, Srinivasan, M.Sc. (India), since 06-15-2004
Skobir, Danijela Anica, Dr.Ing. (Slovenia), since 01-15-2004
Spiegel, Michael, Priv.-Doz. Dr.rer.nat. (*group head*)
Stempniewicz, Magdalena, Dipl.-Ing. (Poland), since 07-01-2004
Stromberg, Christian, Dr.rer.nat., since 10-01-2003
Sun, Guoguang, Dipl.-Ing. (China), since 01-15-2004
Tan, Kengsoong, Dr. (Malaysia), since 05-27-2003
Titz, Tobias, Dipl.-Phys., since 03-15-2004
Vander Kloet, Jana, Dipl.-Phys. (Canada)
Vlasak, René, Dipl.-Phys., since 07-15-2003
Vuolo, Diogo, Dipl.-Chem. (*guest*, Brazil), 09-01-2004 to 10-31-2004
Wapner, Kristof, Dipl.-Chem.
Wang, Xuemei, M.Sc. (China), since 05-01-2004
Wicinski, Mariusz, Dipl.-Chem. (Poland), until 09-30-2003
Wilson, Benjamin, Dr. (UK), since 05-15-2003
Yadav, Amar Prasad, Dr.-Ing. (Nepal), since 05-05-2004
Yan, Jiawei, Dr. (China), since 06-04-2004
Yang, Lihong, Dr. (China)
Yu, Xingwen, Dr. (China), until 08-31-2003
Zhang, Zhihong, Dr. (China), 04-01-2004 to 08-31-2004

Materials Technology

Frommeyer, Georg, Prof. Dr.-Ing. (*head of department*)
Bernst, Reinhard, Dipl.-Phys., since 09-01-2003
Brokmeier, Klaus, Dipl.-Ing.
Brüx, Udo, Dipl.-Phys.
Deges, Johannes, Dipl.-Phys.
Eleno, Luiz Tadeu Fernandes, M.Sc. (Brazil), since 05-01-2004

Falat, Ladislav, Dipl.-Ing. (Slowakia), until 09-30-2004
Fischer, Rainer, Dr.-Ing.
Gnauk, Joachim, Dr.rer.nat. (*group head*)
Jiménez, José, Dr. (*guest*, Spain) 02-21-2004 to 03-12-2004, 07-14-2004 to 08-25-2004
Knippscheer, Sven, Dipl.-Ing., until 06-15-2003
Konrad, Joachim, Dipl.-Ing., since 02-01-2003 (50%)
Milenkovic, Srdjan, Dr.-Ing. (Serbia and Montenegro), since 07-01-2003
Palm, Martin, Dr.rer.nat, since 06-01-2004
Rablbauer, Ralf, Dipl.-Phys., until 04-30-2004
Schneider, André, Dr.rer.nat. (*group head*)
Stein, Frank, Dr.rer.nat., since 06-01-2004
Strondl, Annika, M.Sc. (Sweden)
Wenke, Rainer, Dipl.-Phys.

Visiting Scientist:

Prof. Dr. James Wittig, Vanderbilt University School of Engineering (USA), 05-28-2004 to 07-02-2004

Metallurgy and Process Technology

Büchner, Achim R., Dr.rer.nat. (*provisional head of department*)
Thiemann, Michael, Dipl.-Phys., until 02-29-2004
Pötschke, Stephan, Dipl.-Ing.

Microstructure Physics and Metal Forming

Raabe, Dierk, Prof. Dr.-Ing. habil. (*head of department*)
Al-Sawalmih, Ali, Dipl.-Phys. (Jordan), since 01-01-2004
Ardehali-Barani, Araz (Germany and Iran) Dipl.-Ing.
Chen, Nan, Dr. (China), until 12-31-2003
Detroy, Sandra, Dipl.-Ing.
Dorner, Dorothee, Dr.rer.nat., since 08-01-2003
Elsner, Alexander, Dipl.-Ing. FH, until 11-30-2003
Fernandes Bastos da Silva, Alice, Dipl.-Ing. (Brazil), since 11-01-2003
Filatov, Dmitri, Dipl.-Ing. (Russia), until 08-31-2004
Godara, Ajay, Dipl.-Ing. (India), since 04-15-2004
Haurand, Hyeon Sook, Dr.rer.nat. (South-Korea), since 03-01-2004



Jia, Juan, M.Sc. (China), since 06-01-2004
Kemnitz, Hans-Dieter, Dr.-Ing. (*head of electronics workshop and of computer centre*)
Klüber, Christian, Dipl.-Ing., until 05-31-2003
Kobayashi, Satoru, Dr. (Japan)
Konrad, Joachim, Dipl.-Ing., since 02-01-2003 (50%)
Kuo, Jui-Chao Dipl.-Ing. (Taiwan), until 04-30-2004
Li, Fei, M.Sc. (*guest*, China), since 10-11-2004
Lücken, Hermann, Dipl.-Ing., until 02-28-2003
Ma, Anxin, M.Sc. (China)
Masato, Ueno (Japan), 09-01-2004 to 10-31-2004
Moss, Matthew Hale, B.Eng. (UK), since 02-01-2004
Ponge, Dirk, Dr.-Ing. (*group head*)
Rajabali, Firoozi, Mohamed, M.Sc. (Iran), since 07-01-2004
Rasp, Wolfgang, Dr.-Ing. (*group head*)
Romano Triguero, Patricia, Dr. (Spain), since 05-01-2004
Roters, Franz, Dr.rer.nat. (*group head*)
Sachs, Christoph, Dipl.-Ing., since 04-15-2004
Sachtleber, Michael, Dipl.-Ing., until 01-31-2004
Sato, Hisashi, Dr.-Ing. (Japan), since 05-10-2004
Scheele, Georg, Dipl.-Ing., until 04-30-2003
Song, Rongjie, Dipl.-Ing. (China)
Storojeva, Lidia, Dr.-Ing. (Russia), until 06-30-2004
Tikhovskiy, Ilya, Dipl.-Ing. (Russia), since 06-01-2004
Thomas, Ingo, Dipl.-Phys. (*guest*)
Varnik, Fatholla, Dr.rer.nat. (Iran and France), since 09-01-2004
Wang, Yanwen, Dr. (China), until 05-31-2004
Wichern, Christian, Dr. (USA)

Yusupov, Artem, Dipl.-Ing. (Russia)
Zaafarani, Nader (*guest*, Egypt)
Zaefferer, Stefan, Dr.-Ing. (*group head*)
Zhao, Zisu, Dr. (China), until 02-14-2003
Visiting Scientists:
Prof. Dr. A. Rollett, Carnegie Mellon University (USA)
Prof. Dr. H.R.Z. Sandim, University of Lorena (Brazil)
Prof. Dr. W. Mao, TU Beijing (China)
Prof. Dr. R. Radovitzky, Massachusetts Institute of Technology (USA)

Physical Metallurgy

Neumann, Peter, Prof. Dr.rer.nat. (*head of department*), until 05-21-2004
Balun, Jozef, Dipl.-Ing. (Slovak Republic), until 07-31-2004
Bernst, Reinhard, Dipl.-Phys., until 08-31-2003
Dovbenko, Oleksandr, Dr. (Ukraine), since 02-01-2004
Eleno, Luiz Tadeu Fernandez, M.Sc. (Brazil), 09-01-2003 to 04-30-2004
Gahn, Ulrich, Dr.rer.nat.
Inden, Gerhard, Prof. Dr.rer.nat. (*group head*), until 12-31-2003
Knezevic, Vida, M.Sc. (Serbia and Montenegro)
Palm, Martin, Dr.rer.nat., until 05-31-2004
Risanti, Doty-Dewi, M.Sc. (Indonesia)
Sauthoff, Gerhard, Priv.-Doz. Dr.rer.nat. (*provisional head of department*, since 05-21-2004), until 11-30-2004
Stallybrass, Charles, Dipl.-Ing. (UK)
Stein, Frank, Dr.rer.nat., until 05-31-2004
Zhang, Jianqiang, Dr. (China), until 08-31-2003



Scientific Honours

Prof. Dr.-Ing. G. Frommeyer achieved honourable membership of „The Order Of The Damask“ for contributions to the understanding of UHC steels. Thermec 2003, International Conference, Madrid, Leagues, Spain, July 2003.

Prof. Dr. H.J. Grabke was awarded the honorary degree Doctor Honoris Causa of the University of Ljubljana, Slovenija, Dec. 2004.

Dr. Y.S. Li and PD Dr. M. Spiegel received the John Stringer Award for the second best poster „High temperature interactions of pure Cr with KCl“, 6th Int. Symposium on High Temperature Corrosion and Protection of Materials, Lez Embiez, France, May 2004.

M.Sc. I. Parezanovic and PD Dr. M. Spiegel received the Best Poster Award for their presentation „Influence of dew point on the selective oxidation of cold rolled DP and IF-steels“, Corrosion in the 21st Century, UMIST, Manchester, UK, July 2004.

Prof. Dr.-Ing. D. Raabe was awarded the Gottfried Wilhelm Leibniz Award of the Deutsche Forschungsgemeinschaft (DFG, German Research Foundation), 2004.

Prof. Dr.-Ing. D. Raabe became new editor of the series „Umformtechnische Schriften“ of the Shaker-Verlag, Aachen, 2004.

Dr.-Ing. W. Rasp became member of the International Advisory Committee of the 10th International Conference on Metal Forming at Akademia Gorniczo-Hutniza Krakau, Polen, 2004.

Dr.-Ing. W. Rasp was invited to be member of the Advisory Board of the journal ISIJ International, published monthly by the Iron and Steel Institute of Japan, 2004.

Dipl.-Min. A. Ruh and PD Dr. M. Spiegel received the Lez Embiez-VI Award for the third best poster „Kinetic investigations on salt melt induced high temperature corrosion of pure metals“, 6th Int. Symposium on High Temperature Corrosion and Protection of Materials, Lez Embiez, France, May 2004.

Dipl.-Ing. C. Sachs received the Springorum Memorial Award (Springorum Denkmünze) of RWTH, Aachen, 2004.

Dipl.-Ing. R. Song, Dr.-Ing. D. Ponge, and Prof. Dr.-Ing. D. Raabe received the TMS 2004 Gold Medal Poster Award, TMS Annual Meeting, Charlotte, USA, 2004.

Prof. Dr. M. Stratmann became member of the board of trustees of the Karl-Winnacker Institute of DECHEMA, Nov. 2003.

Prof. Dr. M. Stratmann was elected to the „Konvent für Technikwissenschaften der Union der deutschen Akademien der Wissenschaften e.V.“ (acatech), Oct. 2004.



Participation in Research Programmes

National:

BMBF

„Characterization of microstructures and properties of ultra-high strength quasieutectoid Fe-C-Al steels containing higher carbon and aluminium contents“

„Development and characterisation of high strength and supra ductile TRIP/TWIP light weight steels based on Fe-Mn-Al-Si“

„Long-term stable high performance joints based on structural adhesives“

„Release systems for the self-healing of polymer/metal interfaces“

„Tailored adhesion mechanisms in composite systems by means of chemical surface functionalisation“

DFG

„Cellulose and cellulose derivates: molecular and supramolecular design“

„Constitution of cementite“

„Development of ferritic iron-aluminium-tantalum alloys with strengthening Laves phase with highest creep strength in corrosive atmospheres“

„Experimental and theoretical studies of strain and orientation gradients in steels on the grain scale“

„Grain boundary mechanics“

„Hardening of iron-chromium-aluminium-nickel-alloys with coherent precipitates“

„Hardening of novel iron-chromium-aluminium-nickel alloys through coherent precipitates“

„Heat resistant ferritic steels-thermodynamic and kinetic calculations of precipitation reactions“

„Heat transfer and heat contact between strip and roll in twin roll casting“

„High temperature corrosion by carburisation of Fe-Al alloys“

„High temperature materials“

„Improvement of formability by superposition of hydrostatic pressure“

„Improvement of the deformation properties of TRIP-, TWIP- and conventional steels by biaxial loading in compression and tension combined with additional torsion“

„Influence of carbide forming elements on the process of metal dusting“

„Influence of the chip removing process with geometrically defined cutting edge on the material properties of intermetallic nickel and titanium aluminides“

„Initial stages and kinetics of oxidation of binary and ternary iron-aluminides“

„Initial stages of high temperature oxidation investigated by VT-STM“

„Investigation of mechanical properties and hot deformation behavior as well as microstructural characterization of Fe₃Al base alloys“

„Investigation of size effects with respect to texture and anisotropy“

„Modeling of phase and microstructure formation under non-equilibrium conditions of Ti-Al laser welded seams“

„Nanofluid mechanics“

„Oxidation and segregation on high strength steels“



„Production of nanowire arrays through directional solidification and their application“

„Scale effect of the tribological interface on metal forming processes“

„Simulation study on scaling effects in nano- and microscale fluid dynamics at deformable metal surfaces“

„Super heat resistant ferritic steels for environmental friendly coal-fired steam electric power plants with steam inlet temperatures of 650°C: alloy development, alloy preparation and study of long-term microstructure evolution“

„Super heat resistant ferritic steels for environmental friendly coal-fired steam electric power plants with steam inlet temperatures of 650°C: thermodynamic and kinetic calculations of precipitation reactions.“

State of NRW

„International Max Research School (IMPRS) for Surface and Interface Engineering in Advanced Materials (SurMat)“

„Intelligent self-healing by nano- and micro-capsules (SurMat)“

„Microstructural aspects of passivity and corrosion of NiTi (SurMat)“

„Use of surface enhanced Raman spectroscopy for studying the adsorption, adhesion and desorption of organic molecules from oxide covered metals (SurMat)“

International:

EU

„European Network surface engineering of new alloys for super high efficiency power generators“

„Numerical modelling / lifetime prediction of delamination polymer coating disbonding and material degradation“

RFCS (ECSC)

„A mechanistic study of wetting and dewetting during hot dip galvanizing of high strength steels“

„Assessment and synthesis of the most relevant tribological tests for the characterization of cold rolling lubricants“

„Advanced modelling of lateral flow and residual stresses during flat rolling“

„Development of electrically conductive polymer coatings for coil coated steel sheets“

„Forming behaviour of corrosion protection primers“

„Fundamental aspects of corrosion and delamination behaviour of novel zinc alloy coatings and Zn-intermetallic phases“

„Heavy warm rolling for the production of thin hot strips“

„High strength long products with improved toughness and fatigue resistance“

„Improving the properties of near net shape cast strip containing copper and tin from scrap“

„Improving the surface quality of continuously cast semis by an understanding of the shell development and growth“

„Materials for increased performance in sustainable fuel combustion“

„Mitigation of formation of chlorine rich deposits affecting on superheater corrosion under co-combustion conditions“

„New approaches in electrolytic cleaning of cold rolled steel sheets“



- PARTICIPATION IN RESEARCH PROGRAMMES -

- „Optimisation of in-service performance of boiler steels by modelling high temperature corrosion OPTICORR“
- „Passive/active transitions during delamination of organic coatings in cyclic corrosion tests“
- „Self-healing at cut-edge of coil coated galvanized steel sheet“
- „Soluble salt contamination on blast cleaned surfaces and the effect on the durability of subsequently applied paint systems“
- „Tailored thin film plasma polymers for surface engineering of coil coated steel“
- „Transformation behaviour of steel in the in-line hot rolling steel processing“



Collaboration with Research Institutes and Industrial Partners

Research Institutes

National:

Betriebsforschungsinstitut, Düsseldorf
Dr. E. Neuschütz

Bremer Institut für angewandte Strahltechnik, BIAS, Bremen
Prof. Dr. G. Sepold

DECHEMA, Frankfurt
Prof. Dr. M. Schütze

Deutsches Zentrum für Luft- und Raumfahrt, Köln
Prof. Dr. D. Herlach

Fachhochschule Osnabrück, Osnabrück
Prof. Dr.-Ing. I.-M. Zylla

Forschungszentrum Jülich GmbH, Jülich
Prof. Dr. L. Singheiser

Fraunhofer-Institut für Fertigungstechnik und angew. Materialforsch., IFAM, Bremen
Prof. Dr. O.-D. Hennemann

Fraunhofer-Institut für Schicht und Oberflächentechnik, Braunschweig
Prof. Dr. C.-P. Klages

Hahn-Meitner-Institut, Berlin
Prof. Dr. W. Reimers, Dr. N. Wanderka

Institut für Materialwissenschaften, Universität, Wuppertal
Prof. Dr. R. Hentschke

Institut für Oberflächenchemie, Universität, Freiburg
Prof. Dr. J. Rühle

Institut für Werkstoffkunde, Technische Hochschule, Darmstadt
Prof. Dr. C. Berger, Dr. A. Scholz

Institut für Werkstoffwissenschaften, Universität, Erlangen-Nürnberg
Prof. Dr. W. Blum, , Dr. K. Durst, Prof. Dr. M. Göken

Max-Planck-Institut für Chemische Physik fester Stoffe
Prof. Y. Grin, Dr. G. Kreiner

Max-Planck-Institut für Kohlenforschung, Mülheim
Prof. Dr. F. Schüth

Max-Planck-Institut für Mikrostrukturphysik, Halle
Prof. Dr. U. Messerschmidt



Max-Planck-Institut für Polymerforschung, Mainz
Prof. Dr. G. Wegener

Technische Hochschule, RWTH, Aachen
Prof. Dr. W. Bleck, Prof. Dr. R. Sahn, Dr. R. Wagner, Dr. M. Winning

Technische Universität Bergakademie, Freiberg
Prof. Dr. R. Kawalla

Technische Universität, Berlin
Prof. Dr. E. Uhlmann

Technische Universität, Braunschweig
Prof. Dr. I. S. Golovin, Prof. Dr. H. Wohlfahrt

Technische Universität, Clausthal
Prof. Dr. Scholz, Prof. Dr. K. Schwerdtfeger, Prof. Dr. K.-H. Spitzer

Technische Universität, Darmstadt
Prof. Dr. C. Berger

Universität, RUB, Bochum
Prof. Dr. G. Eggeler, Prof. Dr. M. Muhler

Universität Düsseldorf, Düsseldorf
Prof. Dr. E. Kisker

Universität, Dresden
Prof. Dr. H.-J. Adler, Prof. Dr. W. Plieth

Universität Gesamthochschule, Siegen
Prof. Dr. H.-J. Christ

Universität, Stuttgart
Prof. Dr. S. Schmander

International:

Aristoteles University, Thessaloniki, Greece
Prof. Dr. D. Tsipas

CEIT, San Sebastian, Spain
Dr. I. Ocaña

Centre de Recherches Metallurgiques, Gent, Belgium
Dr. C. Mesplont

Centro Nacional de Investig. Metallurgicas, Madrid, Spain
Dr. J. A. Jimenez, Dr. M. Morcillo Linares

Centro Sviluppo Materiali S.p.A, Rome, Italy
Dr.-Ing. E. Anelli, Dr.-Ing. F. Cusumano, Dr. A. Gotti, Dr. I. Salvatori

CIRIMAT, Toulouse, France
Dr. J. Lacaze



Department of Aeronautics and Astronautics, MIT, Cambridge, USA
Prof. Dr. P. Radowitzky

Fudan University, Shanghai, China
Prof. Dr. D. Zhao

Institute for Energy, Joint Research Centre, JRC, Petten, Netherlands
Dr. D. Dexter

Institute of Physics of Materials, Acad. of Sci., Brno, Czech Republic
Prof. Dr. A. Kroupa

Institut für Physikalische Chemie der Universität, Vienna, Austria
Prof. Dr. J. C. Schuster

IPL, Danmarks Tekniske Universitet Lyngby and Elsa/Elkraft, Lyngby, Dänemark
Dr. J. Hald

IWS, Technische Universität, Graz, Austria
Prof. Dr. H. Cerjak, Dr. E. Kozeschnik

KTH, Stockholm, Sweden
Prof. Dr. J. Ågren, Prof. Dr. B. Sundman

Laboratoire de Thermodynamique et Physicochimie Metallurg., Grenoble, France
Dr. A. Pasturel

MEFOS - The Foundation for Metallurgical Research, Lulea, Sweden
Dr. A. Johnson, Dr. P. Siderstam

Swedish Institute for Metals Research, Stockholm, Sweden
Dr. B. Hutchinson

Tohoku Universität, Sendai, Japan
Prof. Dr. K. Ishida, Prof. Dr. M. Sluiter

UMIST, Manchester, UK
Prof. Dr. H. Stott

Universidad Complutense, Madrid, Spain
Prof. Dr. L. Peres

Universidad Nacional de San Luis, Argentina
Dr. F. Nieto

Universidade, Aveiro, Portugal
Prof. Dr. M. Ferreira

Universidade, Lisbon, Portugal
Prof. Dr. A. Simões

University, Limerick, Irland
Prof. Dr. M. Pomeroy

University of Science and Technology, Beijing, China
Prof. Dr. M. Weimin



University of Technology, HUT, Finland
Prof. Dr. L. Otaniemi

University Xiamen, China
Prof. Dr. L. Changjian, Prof. Dr. T. Zhongqun

Industrial Partners

National:

AIF, Köln
AVIF, Ratingen
Bayerische Motorenwerke AG, München
Benteler Automobil GmbH & Co.KG, Paderborn
Berkenhoff GmbH, Heuchelheim
Betriebsforschungsinstitut VDEh, Düsseldorf
Brockhaus Messtechnik, Kaschke KG, Düsseldorf
Brose Fahrzeugteile GmbH & Co. KG, Coburg
CAU, Kiel
CHEMETALL GmbH, Frankfurt/M.
CIS Solartechnik GmbH, Berlin
Clausthaler Umwelttechnik-Institut GmbH, Clausthal
Continental AG, Hannover
CORUS Aluminium GmbH, Voerde
DaimlerChrysler AG, Stuttgart
Dechema Karl Winnacker Institut, Frankfurt/M.
DOC Dortmunder Oberflächen Centrum GmbH, Dortmund
Edelstahlwerke Buderus AG, Wetzlar
Emitec GmbH, Hörselberg
Ford Forschungszentrum, Aachen
Groche & Tilgner, Kalletal
H.C. Starck GmbH, Laufenburg
Haereus GmbH, Hanau
Henkel GmbH, Düsseldorf
Houghton Deutschland GmbH, Aachen
Innovationsgesell. für fortgeschr. Prod.-Syst. in der Fahrzeugindustrie mbH, Berlin
Inprotec, Heitersheim
ISPAT GmbH, Duisburg
Krupp VDM GmbH, Altena
Lechbruk und Gesellschaft für Elektrometallurgie mbH, Nürnberg
Mannesmann-Forschungsinstitut, Duisburg
MK Metallfolien GmbH, Hagen
MTU GmbH, München
Muhr & Bender GmbH, Attendorn
Niobium Products Company GmbH, Düsseldorf
Rasselstein GmbH, Andernach
Rheinzink GmbH, Datteln
Robert Bosch GmbH, Stuttgart
Salzgitter AG, Peine
Salzgitter AG, Salzgitter
Schloemann-Siemag AG, SMS, Demag, Düsseldorf
Schmidt & Clemens GmbH & Co.KG Edelstahlwerk, Lindlar
Siemens AG Power Generation, Mülheim
Siemens AG, Erlangen
SJM Co. Ltd., Ludwigshafen



Stahlwerke Ergste Westig GmbH, Schwerte
Stefanie Geisler Stahlinstitut VDEh, Düsseldorf
TESA, Hamburg
ThyssenKrupp Electrical Steel GmbH, Bochum
ThyssenKrupp Stahl AG, Duisburg
VAW Aluminium AG, Bonn
VDFI, Hagen
VFWH, Düsseldorf
Volkswagen Ag, Wolfsburg

International:

Arceralia, Aviles, Spain
Aceralia Corporacion Siderurgica S.A., Basauri-Vizcaya, Spain
Alcoa Inc., Pennsylvania, USA
Arcelor Research S.A., Metz, France
Arcelor Research S.A., Puteaux, France
Bekaert, Zwevegem, Belgium
Böhler Edelstahl GmbH & Co KG, Kapfenberg, Austria
British Steel Teesside Technology Centre, Middlesbrough, U.K.
Christian-Doppler-Labor, CD Labor, Vienna, Austria
Corus Technology B.V., IJmuiden, Netherlands
Corus UK Ltd, Sheffield, U.K.
Enel Produzione SpA, Milan, Italy
Fundacion INASMET, San Sebastian, Spain
Fundacion ITMA, Llanera, Spain
Galvalange SARL, Dudelange, Luxemburg
ILVA/Riva, Novi Ligure, Italy
Institut de Recherches de la Siderurgie Francaise, IRSID, Maizières-les-Metz, France
Instituto de Soldadura e Qualidade, Oeiras, Portugal
Kawasaki Steel, Chiba, Japan
OCAS N.V., Zelzate, Belgium
Profil ARBED, Esch-sur-Alzette, Louxemburg
Rautaruukki, Oulu, Finland
Recherche Et Developpement Du Groupe Cockerill Sambre SCRL, Liège, Belgium
Rexroth Hyraudyne, Boxtel, Netherlands
Shell Global Solutions Intern. B.V., Amsterdam, Netherlands
Sidenor I + D, Vizcaya, Spain
Treibacher Auermet Produktionsges. mbH, Treibach-Althofen, Austria
Vattenfall Utveckling AB, Aelvkarleby, Sweden
Voest Alpine Stahl Donawitz GmbH, Leoben-Donawitz, Austria
Voest Alpine Stahl Linz GmbH, Linz, Austria



Patents and Licences

| Date of Issue | Description | Inventors |
|-----------------|---|---|
| Apr. 03, 2003 | Verwendung von Stahlpulver auf der Basis Fe-Cr-Si für korrosionsbeständige Beschichtungen (DE Patent No. 198 03 084.3) | Grabke, H.-J., Prof. Dr. (30%) Sauthoff, G., PD Dr. (20%) Schroer, C., Dr. (30%) Spiegel, M., PD Dr. (20%) |
| Aug. 1, 2003 | Light-weight steel and its use for car parts and façade linings (Japan Patent) | Frommeyer, G., Prof. Dr.-Ing. |
| Febr. 19, 2004 | Leichtbaustahl und seine Verwendung (DE Patent No. 198 20 806.5) | Frommeyer, G., Prof. Dr.-Ing. |
| March 04, 2004 | TiAl-Legierung mit Cu und ihre Verwendung (DE Patent No. 198 12 444.9) | Frommeyer, G., Prof. Dr.-Ing. (40%) Knippscheer, S., Dr.-Ing. (20%) Wesemann, J., Dr.-Ing. (40%) |
| Date of Pending | Description | Inventors |
| July 3, 2003 | Beta-Titanlegierung, Verfahren zur Herstellung eines Warmwalzproduktes aus einer solchen Legierung und deren Verwendung (DE Patent No. 103 29 899.1) | Frommeyer, G., Prof. (20%) Knippscheer, S., Dr.-Ing. (20%) Schauerte, O., Dr., Volkswagen AG (20%) Sibum, H., Dr., Deutsche Titan GmbH (40%) |
| Febr. 19, 2004 | Umformbarer, gut kalt tiefziehfähiger Leichtbaustahl (DE Patent No.103 61 952.6) | Frommeyer, G., Prof. Dr.-Ing. (11.1%) Brüx, U., Dipl.-Ing. (11.1%) Brokmeier, K., Dipl.-Ing. (11.1%) TU Clausthal (33.3%) Salzgitter AG (33.3%) |



Conferences, Symposia, and Meetings Organized by the Institute

2003

G. Sauthoff and M. Palm organized and chaired the 12th meeting of the Fachausschuss Intermetallische Phasen (technical committee intermetallic phases) of the DGM (Deutsche Gesellschaft für Materialkunde, German Materials Research Society). 66 participants attended the meeting devoted to „Entwicklung und Anwendung neuer Leichtbauwerkstoffe auf der Basis des γ -Titanaluminids TiAl“ („Development and application of novel light-weight materials on the basis of γ -TiAl“) with 16 presentations, most of them from the industry. The meeting was held at the Max-Planck-Institute, Düsseldorf, Jan. 15 till 16, 2003.

The *Max Planck Institute* organized a symposium „Future trends in metallurgy and materials development“. 14 presentations were given for nearly 80 participants at the Max Planck Institute, Düsseldorf, March 31 till April 1, 2003.

S. Zaeferrer and D. Raabe chaired the international conference on Modern Methods in Texture Research (MOTEX), with 150 attendees, at the Max Planck Institute, Düsseldorf, Juni 23 till 25, 2003.

D. Raabe chaired the 16th international conference on Soft Magnetic Materials (SMM 16) with 300 attendees at the Roy-Lichtenstein Conference Center, University of Düsseldorf, Sept. 9 till 12, 2003.

A. W. Hassel and M. Stratmann organized the 19th GfKORR (Gesellschaft für Korrosionsschutz e.V., Society for Corrosion Protection) Arbeitskreis „Korrosion und Korrosionsschutz von Aluminium und Magnesium“ (working party „Corrosion and corrosion protection of aluminium and magnesium“) and the 12th GfKORR Arbeitsgruppe „Kontaktkorrosion“ (working party „Contact corrosion“). This 2 days seminar with 22 participants from industry and academia was held at the Max Planck Institute, Düsseldorf, Oct. 21 till 22, 2003.

F. Roters organized the conference of the Fachausschuss Computersimulation (technical committee computer simulation) of the DGM, entitled „Simulation von Schädigung und Versagen“ („Simulation of damage and failure“). 14 papers were presented to more than 30 participants from 2 countries. The conference was held at the Max Planck Institute, Düsseldorf, Nov. 24, 2003.

D. Ponge and D. Raabe chaired the Warmumformtag (Hot-Metal Forming conference) with 150 attendees at the Max Planck Institute, Düsseldorf, Dec. 5, 2003.

2004

G. Sauthoff and M. Palm organized and chaired the 13th annual meeting of the Fachausschuss Intermetallische Phasen (technical committee intermetallic phases) of the DGM with 30 participants and 6 presentations at the Max-Planck-Institute, Düsseldorf, Jan. 14, 2004.

M. Palm and A. Schneider organized and chaired the colloquium „Current understanding of phase equilibria and transformations“ on the occasion of Prof. Gerhard Inden's 65th birthday. Approximately 120 guests attended the four invited presentations at the Steel Institute VDEh, Düsseldorf, Jan. 23, 2004.

J. Konrad and M. Palm organized the „Discussion meeting on the development of innovative iron aluminium alloys“ for the presentation of the joint scientific topic „Iron aluminium based materials“. Approximately 70 participants from 4 countries, many of them from industry, attended the 15 presentations at the Max Planck Institute, Düsseldorf, March 9, 2004.



The *Japan Society for the Promotion of Science* and the *Deutsche Gesellschaft der JSPS-Stipendiaten e.V.* jointly organized the symposium „Frontier in nanoscience“. *A. W. Hassel* as a member of the „Deutsche Gesellschaft der JSPS-Stipendiaten e.V.“ was involved in the preparation and as a convener in the accomplishment. The topic „Frontier in nanoscience“ attracted around 200 participants from academia, industry and scientific organisations at the congress centre Rotes Ross, Halle/Saale, May 14 till 15, 2004.

The *Max Planck Institute* held a colloquium in honour of Prof. Dr. P. Neumann on the occasion of his retirement. About 150 guests attended the colloquium at the Steel Institute VDEh, Düsseldorf, July 6, 2004.

F. Roters organized the meeting of the Fachausschuss Computersimulation of the DGM, entitled „Werkstoffmodelle für die Simulation von Leichtmetallen“ („Materials models for the simulation of light metals“). 10 papers were presented to more than 20 participants from 2 countries. The meeting was held at Hydro Aluminium Deutschland GmbH, Bonn, Nov. 15, 2004.

G. Grundmeier as head of the Christian Doppler Laboratory for Polymer/Metal Interfaces conducted the workshop „Applied surface and interface analysis for thin film coated metals“, as part of the Surface Technology Days with 45 participants from industry and academia at the Max Planck Institute, Düsseldorf, Dec. 1 till 2, 2004.

M. Palm organized a workshop on the „Diffusion Couple Technique“ in the framework of COST 535. 40 participants from 12 countries attended 7 lecturers and 16 presentations at the Max Planck Institute, Düsseldorf, Dec. 6 till 7, 2004.



Institute Colloquia and Invited Seminar Lectures

2003

Mudali, M., U.K., Indira Gandhi Centre for Atomic Research, Kalpakkam, India:
Metallurgy and corrosion aspects of ancient Delhi iron pillar (02-07-2003)

Wöll, C., Ruhr-Universität, Bochum:
Surface chemistry on metal oxides: Results of molecular beam scattering (02-11-2003, Colloquium)

Brokmeier, H.-G., GKSS-Forschungszentrum, Geesthacht:
Texturanalytik mittels Neutronen und harten Röntgenstrahlen (03-25-2003, Colloquium)

Godfrey, A., Tsinghua University, Beijing, China:
Problems associated with orientation noise in EBSD data (04-07-2003)

Butt, H.J., MPI für Polymerforschung, Mainz:
Using the atomic force microscope to study confined liquids (04-08-2003, Colloquium)

Frankel, G.S., Ohio State University, Columbus, USA:
application of scanning Kelvin Probe Force microscopy for studies of corrosion
(05-05-2003)

Brill, U., Thyssen Krupp VDM, Altona:
Verfestigungsmechanismen von Hochtemperaturwerkstoffen (05-08-2003, Colloquium)

Müller-Plathe, F., Universität, Bremen:
Soft Surfaces: What can simulation contribute? (05-13-2003, Colloquium)

Davenport, A., University of Birmingham, UK:
Microstructural effects in the corrosion and surface finishing of aluminium alloys
(05-23-2003)

Kelly, T., Image Scientific Instruments Corp., Madison, USA:
3D atomic-scale compositional imaging with local electrode atom probes (05-27-2003)

Bolt, H., MPI für Plasmaphysik, Garching:
Werkstoffe für die plasmabelasteten Werkstoffe von Fusionsanlagen (06-03-2003, Colloquium)

Mücklich, F., Universität des Saarlandes, Saarbrücken:
Surface modification by laser interference induced periodic treatment (06-10-2003, Colloquium)

Dreyer, W., Weierstraß-Institut für angewandte Analysis und Stochastik, Berlin:
On mechanics and thermodynamics of phase transitions involving disordered and ordered solids (06-13-2003, Colloquium)

Blavette, D., Université, Rouen, France:
3D atomic-scale observation of materials using atom-probe tomography (06-23-2003, Colloquium)

Demura, M., National Institute of Materials Science, Tsukuba, Japan:
Mechanical properties of Ni₃Al cold-rolled foils (06-26-2003)



Asteman, H., Chalmers University, Gothenburg, Sweden:

The effect of water vapour induced chromium evaporation on the high temperature oxidation of Cr_2O_3 forming alloys (06-30-2003)

Sakairi, D., Hokkaido University, Sapporo, Japan:

Micro surface patterning on aluminum by laser irradiation and AFM tip processing (07-04-2003)

Rösler, J., TU, Braunschweig:

Superalloy research: From high temperature alloys for power plants to nanoporous materials (07-08-2003, Colloquium)

Takeyama, M., Institute of Technology, Tokyo, Japan:

Physical metallurgy of titanium aluminides and other materials (07-16-2003, Colloquium)

Macdougall, B., National Research Council of Canada, Ottawa, Canada:

Role of nanotechnology in environmental electrochemistry and energy conversion: its academic strength as opposed to applied weakness (07-28-2003)

Kasser, K., Universität Magdeburg:

Numerical approaches to solidification problems (08-19-2003, Colloquium)

Wang, Y., Ohio State University, USA:

Quantitative phase field modeling of microstructural evolution (08-26-2003, Colloquium)

Ozolins, V., University of California, Los Angeles, USA:

Atomic displacements and phase diagrams of bulk and surface alloys (09-02-2003, Colloquium)

Rettenmayr, M., Universität, Jena:

The role of local supersaturation during microstructure evolution (10-07-2003, Colloquium)

Lipowski, R., MPI of Colloids and Interfaces, Potsdam:

Structured surfaces and wetting phenomena (10-14-2003, Colloquium)

Windl, W., Ohio State University, Columbus, USA:

Physic-based multiscale modeling – from semiconductors to structural materials (10-20-2003, Colloquium)

Stiller, K., University, Göteborg, Sweden:

Investigation of microstructure and chemistry of materials using high-resolution methods (10-29-2003, Colloquium)

Harste, K., Wüstner, E., Saarstahl, Völklingen:

Innovative solutions for the production of wire, rod and bar (11-12-2003, Colloquium)

Vehoff, H., Universität des Saarlandes, Saarbrücken:

When the microstructure meets the specimens size – effects of microstructure and size on mechanical properties examined by nanoindentation and in situ mechanical tests in a SEM (12-09-2003, Colloquium)

Müller, S., Universität Erlangen-Nürnberg, Erlangen:

Ab-initio thermodynamics of metal alloys: From the atomic to the mesoscopic scale (12-10-2003, Colloquium)

Neugebauer, J., Universität, Paderborn:

Materials design on the computer (12-16-2003, Colloquium)

Blöchl, P., TU, Clausthal:

Interfacing silicon with high-K oxides (12-19-2003, Colloquium)



2004

Schmuki, P., Universität Erlangen-Nürnberg, Erlangen:
Approaches in electrochemical nanotechnology (01-20-2004, Colloquium)

Frauenheim, T., Universität, Paderborn:
Theoretical approaches to understand complex materials structures, functions and biomolecular processing (02-10-2004, Colloquium)

Nagai, K., Steel Research Center, NIMS, Tsukuba, Japan:
Ultrafine grained steels (02-26-2004, Colloquium)

Herzer, G., Vacuumschmelze, Hanau:
To catch a thief – magnetic materials for electronic article surveillance (03-08-2004, Colloquium)

Geers, M., University Eindhoven, NL:
Multi-scale modelling of the crystal mechanics of FCC-metals (03-16-2004)

Ernst, F., Case Western Reserve University, Cleveland, Ohio USA:
Colossal supersaturation with interstitial atoms: a new concept for advanced structural alloys (03-23-2004, Colloquium)

Kostorz, G., ETH, Zürich, Switzerland:
Microstructure of alloys from neutron scattering (04-20-2004, Colloquium)

Becker, K., Universität, Braunschweig:
Spectroscopic investigations of high-temperature processes in oxides (05-11-2004, Colloquium)

Schneider, J., RWTH, Aachen:
Machineable carbides – a contradiction in terms? (06-02-2004, Colloquium)

Mohles, V., RWTH, Aachen:
Versetzungssimulationen zur kritischen Schubspannung ausscheidungsgehärteter Metalle (06-08-2004, Colloquium)

McQueen, H.J., Concordia University, Montreal, Canada:
Simulation of rolling in Al, Al-5Mg and Al-0.65 Fe (06-14-2004)

Link, T., TU Berlin:
Creep of nickel base superalloys: new deformation mechanisms at high temperatures and low stresses(06-17-2004)

Pundt, A., Universität, Göttingen:
Hydrogen in nano-sized metals (07-13-2004, Colloquium)

Löffler, J., ETH, Zürich, Switzerland:
Mesoscopic and multiphase metallic systems – challenges and perspectives (07-15-2004, Colloquium)

Hiramoto, S., EPFL Lausanne, Lausanne, Switzerland and NIMS, Tsukuba, Japan:
Investigation of various factors of Ti-6Al-4V alloy (in EPFL); Corrosion behaviour of biometals with culturing cells (in NIMS) (09-02-2004)

Widdel, F., MPI für marine Mikrobiologie, Bremen:
Iron and bacteria multiple connections with consequences (09-07-2004)



Mortensen, A., EPF, Lausanne, Switzerland:

Infiltrated alumina particle reinforced aluminium matrix composites (09-28-2004, Colloquium)

Eckert, J., TU, Darmstadt:

Recent advances in the design of metastable materials for engineering applications (10-04-2004, Colloquium)

Müller, S., MPI für Mathematik in den Naturwissenschaften, Leipzig:

Mathematical tools for multiscale problems: phase transitions, shape-memory and dislocation structures (10-07-2004, Colloquium)

Eggeler, G., Ruhr-Universität, Bochum:

New results on the multiple-step martensitic transformation in Ni-rich shape memory alloys (10-13-2004, Colloquium)

Mitterer, C., Universität Leoben, Austria:

Multifunctional nano-structured hard coatings for wear protection (10-28-2004, Colloquium)

Epple, M., Universität, Essen:

Biomaterials on the basis of metals, polymers, and ceramics (11-29-2004, Colloquium)

Pyzalla, R., Institut für Werkstoffwissenschaften, TU, Wien, Austria

Synchrotron radiation: new perspectives in materials science and technology (12-13-2004, Colloquium)

Singheiser, L., FZ, Jülich:

Improvement of oxidation resistance of ferritic steels by alloying additions (12-14-2004, Colloquium)

Weber, L., Laboratoire de Métallurgie Mécanique, EPFL, Lausanne, Switzerland:

Diamond-based composites as new materials for high-power heat-sink applications (12-16-2004, Colloquium)



Lectures and Teaching at University

G. Frommeyer, TU Clasthal: Physikalische Metallkunde und Technologie der hochschmelzenden krz. Metalle, WS 2002/2003, WS 2003/2004, SS 2004.

G. Grundmeier, M. Stratmann, and M. Rohwerder, Ruhr-Univ. Bochum: Funktionelle Schichten auf Metallen - Vom Korrosionsschutz zum Lotus-Effekt, SS 2003.

G. Grundmeier and M. Rohwerder, Ruhr-Univ. Bochum: Oberflächenmodifikation von Metallen – Vom Korrosionsschutz zum Lotuseffekt, SS 2003, SS 2004.

A. W. Hassel, Univ. Düsseldorf: Thermodynamische Rechenübungen für Diplomchemiker und Wirtschaftschemiker, SS 2004.

P. Neumann, Univ. Düsseldorf: Versetzungen in Metallen, Werkstoffwissenschaftliche Mechanik, WS 2003/2004.

D. Raabe, RWTH Aachen: Computational Materials Science (Prozess- and Werkstoffmodellierung), WS 2002/2003, WS 2003/2004.

D. Raabe, RWTH Aachen: Polykristallmechanik Grundlagen, SS 2003.

D. Raabe, RWTH Aachen: Micromechanics of Materials, SS 2003, SS 2004.

D. Raabe, MPIE: Micromechanics of Materials, WS 2003/2004.

D. Raabe, MPIE: Computational Materials Science, WS 2003/2004.

D. Raabe, RWTH Aachen: Ethymology and History of Metals, WS 2002/2003, WS 2003/2004.

D. Raabe, Univ. Dortmund: Computational Materials Science, SS 2004.

D. Raabe and F. Roters, RWTH Aachen: Prozeß- und Werkstoffmodellierung, Aspekte der mesoskopischen und der Gefügesimulation, WS 2003/2004.

F. Roters, RWTH Aachen: Prozess- and Werkstoffsimulation, WS 2004/2005.

G. Sauthoff, RWTH Aachen: Einführung in die Werkstofftechnik (für Wirtschaftswissenschaftler), Teil 2: Werkstoffkunde der Nicht-Eisen-Metalle, SS 2003, SS 2004.

M. Spiegel, RWTH Aachen: Korrosion keramischer Werkstoffe, WS 2002/2003, WS 2003/2004.



Oral and Poster Presentations

2003

Akiyama, E., A. W. Hassel and M. Stratmann: A study of current transients caused by single particle impact on electrodes. (13th Asian Pacific Corrosion Control Conference, 11-16 till 11-21, 2003, Osaka, Japan)

Akiyama, E., A. W. Hassel and M. Stratmann: Measurements of electrochemical responses caused by a single particle impact in slurry impingement. (50th Zairyo-to-Kankyo Meeting, 11-05 till 11-07, 2003, Okinawa, Japan)

Balun, J., G. Inden, L. T. F. Eleno and C. G. Schoen: Phase equilibria in the ternary Fe-Rh-Ti system. (TMS Annual Meeting 2003, International Symposium on Intermetallic and Advanced Metallic Materials – A Symposium dedicated to Dr. C.T. Liu, 03-02 till 03-06, 2003, San Diego, USA)

Balun, J., P. Unucka, G. Inden and A. Kroupa: Thermodynamic assessment of Laves phase and μ -phase in Ta-X-V systems. (CALPHAD XXXII, 05-25 till 05-30, 2003, La Malbaie, Quebec, Canada)

Baumert, B., M. Stratmann and M. Rohwerder: Formability of ultra-thin plasma-polymer films deposited on metal sheet: mesoscopic and nanoscopic aspects of defect formation. (MRS Fall Meeting, 12-01 till 12-05, 2003, Boston, MA)

Bengtsson Blücher, D., J.-E. Svensson, M. Rohwerder and M. Stratmann: Scanning Kelvin probe force microscopy, a useful tool for studying atmospheric corrosion. (204th Meeting - Orlando, Florida, 10-12 till 10-16, 2003, Orlando, Florida)

Büchner, A. R. and S. Pötschke: Gefügeeinstellung beim Bandgießen mit Inline-Warmwalzen. (VDEh-Ausschuss für metallurgische Grundlagen, Stahlzentrum VDEh, 12-17, 2003, Düsseldorf)

Cha, S. C., D. Vogel and M. Spiegel: Fundamental studies on alkali chloride induced corrosion during combustion of biomass. (18. Stahlkolloquium, Eurogress, 09-25 till 09-26, 2003, Aachen)

Elsner, A. and R. Kaspar: Deep-drawable steel strip produced by ferritic rolling. (Lecture at the International Conference on Processing & Manufacturing of Advanced Materials THERMEC, 06-10, 2003, Leganes, Madrid, Spain)

Frommeyer, G.: Neuere Entwicklungen der Stahlforschung: Hochfeste und supraduktile TRIP/TWIP Leichtbaustähle. (Nordrhein-Westfälische Akademie der Wissenschaften, 07-09, 2003, Düsseldorf)

Frommeyer, G.: Structures and properties of advanced high-strength and supra-ductile light-weight steels. (42th Conference of Metallurgists; COM, 08-24 till 08-27, 2003, Vancouver, Canada)

Frommeyer, G.: Structures and properties of the refractory silicides Ti_5Si_3 and $TiSi_2$ and Ti-Si-(Al) eutectic alloys. (NATO Advanced Research Workshop: Metallic Materials with high Structural Efficiency, 09-07 till 09-13, 2003, Kiev, Ukraine)

Frommeyer, G.: Superplasticity at higher strain rates in hypereutectoid Fe-1.3-6.5Al(Sn) steels. (THERMEC, 07-07 till 07-11, 2003, Madrid, Spain)

Frommeyer, G.: Superplastizität und superplastische Blechumformung von Duplex-Stählen am Beispiel der Qualität X 12 Cr Ni Mo (N) 22-5-3. (VDI Seminar: Innovative Rostfreistähle, 06-26, 2003, VDI-Zentrum, Düsseldorf)

Frommeyer, G. and U. Brüx: Structures and properties of advanced high-strength and supra-ductile light-weight steels. (EUROMAT, 09-01 till 09-04, 2003, Lausanne, Schweiz)

Frommeyer, G. and S. Knippscheer: Alternative Perspektiven und Möglichkeiten von TiAl-Basislegierungen. (Fach-ausschusstagung Intermetallische Phasen, MPI für Eisenforschung, 01-15 till 01-16, 2003, Düsseldorf)

Frommeyer, G. and S. Knippscheer: Enhanced superplasticity and superplastic forming of ultra fine-grained TiAl-(Mo, Si) alloys. (Ti-2003, 07-13 till 07-18, 2003, Hamburg)

Frommeyer, G. and S. Knippscheer: Mikrostrukturen, Eigenschaften und Anwendungen neuentwickelter Leichtbauwerkstoffe auf der Basis von Titanaluminiden. (Diehl Symposium, 11-21, 2003, Lengenfeld)

Fushimi, K., A. W. Hassel and M. Stratmann: Passive film formed on shape memory NiTi-alloy in sulfuric acid. (13th Asian Pacific Corrosion Control Conference, 11-16 till 11-21, 2003, Osaka, Japan)

Grabke, H. J.: High temperature corrosion of pyrolysis tubes. (European Federation of Corrosion Workshop „Metal Dusting, Carburisation and Nitridation“, DECHEMA, 01-30 till 01-31, 2003, Frankfurt)

Grabke, H. J.: Korrosion in gemischten Gasen I: Grundlagen - Thermodynamik, Stabilitätsdiagramme, Aufkohlung, Metal Dusting, Sulfidierung. (DGM - Fortbildungsseminar, 10-07 till 10-09, 2003, Jülich)

Grabke, H. J.: Segregation and oxidation. (The Thursday Evening Talk at Gordon Research Conference on High Temperature Corrosion, 07-20 till 07-25, 2003, New London NH, USA)



Grabke, H. J., E. M. Müller-Lorenz, S. Strauss and D. Vogel: Corrosion of steels and Ni-base alloys under Kalina-cycle conditions (NH₃-H₂O, 500°C). (European Federation of Corrosion Workshop „Metal Dusting, Carburisation and Nitridation“, DECHEMA, 01-30 till 01-31, 2003, Frankfurt)

Grundmeier, G. and B. Roßenbeck: Spectroscopic, microscopic and electrochemical investigations of protective model latex films on iron. (GDCH Jahrestagung, 10-06 till 10-10, 2003, Munich)

Grundmeier, G.: Tailored adhesion promoting and corrosion resistant ultra-thin plasma polymer films at polymer/metal interfaces. (EVC, 06-23 till 06-27, 2003, Berlin)

Grundmeier, G., M. Stratmann and B. Roßenbeck: Spectroscopic, microscopic and electrochemical investigations of protective model latex films on iron. (ECASIA, 10-05 till 10-10, 2003, Berlin)

Hassel, A. W., S. Bonk, M. Wicinski and M. Stratmann: Corrosion of zinc coated steel sheets under cyclic corrosion conditions. (13th Asian Pacific Corrosion Control Conference, 11-02 till 11-16, 2003, Osaka, Japan)

Hausbrand, R., M. Stratmann and M. Rohwerder: Delaminationsschutz mit neuartigen Zinklegierungsschichten. (API-Tagung, API-Preisvortrag, „Die Lackindustrie auf dem Wege zur sanften Chemie?“, 09-15 till 09-17, 2003, Rostock-Warnemünde)

Inden, G.: Computerunterstützte Thermodynamik. (Kontaktstudium Werkstofftechnik Stahl, Teil I: Grundlagen, 06-22 till 06-24, 2003, Aachen)

Inden, G.: Simulation of diffusion controlled transformations in multicomponent systems. (DECHEMA Workshop on Diffusion Modelling, 12-17 till 12-18, 2003, Frankfurt)

Inden, G.: Simulation of precipitation in multicomponent systems. (Colloque Précipitation, 10-06 till 10-10, 2003, Autrans, France)

Inden, G.: Überlegungen zu Nichtgleichgewichtsumwandlungen. (THERMOCALC - Anwendertreffen, 06-11 till 06-13, 2003, Aachen)

Inden, G., C. Hutchinson and Y. Bréchet: Interfacial condition at the moving interfaces during steady and non-steady state growth of ferrite from austenite in Fe-C-X alloys. (Symposium on Mechanical Working and Steel Processing Conference, TMS Meeting Materials Science & Technology, 11-09 till 11-12, 2003, Chicago, USA)

Knezevic, V. and G. Sauthoff: Strengthening of martensitic/ferritic 12%Cr model steels through Laves phase precipitation. (Euromat 2003, 8th European Congress on Advanced Materials and Processes, 09-01 till 09-05, 2003, Munich)

Kobayashi, S., S. Zaefferer, A. Schneider, D. Raabe and G. Frommeyer: Slip system determination by rolling texture measurements around the strength peak temperature in a Fe₃Al-based alloy. (Intern. Conf. on Strength of Materials, ICSMA 13, 08-29 till 09-02, 2003, Budapest, Hungary)

Konrad, J.: Thermomechanische Behandlung von Fe₃Al-Basislegierungen-Voruntersuchungen zu Konstitution und Umformverhalten. (MPI für Eisenforschung 07-23, 2003, Düsseldorf)

Konrad, J.: Thermomechanical treatment of Fe₃Al base alloys –texture evolution and inheritance. (Kolloquium Dr. Lacaze, MPI für Eisenforschung, 12-08, 2003, Düsseldorf)

Kuo, J. C., D. Raabe, S. Zaefferer, F. Roters, Z. Zhao and M. Winning: Microstructure mechanics: investigation on deformation behaviour of grain boundaries. (Plasticity 2003, 07-10, 2003, Quebec, Canada)

Li, Y. S. and M. Spiegel: Degradation performance of Al-containing alloys and intermetallics by molten ZnCl₂/KCl. (Corrosion Science in the 21st Century, UMIST, 07-06 till 07-11, 2003, Manchester, UK)

Martinz, H. P., H. J. Grabke and E. M. Müller-Lorenz: Metal dusting resistance of high-chromium alloys. (European Federation of Corrosion Workshop „Metal Dusting, Carburisation and Nitridation“, DECHEMA, 01-30 till 01-31, 2003, Frankfurt)

Müller-Lorenz, E. M. and H. J. Grabke: Metal dusting behaviour of welded Ni-base alloys with different surface finish. (European Federation of Corrosion Workshop „Metal Dusting, Carburisation and Nitridation“, DECHEMA, 01-30 till 01-31, 2003, Frankfurt)

Palm, M.: Determination and application of the Al-Ti and Al-Fe-Ti phase diagrams. (Colloquium at ONERA, Colloquium at Université de Rouen, 09-15 till 09-16, 2003, Chatillon / Rouen, France)

Parezanovic, I. and M. Spiegel: Influence of dew point on the selective oxidation of cold rolled DP and IF-steels. (18. Stahlkolloquium, Eurogress, 09-25 till 09-26, 2003, Aachen)

Parezanovic, I. and M. Spiegel: Influence of dew point on the selective oxidation of cold rolled DP and IF-steels. (Corrosion Science in the 21st Century, UMIST, 07-06 till 07-11, 2003, Manchester, UK)

Parezanovic, I. and M. Spiegel: Surface modification of different Fe-Si and Fe-Mn alloys by oxidation/reduction treatments. (EUROCORR, 09-29 till 10-03, 2003, Budapest, Hungary)



Parezanovic, I. and M. Spiegel: Surface modification of Fe-Si and Fe-Mn alloys by oxidation reduction treatments. (Gordon Research Conference on High Temperature Corrosion, 10-20 till 10-25, 2003, New London, NH, USA)

Pippel, E., J. Woltersdorf and H. J. Grabke: Microprocesses of metal dusting on iron-nickel alloys and their dependence on composition. (European Federation of Corrosion Workshop „Metal Dusting, Carburisation and Nitridation“, DECHEMA, 01-30 till 01-31, 2003, Frankfurt)

Ponge, D.: Hochfeste Baustähle und deren schweißtechnische Verarbeitung. (Berufsbildung Deutscher Verband für Schweißen und verwandte Verfahren e. V., 10-09, 2003, Hamburg)

Raabe, D.: Experiment und Theorie der Oberflächen- und Polykristallmechanik. (Kolloquiumsvortrag an der Technischen Universität, 01-27, 2003, Hamburg-Harburg)

Raabe, D.: Experiments and theory of surface- and polycrystal mechanics. (Colloquium Lecture at the Technical University, 01-25, 2003, Hamburg-Harburg)

Raabe, D.: Microstructure mechanics: investigation on deformation behaviour of grain boundaries. (Keynote lecture at Plasticity 2003, 07-07, 2003, Quebec, Canada)

Raabe, D.: Polycrystal mechanics in experiment and theory. (Keynote lecture at the Breitenau Materials Conference, 08-20, 2003, Breitenau)

Raabe, D.: Polycrystal mechanics in experiment and theory. (Massachusetts Institute of Technology, 07, 2003, Cambridge, USA)

Raabe, D.: Polycrystal mechanics in experiment and theory. (NATO Conference, 08, 2003, Freiburg)

Raabe, D.: Polycrystal mechanics of metals and polymers - experiments and theory. (Colloquium Lecture at the Massachusetts Institute of Technology, 12-05, 2003, Cambridge, USA)

Raabe, D.: Simulation of texture and anisotropy during metal forming with respect to scaling aspects. (Lecture at the 1st Colloquium on Process Scaling, 10-03, 2003, Bremen)

Raabe, D.: Texturen und Kristallmechanik. (Kolloquium, TU, 01-20, 2003, Darmstadt)

Raabe, D.: Textures and Crystal Mechanics. (Colloquium Lecture at the Materials Department at the Technical University, 01-20, 2003, Darmstadt)

Risanti, D. D. and G. Sauthoff: Strengthening of hot corrosion-resistant Fe-Al alloys through Laves phase precipitation. (Euromat 2003, 8th European Congress on Advanced Materials and Processes, 09-01 till 09-05, 2003, Munich)

Rohwerder, M.: Fundamental aspects of delamination. (Corrosion Science in the 21st Century, UMIST, 07-06 till 07-11, 2003, Manchester, UK)

Rohwerder, M.: Scanning Kelvin probe force microscopy (SKPFM) – nanoskopische Aspekte der Korrosion. (4. Workshop Rasterkraftmikroskopie in der Werkstoffwissenschaft, Universität, 02-20 till 02-21, 2003, Münster)

Roters, F.: Application of the texture component crystal plasticity FEM to forming simulation. (THERMEC, 07-10, 2003, Madrid, Spain)

Roters, F.: Crystal plasticity FEM from grain scale plasticity to anisotropic sheet forming behaviour. (13th international Workshop on Computational Modelling of the Mechanical Behaviour of Materials, 09-22, 2003, Magdeburg)

Roters, F.: Numerische Simulation der Metallumformung und Rekristallisation. (Workshop, Simulation und numerische Modellierung, Materials Valley e.V., 11-06, 2003, Mainz)

Ruh, A. and M. Spiegel: Kinetic investigations on molten salt induced corrosion of pure iron. (EUROCORR, 09-29 till 10-03, 2003, Budapest, Hungary)

Schneider, A.: Computer-Simulation von Phasengleichgewichten und diffusionskontrollierten Phasenumwandlungen in Eisenbasislegierungen mit Thermo-Calc und DICTRA. (Thermo-Calc-DICTRA Anwendertreffen, 06-12 till 06-13, 2003, Aachen)

Schneider, A.: How to make high-temperature materials last longer. (Colloquium – Department of Materials, 11-27, 2003, Oxford, UK)

Schneider, A., L. Falat, G. Sauthoff and G. Frommeyer: Microstructures and mechanical properties of Fe-Al-C and Fe-Al-M-C (M = Ti, V, Nb, Ta) alloys. (TMS Annual Meeting - Intern. Symp. Intermetallic and Advanced Metallic Materials - A Symposium Dedicated to Dr. C. T. Li on His 65th Birthday, 03-02 till 03-06, 2003, San Diego, CA)

Schneider, A. and H. J. Grabke: Effect of H₂S on metal dusting. (EFC-Workshop: Metal Dusting, Carburisation and Nitridation, 01-30 till 01-31, 2003, Frankfurt)

Schneider, A. and G. Sauthoff: Iron-aluminium alloys with strengthening carbides and intermetallic phases for high-temperature applications. (THERMEC, 07-07 till 07-11, 2003, Leganes, Madrid, Spain)



- Schneider, A., J. Zhang and G. Inden:** Metal dusting of Fe₃Al-based alloys. (Annual Meeting, Symposium: International Symposium on Intermetallics and Advanced Metallic Materials, 06-02, 2003, San Diego, California, USA)
- Schneider, A., J. Zhang, G. Inden and G. Frommeyer:** Carburisation of Fe₃Al-based alloys in CO-H₂-H₂O mixtures. (EFC-Workshop: Metal Dusting, Carburisation and Nitridation, 01-30 till 01-31, 2003, Frankfurt)
- Spiegel, M.:** Corrosion protection and electronic conductivity: Spinel forming stainless steels as CCC for MCFC. (Gordon Research Conference on High Temperature Corrosion, 10-20 till 10-25, 2003, New London, NH, USA)
- Spiegel, M.:** Factors affecting the high temperature corrosion resistance of coatings in waste fired plant. (Corrosion Science in the 21th Century, 07-06 till 07-11, 2003, UMIST Manchester, UK)
- Spiegel, M.:** Korrosion in Müllverbrennungsanlagen. (DGM-Fortbildungsseminar, Hochtemperaturkorrosion, 10-08 till 10-09, 2003, Jülich)
- Spiegel, M.:** Salzschnmelzeninduzierte Hochtemperaturkorrosion. (VDI Wissensforum, 06-24, 2003, Göttingen)
- Spiegel, M.:** The high temperature reactions group at the MPI für Eisenforschung. (18th Stahlkolloquium, Eurogress, 09-25 till 09-26, 2003, Aachen)
- Spiegel, M. and H. J. Grabke:** Korrosion durch Chlor und Chloride. (DGM-Fortbildungsseminar, Hochtemperaturkorrosion, 10-08 till 10-09, 2003, Jülich)
- Spiegel, M., Warnecke and R. Enders, M.:** Korrosion durch Beläge und Salzschnmelzen. (VGB Fachtagung: Thermische Abfallverwertung, 03-20, 2003, Nürnberg)
- Stallybrass, C. and G. Sauthoff:** Ferritic Fe-Al-Ni-Cr alloys for high temperature applications. (Thirteenth International Conference on the Strength of Materials, ICSMA XIII, 08-25 till 08-30, 2003, Budapest, Hungary)
- Stein, F.:** Laves Phasen – Struktur und Stabilität. (MPI für Festkörperforschung, 11-26, 2003, Stuttgart)
- Stein, F., M. Palm and G. Sauthoff:** Coexistence of Laves phase polytypes in the Co-Nb system. (Workshop „Laves Phases II“, 02-04, 2003, Dresden)
- Stein, F., M. Palm and G. Sauthoff:** Structures and stability of Laves phases. (TMS Annual Meeting - Intern. Symp. Intermetallic and Advanced Metallic Materials - A Symposium Dedicated to Dr. C. T. Liu on His 65th Birthday, 03-02 till 03-06, 2003, San Diego, CA)
- Storojeva, L., C. Escher, R. Bode and K. Hulka:** Stabilization and processing concept for the production of ULC steel sheet with bake hardenability. (Lecture at the International Forum for the Properties and Application of IF Steels, 05-13, 2003, Tokyo, Japan)
- Storojeva, L., R. Kaspar and D. Ponge:** Ferritic-pearlitic steel with deformation induced spheroidized cementite. (Lecture at the International Conference on Processing & Manufacturing of Advanced Materials THERMEC, 06-08, 2003, Leganes, Madrid, Spain)
- Stratmann, M.:** Adhesion and deadhesion of organic coatings. (Penary lecture, 13th Asian Pacific Corrosion Control Conference, Hokkaido University, 11-27, 2003, Sapporo, Japan)
- Stratmann, M.:** High-tech and steel novel concepts in the surface technology of steel. (The 21st Century in Global Heat Treating, LOI, 04-04, 2003, Essen)
- Stratmann, M.:** High-tech and steel – novel concepts in the surface technology of steel. (Plenary lecture, 13th Asian Pacific Corrosion Control Conference, JFE Steel, 11-26, 2003, Chiba, Japan)
- Stratmann, M.:** Knowledge based multifunctional surface layers for mass produced materials. (EOI, MPI für Eisenforschung, 08-09, 2003, Düsseldorf)
- Stratmann, M.:** Knowledge based multifunctional surface layers for mass produced materials. (EU, 02-05, 2003, Brüssel, Belgium)
- Stratmann, M.:** Neuartige Zink-Legierungsüberzüge: Maßgeschneiderte halbleitende Oxide für verbesserten Korrosionsschutz und eine verbesserte Haftung organischer Beschichtungen. (DGM-Tag, 07-10 till 07-11, 2003, Erlangen)
- Stratmann, M.:** Neues vom Stahl: von ungewöhnlichen Legierungen bis zu maßgeschneiderten Oberflächen. (GDCh – Vorträge, Ortsverband Ruhr, 12-18, 2003, Mülheim)
- Stratmann, M.:** Surface modification of iron based alloys for improved corrosion resistance and adhesion. (Plenary lecture, EUROCORR, 09-28 till 10-02, 2003, Budapest, Hungary)
- Stratmann, M.:** Untersuchungen zum Delaminationsverhalten von polymerbeschichteten verzinkten und unverzinkten Stahloberflächen mit der Rasterkelvinsonde bei klimatischen Wechselstestbedingungen. (3. Stahl-Symposium / Werkstoffe, Anwendung, Forschung, Stahlzentrum VDEh, 03-12, 2003, Düsseldorf)



Stratmann, M., R. Hausbrand and M. Rohwerder: Novel zinc alloy coatings: tailored semiconducting oxides for improved corrosion protection and adhesion of organic coatings. (Plenary lecture, 13th Asian Pacific Corrosion Control Conference, 11-16 till 11-21, 2003, Osaka, Japan)

Stratmann, M., R. Hausbrand, M. Rohwerder, Ch. Wapner and G. Grundmeier: Surface modification of iron based alloys for improved corrosion resistance and adhesion. (Penary lecture, 13th Asian Pacific Corrosion Control Conference, Corrosion Symposium in NIMS, 11-25, 2003, Tsukuba, Japan)

Thiemann, M. and A. R. Büchner: Investigation of shell formation on metallic surfaces under different cooling rates. (METEC Congress 03, 06-16 till 06-20, 2003, Düsseldorf)

Tsuri, S., A. W. Hassel and M. Stratmann: Electrochemical behaviour of low alloy Steels during Atmospheric Corrosion. (13th Asian Pacific Corrosion Control conference, 11-16 till 11-21, 2003, Osaka, Japan)

Wang, Y., C. Klüber, F. Roters and D. Raabe: Investigation of nano indentation pile-up patterns in copper single crystals. (EUROMAT, 09-02, 2003, Lausanne, Schweiz)

Wang, Y., F. Roters and D. Raabe: Simulation of texture and anisotropy during metal forming with respect to scaling aspects. (1st Colloquium Process Scaling, 10-28, 2003, Bremen)

Wapner, K., M. Stratmann and G. Grundmeier: Scanning Kelvin probe measurements of electrode potentials at adhesive/metal interfaces in corrosive environments. (Bunsentagung, 05, 2003, Kiel)

Wöllmer, S., S. Zaefferer, M. Göken, T. Mack and U. Glatzel: Characterization of phases of aluminized nickel base superalloys. (Intern. Conf. on Strength of Materials, ICSMA 13, 08-27 till 08-28, 2003, Budapest, Hungary)

Yu, X.-W. and M. Rohwerder: Molecular scale aspects of cathodic delamination. (Electrochem. 2003, 44th Corrosion Symposium, 09-30, 2003, Southampton, UK)

Zaefferer, S.: Microstructural characterization of low alloyed TRIP steels by SEM and TEM techniques. (THERMEC, 07-10, 2003, Madrid, Spain)

Zaefferer, S.: Microstructural characterization of low alloyed TRIP steels by SEM and TEM techniques. (Seminar des Instituts für Eisenhüttenkunde der RWTH, 05-21, 2003, Aachen)

Zaefferer, S.: Microstructure formation and phase transformation mechanisms in low alloyed TRIP steels. (Gemeinsames Kolloquium der Institute für Metallkunde Aachen, Düsseldorf, Ghent und Leuven, 10-22, 2003, Aachen)

Zaefferer, S.: Microtexture measurements: a powerful tool to understand microstructures. (Microtexture measurements, 07-01, 2003, Berlin)

Zaefferer, S.: Microtexture measurements: a powerful tool to understand microstructures. (Seminar des Geologischen Instituts, 05-19, 2003, Bochum)

Zaefferer, S.: Microtexture measurements: a powerful tool to understand microstructures. (MPI für Eisenforschung, 02-27, 2003, Düsseldorf)

Zaefferer, S.: Some topics of experimental texture and microstructure research at the MPIE. (Intern. Workshop on Modern Texture Research in Engineering Materials, MoteX, 06-24, 2003, Düsseldorf)

Zhang, J., A. Schneider and G. Inden: Metal dusting of iron in CO-H₂-H₂O mixtures at 700 °C. (EFC-Workshop: Metal Dusting, Carburisation and Nitridation, 01-30 till 01-31, 2003, Frankfurt)

2004

Balun, J., J. Houserova, A. Kroupa and G. Inden: The modelling of important intermetallic phases, existing in Fe-based systems by the combined CALPHAD and ab-initio approach. (CALPHAD XXXIII, 05-30 till 06-04, 2004, Krakow, Poland)

Bernst, R., M. Spiegel and A. Schneider: Metal dusting of Fe-Al alloys at 600 °C in CO-H₂-H₂O gas mixtures. (EUROCORR, 09-12 till 09-16, 2004, Nice, France)

Bernst, R., M. Spiegel and A. Schneider: Metal dusting of Fe-Al alloys. (Discussion Meeting on the Development of Innovative Iron Aluminium Alloys, MPI für Eisenforschung, 03-09, 2004, Düsseldorf)

Büchner, A. R. and M. Thiemann: Analyse des Wärmeübergangs von Stahlschmelze in Metallsubstrate. (Werkstoffwoche, 09-21 till 09-23, 2004, Munich)

Büchner, A. R. and M. Thiemann: Twin roll strip casting of steel - studies of heat transfer into the rolls. (Deutsch-Chinesisches Seminar des Stahlzentrum VDEh, 10-18 till 10-20, 2004, Beijing, China)

Cha, S.C. and M. Spiegel: Fundamental studies on alkali chloride induced corrosion during combustion of biomass. (6th Int. Symposium on High temperature Corrosion and Protection of Materials, 05-16 till 05-21, 2004, Lez Embiez, France)



Cha, S.C. and M. Spiegel: Local reactions between NaCl and KCl particles and metal surfaces. (EUROCORR 04, 09-12 till 09-17, 2004, Nice, France)

Cha, S.C. and M. Spiegel: Local reactions of KCl particles with Fe, Ni and Cr surfaces. (EFC Workshop: Novel approaches to the improvement of high temperature corrosion resistance, DECHEMA, 10-27 till 10-29, 2004, Frankfurt)

Cha, S.C. and M. Spiegel: Studies on the local reactions of thermophoretic deposited alkali chloride particles on iron surfaces. (NACE CORROSION, 03-28 till 04-02, 2004, New Orleans, USA)

Deges, J., L. Falat, S. Kobayashi, J. Konrad, M. Palm, B. Pöter, D. Risanti, A. Schneider, C. Stallybrass and F. Stein: Brittle-to-ductile transition temperatures (BDTT) of Fe-Al alloys in dependence of the Al-content. (Discussion Meeting on the Development of Innovative Iron Aluminium Alloys, MPI für Eisenforschung, 03-09, 2004, Düsseldorf)

Ehahoun, H., M. Stratmann and M. Rohwerder: Kinetics of O₂-reduction at model interfaces investigated with a scanning Kelvin probe using an O₂-insensitive Ag/AgCl/KCl – tip. (ISE Annual Meeting, 09-19 till 09-24, 2004, Thessaloniki, Greece)

Eleno, L. T. F., J. Balun, G. Inden, J. Houserova and A. Schneider: Experimental study and thermodynamic modelling of the Fe-Ta equilibrium phase diagram. (TOFA, Discussion Meeting on Thermodynamics of Alloys, 09-12 till 09-17, 2004, Vienna, Austria)

Falat, L., A. Schneider, G. Sauthoff and G. Frommeyer: Iron aluminium alloys with strengthening carbides and intermetallic phases for high-temperature applications. (Discussion Meeting on the Development of Innovative Iron Aluminium Alloys, MPI für Eisenforschung, 03-09, 2004, Düsseldorf)

Fink, N., B. Wilson and G. Grundmeier: Fundamental investigations of interfacial processes during the formation of amorphous conversion layers on zinc coated steel. (55th Annual Meeting of the International Society of Electrochemistry (ISE), 09-19 till 09-24, 2004, Thessaloniki, Greece)

Frenznick, S., M. Stratmann and M. Rohwerder: Galvanizing of defined model samples: On the road to a fundamental physical understanding of hot-dip galvanizing. (GALVATECH, 04-04 till 04-07, 2004, Chicago, USA)

Frommeyer, G.: Development - properties - application of Ti-based Ti-Si(Al) alloys. (ELKEM, 03-01 till 03-03, 2004, Kristiansand, Norway)

Frommeyer, G.: Innovative steel concepts for long products. (ISPAT, 01-16, 2004, Duisburg)

Frommeyer, G.: Mikrostruktur und Eigenschaften hoch-siliziumhaltiger Titanlegierungen. (Meeting, 09-16, 2004, Bestwig)

Frommeyer, G.: Sind Legierungen der intermetallischen Phasen TiAl und NiAl zukünftige Strukturwerkstoffe?. (VDI Seminar, 11-22 till 11-23, 2004, VDI-Zentrum, Düsseldorf)

Frommeyer, G.: Structures, properties and applications of selected intermetallics and chromium alloys. (Meeting, 03-31 till 04-01, 2004, Plansee, Tirol, Austria)

Frommeyer, G.: Superplasticity at higher strain rates in ultrafine grained α -titanium / Ti_xMe_y-intermetallic Ti-8Fe-4Al, Ti-10Co-4Al and Ti-10Ni-4Al alloys. (Euro-SFP Albi, 07-07 till 07-09, 2004, France)

Frommeyer, G., C. Derder and J. A. Jiménez: High temperature plasticity -superplasticity and creep- of Fe₃Al based alloys. (Discussion Meeting on the Development of Innovative Iron Aluminium Alloys, MPI für Eisenforschung, 03-09, 2004, Düsseldorf)

Frommeyer, G., S. Knippscheer and R. Rablbauer: Hochtemperatur-Leichtbauwerkstoffe auf der Basis intermetallischer Phasen. (Metallographie-Tagung, 09-29 till 10-01, 2004, Bochum)

Frommeyer, G., Z. G. Liu, J. Wesemann and N. Wanderka: Investigations on D0₃/B2 ordering in Fe₃Al by X-ray diffraction, TEM and APFIM. (Discussion Meeting on the Development of Innovative Iron Aluminium Alloys, MPI für Eisenforschung, 03-09, 2004, Düsseldorf)

Gnauk, J.: Modellierung der Erstarrung peritektischen Stahls und des Übergangs von gerichteter zu ungerichteter Erstarrung beim Strangguss. (Werkstoffwoche, 09-21 till 09-23, 2004, Munich)

Grabke, H. J.: High temperature corrosion by sulfur, carbon, nitrogen and chlorine, in mixed environments and under salt deposits.. (High Temperature Corrosion Course 2004, 06-08 till 06-10, 2004, Chalmers Tekniska Högskola, Göteborg, Sweden)

Grabke, H. J.: Korrosion in gemischten Gasen I: Grundlagen - Thermodynamik, Stabilitätsdiagramme, Aufkohlung, Metal Dusting, Sulfidierung. (DGM - Fortbildungsseminar, 11-15 till 11-17, 2004, Jülich)

Grabke, H. J.: Oxidation of pure metals, linear and parabolic kinetics, surface and interface reactions, Wagner's theory of diffusion controlled oxide growth. Oxidation of alloys, binary and ternary base alloys and steels, formation of protective scales, reactive element effect.. (High Temperature Corrosion Course 2004, 05-03 till 05-06, 2004, Chalmers Tekniska Högskola, Göteborg, Sweden)



Grabke, H. J.: Supersaturation of iron with nitrogen, hydrogen or carbon and the consequences. (12th Conference on Materials and Technology, 09-27 till 09-29, 2004, Portoroz, Slovenija)

Grundmeier, G.: Combined in-situ IRRAS and Kelvin probe studies of plasma modifications on polymers and metals. (COST 527 Workshop, 06-10 till 06-12, 2004, Sant Feliu, Spain)

Grundmeier, G.: Grundlagen und Anwendung einer neuen höhenregulierten Raster-Kelvin-Sonde für die Korrosionsforschung und Haftung auf Oberflächen. (79. AGEF-Symposium, 25 Jahre Elektrochemie in Düsseldorf, Universität, 11-18 till 11-19, 2004, Düsseldorf)

Grundmeier, G., C. Stromberg, N. Fink and B. Wilson: Spectroscopic, microscopic and electrochemical studies of adhesion promoting thin layers at polymer/metal interfaces. (Kurt-Schwabe-Symposium, 06-13 till 06-17, 2004, Helsinki, Finland)

Grundmeier, G., K. Wapner and M. Stratmann: Applications of a new height regulated scanning Kelvin probe for the study of polymer/metal interfaces in corrosive environments. (ICEPAM, 06-16 till 06-18, 2004, Helsinki, Finland)

Grundmeier, G., K. Wapner and M. Stratmann: Tailored adhesion promoting and corrosion resistant thin plasma polymer films at adhesion/metal interface. (Ninth International Conference on Plasma Surface Engineering, 09-19 till 09-24, 2004, Garmisch-Partenkirchen)

Grundmeier, G., K. Wapner, B. Schönberger and M. Stratmann: Fundamentals and Applications of a new height regulated scanning Kelvin probe in corrosion and adhesion science. (ISE, 09-19 till 09-24, 2004, Thessaloniki, Greece)

Grundmeier, G., K. Wapner, B. Schönberger and M. Stratmann: Non-destructive, real time in-situ measurement of de-adhesion processes at buried adhesive/metal interfaces by means of a new scanning Kelvin probe blister test. (Annual Meeting of the American Adhesion Society, 02-15 till 02-20, 2004, Wilmington, USA)

Hassel, A.W.: Elektrochemie mit und an Nanoelektroden-Arrays. (79. AGEF-Symposium, 25 Jahre Elektrochemie, Universität, 11-18 till 11-19, 2004, Düsseldorf)

Hassel, W., S. Bonk, M. Wicinski and M. Stratmann: Korrelation zwischen Klimawechseltest und Freibewitterung. (GFKORR Expertengespräch Organische Beschichtungen, 10-02, 2004, Iserlohn)

Hassel, W., K. Fushimi and M. Stratmann: Aktivierung und Passivierung einer Nickel Titan Formgedächtnislegierung. (DGM Fachausschuss Intermetallische Phasen, MPI für Eisenforschung, 01-14, 2004, Düsseldorf)

Hassel, W., K. S. Tan and M. Stratmann: Examination of particle-surface contact under tribo-corrosion conditions with a novel low force micro indenter. (55th Meeting of the International Society of Electrochemistry, 09-19 till 09-24, 2003, Thessaloniki, Greece)

Hassel, W., K. S. Tan, A. Smith and M. Stratmann: Detektion von Elementarprozessen der Tribokorrosion. (Bunsen-tagung, 05-20 till 05-22, 2004, Dresden)

Inden, G.: Cementite decomposition in high carburizing atmospheres. (Colloquium: Div. Physical Metallurgy, Royal Institute of Technology, 03-18, 2004, Stockholm, Sweden)

Inden, G.: Computerberechnung von Phasengleichgewichten und Umwandlungen – Instrument für Legierungs- und Wärmebehandlungsoptimierung. (Numerische Simulation, Verarbeitungsprozesse und prozessgerechte Bauteilgestaltung, 11-02 till 11-03, 2004, Bayreuth)

Inden, G.: DICTRA: Von der Idee zur Anwendung. (THERMOCALC - Anwendertreffen, ACCESS, 06-24 till 06-25, 2004, Aachen)

Inden, G.: How far do we get with the local equilibrium hypothesis? (Symposium: Thermodynamics and kinetics of migrating interfaces in steels and complex alloys, 12-02 till 12-03, 2004, Stockholm, Sweden)

Inden, G.: Simulation of precipitation reactions in multi-component systems. (Colloquium: Institute of Physics of Materials, Academy of Sciences of the Czech Republic, 09-03, 2004, Brno, CZ)

Inden, G. and A. Schneider: DICTRA simulation of precipitation reactions in ferritic steels. (CALPHAD XXXIII, 05-30 till 06-04, 2004, Krakow, Poland)

Knezevic, V., J. Balun, G. Sauthoff, A. Schneider and G. Inden: Design of ferritic/martensitic heat resistant 650 °C steels supported by thermodynamic modelling. (Werkstoffwoche, 09-21 till 09-23, 2004, DGM Munich)

Knezevic, V. and G. Sauthoff: Improvement of creep strength of heat-resistant martensitic/ferritic 12% Cr steels. (Fourth International Conference on Advances in Materials Technology for Fossil Power Plants, 10-26 till 10-28, 2004, Hilton Head Island, SC)

Kobayashi, S., S. Zaefferer, A. Schneider and D. Raabe: Optimisation of precipitation for controlling recrystallization of wrought Fe₃Al based alloys. (Treffen des Fachausschusses Intermetallische Phasen, 01-14, 2004, MPI Eisenforschung, Düsseldorf)

Konrad, J.: Hot rolling behaviour and plastic anisotropy of Fe₃Al-based alloys. (Discussion Meeting on the Development of Innovative Iron Aluminium Alloys, MPI für Eisenforschung, 03-09, 2004, Düsseldorf)



- Konrad, J.:** Nucleation mechanisms of recrystallization in warm rolled Fe₃Al base alloys. (Discussion Meeting on the Development of Innovative Iron Aluminium Alloys, MPI für Eisenforschung, 03-09, 2004, Düsseldorf)
- Konrad, J.:** Texturwicklung beim Warmwalzen und bei der Rekristallisation von Fe₃Al-Basislegierungen. (Sitzung des DFG Fachausschuss Intermetallische Phasen, MPI für Eisenforschung, 01-14, 2004, Düsseldorf)
- Konrad, J., A. Schneider and S. Zaeferrer:** Texture Evolution during thermomechanical treatment of Fe₃Al Base alloys. (Kolloquium Prof. J.J. Jonas, MPI für Eisenforschung, 06-09, 2004, Düsseldorf)
- Konrad, J., S. Zaeferrer, A. Schneider, D. Raabe and G. Frommeyer:** Texturwicklung beim Warmwalzen und bei der Rekristallisation von Fe₃Al-Basislegierungen. (Treffen des Fachausschusses Intermetallische Phasen, 01-14, 2004, MPI Eisenforschung, Düsseldorf)
- Li, Y.S. and M. Spiegel:** High temperature interactions of pure Cr with KCl. (6th Int. Symposium on High temperature Corrosion and Protection of Materials, 05-16 till 05-21, 2004, Lez Embiez, France)
- Lill, K. A., M. Stratmann, G. Frommeyer and A. W. Hassel:** On the corrosion resistance of a new class of FeCrAl light weight-ferritic steels. (55th Meeting of the International Society of Electrochemistry, 09-19 till 09-24, 2003, Thessaloniki, Greece)
- Neumann, P.:** Kompatibilitätsspannungen – ein Schlüssel zum Verständnis der Ermüdungsrisbildung an Korngrenzen. (Kolloquium, Universität, 06-15, 2004, Erlangen)
- Neumann, P.:** Material separation by plastic deformation. (Meeting, 06-23 till 06-25, 2004, Brno, CZ)
- Paliwoda-Porebska, G., A. Michalik and M. Rohwerder:** Conducting polymer coatings for corrosion protection: pros and cons. (Gordon Research Conference on Aqueous Corrosion, 07-25 till 07-30, 2004, New London, NH, USA)
- Paliwoda-Porebska, G., A. Michalik, M. Stratmann and M. Rohwerder:** Conducting polymer coatings for corrosion protection: pros and cons. (ISE Annual Meeting, 09-19 till 09-24, 2004, Thessaloniki, Greece)
- Palm, M.:** Concepts derived from phase diagram studies for the strengthening of Fe-Al-based alloys. (Discussion Meeting on the Development of Innovative Iron Aluminium Alloys, MPI für Eisenforschung, 03-09, 2004, Düsseldorf)
- Palm, M., M. Eumann and G. Sauthoff:** Improving properties of Fe-Al based alloys by increasing the stability range of DO3/L21 order. (Discussion Meeting on the Development of Innovative Iron Aluminium Alloys, MPI für Eisenforschung, 03-09, 2004, Düsseldorf)
- Palm, M. and J. Lacaze:** Assessment of the Al-Fe-Ti system. (Thermodynamics of Alloys, TOFA, 09-12 till 09-17, 2004, Vienna, Austria)
- Palm, M., D. D. Risanti, C. Stallybrass, F. Stein and G. Sauthoff:** Strengthening of corrosion-resistant Fe-Al alloys through intermetallic precipitates. (Discussion Meeting on the Development of Innovative Iron Aluminium Alloys, MPI für Eisenforschung, 03-09, 2004, Düsseldorf)
- Palm, M.:** Evaluation of Concentration Profiles by EPMA. (Workshop „The Diffusion Couple Technique“, COST 535 Working Group Meeting, MPI für Eisenforschung, 12-06 till 12-07, 2004, Düsseldorf)
- Parezanovic, I., B. Poeter and M. Spiegel:** B and N segregation on dual phase steel after annealing. (DIMAT, 07-18 till 07-23, 2004, Krakow, Poland)
- Parezanovic, I. and M. Spiegel:** Influence of B, S, P, Si and C segregation on the selective oxidation of dual phase and interstitial free steels. (GALVATECH, 04-04 till 04-07, 2004, Chicago, USA)
- Park, E., B. Hüning and M. Spiegel:** Effects of heat treatment on the oxide layer of Fe-15 at.% Cr alloy surface. (EUROCORR, 09-12 till 09-17, 2004, Nice, France)
- Park, E., B. Hüning and M. Spiegel:** Annealing of Fe-15Cr alloy in N₂- 5% H₂ gas mixture: Effect of hydrogen concentration. (DIMAT, 07-18 till 07-23, 2004, Krakow, Poland)
- Ponge, D.:** Arbeiten des MPI für Eisenforschung auf dem Gebiet der feinkörnigen Stähle. (VDEh-Ausschuss des Werkstoffausschusses, Stahlzentrum VDEh, 03, 2004, Düsseldorf)
- Ponge, D.:** Bericht aus der Arbeitsgruppe Weiterentwicklung Umformdilatometer. (VDEh-Werkstoffausschuss, Arbeitskreis Umformdilatometrie, Stahlzentrum VDEh, 04-21, 2004, Düsseldorf)
- Ponge, D.:** Bericht aus der Arbeitsgruppe Weiterentwicklung Umformdilatometer. (VDEh-Werkstoffausschuss, Arbeitskreis Umformdilatometrie, Stahlzentrum VDEh, 06-14, 2004, Düsseldorf)
- Ponge, D.:** Charakterisierung des Umwandlungsverhaltens bei der Simulation moderner Direktwalzprozesse. (VDEh-Werkstoffausschuss, Unterausschuss für Metallographie, Werkstoffanalytik und -simulation, Stahlzentrum VDEh, 05-12, 2004, Düsseldorf)
- Ponge, D.:** Warmumformbarkeit von Stahl. (Seminar 15/04, Kontaktstudium Werkstofftechnik Stahl, Teil III, Technologische Eigenschaften, Institut für Bildung, Stahlzentrum VDEh, 06-14, 2004, Düsseldorf)



Ponge, D., R. Song and R. Kaspar: The effect of Mn on the microstructure and mechanical properties after heavy warm rolling of C-Mn steel. (Lecture at the TMS annual meeting in Charlotte, 03-16, 2004, North Carolina, USA)

Pöter, B., F. Stein, M. Palm and M. Spiegel: Oxidation behaviour of Fe-Al alloys analysed using in- and ex-situ techniques. (EUROCORR, 09-12 till 09-16, 2004, Nice, France)

Pöter, B., F. Stein and M. Spiegel: Initial stages of Al_2O_3 growth on Fe-Al intermetallic phases. (EMPG X Conference, 04-04 till 04-07, 2004, Frankfurt)

Pöter, B., F. Stein, M. Spiegel and M. Stratmann: Anfangsstadien der Oxidation von intermetallischen Fe-Al Phasen. (38. Metallographietagung der DGM, 09-29 till 10-01, 2004, Bochum)

Pöter, B., F. Stein, D. Vogel and M. Spiegel: Al_2O_3 growth on Fe-Al intermetallic phases. (ANKA Users Meeting, 09-23 till 09-24, 2004, Karlsruhe)

Pötschke, S. and A. R. Büchner: Influence of inline hot rolling on twin roll cast LC-steel. (2nd Int. Conf. and Exhibition on New Developments in Metallurgical Process Technology, 09-19 till 09-21, 2004, Riva del Garda, Italy)

Raabe, D.: Computational steels. (Keynote lecture at the 19. Aachener Stahl Kolloquium, RWTH, 03-06, 2004, Aachen)

Raabe, D.: Crystal mechanics in metals and polymers – experiments and simulations. (Colloquium Lecture at Forschungszentrum Karlsruhe, 10-12, 2004, Karlsruhe)

Raabe, D.: Crystal plasticity simulations in materials testing. (Keynote lecture at the International Materials Testing Conference, 11-20, 2004, Neu-Ulm)

Raabe, D.: Crystal plasticity simulations in metals. (Colloquium Lecture at the Massachusetts Institute of Technology, 09-30, 2004, Cambridge, USA)

Raabe, D.: Kristallmechanik in Metallen. (Lecture at the Rheinland-Pfälzische Akademie der Wissenschaften, 10-12, 2004, Mainz)

Raabe, D.: Microstructure scales in materials simulation. (Lecture at the Gordon Conference on Physical Metallurgy, 07-12, 2004, New Hampshire, USA)

Raabe, D.: Moderne Simulationskonzepte für den Werkstoff Stahl und seine Anwendungen. (VDEh-Werkstoffausschuss, Stahlzentrum VDEh, 02-02, 2004, Düsseldorf)

Raabe, D.: Recrystallization in polymers – experiments and simulations. (Invited Keynote lecture, 2nd International Conference on Recrystallization and Grain Growth, REX&GG, 08-02, 2004, Annecy, France)

Raabe, D.: Simulation of abnormal grain growth in FeSi steels. (Keynote lecture at the TMS Fall Meeting, 09-26 till 09-29, 2004, New Orleans, Louisiana, USA)

Raabe, D.: Simulations and experiments on micromechanics in metals and polymers. (Colloquium, Department for Theoretical Physics; University, 01-20, 2004, Paderborn)

Raabe, D.: Textures and micromechanics in experiment and theory on metals and semi-crystalline polymers. (Joint Colloquium of the University of Vienna and Technical University, 05-05, 2004, Vienna, Austria)

Raabe, D.: The texture component crystal plasticity finite element method. (Keynote lecture at the Third GAMM, Society for Mathematics and Mechanics, Seminar on Microstructures, University of Stuttgart, 01-08, 2004, Stuttgart)

Raabe, D. and F. Roters: Physically-based large-scale texture and anisotropy simulation for automotive sheet forming. (TMS Fall meeting, 09-26 till 09-29, 2004, New Orleans, Louisiana, USA)

Raacke, J., M. Giza and G. Grundmeier: In-situ IR-spectroscopic and Kelvin probe investigations of plasma modified model substrates. (9th International Conference on Plasma Surface Engineering, 09-13 till 09-17, 2004, Garmisch-Partenkirchen)

Risanti, D. D. and G. Sauthoff: Entwicklung ferritischer Eisen-Aluminium-Tantal-Legierungen mit verstärkender Laves-Phase für Anwendungen bei hohen Temperaturen. (Werkstoffwoche, Kongress für innovative Werkstoffe, Verfahren und Anwendungen, DGM, 09-21 till 09-23, 2004, Munich)

Risanti, D. D. and G. Sauthoff: Iron-aluminide-base alloys with strengthening Laves phase for structural applications at high temperatures. (The Fifth Pacific RIM International Conference on Advanced Materials and Processing, 11-02 till 11-05, 2004, Beijing, China)

Risanti, D. D. and G. Sauthoff: Strengthening of iron aluminide alloys by atomic ordering and Laves phase precipitation for high-temperature application. (Discussion Meeting on the Development of Innovative Iron Aluminium Alloys, MPI für Eisenforschung, 03-09, 2004, Düsseldorf)

Rohwerder, M., R. Hausbrand and M. Stratmann: Development of zinc-alloy Coatings with inherent delamination stability for organic coatings. (GALVATECH, 04-04 till 04-07, 2004, Chicago, USA)



Rohwerder, M., R. Hausbrand and M. Stratmann: The role of the electrode potential at the buried polymer/metal interface on electrochemically driven delamination: the case MgZn₂. (ISE Annual Meeting, 09-19 till 09-24, 2004, Thessaloniki, Greece)

Rohwerder, M., A. Michalik, G. Paliwoda and M. Stratmann: Leitfähige Polymere für den Korrosionsschutz: Chancen and Risiken. (Plenary lecture, DGO (GDCh) Jahrestagung, 09-08 till 09-10, 2004, Graz, Österreich)

Rohwerder, M. and M. Stratmann: Delamination of organic coatings from galvanized steel: A fundamental overview. (GALVATECH, 04-04 till 04-07, 2004, Chicago, USA)

Rohwerder, M. and M. Stratmann: The effect of oxygen reduction on the self-assembly and stability of thiol monolayer films. (205th Meeting of the ECS, 05-09 till 05-14, 2004, San Antonio, USA)

Roßenbeck, B. and G. Grundmeier: Structure and stability of pigmented model latex coatings on iron. (Kurt-Schwabe-Symposium, 06-13 till 06-17, 2004, Helsinki, Finnland)

Roters, F.: Das Anwendungspotential der Kristallplastizitäts-Finite-Elemente-Methode aus Sicht der werkstoffphysikalischen Grundlagen. (Werkstoffwoche, 09-22 till 09-27, 2004, Munich)

Roters, F., A. Ma and D. Raabe: The texture component crystal plasticity finite element method. (Third GAMM-Seminar on Microstructures, 01-09, 2004, Stuttgart)

Roters, F., Z. Zhao and D. Raabe: Development of a grain fragmentation criterion and its validation using crystal plasticity FEM simulations. (MPI für Eisenforschung 2004, Düsseldorf)

Ruh, A. and M. Spiegel: Influence of gas phase composition on the kinetics of chloride melt induced corrosion. (EFC Workshop: Novel approaches to the improvement of high temperature corrosion resistance, DECHEMA, 10-27 till 10-29, 2004, Frankfurt)

Ruh, A. and M. Spiegel: Influence of HCl and water vapour on the corrosion kinetics of Fe beneath molten ZnCl₂/KCl. (EUROCORR, 09-12 till 09-17, 2004, Nice, France)

Ruh, A. and M. Spiegel: Kinetic investigations on salt melt induced high temperature corrosion of pure metals. (6th Int. Symposium on High Temperature Corrosion and Protection of Materials, 05-16 till 05-21, 2004, Lez Embiez, France)

Sanchez-Pasten, M., E. Strauch and M. Spiegel: High temperature corrosion of metallic materials in simulated waste incineration conditions at 300 – 600 °C. (EFC Workshop: Novel approaches to the improvement of high temperature corrosion resistance, DECHEMA, 10-27 till 10-29, 2004, Frankfurt)

Sauthoff, G.: Eisenaluminid-Werkstoffentwicklungen in den USA. (DGM-Fachausschuss Intermetallische Phasen, MPI für Eisenforschung, 01-14, 2004, Düsseldorf)

Sauthoff, G.: Eisen-Aluminium-Legierungen - Legierungskonzepte für neue Hochtemperaturlegierungen. (DGM-Fachausschuss Intermetallische Phasen, MPI für Eisenforschung, 01-14, 2004, Düsseldorf)

Sauthoff, G.: Intermetallische Phasen - Erwartungen und Probleme. (Werkstofftechnische Kolloquien im IWW, 02-03, 2004, Magdeburg)

Sauthoff, G.: Opening and introduction to Fe-Al. (Discussion Meeting on the Development of Innovative Iron Aluminium Alloys, MPI für Eisenforschung, 03-09, 2004, Düsseldorf)

Schneider, A., M. Palm, F. Stein, and G. Sauthoff: Strengthening of iron aluminide alloys for high temperature applications. (Symposium „Integrative and Interdisciplinary Aspects of Intermetallics“ MRS Fall Meeting 2004, 11-29. till 12-3, 2004, Boston, Massachusetts, USA)

Schneider, A., C. Stallybrass, G. Sauthoff, A. Cerezo and G. D. W. Smith: Three-dimensional atom probe studies of phase transformations in Fe-Al-Ni-Cr alloys with B2-ordered NiAl precipitates. (49th International Field Emission Symposium, IFES 04, 07-12 till 07-15, 2004, Graz, Austria)

Schneider, A., J. Zhang, R. Bernst and G. Inden: Thermodynamics and kinetics of phase transformations during metal dusting of iron and iron-based alloys. (CALPHAD XXXIII, 05-30 till 06-04, 2004, Krakow, Poland)

Schuster, J. C. and M. Palm: Re-assessment of the Al-Ti system. (Thermodynamics of Alloys, TOFA, 09-12 till 09-17, 2004, Vienna, Austria)

Skobir, D. and M. Spiegel, St. Arvelakis, A. Milewska, F.J. Perez: Deposit induced corrosion of CVD coatings, steels and model alloys in simulated biomass combustion atmospheres. (EFC Workshop: Novel Approaches to the Improvement of High Temperature Corrosion Resistance, DECHEMA, 10-27 till 10-29, 2004, Frankfurt)

Song, R.: Microstructure and mechanical properties of ultrafine grained steels. (Institutsseminar am Institut für Eisenhüttenkunde, RWTH, 06-03, 2004, Aachen)

Song, R.: Ultrafine grained steel after heavy warm deformation of ferritic pearlitic C-Mn steels. (TMS Annual Meeting, 03-14 till 03-18, 2004, Charlotte, North Carolina, USA)



Song, R., D. Ponge and R. Kaspar: Microstructure and mechanical properties of ultrafine grained steels. (Lecture at the Workshop KUL-Uni-Gent-RWTH-MPIE, 04-07, 2004, Gent, Belgium)

Song, R., D. Ponge and R. Kaspar: Review of the properties and methods for production of ultrafine grained steels. (Lecture at the SMEA Conference, 06-20 till 06-20, 2004, Sheffield, UK)

Spiegel, M. and H. J. Grabke: Korrosion durch Chlor und Chloride. (DGM-Fortbildungsseminar, Hochtemperaturkorrosion, 11-15 till 11-17, 2004, Jülich)

Spiegel, M.: Fundamental aspects of fireside corrosion in waste and biomass fired plants. (Invited lecture, 6th Int. Symposium on High Temperature Corrosion and Protection of Materials, 05-16 till 05-21, 2004, Lez Embiez, France)

Spiegel, M.: Korrosion in Müllverbrennungsanlagen. (DGM-Fortbildungsseminar, Hochtemperaturkorrosion, 11-15 till 11-17, 2004, Jülich)

Spiegel, M.: Salzschnmelzeninduzierte Hochtemperaturkorrosion. (VDI, 05-04, 2004, Göttingen)

Stallybrass, C. and G. Sauthoff: Effect of heat treatment on the mechanical behaviour of novel ferritic Fe-Al-Ni-Cr alloys hardened with intermetallic (Ni,Fe)Al precipitates. (Discussion Meeting on the Development of Innovative Iron Aluminium Alloys, MPI für Eisenforschung, 03-09, 2004, Düsseldorf)

Stallybrass, C., A. Schneider and G. Sauthoff: Mechanisches Verhalten neuartiger ferritischer Fe-Al-Ni-Cr Legierungen mit intermetallischen (Ni,Fe)Al Ausscheidungen bei hohen Temperaturen. (Werkstoffwoche, Kongress für innovative Werkstoffe, Verfahren und Anwendungen, DGM, 09-21 till 09-23, 2004, Munich)

Stein, F., A. Schneider and G. Frommeyer: Quaternary Fe₃Al-based alloys with transition metals: effect of alloying additions on the order-disorder transitions and the mechanical behaviour. (Discussion Meeting on the Development of Innovative Iron Aluminium Alloys, MPI für Eisenforschung, 03-09, 2004, Düsseldorf)

Stein, F., D. Jiang, M. Palm and G. Sauthoff: Laves phase polytypism in the Co-Nb system. (TOFA 2004 - Discussion Meeting on Thermodynamics of Alloys, 09-12 till 09-17, 2004, Vienna, Austria)

Stein, F., G. Sauthoff and M. Palm: Experimental determination of the ternary Fe-Al-Zr phase diagram. (Discussion Meeting on the Development of Innovative Iron Aluminium Alloys, MPI für Eisenforschung, 03-09, 2004, Düsseldorf)

Stein, F., M. Palm and G. Sauthoff: Mechanical properties of two-phase iron aluminium alloys with Zr(Fe,Al)₂ Laves phase or Zr(Fe,Al)₁₂τ₁ phase. (Discussion Meeting on the Development of Innovative Iron Aluminium Alloys, MPI für Eisenforschung, 03-09, 2004, Düsseldorf)

Stein, F.: Structure and stability of Laves phases in binary and ternary systems. (CEA Saclay, 03-26, 2004, Gif-sur-Yvette, France)

Stratmann, M.: From novel alloys to tailored surfaces. (University, Metallurgy and Materials Department, 03-17, 2004, Birmingham, UK)

Stratmann, M.: From novel alloys to tailored surfaces. (University, Metallurgy and Materials, Seminar, 03-18 till 03-18, 2004, Cambridge, UK)

Stratmann, M.: Maßgeschneiderte halbleitende Oxide zur Verbesserung des Korrosionswiderstandes und der Adhäsion organischer Schichten. (79th AGEF-Symposium, 25 Jahre Elektrochemie, Universität, 11-18 till 11-19, 2004, Düsseldorf)

Stratmann, M.: Moderne Schutzschichtsysteme auf der Basis molekularer Grenzflächenkonzepte. (25th Sitzung, Nordrhein-Westfälische Akademie der Wissenschaften, 03-10, 2004, Düsseldorf)

Stratmann, M.: Moderne Schutzsysteme für Stahloberflächen auf der Basis maßgeschneiderter Zinklegierungen. (5th Fachsymposium Oberflächentechnik in Dortmund, DOC, 11-30, 2004, Dortmund)

Stratmann, M.: Neuartige Zink-Legierungsüberzüge: Maßgeschneiderte halbleitende Oxide für verbesserten Korrosionsschutz und eine verbesserte Haftung organischer Beschichtungen. (Seminar, Leibniz-Institut für Festkörper- und Werkstoffforschung, 01-29, 2004, Dresden)

Stratmann, M.: Steel News: From novel alloys to tailored surfaces. (Fritz-Haber-Institut, Abteilung Physikalische Physik, 02-18, 2004, Berlin)

Stratmann, M.: Tailored semiconducting oxides for improved corrosion resistance and adhesion of organic coatings. (ARCELOR Surfschool, 10-18 till 10-20, 2004, Thionville, France)

Stratmann, M.: Tailored semiconducting oxides for improved corrosion resistance and adhesion of organic coatings. (Gordon Research Conference on Aqueous Corrosion, 07-25 till 07-30, 2004, New London, NH, USA)

Stratmann, M.: The scientist's view – project ideas for FP7. (Building Excellence, Facing the Needs of Framework Programme 7, 11-22, 2004, Brussels, Belgium)

Thomas, I., S. Zaeferrer, F. Friedel and D. Raabe: Orientation dependent growth behaviour of subgrain structures in IF steel. (2nd International Joint Conference on Recrystallization and Grain Growth, 08-31, 2004, Annecy, France)



Wapner, K. and G. Grundmeier: Application of the scanning Kelvin probe for the study of de-adhesion processes at thin film engineered adhesive/metal interfaces. (Annual Meeting of the American Adhesion Society, 02-15 till 02-20, 2004, Wilmington, USA)

Wapner, K. and G. Grundmeier: Extended Abstract: „Water diffusion measurements in a model adhesive/silicon lap joint using FTIR-spectroscopy: differentiation between bulk and interfacial diffusion. (Euradh/Adhesion, 09-05 till 09-09, 2004, Freiburg)

Wapner, K., M. Stratmann and G. Grundmeier: Extended Abstract: Non-destructive, in-situ measurement of de-adhesion processes at buried adhesive/metal interfaces by means of a new scanning Kelvin probe blister test. (Euradh/Adhesion, 09-05 till 09-09, 2004, Freiburg)

Wicinski, M., A. W. Hassel and M. Stratmann: Corrosion under cyclic conditions monitored by a simultaneous scanning Kelvin probe and galvanic current measurement. (55rd Meeting of the International Society of Electrochemistry, 09-19 till 09-24, 2004, Thessaloniki, Greece)

Wilson, B., N. Fink and G. Grundmeier: Interfacial reactions during the formation of amorphous anti-corrosion coatings on zinc coated steel. (Gordon Research Conference on Aqueous Corrosion, Colby-Sawyer College, 07-25 till 07-30, 2004, New London, NH, USA)

Wilson, B., N. Fink and G. Grundmeier: Interfacial reactions during the formation of ultra-thin amorphous anti-corrosion coatings on zinc coated steel. (45th Corrosion Science Symposium, Sheffield Hallam University, 09-05 till 09-08, 2004, Sheffield, S. Yorkshire, UK)

Yang, L. and Guido Grundmeier: Nanomechanical studies of thin tailored plasma polymers on organic coatings. (5th European Symposium on Nano-mechanical Testing, 09-07 till 09-09, 2004, Hückelhoven)

Zaefferer, S.: Electron backscatter diffraction (EBSD): a powerful tool to understand microstructures. (Instituts-kolloquium im Fachbereich Material-und Geowissenschaften der TU, 05-17, 2004, Darmstadt)

Zaefferer, S.: High resolution EBSD investigations of the recrystallization behaviour of a cold rolled Ni3Al single crystal. (2nd International Joint Conference on Recrystallization and Grain Growth, 08-31, 2004, Annecy, France)

Zaefferer, S.: Investigation of the bainitic phase transformation in a low alloyed TRIP steel using EBSD and TEM. (Material Science and Technology, 09-27 till 09-30, 2004, New Orleans, USA)

Zaefferer, S.: Microtexture measurements: a powerful tool to understand microstructures. (Institutsseminar am Institut für metallische Werkstoffe, Universität, 05-12, 2004)

Zaefferer, S.: Phase identification by electron backscatter diffraction (EBSD). (Werkstoffwoche, 09-21, 2004, Munich)

Zaefferer, S.: The investigation of the correlation between texture and microstructure on a submicrometer scale in the TEM. (Seminar des Instituts für Geologie, ETH, 02-02, 2004, Zürich, Schweiz)

Zaefferer, S., N. Chen and D. Dörner: New ideas and investigations concerning the development of the Goss texture. (Treffen des Fachausschusses Texturen, TU, Institut für Physik, 04-02, 2004, Dresden)

Zaefferer, S., N. Chen, J. C. Kuo and S. Kobayashi: On the EBSD activities at the MPIE. (EBSD meeting of the Royal Microscopy Society, University, 04-20, 2004, Sheffield, UK)

Zaefferer, S., J. Ohlert and W. Bleck: Influence of thermal treatment on the microstructure and mechanical properties of a low alloyed TRIP steel. (Werkstoffwoche, 09-21, 2004, Munich)



Publications

2002 (residual since Scientific Report 2001 / 2002)

Books, Book Chapters, and Editorial Work

Neumann, P., G. Inden and G. Sauthoff. Max-Planck-Institut für Eisenforschung GmbH, Düsseldorf - Abteilung Physikalische Metallkunde. In: Jahrbuch Stahl 2003, Verlag Stahleisen GmbH, Düsseldorf, Band 1, p. 373-386 (2002)

Publications in Scientific Journals

Rebhan, M., M. Rohwerder and M. Stratmann: Electrochemical properties of iron covered by CVD-silicon and silicon-organic molecules. *Materials and Corrosion* **52**, 936-939 (2002)

Rebhan, M., M. Rohwerder and M. Stratmann: Formation of mesoscopic structures by the CVD of SiH₄ on Fe(100). *Chemical Vapor Deposition* **8**, 259-261 (2002)

Conference Papers, Final Reports, and Other Publications

Müller-Lorenz, E. M., H. J. Grabke and M. Zinke: Metal dusting resistance of welded Nickel-based alloys. In: EUROCORR 01, (Ed.) Associazione Italiana di Metallurgia, AIM, Milano, Italy (2002) CD-ROM

Schneider, A. and G. Sauthoff. Intermetallic alloys and ferritic steels for high-temperature applications. In: Proc. 9th Intern. Conf. Ultra-High Purity Base Metals (UHPM-2002), (Eds.) K. Abiko, S. Takaki. (2002) 133

2003

Books, Book Chapters, and Editorial Work

Bard, A. J. and M. Stratmann (Eds.): Encyclopaedia of electrochemistry. Wiley-VCH, Weinheim, Vol. 2: Interfacial Kinetics and Mass Transport (Ed.: E. Calvo), isbn 3-527-30394-4; Vol. 3: Instrumentation and Electroanalytical Chemistry (Ed.: Pat Unwin), isbn 3-527-30395-2; Vol. 4: Corrosion and Oxide Films (Eds.: M. Stratmann and J. Frankel), isbn 3-527-30396-0 (2003)

Büchner, A. R.: Aktivitäten zum Dünnbandgießen. In: Jahrbuch Stahl 2004, Band 1, (Ed.) Stahlinstitut VDEh Verlag Stahleisen Düsseldorf, Düsseldorf, isbn: 3-514-00698-9, p. 383-389 (2003)

Frankel, G. S. and M. Rohwerder: Electrochemical techniques for corrosion. In: Encyclopedia of Electrochemistry, Volume 4, Corrosion, (Eds.) M. Stratmann, G.S. Frankel. Wiley-VCH, Weinheim, p. 687-723 (2003)

Frommeyer, G. and S. Knipscheer: Aluminium intermetallics. In: Handbook of Aluminium, Vol. 2, (Eds.) G.B. Totten, D.S. MacKenzie, M. Dekker. Marcel Dekker, Inc., New York, p. 603-630 (2003)

Frommeyer, G. and S. Knipscheer: Aluminium-based metal matrix composites. In: Handbook of Aluminium, Vol. 2, (Eds.) G.B. Totten, D.S. MacKenzie, M. Dekker. Marcel Dekker, New York, p. 631-672 (2003)

Grabke, H.J. and G. Holzäpfel: High-temperature corrosion of metals by gases. In: Encyclopedia of Electrochemistry, Vol. 4, Corrosion and Oxide Films, (Eds.) A.J. Bard, M. Stratmann, G.S. Frankel. Wiley-VCH, Weinheim, p. 623-661 (2003)

Grundmeier, G.: Funktionalisierung von Stahloberflächen mit dünnen Plasmapolymerschichten. In: Jahrbuch der Oberflächentechnik 59, (Ed.) A. Zielonka, G. Eugen. Leuze-Verlag, Bad Saulgau, p. 109-117 (2003)



Grundmeier, G. and A. Simões: Corrosion protection of metals by organic coatings. In: Encyclopaedia of Electrochemistry, Vol. 4, (Eds.) E.J. Bard, M. Stratmann. Wiley VCH, Weinheim, p. 500-566 (2003)

Inden, G.: Computer modelling of diffusion controlled transformations. In: Thermodynamics, Microstructures and Plasticity, (Eds.) A. Finel, M. Verron. Kluwer Acad. Publ., Dordrecht, p. 135-153 (2003)

Schultze, J. W and A. W. Hassel: Passivity of metals, alloys and semiconductors. In: Encyclopedia of Electrochemistry, Vol. 4, Corrosion and Oxide Films, (Eds.) A.J. Bard, M. Stratmann, G.S. Frankel. Wiley-VCH, Weinheim, p. 188-189, 216-270 (2003)

Spiegel, M.: Molten salts-induced corrosion of metals (Hot Corrosion). In: Encyclopedia of Electrochemistry, Vol. 4, Corrosion and Oxide Films, (Eds.) A. Bard, M. Stratmann. Wiley-VCH, Weinheim, p. 597-622 (2003)

Publications in Scientific Journals

Carpentier, J., P. Thiemann, V. Barranco and G. Grundmeier: Tailored thin plasma polymers for the corrosion protection of metals. *Surface and Coatings Technology* **173-174**, 996-1001 (2003)

Chen, N., S. Zaefferer, L. Lahn, K. Günther and D. Raabe: Effects of topology on abnormal grain growth in silicon steel. *Acta Materialia* **51**, 1755-1765 (2003)

Deges, J., A. Schneider, R. Fischer and G. Frommeyer: APFIM investigations on quasi-binary hypoeutectic NiAl-Re alloys. *Materials Science and Engineering* **A353**, 80-86 (2003)

Ducher, R., F. Stein, M. Palm and J. Lacaze: A re-examination of the liquidus surface of the Al-Fe-Ti System. *Zeitschrift für Metallkunde* **94**, 396-410 (2003)

Eleno, L. T. F. and C. G. Schön: CVM calculation of the b.c.c. Co-Cr-Al phase diagram. *Calphad* **27**, 335-342 (2003)

Eleno, L. T. F., C. G. Schön, J. Balun and G. Inden: Prototype calculations of B2 miscibility gaps in ternary b.c.c. systems with strong ordering tendencies. *Intermetallics* **11**, 1245-1252 (2003)

Elsner, A. and R. Kaspar: Deep-drawable steel strip produced by ferritic rolling. *Materials Science Forum* **426-432**, 1349-1354 (2003)

Fischer, R., G. Frommeyer and A. Schneider: APFIM investigations on site preferences, superdislocations, and antiphase boundaries in NiAl(Cr) with B2 superlattice structure. *Materials Science and Engineering* **A353**, 87-91 (2003)

Frommeyer, G., U. Brück and P. Neumann: Supra-ductile and high-strength manganese-TRIP/TWIP steels for high energy absorption purposes. *Iron and Steel Institute of Japan International* **43**, 438-446 (2003)

Frommeyer, G., H. Hofmann and J. Löhr: Structural superplasticity at high strain rates of super duplex stainless steel Fe-25Cr-7Ni-3Mo-0.3N. *Steel Research* **74**, 338-344 (2003)

Grabke, H. J.: Metal dusting. *Material and Corrosion* **54**, 736-746 (2003)

Grabke, H. J.: Nitrierung als Korrosionsprozess. *Härtereitechnische Mitteilungen* **58**, 69-73 (2003)

Grabke, H. J., H. P. Martinz and E. M. Müller-Lorenz: Metal dusting resistance of high chromium-alloys. *Material and Corrosion* **54**, 860-893 (2003)

Grabke, H. J., E. M. Müller-Lorenz and M. Zinke: Metal dusting behaviour of welded Ni-base alloys with different surface finish. *Material and Corrosion* **54**, 785-792 (2003)

Grabke, H. J. and M. Spiegel: Occurrence of metal dusting – referring to failure cases. *Material and Corrosion* **54**, 799-804 (2003)

Grabke, H. J., S. Strauss and D. Vogel: Nitridation in NH₃-H₂O mixtures. *Material and Corrosion* **54**, 895-901 (2003)

Grundmeier, G., M. Brettmann and P. Thiemann: In-situ spectroscopic and corrosion studies of ultra-thin gradient plasma polymer layers on zinc. *Applied Surface Science* **217**, 223-232 (2003)



Hassel, A. W. and M. Stratmann: Microscopic and nanoscopic aspects of corrosion and corrosion protection – Editorial. *Electrochimica Acta* **48**, XI (2003)

Hausbrand, R., M. Stratmann and M. Rohwerder: Delamination resistant zinc alloys: simple concept and results on the system zinc-magnesium. *Steel Research International* **74**, 453-458 (2003)

Herrmann, J., G. Inden and G. Sauthoff: Deformation behaviour of iron-rich iron-aluminium alloys at low temperatures. *Acta Materialia* **51**, 2847-2857 (2003)

Herrmann, J., G. Inden and G. Sauthoff: Deformation behaviour of iron-rich iron-aluminium alloys at high temperatures. *Acta Materialia* **51**, 3233-3242 (2003)

Kuo, J.-C., S. Zaefferer, Z. Zhao, M. Winning and D. Raabe: Deformation behaviour of aluminium-bicrystals. *Advanced Engineering Materials* **5**, 563-566 (2003)

Lima, E. B. F., A. R. Pyzalla, W. Reimers, J.-C. Kuo and D. Raabe: Mosaic size distributions in an aluminium bi-crystal deformed by channel die plane strain compression. *Journal of Neutron Research* **11**, 209-214 (2003)

Lobnig, R., J. D. Sinclair, M. Unger and M. Stratmann: Mechanism of atmospheric corrosion of copper in the presence of ammonium sulphate particles – Effect of surface particle concentration. *Journal of the Electrochemical Society* **150**, A835-A849 (2003)

Ma, A.: Implicit scheme of RVE calculation for f.c.c. polycrystals. *Computational Materials Science* **27**, 471-479 (2003)

Maupai, S., A. S. Dakkouri, M. Stratmann and P. Schmuki: Tip-induced nanostructuring of Au₃Cu(001) with an electrochemical scanning tunneling microscope. *Journal of the Electrochemical Society* **150**, C111-C114 (2003)

Palm, M., J. Preuhs and G. Sauthoff: Production-scale processing of a new intermetallic NiAl-Ta-Cr alloy for high-temperature application: Part I. Production of master alloy remelt ingots and investment casting of combustor liner model panels. *Journal of Materials Processing Technology* **136**, 1-3, 105-113 (2003)

Palm, M., J. Preuhs and G. Sauthoff: Production scale processing of a new intermetallic NiAl-Ta-Cr alloy for high-temperature application: Part II. Powder metallurgical production of bolts by hot isostatic pressing. *Journal of Materials Processing Technology* **136**, 1-3, 114-119 (2003)

Pippel, E., J. Woltersdorf and H. J. Grabke: Microprocesses of metal dusting on iron – nickel alloys and their dependence on composition. *Material and Corrosion* **54**, 747-751 (2003)

Raabe, D.: Overview on basic types of hot rolling textures of steels. *Steel Research* **74**, 327-337 (2003)

Raabe, D. and F. Roters: A new finite element method for predicting anisotropy of steels. *Steel Research* **74**, 181-182 (2003)

Raabe, D., M. Sachtleber, H. Weiland, G. Scheele and Z. Zhao: Grain-scale micromechanics of polycrystal surfaces during plastic straining. *Acta Materialia* **51**, 1539-1560 (2003)

Rablbauer, R., G. Frommeyer and F. Stein: Determination of the constitution of the quasi-binary eutectic NiAl-Re system by DTA and microstructural investigations. *Materials Science and Engineering* **A343**, 301-307 (2003)

Rasp, W. and C. M. Wichern: A survey of the morphology of surface features during metal-forming operations. *Steel Research International* **74**, 300-303 (2003)

Rebhan, M., M. Rohwerder and M. Stratmann: Delamination of polymeric coatings on silidized iron. *Materials and Corrosion - Werkstoffe und Korrosion* **54**, 19-22 (2003)

Rohwerder, M., E. Hornung and M. Stratmann: Microscopic aspects of electrochemical delamination: an SKPFM study. *Electrochimica Acta* **48**, 1235-1243 (2003)

Roters, F.: A new concept for the calculation of the mobile dislocation density in constitutive models of strain hardening. *Physica Status Solidi (b)* **240**, 68-74 (2003)

Roters, F.: Simulation der Umformung von metallischen Werkstoffen nach der Texturkomponenten-Kristallplastizitäts-FEM. *Simulation* **1**, 50-53 (2003)



Roters, F.: Application of the texture component crystal plasticity FEM to forming simulation. *Materials Science Forum* **426-432**, 3673-3678 (2003)

Schneider, A., L. Falat, G. Sauthoff and G. Frommeyer. Constitution and microstructures of Fe-Al-M-C (M=Ti, V, Nb, Ta) alloys with carbides and laves phase. *Intermetallics* **11**, 443-450 (2003)

Schneider, A. and H. J. Grabke. Effect of H₂S on metal dusting of iron. *Materials and Corrosion* **54**, 793-798 (2003)

Schneider, A. and J. Zhang. Metal dusting of ferritic Fe-Al-M-C (M=Ti, V, Nb, Ta) alloys in CO-H₂-H₂O gas mixtures at 650 °C. *Materials and Corrosion* **54**, 778-784 (2003)

Shirtcliffe, N. J., M. Stratmann and G. Grundmeier. In situ infrared spectroscopic studies of ultrathin inorganic film growth on zinc in non-polymerizing cold plasmas. *Surf Interface Anal* **35**, 799-804 (2003)

Spiegel, M.: Fundamental aspects of chlorine induced corrosion in power plants. *Materials at High Temperatures* **20**, 2 (2003)

Spiegel, M.: The role of molten salts in the corrosion of metals in waste incineration plants. *Trans Tech Publications, Switzerland, Molten Salt Forum* **7**, 253-268 (2003)

Spiegel, M., A. Zahs. and H.J. Grabke. Fundamental aspects of chlorine induced corrosion in power plants. *Materials at High Temperatures*, **20**, 153-159 (2003)

Stein, F., A. Schneider and G. Frommeyer. Flow stress anomaly and order-disorder transitions in Fe₃Al-based Fe-Al-Ti-X alloys with X=V, Cr, Nb, or Mo. *Intermetallics* **11**, 71-82 (2003)

Storojeva, L., R. Kaspar and D. Ponge. Ferritic-Pearlitic Steel with deformation induced spheroidized cementite. *Materials Science Forum* **426-432**, 1169-1174 (2003)

Thieman, M. and A. R. Büchner. Heat Flux Density and Heat Transfer Coefficient between Steel Melt and Metallic Substrates. *Steel Research* **74**, 732-738 (2003)

Thomas, I., S. Zaefferer, F. Friedel and D. Raabe. High resolution EBSD investigation of deformed and partially recrystallized IF steel. *Advanced Engineering Materials* **5**, 566-570 (2003)

Vander Kloet, J., W. Schmidt, A. W. Hassel and M. Stratmann. The role of chromate in filiform corrosion inhibition. *Electrochimica Acta* **48**, 1211-1222 (2003)

Wöllmer, S., S. Zaefferer, M. Göken, T. Mack and U. Glatzel. Characterization of phases of aluminized nickel base superalloys. *Surface and Coating Technology* **167**, 83-96 (2003)

Zaefferer, S.: A study on active deformation systems in titanium alloys: dependence on alloy composition and correlation with the deformation texture. *Materials Science and Engineering* **A344**, 20-30 (2003)

Zaefferer, S.: High resolution crystal orientation measurement techniques for the study of nucleation processes during recrystallization in heavily deformed metals. *La Revue de Métallurgie* **1**, 891-901 (2003)

Zaefferer, S.: Investigation of the correlation between texture and microstructure on a submicrometer scale in the TEM. *Advanced Engineering Materials* **5**, 745-752 (2003)

Zaefferer, S.: Microstructural characterization of multiphase steels. *Materials Science Forum* **426-432**, 1361-1366 (2003)

Zaefferer, S., J.-C. Kuo, Z. Zhao, M. Winning and D. Raabe. On the influence of the grain boundary misorientation on the plastic deformation of aluminum bicrystals. *Acta Materialia* **51**, 4719-4735 (2003)

Zhang, J., A. Schneider and G. Inden. Characterisation of the coke formed during metal dusting of iron CO-H₂-H₂O gas mixtures. *Corrosion Science* **45**, 1329-1341 (2003)

Zhang, J., A. Schneider and G. Inden. Coke formation during metal dusting of iron in CO-H₂-H₂O gas with high CO content. *Materials Science and Corrosion* **54**, 770-777 (2003)



Zhang, J., A. Schneider and G. Inden: Effect of gas composition on cementite decomposition and coke formation of iron. *Corrosion Science* **45**, 281-299 (2003)

Zhang, J., A. Schneider and G. Inden: α -Fe layer formation during metal dusting of iron in CO-H₂-H₂O gas mixtures. *Materials and Corrosion* **54**, 763-769 (2003)

Zhong, Q., N. Xu, G. Zhou and M. Rohwerder: Study of electronic-ionic conducting transformation of temporarily protective oil coating in salt solution. *Materials and Corrosion* **54**, 97-105 (2003)

Conference Papers, Final Reports, and Other Publications

Akiyama, E., A. W. Hassel and M. Stratmann: A study of current transients caused by single particle impact on electrodes. IN: Proc. Asian Pacific Corr. Contr. Conf. 13, C02 (2003) 1-8

Brüx, U. and G. Frommeyer: High-strength light-weight steels based on Fe-Mn-Al-C microstructures - mechanical properties. In: Dislocations, Plasticity and Metal Forming, (Ed.) Khan, A.S. Neat Press, Fulton, Maryland, USA (2003) 169-171

Filatov, D., O. Pawelski and W. Rasp: Laboratory tests on brittle-ductile behaviour of scale in the roll gap during hot rolling. In: Proc. 3rd European Rolling Conf., METEC Congress (2003) 103-108

Frommeyer, G. and R. Rablbauer: High temperature resistant intermetallic Ni-Al-based alloys with refractory metals Cr, Mo, Re. In: Proceedings of MRS Fall Meeting (2003) 193-207

Fushimi, K., A. W. Hassel and M. Stratmann: Passive film formed on shape memory NiTi-alloy in sulfuric acid. In: Proceed. Asian Pacific Corr. Contr. Conf. 13, L06 (2003) 1-8

Hassel, W., S. Bonk, M. Wicinski and M. Stratmann: Corrosion of zinc coated steel sheets under cyclic corrosion conditions. In: Proceed. Asian Pacific Corr. Contr. Conf. 13, P03 (2003) 1-6

Inden, G. and C. R. Hutchinson: Interfacial conditions at the moving interface during growth of ferrite from austenite in Fe-C-(X) alloys. In: Proceedings of the Symposium on the Thermodynamics, Kinetics, Characterization and Modelling of Austenite Formation and Decomposition, (Eds.) E.B. Damm, M.J. Erwin, TMS, Warrendale (2003) 65-79

Kuo, J. C., D. Raabe, S. Zaeferrer, F. Roters, Z. Zhao and M. Winning: Characterizing the grain boundary effect in bicrystal deformation. In: Proceedings of the Tenth International Symposium on Plasticity and its Current Applications (Plasticity 03), (Ed.) A.S. Khan. Neat Press, Fulton, Maryland, USA. Dislocations, Plasticity and Metal Forming, (2003) 543-545

Le Papillon, Y., W. Jäger, M. König, B. Weisgerber and M. Jauhola: Determination of high temperature surface crack formation criteria in continuous casting and thin slab casting. Meeting: Final Report ECSC 7210-PR/084 in Luxemburg. European Commission, Luxemburg, isbn: 92-894-6420-8 (2003) 1-161

Li, Y. S. and M. Spiegel: Degradation performance of Al-containing alloys and intermetallics by molten ZnCl₂/KCl. In: *Corrosion Science in the 21st Century*, UMIST, Manchester, UK (2003) CD-ROM

Parezanovic, I. and M. Spiegel: Influence of dew point on the selective oxidation of cold rolled DP and IF-steels. In: *Corrosion Science in the 21st Century*, UMIST, Manchester, UK (2003) CD-Rom

Parezanovic, I. and M. Spiegel: Surface modification of different Fe-Si and Fe-Mn alloys by oxidation/reduction treatments. In: EUROCORR 03, Budapest, Hungary (2003) CD-ROM

Raabe, D., F. Roters and Y. Wang: Simulation of texture and anisotropy during metal forming with respect to scaling aspects. In: Proceedings of the 1st Colloquium of DFG Priority Program Process Scaling, Process Scaling, Strahl-technik Volume 24, (Eds.) F. Vollertsen, F. Hollmann. BIAS Verlag, Bremen (2003) 99-106

Rasp, W.: Investigation of the tribology of cold rolling using mechanical simulation techniques. In: XXII. Verformungskundliches Kolloquium (2003) 118-123

Rasp, W.: Manufacturing of autobody sheets with improved formstiffness by cold rolling. In: Proc. Int. Deep Drawing Research Group (IDDRG) Conf., Bled, Slovenia (2003) 261-271



Rasp, W., C. M. Wichern and L. Krone: Deformation of idealized lubrication pockets during plane-strain upsetting. In: Proc. 6th Int. ESAFORM Conf. on Material Forming (2003) 755-758

Rohwerder, M., E. Hornung and X.-W. Yu: Delamination of polymer coatings from metal substrates: submicroscopic and molecular aspects. In: Mater. Res. Soc. Symp. Proc. Vol. 734 (2003) B2.8.1-B2.8.6

Ruh, A. and M. Spiegel: Kinetic investigations on molten salt induced corrosion of pure iron. In: EUROCORR 03, Budapest, Hungary (2003) CD-ROM

Sauthoff, G.: Titan-Aluminid-Legierungen - eine Werkstoffgruppe mit Zukunft, Vorwort. Forschungszentrum Jülich - Projektträger Jülich (PTJ), Jülich, isbn: 3-89336-318-1 (2003)

Spiegel, M.: Factors affecting the high temperature corrosion resistance of coatings in waste fired plant. In: Corrosion Science in the 21th Century UMIST, Manchester, UK (2003) CD-ROM

Storojeva, L., C. Escher, R. Bode and K. Hulka: Stabilization and processing concept for the production of ULC steel sheet with bake hardenability. In: IF STEELS, (Ed.) H. Takechi. The Iron and Steel Institute of Japan, Japan (2003) 294-297

Stratmann, M., R. Hausbrand and M. Rohwerder: Novel zinc alloy coatings: tailored semiconducting oxides for improved corrosion protection and adhesion of organic coatings. In: Proceedings of 13th Asian Pacific Corrosion Control Conference, Osaka University. Japan Society of Corrosion Engineering, PL-5 (2003) 1-7

Tsuri, S., A. W. Hassel and M. Stratmann: Electrochemical behaviour of low alloy steels during atmospheric corrosion. In: Proceed. Asian Pacific Corr. Contr. Conf. 13, A05 (2003) 1-8

Wöllmer, S., S. Zaefferer, M. Göken, T. Mack and U. Glatzel: Characterization of phases of aluminized nickel base superalloys. In: Proceedings ICSMA-13 (2003) 364

2004

Books, Book Chapters, and Editorial Work

Bard, A. J. and M. Stratmann (Eds.): Encyclopaedia of electrochemistry. Wiley-VCH, Weinheim, Vol. 5: Electrochemical Engineering (Ed.: Digby D. MacDonald), Vol. 7: Inorganic Chemistry (Ed.: William E. Geiger), Vol. 8: Organic Electrochemistry (Ed.: Hans J. Schäfer), isbn 3-527-30400-2, Vol. 10: Modified Electrodes (Ed.: Israel Rubinstein) (2004)

Raabe, D.: Cellular, lattice gas, and Boltzmann automata. In: Continuum Scale Simulation of Engineering Materials, (Eds.) D. Raabe, F. Roters, F. Barlat, L.-Q. Chen. Wiley-VCH, Weinheim, isbn: 3-527-30760-5 (2004)

Raabe, D.: Drowning in data - a viewpoint on strategies for doing science with simulations. In: Handbook of Materials Modelling, Vol. 1: Methods and Models, (Ed.) S. Yip. Kluwer-Springer, Berlin (2004)

Raabe, D.: Volume 6, Zeitschrift für Metallkunde (2004)

Raabe, D., F. Roters, F. Barlat and L.-Q. Chen (Eds.): Continuum scale simulation of engineering materials fundamentals - microstructures - process applications. Wiley-VCH, Weinheim, isbn: 3-527-30760-5, p. 855 (2004)

Roters, F.: The texture component crystal plasticity finite element method. In: Continuum Scale Simulation of Engineering Materials, (Eds.) Raabe, D.; Roters, F. Barlat, L.Q. Chen. Wiley-VCH, Weinheim (2004)

Schneider, A. and G. Inden: Computer simulation of diffusion controlled phase transformations. In: Continuum scale simulation of engineering materials: Fundamentals – Microstructures – Process Applications, (Eds.) D. Raabe, L.Q. Chen, F. Barlat; F. Roters. Wiley-VCH Verlag, Weinheim, p. 3-36 (2004)



Publications in Scientific Journals

Barranco, V., J. Carpentier and G. Grundmeier: Correlation of morphology and barrier properties of thin microwave plasma polymer films on metal substrate. *Electrochimica Acta* **49**, 1999-2013 (2004)

Barranco, V., P. Thiemann, H. K. Yasuda, M. Stratmann and G. Grundmeier: Spectroscopic and electrochemical characterisation of thin cathodic plasma polymer films on iron. *Applied Surface Science* **229**, 87-96 (2004)

Bastos, A.C., C. Oswald, L. Engl, G. Grundmeier and A.M. Simoes: Formability of organic coatings – an electrochemical approach. *Electrochimica Acta* **49**, 3947-3955 (2004)

Baumert, B., M. Stratmann and M. Rohwerder: The deformation response of ultra-thin polymer films on steel sheet in a tensile straining test: the role of slip bands emerging at the polymer/metal interface. *Zeitschrift für Metallkunde* **95**, 447-455 (2004)

Bonk, S., M. Wicinski, A. W. Hassel and M. Stratmann: Electrochemical characterizations of precipitates formed on zinc in alkaline sulphate solution with increasing pH values. *Electrochemistry Communicatio*s **6**, 800-804 (2004)

Büchner, A. R.: Thin strip casting of steel with a twin roll caster - correlation between feeding system and strip quality. *Steel Research Int.* **755**, 5-12 (2004)

Cha, S.C. and M. Spiegel: Fundamental studies on alkali chloride induced corrosion during combustion of biomass, *Materials Science Forum* **461-464**, 1055-1062 (2004)

Deges, J., R. Fischer, G. Frommeyer and A. Schneider: Atom probe field ion microscopy investigations on the intermetallic $\text{Ni}_{49.5}\text{Al}_{49.5}\text{Re}_1$ alloy. *Surface and Interface Analysis* **36**, 533-539 (2004)

Dinh, H. T., J. Kuever, M. Mußmann, A. W. Hassel, M. Stratmann and F. Widde: Iron corrosion by novel anaerobic microorganisms. *Nature* **427**, 829-832 (2004)

Dorner, D., L. Lahn and S. Zaefferer: Investigation of the primary recrystallization microstructure of cold rolled and annealed Fe 3% Si single crystals with Goss orientation. *Material Science Forum* **467-470**, 129-134 (2004)

Eleno, L. T. F., C. G. Schön, J. Balun and G. Inden: Experimental study and cluster Variation modelling of the A2/B2 equilibria at the Ti-rich side of the Ti-Fe system. *Zeitschrift für Metallkunde* **95**, 464-468 (2004)

Elsner, A., R. Kaspar, D. Ponge, D. Raabe and S. van der Zwaag: Recrystallitexture of cold rolled and annealed IF steel produced from ferritic rolled hot strip. *Materials Science Forum* **467-470**, 257-262 (2004)

Eumann, M., M. Palm and G. Sauthoff: Alloys based on Fe_3Al or FeAl with strengthening Mo_3Al precipitates. *Intermetallics* **12**, 625-633 (2004)

Eumann, M., M. Palm and G. Sauthoff: Iron-rich iron-aluminium-molybdenum alloys with strengthening intermetallic mu-phase and r-phase precipitates. *Steel Research International* **75**, 62-73 (2004)

Filatov, D., O. Pawelski and W. Rasp: Hot-rolling experiments on deformation behaviour of oxide scale. *Steel Research International* **75**, 20-25 (2004)

Frommeyer, G., R. Fischer, J. Deges, R. Rablbauer and A. Schneider: APFIM investigations on site occupancies of the ternary alloying elements Cr, Fe, and Re in NiAl. *Ultramicroscopy* **101**, 139-148 (2004)

Grabke, H. J.: Supersaturation of iron with nitrogen, hydrogen or carbon and the consequences. *Materiali in Tehnologije* **38**, 25-36 (2004)

Grabke, H. J., M. Spiegel and A. Zahs: Role of alloying elements and carbides in the chlorine-induced corrosion of steels and alloys. *Materials Research* **7**, 89-95 (2004)

Grabke, H. J. and Z. Tökei: Initial oxidation of a 9 % CrMo- and a 12 % CrMoV – steel. *Steel Research International* **75**, 38-46 (2004)

Grundmeier, G., P. Thiemann, J. Carpentier, N. Shirtcliffe and M. Stratmann: Tailoring of the morphology and chemical composition of thin organosilane microwave plasma polymer layers on metal substrates. *Thin Solid Films* **446**, 61-71 (2004)



Hassel, A. W.: Surface treatment of NiTi for medical applications. *Minimally Invasive Therapy & allied Technologies*, **13**, 240-247 (2004)

Heikinheimo, L., K. Hack, D. Baxter, M. Spiegel, U. Krupp, M. Hamalainen and M. Arponen: Optimisation of in-service performance of boiler steels by modelling high temperature corrosion – EU FP5OPTICORR project. *Materials Science Forum* **461-464**, 473-480 (2004)

Herrmann, J., G. Inden and G. Sauthoff: Deformation behaviour of iron-rich iron-aluminium alloys with ternary transition metal additions. *Steel Research International* **75**, 339-342 (2004)

Herrmann, J., G. Inden and G. Sauthoff: Microstructure and deformation behaviour of iron-rich iron-aluminium alloys with ternary carbon and silicon additions. *Steel Research International* **75**, 343-352 (2004)

Kobayashi, S., S. Zaeferrer, A. Schneider, D. Raabe and G. Frommeyer: Effect of the degree of order and the deformation microstructure on the kinetics of recrystallization in a Fe₃Al ordered alloy. *Materials Science Forum* **467-470**, 153-158 (2004)

Konrad, J., S. Zaeferrer and A. Schneider: Investigation of nucleation mechanisms of recrystallization in warm rolled Fe₃Al base alloys. *Materials Science Forum* **467-470**, 75-80 (2004)

Li, Y.S., M. Sanchez-Pasten and M. Spiegel: High temperature interaction of pure Cr with KCl, *Materials Science Forum* **461-464**, 1047-1053 (2004)

Li, Y.S. and M. Spiegel: Internal oxidation of Fe-Al alloys in KCl-air atmosphere at 650 °C. *Oxidation of Metals* **61**, 314 (2004)

Li, Y.S. and M. Spiegel: Models describing the degradation of FeAl and NiAl alloys induced by ZnCl₂/KCl melt at 400-450 °C. *Corrosion Science* **46**, 2009-2023 (2004)

Löffler, F., M. Palm and G. Sauthoff: Iron-rich iron-titanium-silicon alloys with strengthening intermetallic laves phase precipitates. *Steel Research International* **75**, 766-772 (2004)

Ma, A. and F. Roters: A constitutive model for fcc single crystals based on dislocation densities and its application to uniaxial compression of aluminium single crystals. *Acta Materialia* **52**, 3603-3612 (2004)

Ma, A., F. Roters and D. Raabe: Numerical study of textures and Lankford values for FCC polycrystals by use of a modified Taylor model. *Computational Materials Science* **29**, 259-395 (2004)

Ostwald, C. and H. P. Grabke: Initial oxidation and chromium diffusion I. Effects of surface working on 9 – 20 % Cr steels. *Corrosion Science* **46**, 1113-1127 (2004)

Palm, M. and G. Sauthoff: Deformation behaviour and oxidation resistance of single-phase and two-phase L21 Fe-Al-Ti alloys. *Intermetallics* **12**, 1345-1359 (2004)

Parezanovic, I. and M. Spiegel: Surface modification of various Fe-Si and Fe-Mn alloys by oxidation/reduction treatments. *Surface Engineering* **20**, 285-291(2004)

Parezanovic, I., E. Strauch and M. Spiegel: Development of spinel forming alloys with improved electronic conductivity for MCFC application. *Journal of Power Sources* **135**, 52-61 (2004)

Poeter, B., F. Stein and M. Spiegel: Initial stages of Al₂O₃ growth on Fe-Al intermetallic phases. *Lithos* **73**, Suppl., S89 (2004)

Raabe, D.: Overview on the lattice Boltzmann method for nano- and microscale fluid dynamics in materials science and engineering. *Modelling and Simulation in Materials Science and Engineering* **12**, R13-R46 (2004)

Raabe, D.: Simulation of spherulite growth during polymer crystallization by use of a cellular automaton. *Materials Science Forum* **467-470**, 603-609 (2004)

Raabe, D. and N. Chen: Recrystallization in deformed and heat treated PET polymer sheets. *Materials Science Forum* **467-470**, 551-556 (2004)

Raabe, D., N. Chen and L. Chen: Crystallographic texture, amorphization, and recrystallization in rolled and heat treated polyethylen terephthalate. *Polymer* **45**, 8265-8277 (2004)



Raabe, D. and J. Ge: Experimental study on the thermal stability of Cr filaments in a Cu–Cr–Ag in situ composite. *Scripta Materialia* **51**, 915-920 (2004)

Raabe, D. and F. Roters: Using texture components in crystal plasticity finite element simulations. *International Journal of Plasticity* **20**, 339-361 (2004)

Rablbauer, R., R. Fischer and G. Frommeyer: Mechanical properties of NiAl-Cr alloys in relation to microstructure and atomic defects. *Zeitschrift für Metallkunde* **95**, 525-534 (2004)

Rasp, W. and C. M. Wichern: Effects of idealized surface geometry on lubricant entrapment during plane-strain upsetting - An FEM Study. *Steel Grips* **2**, (2004)

Roters, F., W. Yanwen, K. Jui-Chao and D. Raabe: Comparison of single crystal simple shear deformation experiments with crystal plasticity finite element simulations. *Advanced Engineering Materials* **6**, 653-656 (2004)

Roters, F., Y. Wang, J.-C. Kuo and D. Raabe: Comparison of single crystal simple shear deformation experiments with crystal plasticity finite element simulations. *Advanced Engineering Materials*, **6**, 653-656 (2004)

Ruh, A. and M. Spiegel: Kinetic investigations on salt melt induced high temperature corrosion of pure metals. *Materials Science Forum* **461-464**, 61 (2004)

Sandim, H. R. Z. and D. Raabe: An EBSD study on orientation effects during recrystallization of coarse-grained niobium. *Materials Science Forum* **467-470**, 519-555 (2004)

Sandim, H. R. Z., M. J. R. Sandim, H. H. Bernardi, J. F. C. Lins and D. Raabe: Annealing effects on the microstructure and texture of a multifilamentary Cu–Nb composite wire. *Scripta Materialia* **51**, 1099-1104 (2004)

Schneider, A. and G. Sauthoff: Iron-aluminium alloys with strengthening carbides and intermetallic phases for high-temperature applications. *Steel Research International* **75**, 55-61 (2004)

Schneider, A., J. Zhang and G. Inden: Metal dusting of binary Fe-Al alloys in CO-H₂-H₂O gas mixtures. *Journal of Corrosion Science and Engineering* **6**, paper 87 (2004)

Schön, C. G., G. Inden and L. T. F. Eleno: Comparison between Monte Carlo and Cluster Variation method calculations in the BCC Fe-Al system including tetrahedron interactions. *Zeitschrift für Metallkunde* **95**, 459-463 (2004)

Song, R., D. Ponge and R. Kaspar: The microstructure and mechanical properties of ultrafine grained plain C-Mn steels. *Steel Research* **75**, 33-37 (2004)

Song, R., D. Ponge, R. Kaspar and D. Raabe: Grain boundary characterization and grain size measurement in an ultrafine grained steel. *Zeitschrift für Metallkunde* **95**, 513-517 (2004)

Stein, F., G. Sauthoff and M. Palm: Phases and phase equilibria in the Fe-Al-Zr system. *Zeitschrift für Metallkunde* **95**, 469-485 (2004)

Stein, F., M. Palm and G. Sauthoff: Structures and stability of Laves phases - Part I: critical assessment of factors controlling Laves phase stability. *Intermetallics* **12**, 713-720 (2004)

Storojeva, L., D. Ponge, R. Kaspar and D. Raabe: Development of microstructure and texture of medium carbon steel during heavy warm deformation. *Acta Materialia* **52**, 2209-2220 (2004)

Storojeva, L., R. Kaspar and D. Ponge: Effects of heavy warm deformation on microstructure and mechanical properties of a medium carbon ferritic-pearlitic steel. *ISIJ International*, **44**, 1211-1216 (2004)

Vander Kloet, J., W. Schmidt, A. W. Hassel and M. Stratmann: The role of chromate in filiform corrosion inhibition. *Electrochimica Acta* **49**, 1673 (2004)

Wang, Y., D. Raabe, C. Klüber and F. Roters: Orientation dependence of nanoindentation pile-up patterns and of nanoindentation microtextures in copper single crystals. *Acta Materialia* **52**, 2229-2238 (2004)

Wapner, K. and G. Grundmeier: Scanning Kelvin probe measurements of the stability of adhesive/metal interfaces in corrosive environments. *Advanced Engineering Materials* **6**, 163-167 (2004)



Wasilkowska, A., M. Bartsch, F. Stein, M. Palm, G. Sauthoff and U. Messerschmidt: Plastic deformation of Fe- Al polycrystals strengthened with Zr-containing Laves phases: Part II. Mechanical properties. *Materials Science and Engineering A* **381**, 1-15 (2004)

Wasilkowska, A., M. Bartsch, F. Stein, M. Palm, K. Sztwiertnia, G. Sauthoff and U. Messerschmidt: Plastic deformation of Fe-Al polycrystals strengthened with Zr- containing Laves phases: part I. microstructure of undeformed materials. *Materials Science and Engineering A* **380**, 9-19 (2004)

Zaefferer, S., J. Ohlert and W. Bleck: A study of microstructure, transformation mechanisms and correlation between microstructure and mechanical properties of a low alloyed TRIP steel. *Acta Materialia* **52**, 2765-2778 (2004)

Zaefferer, S.: The electron backscatter diffraction technique - a powerful tool to study microstructures by SEM. *JEOL News* **39**, 10-15 (2004)

Zhang, J., A. Schneider and G. Inden: Cementite decomposition and coke gasification in He and H₂-He gas mixtures. *Corrosion Science* **46**, 667-679 (2004)

Zhang, J., A. Schneider and G. Inden: Metal dusting of iron in CO-H₂-H₂O gas mixtures at 600 °C. *Journal of Corrosion Science and Engineering* **6**, paper 100 (2004)

Zhong, Q.D., M. Rohwerder and Z. Zhang: Study of lubricants and their effect on the anti-corrosion performance as temporarily protective oil coatings. *Surface & Coatings Technology* **185**, 234-239 (2004)

Zhong, Q.D., M. Rohwerder, Z. Zhao and Z. Jin: Semiconducting behavior of temporarily protective oil coating on the surface of AISI 304 stainless steel in 5% Na₂SO₄ solution during its degradation. *Journal of the Electrochemical Society* **151**, B446-B452 (2004)

Conference Papers, Final Reports, and Other Publications

Baumert, B., M. Stratmann and M. Rohwerder: Formability of ultra-thin plasma polymer films deposited on metal sheet: mesoscopic and nanoscopic aspects of defect formation. In: *Materials Research Society Symp. Proc. Vol. 795* (2004) U5.23.1-U5.23.6

Büchner, A. R. and M. Thiemann: Twin roll strip casting of steel – studies of heat transfer into the rolls. In: *1st Chinese-German Seminar on Fundamentals of Iron and Steelmaking*, (Ed.) Steel Institute VDEh. The Chinese Society for Metals, Beijing, China (2004) 276-286

Cha, S.C. and M. Spiegel: Local reaction between NaCl and KCl particles and metal surfaces. In: *Proceedings of EUROCORR 04*, Nice, France (2004)

Cha, S.C. and M. Spiegel: Studies on the local reactions of thermophoretic deposited alkali chloride particles on metal surfaces. In: *NACE CORROSION*, New Orleans (2004) No 04533

Frenznick, S., M. Stratmann and M. Rohwerder: Galvanizing of defined model samples: on the road to a fundamental physical understanding of hot-dip galvanizing. In: *GALVATECH* (2004) 411-417

Frommeyer, G.: Superplasticity at higher strain rates in ultrafine grained α -titanium / Ti_xMe_y-intermetallic Ti-8Fe-4Al, Ti-10Co-4Al and Ti-10Ni-4Al alloys. In: *Third European Conference on Super Plastic Forming*, (Eds.) G. Bernhart, T. Cutard, P. Lours. Cépaduès-Éditions, Toulouse, France (2004) 57-64

Frommeyer, G. and S. Knippscheer: Enhanced superplasticity of fine-grained gamma TiAl(Mo, Cr, Si) Alloys. In: *Ti-2003 Science and Technology*, (Eds.) G. Lütjering, J. Albrecht. Wiley-VCH, Weinheim (2004) 2249-2256

Frommeyer, G. and R. Rosenkranz: Structures and properties of the refractory silicides Ti₅Si₃ and TiSi₂ and Ti-Si-(Al) eutectic alloys. In: *Nato Science Series II. Mathematics, Physics and Chemistry*. (Eds.) O.N. Senkov, D.B. Miracle, S.A. Firstov. *Nato Science Series Vol. 146, Part 5*, Kluwer Academic Publishers, Dordrecht (2004) 287-308

Knippscheer, S. and G. Frommeyer: Effects of ternary alloying elements on constitution and mechanical properties of TiAl base alloy. In: *Ti-2003 Science and Technology*. (Eds.) G. Lütjering, J. Albrecht. Wiley-VCH, Weinheim (2004) 2231-2238



Konrad, J., A. Guenther, S. Zaefferer and D. Raabe: Texture analysis of a coarse grained Fe₃Al cast alloy by neutron scattering. GeNF-Experimental Report 2003, 183-185 (2004)

Parezanovic, I. and M. Spiegel: Influence of B, S, P, Si and C segregation on the selective oxidation of dual phase and interstitial free steels. In: Proceedings of GALVATECH, USA, Chicago (2004)

Parezanovic, I., B. Poeter and M. Spiegel: B and N segregation on dual phase steel after annealing. In: Defect and Diffusion Forum, DIMAT, Krakow, Poland (2004)

Park, E., B. Hüning and M. Spiegel: Annealing of Fe-15Cr alloy in N₂- 5% H₂ gas mixture: Effect of hydrogen concentration. In: Defect and Diffusion Forum, DIMAT, Krakow, Poland (2004)

Park, E., B. Hüning and M. Spiegel: Effects of heat treatment on the oxide layer of Fe-15 at.% Cr alloy surface. In: Proceedings of EUROCORR 04, Nice, France (2004)

Pöter, B., F. Stein, M. Palm and M. Spiegel: Oxidation behaviour of Fe-Al alloys analysed using in- and ex-situ techniques. In: Proceedings of EUROCORR 04, Nice, France (2004)

Pötschke, S. and A. R. Büchner: Influence of in-line hot rolling on twin roll cast LC-steel. In: Proceedings of 2nd International Conference & Exhibition on New Development in Metallurgical Process Technology. (Ed.) Editors Associazione Italiana di Metallurgia, Milano (2004) CD-ROM

Prakash, U., G. Sauthoff, N. Parvathavarthini and R. K. Dayal: Hydrogen effects in iron aluminides containing carbon. In: International Symposium on Recent Advances in Inorganic Materials (RAIM 02) , (Eds.) D. Bahadur, S. Vitta, O. Prakash. Narosa Publishing House, New Delhi. Inorganic Materials: Recent Advances, (2004) 148-152

Rasp, W. and D. Filatov: Final report - Untersuchungen zum spröd-duktilen Zunderverhalten beim Warmwalzen. Bericht Nr. AW 130 des VFWH im VDEh in Düsseldorf. (2004)

Rohwerder, M., R. Hausbrand and M. Stratmann: Development of zinc-alloy coatings with inherent delamination stability for organic coatings. In: GALVATECH (2004) 971-976

Roters, F., A. Ma and D. Raabe: Kristallplastische Simulation in der Werkstoffprüfung. In: Proceedings of the 2004-Materials-Testing Conference of DGM in Neu-Ulm. DGM-Verlag, (2004) 1

Ruh, A. and M. Spiegel: Influence of HCl and water vapour on the corrosion kinetics of Fe beneath molten ZnCl₂/KCl. In: Proceedings of EUROCORR 04, Nice, France (2004)

Song, R., R. Kaspar, D. Ponge and D. Raabe: The effect of Mn on the microstructure and mechanical properties after heavy warm rolling of C-Mn steel. In: Ultrafine Grained Materials III. (Eds.) Y.T. Zhu, T.G. Langdon, R.Z. Valiev. TMS, Charlotte, North Carolina, USA (2004) 445-450

Uhlmann, E., G. Frommeyer, S. Herter, S. Knippscheer and J. M. Lischka: Studies on the conventional machining of TiAl-Based Alloys. In: Ti-2003, 10th World Conference on Titanium. (Eds.) G. Lütjering, J. Albrecht. Wiley-VCH, Weinheim (2004) 2293-2238

Zaefferer, S.: Caractérisation de la microtexture: quand faut-il utiliser le microscope électronique à transmission?. L'Analyse EBSD, Principes et Applications (2004) 161-170



Doctoral and Diploma Theses

Doctoral Theses

2002 (residual since Scientific Report 2001/2002)

Dr.-Ing. Reichert, A.: Dreidimensionale Finite-Elemente-Analyse der Dickenreduktion beim Stranggießen. In: Shaker-Verlag Aachen, isbn: 3-8322-1315-5. Technische Universität, Hannover (2002)

2003

Dr.-Ing. Gehrman, R.: Texturen von Magnesium. RWTH Aachen (2003)

Dr. rer. nat. Hausbrand, R.: Elektrochemische Untersuchungen zur Korrosionsstabilität von polymerbeschichtetem Zink-Magnesiumüberzug auf Stahlband. Ruhr-Universität, Bochum (2003)

Dr.-Ing. Kuo, J.-C.: Mikrostrukturmechanik von Bikristallen mit Kippkorngrenzen. In: Shaker-Verlag, D82. RWTH, Aachen (2003)

Dr.-Ing. Liebeherr, M.: Kornwachstum und Texturen einer Ni-Basis ODS-Superlegierung. RWTH, Aachen (2003)

Dr.-Ing. Marx, V.: Simulation der Rekristallisation mittels zellulärer Automaten. RWTH, Aachen (2003)

Dr.-Ing. Park, C.-M.: Mikrotransformationstexturen im Stahl mittels Orientierungsmikroskopie im hochauflösenden Rasterelektronenmikroskop. RWTH Aachen (2003)

Dr.-Ing. Wengenroth, W.: Möglichkeiten und Grenzen der plastischen Formgebung von Rundstäben mit dem Dieless-Drawing-Verfahren. In: Umformtechnische Schriften, Band 108. Aachen, Shaker-Verlag. RWTH, Aachen (2003)

2004

Dr.-Ing. Balun, J.: Phase Equilibria in Fe-Rh-X (X=Ti,Co) Systems. In: Shaker-Verlag, D82, isbn: 3-8322-2959-0. RWTH, Aachen (2004)

Dr.-Ing. Büscher, M.: Lernen mit Simulationen: Erstellung einer interaktiven und objektorientierten Lernsoftware für die Materialkunde. RWTH, Aachen (2004)

Dr. Dewobroto, N.: Evolution de la microstructure et de la texture lors de la recristallisation statique d'alliages de symétrie hexagonale (alliages Ti et Zr). University, Metz, France (2004)

Dr.-Ing. Eisen, S.: Beitrag zur lokale Breitung beim Flachwalzen. In: Umformtechnische Schriften, Band 115. Aachen: Shaker Verlag. RWTH, Aachen (2004)

Dr.-Ing. Fischer, R.: Strukturelle Charakterisierung auf atomarer Skala von unlegiertem und chromhaltigem NiAl mit B2-Überstrukturgitter mit der Atomsonden-Feldionenmikroskopie. In: Shaker Verlag Aachen, isbn: 3-8322-3098-X. Technische Universität, Clausthal (2004)

Dr.-Ing. Heckmann, C.-J.: Schmelzenzufuhr und Bandoberflächenqualität beim Zweirollengießverfahren. In: Shaker-Verlag Aachen, isbn: 3-8322-2885-3. Technische Universität, Clausthal (2004)

Dr.-Ing. Pohl, H.: Optimierung der Prozessparameter beim Direkteinsatz dünner Brammen bezüglich der mechanischen und bruchmechanischen Eigenschaften von Ti-Mikrolegierten Stählen. RWTH, Aachen (2004)

Dr.-Ing. Schinkinger, B.: Schichtanalytische und elektrochemische Untersuchungen zur Abscheidung dünner SiO₂- und Organosilanschichten auf verzinktem Stahl. Ruhr-Universität, Bochum (2004)



Dr.-Ing. Song, R.: Processing, microstructure, and properties of ultrafine grained steels. RWTH, Aachen, (2004)

Dr. Verbeken, K.: Orientation selection in ultra low carbon steel during thermally activated phenomena induced by cold deformation. University, Ghent, Belgium (2004)

Diploma Theses

2002 (residual since Scientific Report 2001/2002)

Tranchant, J.: Deformation of semi-brittle intermetallic material under superimposed hydrostatic pressure. Ecole Centrale de Nantes, Nantes (2002)

Krone, L.: Untersuchung des Einflusses definierter Schmierverhältnisse am Beispiel des Flachstauchversuches. TU, Clausthal (2002)

2003

Kaushal, C.: Untersuchung der Abhängigkeit des Ölaustrags von der Oberflächenfeinstruktur beim Auswalzen gedoppelter Aluminiumfolien. HS Niederrhein, Krefeld (2003)

2004

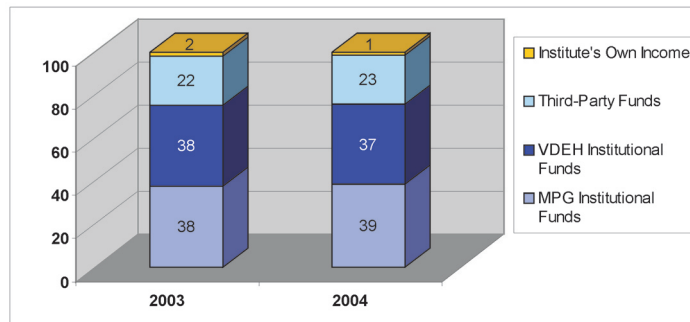
Willutzki, S.: Entwicklung und Charakterisierung hochfester Beta-Titan-Legierungen für Fahrzeugkomponenten. Gerhard-Mercator Universität GH, Duisburg (2004)



Budget of the Institute

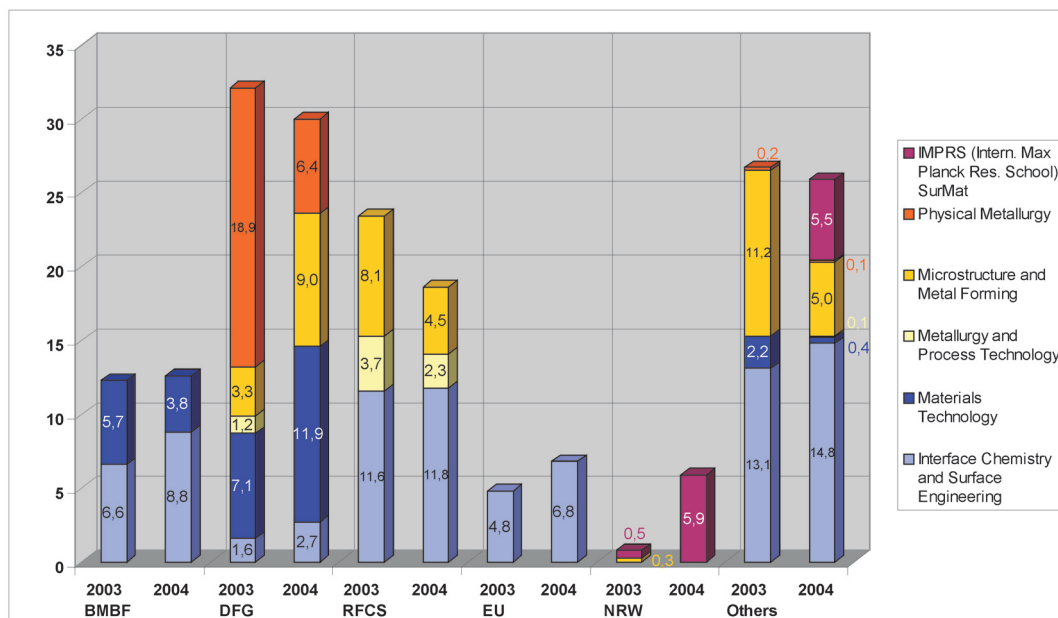
Revenue

(percentual contributions to total revenue without appointment-related investment funds and general reconstruction of the buildings; year 2004 data estimated)



Third-Party Funds

(percentual contributions to total revenue including personnel, material, investments; year 2004 data estimated)

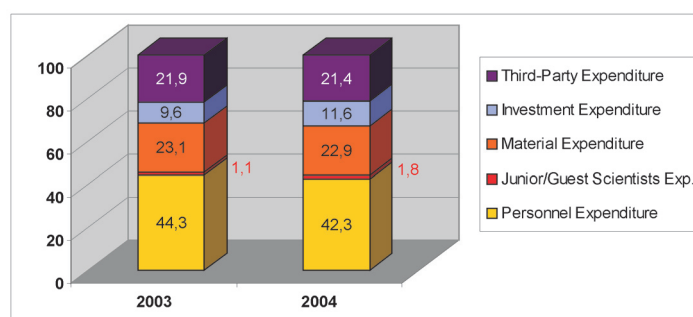


BMBF: Ministry of Science and Education
 DFG: German Science Foundation
 RFCS: Research Fund for Coal and Steel
 (European Coal and Steel Community - ECSC)

EU: European Community
 NRW: North Rhine-Westphalia

Expenditure

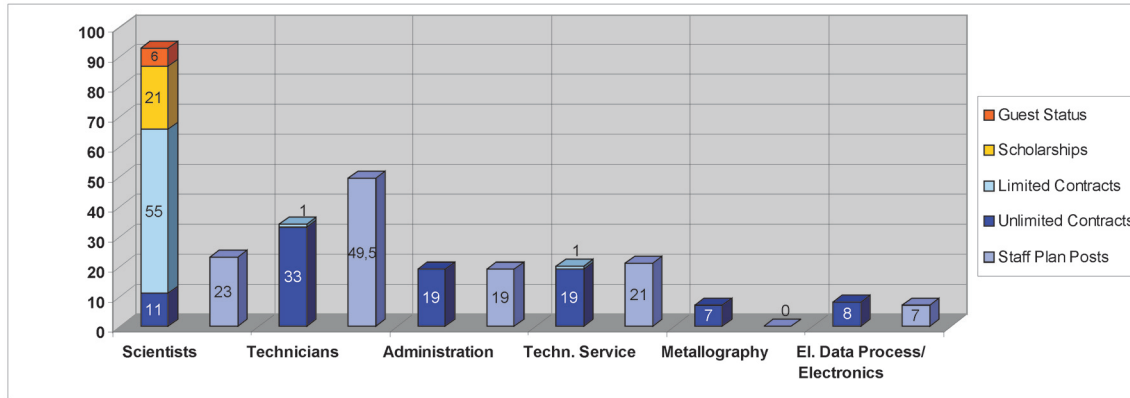
(percentual distribution of total expenditure; investments include large-scale apparatus, electronic data processing, appointment-related investments, separate investment for basic equipment; year 2004 data estimated)



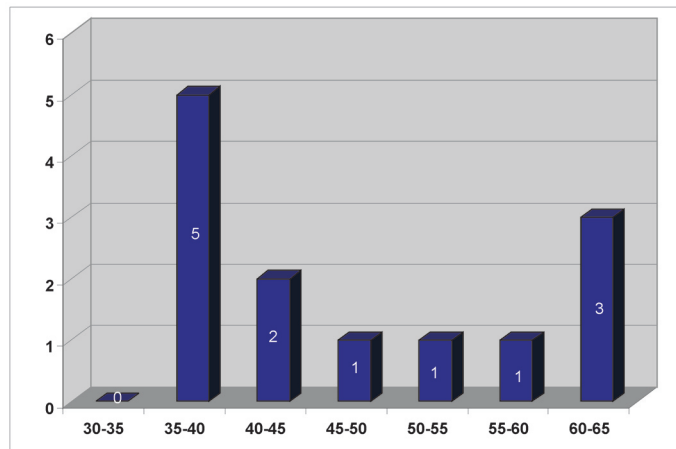


Personnel Structure

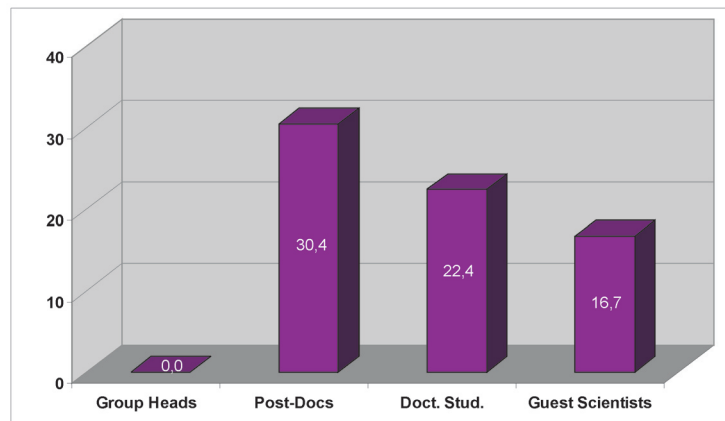
Number of Scientific / Non-Scientific Employees (Dec. 2004, estimated)
(exclusive of department heads)



Age Distribution: Number of Scientists with Unlimited Contracts (Dec. 2004, estimated)
(total number: 13; exclusive of department heads)

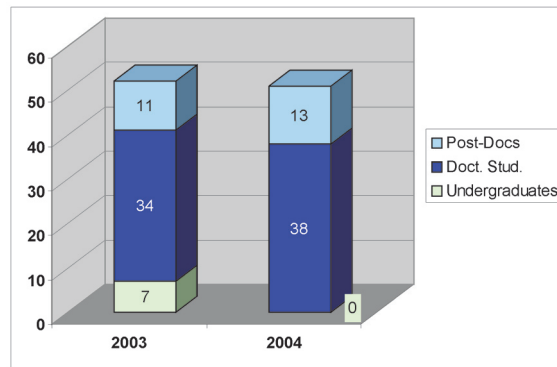


Female Scientists (Dec. 2004, estimated)
(percentual number with respect to different contracts; exclusive of department heads)

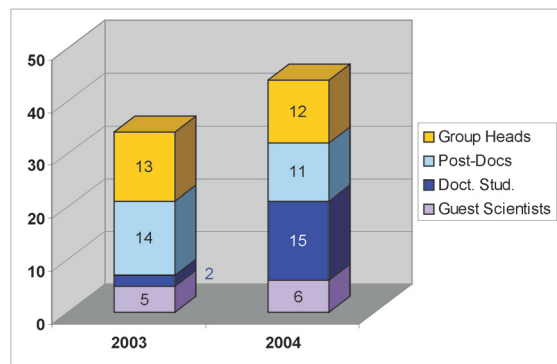




Number of Junior Scientists Financed via Third-Party Funds
(year 2004 data estimated)



Number of Junior Scientists not Financed via Third-Party Funds
(year 2004 data estimated)





The Institute in Public

Prof. Dr.-Ing. Raabe was awarded the *Gottfried Wilhelm Leibniz Price 2004* by the German Research Foundation, DFG, on Dec. 5, 2003. On this occasion and during the following months, a lot of newspapers devoted articles to the price winner and his working field. Among them were: Berliner Zeitung, Chemische Rundschau, Der Tagesspiegel, Die Welt, FAZ, Financial Times Deutschland, Hamburger Abendblatt, Münstersche Zeitung, NRZ and NRZ am Sonntag, Rheinische Post, Schwäbische Zeitung, Stuttgarter Zeitung, Süddeutsche Zeitung, VDI Nachrichten, Westfälische Nachrichten, WZ.

Several articles were published by authors of the MPIE in newspapers and popular scientific journals:

Prof. G. Frommeyer:

Ausgekochter Stahl für das Auto von morgen, „Max-Planck-Forschung“, 3/2004;
Extrem dehnbarer Stahl, Prof. Dr. G. Frommeyer in „Die Welt“, Oct. 23, 2004;
Superleichter Stahl für Autobau entwickelt, „Rheinische Post“, Oct. 23, 2004;
Neuer Stahl fast so dehnbar wie Gummi, „Die Welt kompakt“, Oct. 25, 2004;
Ausgeklügelter Stahl für die Autos von morgen, „Hamburger Abendblatt“, Oct. 25, 2004.

Dr. M. Rohwerder, Prof. Dr. M. Stratmann:

Moderne Konzepte für den Korrosionsschutz, Haftende Hüllen für neue Stähle, „RUBIN Wissenschaftsmagazin“, 96-101, 2004.

The „*Tag der Technik*“ (*Technology Day*) was organized by the City of Düsseldorf and the Federal Ministry of Education and Research (BMBF) on June 18 and 19, 2004. Within the framework of the „Year of Technics“, the Max-Planck-Institute and the Steel Institute VDEh appeared in public with a joint tent and several presentations on the Gründgens-Platz in Düsseldorf, just in front of the main theatre. Under the headline „Stahl - Vielfalt der Eigenschaften, Vielfalt der Chancen“ („steel - variety of properties, variety of prospects“) a playful-interactive event was held to demonstrate the characteristics of steel. Examples were presented by the members of the Max Planck Institute's metallography group (s. Fig.). There was a great deal of information and a CD-ROM containing answers to training, studying, jobs and carriers within the steel industry. Besides, the theatre group of the Goethe Gymnasium Düsseldorf, the partner school of the Steel Institute VDEh, entertained the visitors.



Members of the metallography group of the MPIE and „junior scientist“ at the *Technology Day*.

On Dec. 17, 2004, the inauguration of the *International Max Planck Research School SurMat* was conducted with the participation of Prof. Dr.-Ing. Dieter Ameling, chairman of the steel institute VDEh, Hannelore Kraft, minister of science and education of the state North Rhine-Westphalia, Meng Shuguang, counsellor of the People's Republic of China and Joachim Erwin, lord mayor of the city of Düsseldorf.

